

Radiation-Induced Copolymerization of Ethylene and Sulfur Dioxide in the Liquid and Gas Phases

P. COLOMBO, J. FONTANA, and M. STEINBERG,
Brookhaven National Laboratory, Upton, New York 11073

Synopsis

The radiation-induced copolymerization of ethylene and sulfur dioxide has been studied in the liquid and gas phases. In the liquid phase, the copolymer composition remained equimolar over a temperature range of 20–160°C. and ethylene pressures of 50–680 atm. The rate of copolymerization in the liquid phase at 680 atm. increased with temperature to a maximum value at ~80°C. Above this temperature the rate steadily decreased to zero at 157°C. because of temperature-dependent depropagation reactions. In the gas phase, copolymers were formed that contained from 9 to 46 mole-% sulfur dioxide. Under constant conditions of temperature, pressure, and radiation intensity, the copolymerization rate in the gas phase increased with increasing sulfur dioxide in the initial gas mixture. The propagating species for the liquid-phase experiments is considered to consist of an equimolar complex molecule of ethylene and sulfur dioxide. For gas mixtures containing an excess molar concentration of ethylene, the propagating species are ethylene and the complex molecule. Infrared spectra show polysulfone structures. Calorimetric and x-ray diffraction analyses indicate crystalline structures for copolymers in the range 9–50 mole-% sulfur dioxide, although a melt transition temperature could not be observed for copolymer containing >31 mole-% sulfur dioxide. Clear uniform film was obtained with copolymers containing up to 31 mole-% SO₂.

INTRODUCTION

The reaction between olefin and sulfur dioxide to form polysulfone by using free-radical catalysts and Co⁶⁰ γ -radiation has been extensively studied.^{1–6} The unique kinetic behavior of these copolymerization reactions have introduced several new concepts which have not been entirely proven by theoretically derived kinetic equations. With very few exceptions, these studies were conducted in the liquid phase by using olefins which do not readily homopolymerize in the presence of free-radical initiators. The copolymers obtained by these investigators were invariably equimolar.

This paper involves a study of the kinetic behavior of ethylene and sulfur dioxide in the liquid and gas phases with the use of Co⁶⁰ γ -radiation for initiating the reactions. The purpose of this study was to investigate further the olefin-sulfur dioxide system with an olefin which readily homopolymerizes⁷ under the conditions prescribed and to characterize some of the copolymer properties.

EXPERIMENTAL

Materials

Ethylene gas containing 99.8 mole-% C_2H_4 , 0.2 mole-% C_1 - C_4 saturated hydrocarbons, and <20 ppm O_2 was obtained from Phillips Petroleum Co. The ethylene gas was used without further purification. Matheson Co. anhydrous-grade sulfur dioxide containing 99.98% by weight SO_2 and 50 ppm moisture was distilled and dried through a vacuum system prior to use.

Apparatus

Reaction Vessel. The reaction vessel used for this study is illustrated in Figure 1. The vessel is made of 316 stainless steel with an i.d. of 2.54 cm. and an internal volume of 100 cc. Both ends of the vessel can be opened to facilitate removal of polymer. A thermocouple well was ex-

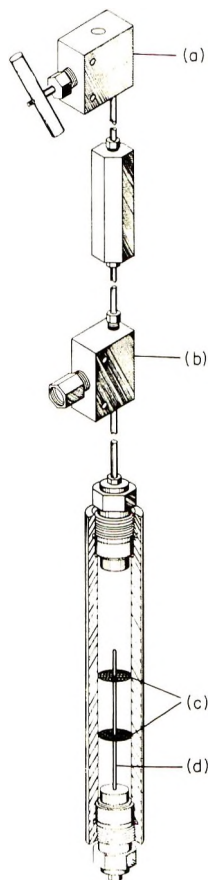


Fig. 1. Schematic of high pressure reaction vessel used for copolymerization reactions in the liquid and gas phases: (a) closure valve; (b) rupture disk assembly; (c) fine mesh screens; (d) thermocouple well.

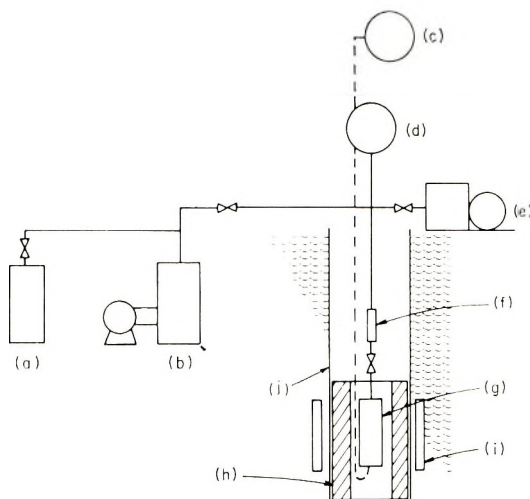


Fig. 2. Schematic of apparatus used for conducting experiments: (a) ethylene supply; (b) compressor; (c) temperature recorder; (d) pressure recorder; (e) vacuum pump; (f) pressure transducer; (g) reaction vessel; (h) oven; (i) ^{60}Co sources; (j) air duct in ^{60}Co water-tank facility.

tended into the center of the vessel through the bottom closure to measure reaction temperatures. The upper closure consists of a rupture disk assembly and valve.

Irradiation Facility. The experiments were conducted in an air duct in a Co^{60} water-tank-type facility shown schematically in Figure 2. Surrounding the reaction vessel inside the air duct was a thermocouple-controlled resistance furnace for controlling the reaction temperature. The vessel was pressurized through a compressor monitored by a pressure transducer located directly above the vessel assembly shown in Figure 1. The reactions were initiated by placing the Co^{60} sources around the air duct. Dosimetry measurements were conducted inside the vessel by using a Fricke dosimeter and secondary standard solar cells.

Procedure

In a two-component system consisting of a gas and a liquid, the composition of the mixture depends on the solubility of the gas in the liquid at various temperatures and pressures. Because of the lack of available data on the solubility of ethylene gas in liquid SO_2 , several experiments were conducted to determine the ethylene concentration in the liquid mixture for a range of conditions used in this work. Data were obtained showing the pressure increase and the ethylene solubility in liquid SO_2 as a function of temperature. A vessel of known volume was initially charged with a measured amount of liquid SO_2 and 340 atm of ethylene gas at 20°C . The temperature in the sealed vessel was then increased to 100°C . in increments of 20°C .; equilibrium pressures were noted at each temperature. The amount of ethylene soluble in SO_2 was calculated from the total initial

mass and from ethylene PVT data obtained under the same conditions of pressure and temperature. Corrections were made for the partial pressure of SO_2 and for the volume expansion of the liquid over the temperature range used.

Liquid-Phase Experiments. A measured amount of distilled SO_2 was condensed into an evacuated reaction vessel to approximately the midpoint between the two fine mesh screens shown in Figure 1. The vessel was then pressurized with ethylene gas at 20°C . through the system shown in Figure 2. This preparatory technique results in a two-phase system, a liquid phase consisting of ethylene dissolved in SO_2 and a gas phase consisting of a mixture of ethylene and SO_2 . The screens shown in Figure 1 serve to separate the polymer formed in each phase. Prior to positioning the Co^{60} sources around the air duct, the charged reaction vessel was heated to the desired temperature. At the termination of the experiment, the Co^{60} sources were removed and the unreacted ethylene and SO_2 were discharged from the vessel. The fraction of polymer that was formed entirely in the liquid phase below the lower screen was recovered. The polymerization rates were calculated based on the known volume below the lower screen.

Gas-Phase Experiments. The gas-phase experiments were prepared by varying mixtures of ethylene and SO_2 . The concentration of SO_2 in the gas mixtures for experiments conducted at 20°C . was limited by the vapor pressure of SO_2 at this temperature. For elevated temperature experiments in the gas phase, the measured amount of SO_2 initially condensed into the reaction vessel at 20°C . was calculated so that the entire mass was in the gas phase at the reaction temperature.

Treatment of Copolymers. The copolymers were heated under vacuum at 40°C . for 48 hr. in order to remove unreacted monomer. To determine if the copolymers were admixed with ethylene homopolymer, the following tests were made. Samples of the powdered copolymers were placed in extraction columns containing Decalin at 130°C . Decalin was used because it is a known solvent for polyethylene. After 4–8 hr., the solutions were examined using precipitation methods, evaporation, and infrared techniques. The copolymers formed in the liquid-phase portion of this work were completely insoluble in Decalin. No trace of ethylene homopolymer could be detected in these samples with the above techniques. The composition of the copolymers calculated from elemental analysis of C, H, S, and O gave a 1:1 structure which also indicates the absence of ethylene homopolymer.

The copolymers formed in the gas phase, having other than equimolar amounts of ethylene and SO_2 , were examined by the same techniques. In this case, however, it was found that the copolymers were partially soluble. The solubility decreased with increasing SO_2 in the copolymer. Elemental analyses of the soluble and insoluble fractions for each sample showed the same composition. Other solvents such as dichlorobenzene and dimethyl sulfoxide gave the same comparative results. In addition to the above tests, the samples were examined with a differential scanning calorimeter.

With careful technique, the presence of admixed polymers could be detected with this instrument by noting the transition temperatures. Based on these exhaustive tests, it was concluded that the material formed in the gas phase was also free of ethylene homopolymer.

In the polymer evaluation section of this paper the transition temperatures were determined with a Perkin-Elmer differential scanning calorimeter (DSC) at a scan speed of 10°C./min. Thermal stability studies were also conducted with the Perkin-Elmer DSC by using the weight-loss method. Infrared spectra were obtained with a Leitz Wetzlar spectrophotometer by using KBr pellets. The x-ray diffraction scans were made by using a North American Phillips diffractometer.

RESULTS AND DISCUSSION

The effect of temperature on the copolymerization rates for experiments conducted in the liquid phase is shown in Figure 3. Prior to irradiation at a prescribed temperature, each vessel was initially charged to a constant mass consisting of 26 g. SO₂ and 340 atm. ethylene gas at 20°C. Table I shows the concentration of ethylene in the mixture and the pressure increase as a function of temperature. Although the data in Table I cover a temperature range of 20–100°C, it is reasonable to assume that the mixtures were rich in SO₂ over the range of temperatures and pressures involved during the course of the reactions in Figure 3. The polymerization rates, were based on the yields of copolymers formed only in the liquid phase under the conditions shown in Figure 3. The kinetic behavior of this reaction appears to be typical of a free-radical polymerization for temperatures of 20–80°C. Above these temperatures, the reaction rate reaches a maximum value and then steadily decreases to a zero rate between 155 and 157°C. This phenomenon was first observed by Snow and Frey,^{1,2} who concluded that for each olefin-SO₂ system there exists a "ceiling temperature" above which little or no polymerization occurs. The ceiling tem-

TABLE I
Solubility Data for Ethylene Gas in Liquid SO₂

Temperature, °C.	Total pressure, atm.	Partial pressure, atm.		Liquid SO ₂ ^c gm/wt %	Ethylene in SO ₂ ^d gm/wt %	Ethylene soluble in SO ₂ gm/wt %
		Ethylene	SO ₂ ^b			
20 ^a	340.0	336.9	3.1	10.99	0.58	5.28
40	432.0	425.9	6.1	10.92	0.71	6.50
60	512.2	501.3	10.9	10.81	0.86	7.95
80	559.3	542.3	17.0	10.62	1.0	9.42
100	689.8	663.3	26.5	10.37	1.18	11.38

^aInitial charge conditions at 20°C. determined gravimetrically.

^bVapor pressure of SO₂ gas from *Matheson Gas Data Book* (1961).

^cLiquid density of SO₂ from *Matheson Gas Data Book* (1961).

^dCalculated from ethylene PVT data obtained under same conditions.

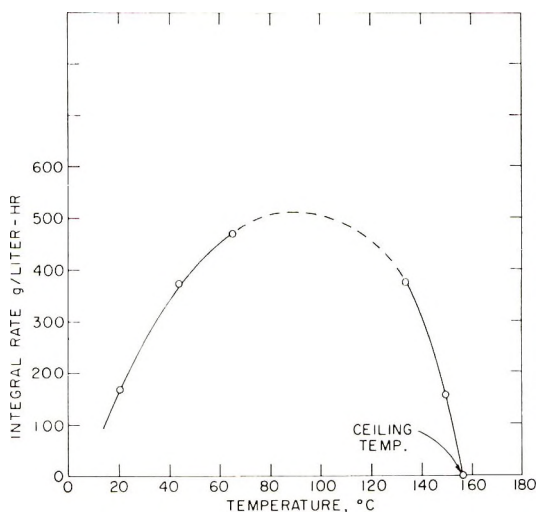


Fig. 3. Effect of temperature on the copolymerization rate of ethylene and sulfur dioxide in the liquid phase. Initial pressure, 340 atm. at 20°C.; radiation intensity, 1.78×10^6 rad/hr.

perature T_c obtained with ethylene under conditions shown in Figure 3 is considerably higher than those reported for other olefin-SO₂ systems.^{2,3} The T_c value observed is in accordance with the work of Cook et al.,³ who demonstrated that the ceiling temperature for olefin polysulfone formation is dependent largely on the structure of the olefin.

Dainton and Ivin⁵ have also shown that within a particular olefin-SO₂ system variations in T_c occur with monomer concentration because of competition of first- and second-order processes.

The primary purpose of this investigation was not to determine T_c values for this system *per se* but to demonstrate the polymerization behavior of an olefin-SO₂ system in the liquid and gas phases with an olefin that is capable of homopolymerizing with the same initiator and under the same conditions of temperature and pressure used to form the polysulfone.⁷ This is in contrast to olefin-SO₂ systems studied by other workers where the olefin does not homopolymerize under the conditions used to form the polysulfone and the reactions were carried out in the liquid phase. The fact that we have obtained a T_c value for the liquid-phase portion of this work substantiates some of the concepts set forth by earlier workers.

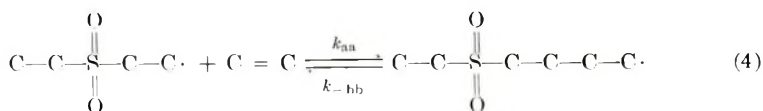
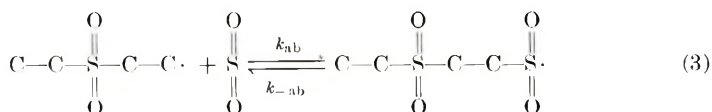
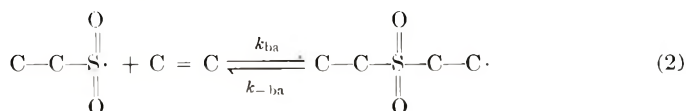
Several explanations for the treatment of the ceiling temperature phenomenon have been suggested;^{2,4} however, the extensive kinetic studies of Dainton and Ivin⁵ have convincingly shown that the observed decline in reaction rate with temperature leading to T_c is due to a depropagation reaction. In considering their scheme relative to the ceiling temperature, several important conditions are upheld: (1) that the copolymer remains equimolar over the temperature range used, and (2) that the decrease in rate or depolymerization is not due to thermal instability of the copolymer.

As mentioned earlier, the copolymers formed in the liquid phase, over the range of temperatures shown in Figure 3, were found to be equimolar. Also, thermal stability studies on an equimolar ethylene-SO₂ copolymer, to be discussed in more detail later, show that the temperature required for the onset of decomposition is much higher than any reaction temperature used during the course of the experiments. This evidence supports Dainton's scheme in that the depolymerization is necessarily a reaction of polymer radicals only. The results obtained in our liquid-phase study can therefore be discussed in accordance with the above concept. Assuming that the propagation and the depropagation reactions are occurring simultaneously, the polymerization rate can be expressed as follows:

$$-d[M]/dt = k_p[P\cdot][M] - k_d[P\cdot] \quad (1)$$

where k_p and k_d are the rate constants for the overall propagation and depropagation reactions, respectively, and $P\cdot$ is a radical chain end. The overall polymerization rate depends on the relative values of k_p and k_d at any given temperature. As the temperature is increased, k_p becomes smaller and the rate decreases to zero when $k_d = k_p[M]$.

Since ethylene is capable of homopolymerizing, it is reasonable to infer that random ethylene to ethylene linkages can occur during the course of the reaction. In spite of other considerations, addition of ethylene to ethylene is most likely to occur in the temperature range where $k_d \cong k_p[M]$. Assuming that propagation and depropagation for this reaction proceeds by successive addition and elimination of ethylene and SO₂ units, a simplified scheme showing the possible chain reactions involved in this system can be represented as shown in eqs. (2)–(4).

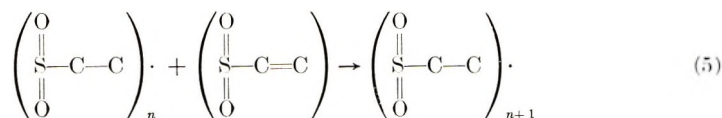


where k_{ab} , k_{ba} , and k_{aa} are the propagating rate constants for addition of SO₂ to ethylene, ethylene to SO₂, and ethylene to ethylene, respectively. The negative values in reactions (2)–(4) represent the corresponding depropagation rate constants. Since sulfur dioxide does not add to itself, a reaction between an SO₂ free-radical chain end and an SO₂ molecule cannot occur. On the basis of the scheme outlined above, the only reactions compatible with the experimental results obtained in the liquid phase are (2) and

(3). It is evident that reaction (4) does not occur, since the copolymers were equimolar.

This unique kinetic behavior has been studied in detail by other workers. Strong evidence of 1:1 olefin-SO₂ complex participation was reported by Dainton and Ivin^{5,8} in their kinetic studies on the 1-butene-SO₂ system. Barb⁹⁻¹¹ also invoked complex participation in his studies on the copolymerization of styrene and SO₂, and postulated that the reacting species are styrene and a 1:1 complex of styrene and SO₂. Walling,¹² however, showed that Barb's data could be derived without involving complex participation by extending the classical copolymer equation to include reversible steps and a penultimate effect.

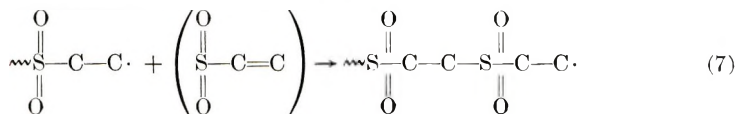
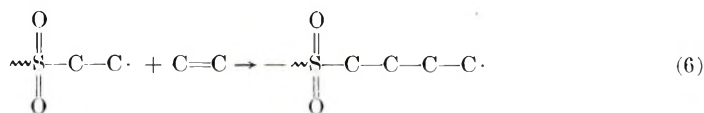
Although the work presented in this paper is insufficient for a detailed kinetic analysis, an evaluation of the data obtained permits us to interpret the results by invoking participation of a 1:1 ethylene-SO₂ complex. With the adoption of this scheme and in accordance with the foregoing discussions, the following general observations can be made in summation of the liquid-phase work: (a) mixtures of ethylene and SO₂ produce equimolar complex molecules; (b) in an ethylene-SO₂ mixture "rich" in SO₂, the ethylene is tied up in complex units, and ethylene-ethylene linkages cannot occur; (c) the reaction therefore proceeds by successive addition of complex molecules resulting in equimolar copolymer as shown in eq. (5):



(d) the decrease in polymerization rate with increasing temperature involves depropagation reactions.

Up to this point we have considered a liquid-phase system whereby the mixture is "rich" in SO₂. Since ethylene-rich mixtures could not be prepared in the liquid phase under conditions used in this work, as shown in Table I, a series of gas-phase experiments was conducted with gas mixtures rich in ethylene. Figure 4 shows the copolymer composition versus the feed composition as mole per cent SO₂ on each axis. The conversions were held to $\approx 2\%$ in order not to appreciably change the initial gas composition.

This series of experiments was conducted at a total pressure of 680 atm. and at 20°C. to minimize any effect due to depropagation reactions. Since the feed composition at 20°C. is limited to the vapor pressure of SO₂, the data are insufficient for obtaining a quantitative determination of copolymer composition over the entire range of feed composition. It is significant, however, to note that under these conditions ethylene polysulfones with SO₂ concentrations up to 32 mole-% can be formed. In being consistent with the concept of a molecular complex, it is suggested that the reacting species are consequently ethylene and equimolar complex molecules of ethylene and sulfur dioxide as shown in eqs. (6) and (7):



The overall polymerization rates for gas-phase reactions over a range of feed compositions are shown in Figure 5. The experiments were conducted at 20°C. and at total pressures of 680 atm. Because of the surprisingly high rates, as compared with the rates obtained with pure ethylene under the same conditions,⁷ the maximum radiation time for each experiment did not exceed 4 min. at an intensity of 178,000 rad/hr. In all cases the copolymers precipitated out of the monomer mixtures. The reactions were, therefore, carried out to low conversions ($\approx 2\%$ by weight) in order to maintain near-homogeneous conditions. No induction periods were observed for these reactions. Each experimental point in Figure 5 represents the overall rate obtained under the conditions described. The data show a progressive increase in rate when the SO₂ concentration in the gas mixture is increased. This phenomenon can be attributed to the relative concentration of monomers. If the rate coefficient for complex addition to ethylene is greater than that for ethylene adding to ethylene, an increase in the concentration of the more reactive species should result in a greater overall rate. Another consideration is the effect of the heterogeneous nature of the system on the rate coefficients. Since the conversions were all carried out to the same low degree, it is unlikely that monomer diffusion had any appreciable effect on the overall rate.

It is commonly known that the copolymerization rate for a free-radical addition-type reaction is dependent on temperature. To a lesser extent

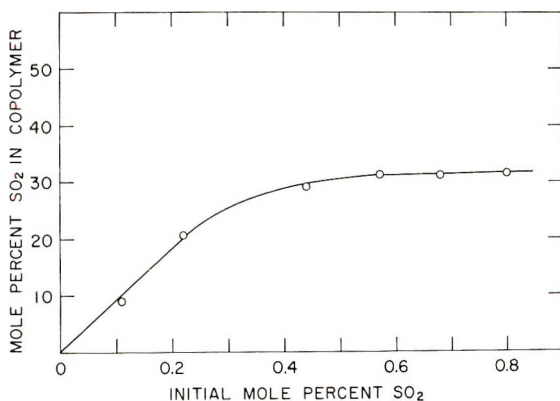


Fig. 4. Copolymerization of ethylene and SO₂ in the gas phase. Effect of SO₂ concentration in initial feed mixture on copolymer composition. Experiments conducted at 20°C., total pressures of 680 atm., and radiation intensity of 1.78×10^5 rad/hr.

TABLE II
Preliminary Data on the Effect of Temperature
on Copolymer Composition and Rate for Gas Phase

Initial mole-% SO ₂ ^a	Reaction temperature, °C.	Copolymer, mole-% SO ₂	Radiation time, min. ^b	Overall rate g./l.-hr.
2.3	71	46.3	6.0	190
2.3	130	46.3	4.0	345
2.3	149	45.8	12.0	110
2.3	161	43.2	120.0	16

^aTotal initial pressure, 340 atm. at 20°C.

^bRadiation intensity, 178,000 rad/hr.

the copolymer composition is also affected by temperature, particularly if the monomer reactivity ratios deviate appreciably from unity. Table II shows experimental data for reactions conducted at temperatures from 71 to 161°C. As indicated in Table II, each vessel was initially charged with the same mass by using a feed mixture containing 2.3 mole-% SO₂.

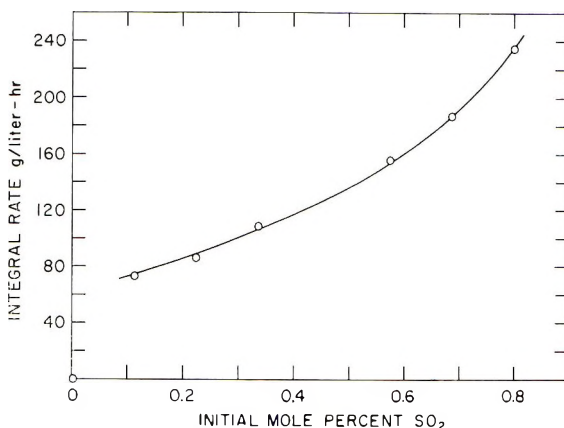
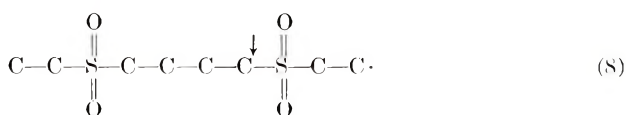


Fig. 5. Copolymerization of ethylene and SO₂ in the gas phase. Effect of initial SO₂ concentration on the polymerization rate. Reaction conditions as in Fig. 4.

Over the range of temperatures given, the entire mass was in the gas phase. The kinetic behavior for this series of gas-phase reactions is similar to that observed for reactions conducted in the liquid phase (Fig. 3). The overall rate increases rapidly with temperature to a maximum and then decreases. It should be noted, however, that the SO₂ concentration in the copolymer decreases with increasing temperature in the range where the rate is also decreasing. These data are consistent with the concept of chain depropagation discussed earlier. Since in this case we have an excess in molar concentration of ethylene in the copolymer composition, as shown in Table II, chain depropagation can occur only until a carbon-carbon bond is reached as shown in eq. (8):



At the stable point in the chain end, indicated by the arrow, the radical can react with an ethylene molecule, a complex molecule, or terminate. As a result, complete depropagation by polymer radical cannot occur and a T_c is not obtained.

POLYMER CHARACTERIZATION

Infrared Spectra

The infrared spectra of copolymers containing (a) 9 and (b) 50 mole-% SO_2 are shown in Figure 6. Both copolymers exhibit strong absorption bands at 7.8 and 9.0 μ because of the asymmetrical and symmetrical SO_2 stretching vibrations. The absorption bands in spectrum (a), with the exception of the sulfone bands, are characteristic of polyethylene. The doublet at 13.7 and 13.9 μ is indicative of four or more carbons in a chain.

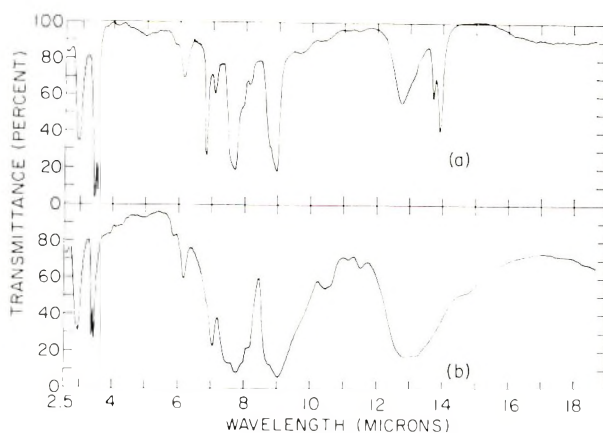


Fig. 6. Infrared spectra of ethylene polysulfones. Copolymer containing (a) 9 mole-% SO_2 and (b) 50 mole-% SO_2 .

In spectrum (b), the relative peak intensities of the doublet at 3.4 μ , due to carbon-hydrogen stretch, are reversed in respect to spectrum (a). The carbon-hydrogen bending vibration band which normally appears at 6.8 μ for most hydrocarbons has shifted to 7.0 μ in spectrum (b). Since spectrum (b) represents an alternating copolymer of ethylene and SO_2 , the doublet at 13.7 and 13.9 μ has disappeared, as expected. The broad absorption at $\approx 13\mu$ has been assigned to carbon-sulfur stretch bands. H_2O bands at 2.9 and 6.1 μ observed in both spectra are due to moisture present in the KBr pellets.

Thermal Stability

Thermal stability measurements were conducted isothermally for copolymer samples containing 9 and 50 mole-% SO_2 . The data obtained over the temperature range 160–350°C. are shown in Figure 7. Each sample was subjected to the indicated temperature for a 1-hr. period. A 50 mole-% SO_2 sample, however, was subjected to a temperature of 160°C. for 4 hr. This sample was formed in the liquid phase under the conditions shown in Figure 3. The fact that the copolymer was thermally stable at this temperature, which is approximately the T_c temperature obtained in Figure 3, shows conclusively that the depropagation that we observed earlier is a reaction of polymer radicals only. The onset of thermal decomposition for the 50% SO_2 samples under the conditions given above was 225°C.

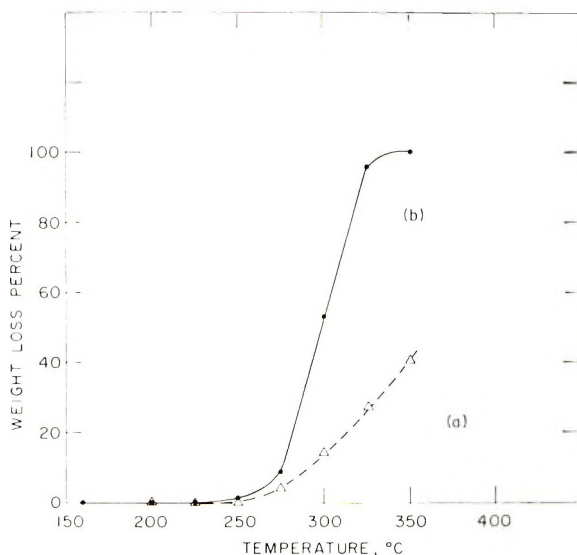


Fig. 7. Thermal stability of ethylene polysulfones. Copolymer containing (a) 9 mole-% SO_2 and (b) 50 mole-% SO_2 .

At temperatures $>275^\circ\text{C}$., decomposition occurred very rapidly. A 100% weight loss was observed at 350°C . No residue was found in the sample container, indicating that the copolymer “unzipped” into its monomer units of ethylene and SO_2 or other volatile components. The pyrolysis products were not analyzed. The activation energies for decomposition for the 9 and 50% SO_2 copolymer samples were calculated to be 31.8 and 43.0 kcal./mole, respectively.

Melting Thermograms

Melt transition temperatures were measured for copolymers containing 9, 20, and 31 mole-% SO_2 . It was surprising to find that over this range

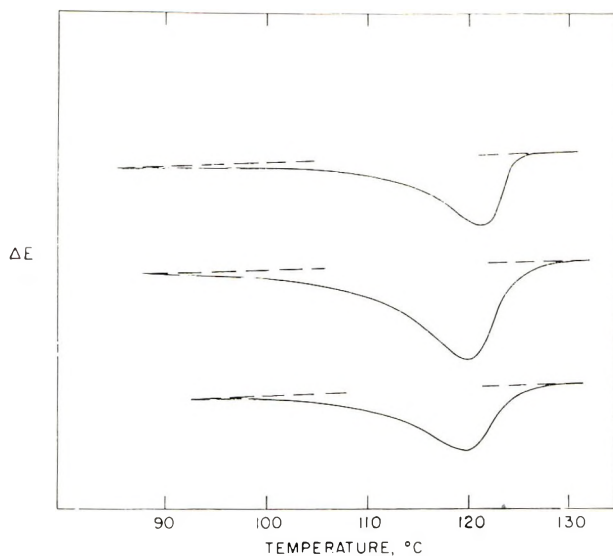


Fig. 8. Melting thermograms of ethylene polysulfones. Lines (a), (b), and (c) run from top to bottom, respectively. Copolymer containing (a) 9 mole-% SO_2 ; (b) 20 mole-% SO_2 ; and (c) 31 mole-% SO_2 .

of copolymer SO_2 concentration the melting points were essentially the same. The melting points for the above copolymers were measured at 126–128°C. and fall in the same range as those obtained for pure polyethylene¹¹ formed under the same conditions of temperature, pressure, and radiation intensity. The possibility of a two-component mixture of polyethylene and ethylene- SO_2 copolymer was excluded, since vigorous fractionation of the samples with preferential solvents for polyethylene did not indicate the presence of homopolymer. The copolymers, in the range of compositions given in Figure 8, produced film that appeared to increase in clarity with increasing SO_2 . Despite the presence of crystallinity, the increase in clarity is probably due to the larger number of smaller crystallites formed. Although the crystal transitions decreased slightly with increasing SO_2 content, the softening points of the copolymers increased. This may be due to the increase in polar groups and possibly to increased stiffness of the chains. The film specimens became less flexible with increasing SO_2 . Melt transitions could not be detected for copolymers containing >44 mole-% SO_2 at temperatures up to the decomposition point.

X-Ray Diffraction

X-ray diffraction traces for ethylene-sulfur dioxide copolymers containing from 9 to 50 mole-% SO_2 are shown in Figure 9. The traces show that crystalline material is formed over the entire range of copolymer compositions up to 50 mole-% SO_2 . Closer inspection of the traces, however, reveals some interesting points. As the SO_2 content increases, the amount of crystallinity apparently decreases. The crystal patterns, particularly

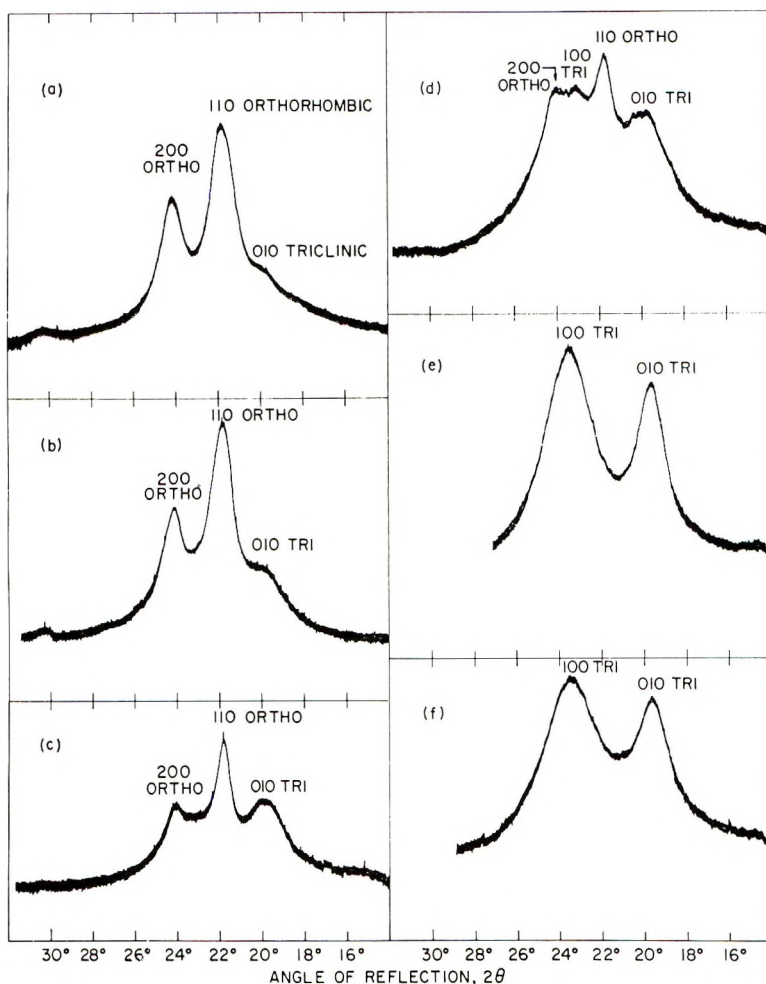


Fig. 9. X-ray diffraction scans of ethylene-SO₂ copolymers: (a) pure polyethylene; (b) 9 mole-% SO₂; (c) 21 mole-% SO₂; (d) 31 mole-% SO₂; (e) 44 mole-% SO₂; (f) 50 mole-% SO₂.

for the lower SO₂ concentrations, closely resemble that for polyethylene. At 9% SO₂, reflections are obtained that are apparently due to both the orthorhombic and triclinic forms of polyethylene. This pattern is very similar to the polyethylene (Fig. 9a) formed by radiation polymerization under the same conditions used to form the polysulfones. The ratio between the triclinic and the orthorhombic forms increases with increasing SO₂ in the copolymer. Between 31 and 44% SO₂ the orthorhombic form can no longer be detected. With increasing SO₂, the x-ray reflections become broader, particularly those for triclinic. This indicates that the crystallite size becomes smaller or the crystallite structure becomes defective or both. The implication is that the material tends to crystallize in

the polyethylene structure but becomes increasingly disrupted by the poorly fitting SO₂ group. Apparently the triclinic can accommodate the SO₂ more easily than the orthorhombic, since this form seems to persist. The disruption due to the SO₂ affects the size, quantity, and perfection of the crystallites as indicated by the line broadening and the increase in amorphous content. With increasing SO₂, the lattice spacings tend to increase in order to accommodate the larger off-size impurity group. Since the copolymers are crystalline even in the range where we failed to observe melt transition temperatures, it appears that there is some lack of sensitivity in the thermal technique used. There is also the possibility that the melt transition temperatures for copolymers containing >31 mole-% SO₂ are higher than the decomposition temperatures.

The authors express their appreciation to D. O. Hummel, University of Cologne, for the infrared spectra, J. Sadofsky and G. Adler, Brookhaven National Laboratory, for the x-ray diffraction work, and L. E. Kukacka, Brookhaven National Laboratory, for carrying out the radiations. This investigation was performed under the auspices of the Division of Isotopes Development, U. S. Atomic Energy Commission.

References

1. R. D. Snow and F. E. Frey, *Ind. Eng. Chem.*, **30**, 176 (1938).
2. R. D. Snow and F. E. Frey, *J. Am. Chem. Soc.*, **65**, 2417 (1943).
3. R. E. Cook, F. S. Dainton, and K. J. Ivin, *J. Polymer Sci.*, **26**, 351 (1957).
4. G. Salomen, *Discussions Faraday Soc.*, **2**, 356 (1947).
5. F. S. Dainton and K. J. Ivin, *Proc. Roy. Soc. (London)*, **212**, 207 (1952).
6. B. G. Bray, J. J. Martin, and L. C. Anderson, *Chem. Eng. Progr.*, **55**, 173 (1959).
7. M. Steinberg, L. E. Kukacka, P. Colombo, and B. Manowitz, *Chem. Eng. Progr.*, in press.
8. F. S. Dainton and K. J. Ivin, *Proc. Roy. Soc. (London)*, **212**, 96 (1952).
9. W. G. Barb, *Proc. Roy. Soc. (London)*, **212**, 66 (1952).
10. W. G. Barb, *Proc. Roy. Soc. (London)*, **212**, 177 (1952).
11. W. G. Barb, *J. Polymer Sci.*, **10**, 49 (1953).
12. C. Walling, *J. Polymer Sci.*, **16**, 315 (1955).
13. P. Colombo, J. Fontana, L. E. Kukacka, and M. Steinberg, *J. Appl. Polymer Sci.*, **9**, 3123 (1965).

Received May 1, 1967

Revised August 22, 1967

Thermogravimetric Analysis of Cellulose

PRONoy K. CHATTERJEE, *Personal Products Company, Division of Johnson & Johnson, Milltown, New Jersey 08850* and CARL M. CONRAD, *Plant Fibers Pioneering Research Laboratory, Southern Utilization Research and Development Division, Agricultural Research Service, U. S. Department of Agriculture, New Orleans, Louisiana*

Synopsis

An application of TGA technique to elucidate the chain reaction mechanism of cellulose pyrolysis is discussed. The mathematical expressions for isothermal kinetics are modified for use with temperature-programmed kinetics. It is shown that in temperature-programmed kinetics, the initial reaction should theoretically be a pseudo zero-order type, whereas the latter part should be a pseudo first-order type. Experimental data from the present study and from the literature are in good agreement with the theory. Energies of activation for the initiation and the propagation steps of cellulose pyrolytic reactions are analyzed from TG data. Various cellulose samples, such as adsorbent cotton, vibratory ball-milled absorbent cotton, mercerized commercial yarn, mercerized and treated commercial yarn, dewaxed-kiered cotton, and microcrystalline cellulose are included in this study. A basic problem which is associated with all thermogravimetric kinetic expressions is also discussed.

INTRODUCTION

The kinetics of pyrolysis of cellulose has been studied extensively during recent years. The need for a better understanding of the kinetics of pyrolysis is not only for development of fundamental knowledge but also for practical utilization in the development of flame-resistant textiles. Although it has been reported in the literature that some salt treatments improve the flame resistance as well as decrease the energy of activation for the decomposition of cellulose,^{1,2} no sound mechanism has yet been proposed. Also, the values of the energy of activation reported in the literature have varied widely, depending upon the technique used and the source of cellulose. In most cases attempts were made to determine the Arrhenius parameters such as reaction order, energy of activation, etc., by empirical approaches. It is difficult to understand the real meaning of the order of reaction applied to the decomposition of long-chain polymer molecules, other than its value as an empirical correlation parameter of the relationship between weight loss and rate of decomposition. An approach to the formulation of kinetic expressions for the fundamental reaction steps of the pyrolysis of cellulose has been published recently.³ In that paper we proposed a chain reaction mechanism in which the major reaction of

cellulose is a two-step process, the initiation step being glucosidic bond scission and the propagation step being levoglucosan formation. The energies of activation for the initiation and propagation steps of the reaction were analyzed. It was also shown in a later communication⁴ that the kinetic data published by Lipska and Parker⁵ are consistent with the chain-reaction mechanism and the initiation and propagation steps could be deduced from the data.

In this paper an application of the TGA technique to elucidate the chain-reaction mechanism is discussed. A comprehensive theoretical treatment has been developed and modified kinetic expressions are presented. Experimental data are analyzed with the aid of the derived equations in order to determine the energy parameters.

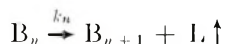
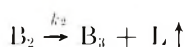
THEORY AND DERIVATION

In view of the proposed mechanism of cellulose pyrolytic decomposition,² the initial reaction would be the breaking of glucosidic bonds and conversion of the linear molecules to lower molecular weight species having either levoglucosan or hydroxyl groups at the end. Once the fragmented molecules are produced, they undergo further decomposition from one end, since they are thermally unstable, and thus levoglucosan molecules are produced. This reaction would continue until the ends of the molecular chains are reached or, due to structure or other factors, a limiting stage is reached which may be the carbonization end point. This latter depolymerization-type reaction could be considered as the propagation step. Thus the mechanism can be represented as:

Initiation:



Propagation:



or



where A denotes initial molecules of cellulose, B_1, \dots, B_n are fragmented molecules, L denotes volatile products, and

$$k_1 = k_2 = \dots = k_n = k_p$$

Therefore, the equation for the initiation reaction is

$$d\sum B_1/dt = k_i A_0 \quad (1)$$

(where B_1 denotes concentration of B_1) and the equation for the propagation reaction is

$$dL/dt = k_p \sum B_n \quad (2)$$

In eqs. (1) and (2), k_i and k_p are constants in isothermal kinetics but are functions of temperature in temperature-programmed kinetics. Assuming the Arrhenius equation for temperature dependence of k , eqs. (1) and (2) can be transformed to eqs. (3) and (4), respectively:

$$d\sum B_1/dt = A_0 Z_i \exp \{-E_i/RT\} \quad (3)$$

and

$$dL/dt = Z_p \exp \{-E_p/RT\} \sum B_n \quad (4)$$

We now assume the following different conditions.

Case I

In case I, only in the early stages of the reaction will all the chains which have been initiated still be reacting according to eq. (3).

Initial Kinetics. Accordingly, at the early stages of the reaction

$$\int_0^{B_n} d\sum B_1 = A_0 Z_i \int_0^t \exp \{-E_i/RT\} dt \quad (5)$$

If the heating rate is a linear function of time,

$$dT/dt = \beta \quad (6)$$

Therefore, eq. (5) can be transformed to eq. (7)

$$\int_0^{B_n} d\sum B_1 = A_0 (Z_i/\beta) \int_{T_0}^T \exp \{-E_i/RT\} dT \quad (7)$$

or,

$$\begin{aligned} \sum B_n &= (A_0 Z_i E_i / R\beta) \left\{ -e^x/x + \int_{-\infty}^x (e^x/x, dx) \right\} \\ &= (A_0 Z_i E_i / R\beta) p(x) \end{aligned} \quad (8)$$

where $x = -E_i/RT$. It is assumed that T_0 is low enough for the lower limit to be negligible. On substituting eq. (8) into eq. (4) there results

$$dL/dt = (A_0 Z_i Z_p E_i / R\beta) p(x) \exp \{-E_p/RT\} \quad (9)$$

If L is expressed in terms of weight, then

$M_L(L) = W_0 - W_r$, where W_0 is initial weight, W_r is weight remaining and M_{M_1} is the molecular weight of L .

Hence,

$$\begin{aligned} M_L(dL/dt) &= -(dW_r/dt) \\ -dW_r/dt &= (M_L A_0 Z_i Z_p E_i / R\beta) p(x) \exp \{-E_p/RT\} \end{aligned} \quad (10)$$

Taking logarithms of both sides yields

$$\log(-dW_r/dt) = (-E_p/2.303RT) + \log p(x) + \log(A_0 Z_i Z_p E_i M_L / R\beta) \quad (11)$$

Now, $p(x)$ can only be solved by approximation. Several series expansions have been reported⁶ and a semiempirical approximation for $p(x)$ was given by Doyle.⁷

For mathematical simplicity, let Doyle's approximation be applied.

$$\log p(x) \cong -2.315 + 0.457x \quad (12)$$

By substituting the $\log p(x)$ value in eq. (11) we get

$$\log(-dW_r/dt) = -(E_p/2.303RT) - 0.457(E_i/RT) - 2.315 + \log(A_0 Z_i Z_p E_i M_L / R\beta) \quad (13)$$

since $x = -E_i/RT$

$$\text{or,} \quad \log(-dW_r/dt) = -(E_p + 1.05 E_i)/2.303R(1/T) + \lambda \quad (14)$$

where λ is a constant.

According to eq. (14), a plot of $\log(-dW_r/dt)$ versus $1/T$ should give a straight line, at least at the early stage, with slope equal to $(E_p + 1.05 E_i)/2.303R$. Thus, E_i can be evaluated from the slope if E_p is determined by the process which will be discussed under propagation kinetics. If a straight line is obtained in the above plot then it may be concluded that the reaction is a pseudo zero-order type,⁸ although order as such has no physical significance.

Propagation Kinetics. As in isothermal kinetics, let us assume that the reaction proceeds according to the above mechanism as long as glucosidic bond scissions are initiated. But gradually all the chains which were initiated will transform to B_n . Thus, B_n and B_{n+1} will appear to be reacting according to eq. (2) where eq. (2) will be independent of eq. (1), and a transition will occur from a two-step reaction to a single-step unzipping reaction (propagation type). Eventually, the active molecules will begin to disappear and $\sum B_n$ will continue to decrease. As this reaction becomes predominant, W_r can be expressed as $M \sum B_n$ by assuming M as the average molecular weight of the active species. The weight remaining W_r can also be expressed as $(L)M_L = W_0 - W_r$, where M_L is the molecular weight of the volatile species L. Therefore, eq. (2) can be transformed as

$$-(1/M_L)(dW_r/dt) = k_p W_r / M \quad (\text{first-order type}) \quad (15)$$

$$-dW_r/dt = (M_L/M)Z_p \exp\{-E_p/RT\} W_r \quad (16)$$

Taking logarithms of eq. (16) yields

$$\{\log(-dW_r/dt) - \log W_r\} = -(E_p/2.303RT) + \log Z_p(M_L/M) \quad (17)$$

By plotting eq. (17) as $[\log(-dW_r/dt) - \log W_r]$ versus $1/T$, the slope E_p can be determined.

Case II

In case II, a stationary state condition is established at an early stage of the reaction, as described for initial kinetics for case I.

$$d\sum B_i/dt = k_i A_0 - k_p \sum B_n = 0 \quad (18)$$

or
$$k_p \sum B_n = k_i A_0$$

Combining eqs. (2) and (18), we get

$$dL/dt = k_p \sum B_n = k_i A_0 \quad (19)$$

Since $(L)M_L = W_0 - W_r$,

$$-dW_r/dt = M_L k_i A_0 = M_L Z_i \exp \{ -E_i/RT \} A_0 \quad (20)$$

or
$$\log (-dW_r/dt) = -(E_i/2.303RT) + \log Z_i A_0 M_L \quad (21)$$

Again, a plot of $\log (-dW_r/dt)$ against $1/T$ will give a straight line as in case I, but in this case the slope will be equal to $E_i/2.303R$. Therefore, it appears that the kinetic treatment will indicate a pseudo zero-order type of reaction whether a stationary state is established or not. Under a non-stationary state the slope will be equal to $(E_p + 1.05E_i)/2.303R$, whereas under a stationary state it will be equal to $E_i/2.303R$. At the present time there is no available technique to confirm a steady-state condition. Of course, a steady-state assumption has been applied frequently in the kinetics of many other chain reactions. In the present case, an increase of temperature will cause an increase in the production of active molecules B_n as well as the rate of the propagation reaction. In the TGA technique, the temperature is continuously increased; therefore, it is not unlikely that when both processes are occurring simultaneously, a stationary concentration of active molecules could be established.

However, the second part of the kinetics remains unaltered and therefore should follow eq. (17).

Case III

Case III presents a more complicated situation in which the initial degradation mechanism is not confined to the initial molecules only but to degraded molecules also. The initiation reaction must now be modified, as

$$d\sum B_n/dt = k_i A_0 + k_i \sum B_n \quad (22)$$

Since this is a rapid reaction, presumably, within a short time $\sum B_n \gg A_0$. Therefore, if the first few per cent of decomposition is neglected, then

$$d\sum B_n/dt = k_i \sum B_n \quad (23)$$

by integration,

$$\log (\sum B_n) = \frac{Z_i E_i}{R\beta} p(x) \quad (24)$$

From eq. (2), and by converting (L) to W_r , we have

$$-dW_r/dt = M_1 k_p \sum B_n = M_1 Z_p \exp \{-E_p/RT\} \sum B_n \quad (25)$$

Combining eqs. (24) and the logarithmic form of (25) yields

$$\log(-dW_r/dt) = -(E_p/2.303RT) + (Z_i E_i/R\beta) p(x) + \log Z_p M_L \quad (26)$$

Again, by applying Doyle's approximation,

$$\log\left(-\frac{dW_r}{dt}\right) = -\frac{1}{T} \left(\frac{E_p}{2.303R} + 2.303 \frac{Z_i E_i T}{R\beta} \exp\{-2.315 - 0.457 x\} \right) + \log Z_p M_L \quad (27)$$

By plotting $\log(-dW_r/dt)$ versus $1/T$ the slope s can be determined for a series of $1/T$ values. (This plot will not give a straight line under the above condition. If it gives a straight line then the conditions I or II is valid and III is not applicable.)

$$\text{Thus, } s = (E_p/2.303R) + 2.303 (Z_i E_i T/R\beta) \exp\{-(2.315 - 0.457 x)\} \quad (28)$$

If E_p is determined by analyzing the latter part of the thermogram [eq. (17)], then $E_p/2.303R$ can be calculated.

$$\text{Hence } \left(s - \frac{E_p}{2.303R}\right) = 2.303 \frac{Z_i E_i T}{R\beta} \exp\{-(2.315 + 0.457 E_i/RT)\} \quad (29)$$

since $x = -E_i/RT$

$$\log\left(s - \frac{E_p}{2.303R}\right) - \log T + 1 = -\frac{E_i}{5RT} + \log \frac{2.303 Z_i E_i}{R\beta} \quad (30)$$

By plotting $\{\log[s - (E_p/2.303R)] - \log T + 1\}$ against $1/T$, the slope E_i can be estimated.

Case IV

In case IV a stationary state condition is established at an early stage of reaction under case III.

$$\frac{d\sum B_n}{dt} = k_i A_0 + k_i \sum B_n - k_p \sum B_n = 0 \quad (31)$$

Therefore,

$$\sum B_n = [k_i/(k_p - k_i)] A_0 \quad (32)$$

From eq. (2) and by changing L to W_r , we have

$$-\frac{dW_r}{dt} = k_p M_1 \sum B_n = \frac{k_i k_p}{k_p - k_i} A_0 M_L \quad (33)$$

$$-\frac{dW_r}{dt} = \frac{Z_i Z_p \exp\{-(E_i + E_p/RT)\}}{Z_p \exp\{-E_p/RT\} - Z_i \exp\{-E_i/RT\}} A_0 M_L \quad (34)$$

This equation can be used to treat the data, but several secondary plots will be required. The error will be highly magnified, and it will be difficult to obtain a good solution of the problem.

From the above discussions, it is obvious that the second part of the pyrolysis (propagation only) can be treated by eq. (17) in all the above cases but no unique equation is derived for the first part of the kinetics. Different equations are obtained depending upon the mechanism of reaction kinetics. If either case I or II is valid, then the derivation ends up with a simple equation, differing only in the expression of the slope from a plot of $\log(-dW_r/dt)$ versus $1/T$. However, E_1 can be easily determined. If a plot of $\log(-dW_r/dt)$ versus $1/T$ does not show a linear relationship, then a more complicated situation, such as case III and IV, can be considered. It is also evident that the kinetic treatment under case IV is very complicated, and the analysis should be pursued only if the data are highly precise.

EXPERIMENTAL

The thermograms were obtained on the Robert L. Stone Co. dynamic thermogravimetric analysis instrument. An Inconel cylindrical crucible, supported on its optical system, was calibrated empty before each pyrolysis experiment by adjusting the potentiometer pen to full scale for whatever weight of sample (0.1 or 0.2 g) was to be used. The samples (Table I)

TABLE I
Characterization and Preparation of Samples

Sample No.	Nature of sample	Type of cellulose	Preparation of sample	Weight of sample, g
1	Cotton yarn (commercial) ^a	Mercerized	20 mesh	0.1
2	Cotton yarn (commercial) ^a	Mercerized	20 mesh	0.2
3	Treated cotton yarn ^b	Mercerized	20 mesh	0.1
4	Treated cotton yarn ^b	Mercerized	20 mesh	0.2
5	Absorbent cotton ^c	Native	20 mesh	0.1
6	Absorbent cotton ^d	Native	Vibration ball-milled	0.1
7	Dewaxed kiered cotton	Native	20 mesh	0.1
8	Microcrystalline cellulose ^e	Native	20 mesh	0.1

^a Commercial mercerized 7/2 yarn.

^b Same as samples 1 and 2, except remercerized and heated 4 hr at 100°C with pyridine.

^c Similar to that used in the previous study.³

^d Sample 5 was vibration ball-milled for 120 min. No crystalline structure could be detected by x-ray diffraction.

^e Sample furnished by American Viscose Corporation.

were ground to pass a 20-mesh sieve and layered approximately midheight of the crucible between portions of the preweighed fired quartz sand (60–140 mesh) sufficient in combination with the sample weight to give one gram total. The dynamic gas was helium, which was passed through the sample at a rate of approximately 165 cc/min.

The temperature of the furnace was raised at the programmed rate of $3^{\circ}\text{C}/\text{min}$ and registered on a potentiometer chart in response to a Pt-Pt, 10% Rh thermocouple located just above the crucible cover. Loss of weight was indicated on the strip chart traveling at 6 in./hr. Only the tar region of pyrolysis was considered and this was usually complete at about 360°C . The chart was ruled in 0.01 part units so that the loss in weight could be read off simply as 1/100 part of the sample weight taken. The computation of the kinetics was carried out by conventional methods.

RESULTS AND DISCUSSION

The analysis of temperature-programmed kinetics is much more complicated than that of isothermal kinetics. In our earlier communications on isothermal kinetics,^{3,4} it was stated that the initial two-step chain reaction mechanism was followed during the final decomposition process by a one-step propagation reaction of the first-order type. The transition region was somewhere between 30 and 45% of total decomposition.

Kinetics of the Propagation Reaction

Assuming that the same mechanism would apply in the temperature programmed kinetics as in the isothermal kinetics, except for the location of the transition region, the complete range of data was treated according to eq. (17) in order to determine E_p . Figures 1 and 2 show the plots

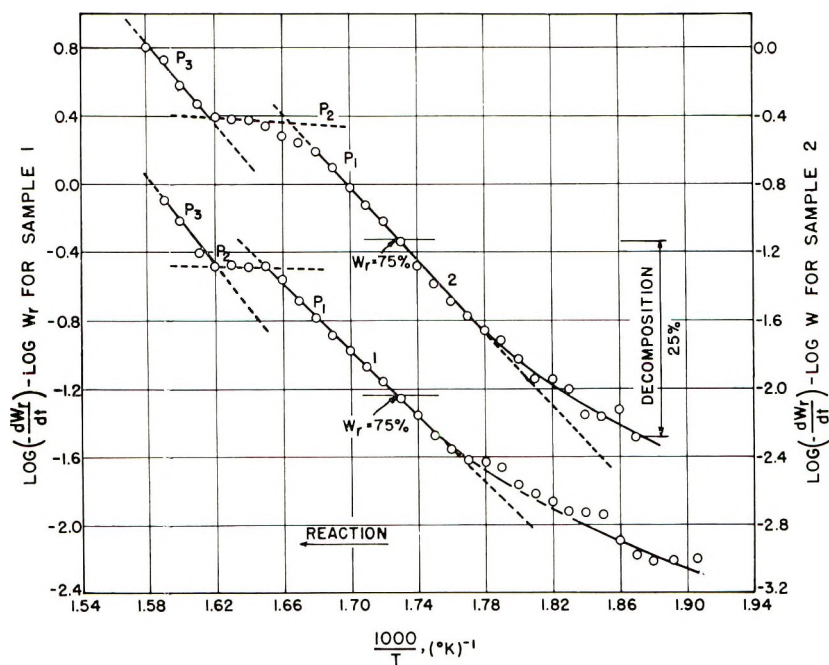


Fig. 1. Application of propagation kinetics to samples 1 and 2 according to eq. (17).

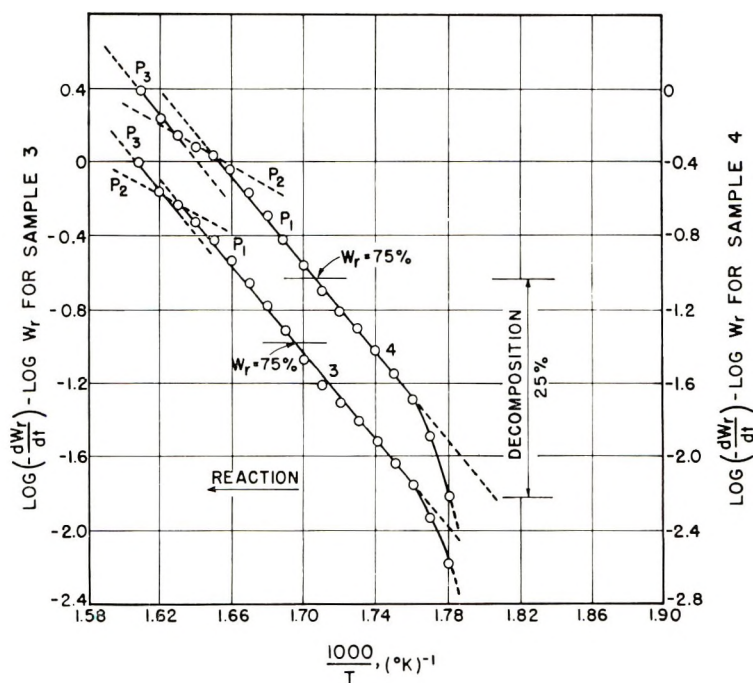


Fig. 2. Application of propagation kinetics to samples 3 and 4 according to eq. (17).

corresponding to two different celluloses, one obtained commercially, the other after heating in a control reaction which did not add any substituent. Plots of two initial weights of each material are presented. Figure 3 shows similar plots of four other cellulose samples (see Table I).

Figures 1 and 2 show that the initial weight of the sample has no significant effect on the shape of the thermogram and also indicate that the characteristic nature of the plot is quite reproducible. It is evident that even if the first 25% of the decomposition is neglected, the data of none of the materials could be accounted for by a single continuous propagation reaction as found in the case of isothermal kinetics.^{3,4}

It is worthy of mention here that aside from any consideration of the suggested mechanism of reaction, determination of the energy of activation on the assumption of first-order kinetics would also lead to exactly the same plot, since eq. (17) represents a general first-order type reaction.⁸ Although Tang and Neill² did not mention anything about the occurrence of a discontinuity in the plot we frequently observed such a discontinuity in a first-order treatment according to the method of Freeman and Carroll⁹ which was adapted by Tang and Neill during their work.

By considering the fact that all these deviations are due to experimental fluctuations, particularly since the plotted figures consist of the derivatives of the primary data, one may attempt to make an approximate fit for a straight line and get an overall crude value of energy of activation. How-

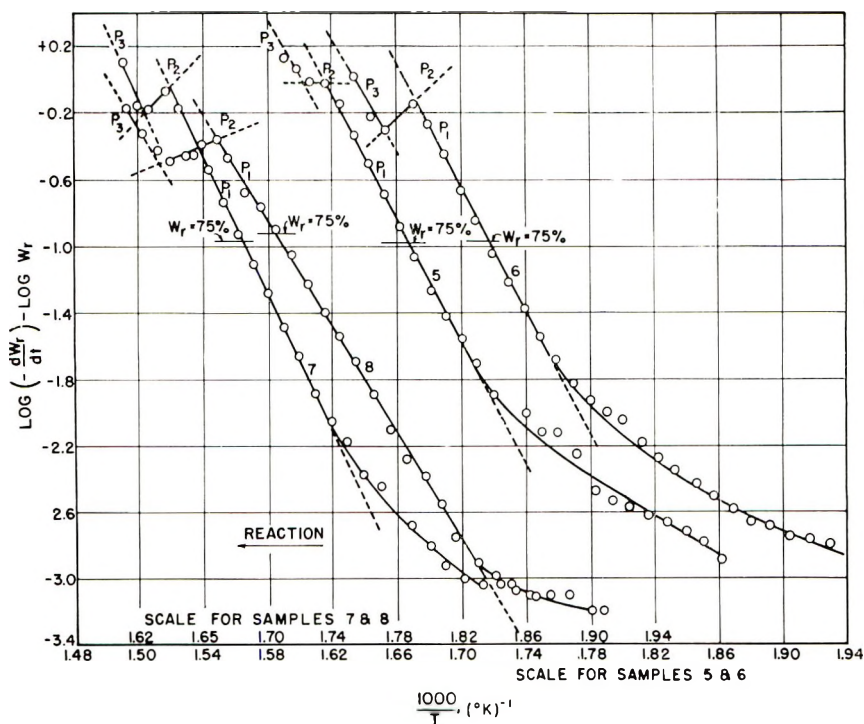


Fig. 3. Application of propagation kinetics to samples 5-8 according to eq. 17.

ever, all the duplicate results in the figures undergo practically identical trends. Therefore, we believe that the curvature or discontinuity represents an actual phenomenon and not just the scattering of the data.

Figure 3 shows the same overall nature of the kinetic plot, including the discontinuity of the propagation reaction as shown in Figures 1 and 2.

Next, an attempt was made to fit the data with straight lines in order to get energies of activation, as would be expected through the occurrence of a series of propagation reactions. In this analysis the initial portion of the decomposition up to a maximum of 25% decomposition was neglected. The straight lines drawn at different segments of the plot were represented by dashed lines. The apparent energies of activation of the reactions, marked P_1 , P_2 , P_3 , etc. in the figures, were determined from the slopes of the straight lines. The values are recorded in Table II.

On considering the propagation reaction only, in the case of the control cellulose (samples 1 and 2) three steps of reactions were observed, P_1 , P_2 , and P_3 . Energies of activation for the corresponding steps are 48, 2, and 54 kcal/mole, respectively. An energy of only 2 kcal/mole is practically a negligible value and may be considered as zero energy of activation. In some cases the energy of activation for step P_2 was found to be less than zero (see Table II). At present, we do not have any sound explanation of this fact. As soon as this abnormal phenomenon is complete, however,

TABLE II
 Ranges of Decomposition and Apparent Energies of Activation
 of the Secondary Decomposition (First-Order Type)

Cotton sample	Approximate range of decomposition, % ^a	Apparent energy of activation, kcal/mole
Commercial yarn (mercerized)	13-79 (P ₁)	48
	79-96 (P ₂)	2
	96-100 (P ₃)	54
Same, treated control	7-91 (P ₁)	54
	91-96 (P ₂)	25
	96-99 (P ₃)	55
Absorbent cotton	10-88 (P ₁)	86
	88-97 (P ₂)	3
	97-100 (P ₃)	82
Absorbent cotton, vibration ball-milled	11-74 (P ₁)	87
	74-95 (P ₂)	<0
	95-99 (P ₃)	80
Dewaxed, kiered	3-91 (P ₁)	95
	91-95 (P ₂)	<0
	95-99 (P ₃)	95
Microcrystalline cellulose	2-74 (P ₁)	74
	74-92 (P ₂)	<0
	92-98 (P ₃)	73

^a Reactions corresponding to indicated range referred to as P₁, P₂, and P₃ in Figures 1, 2, and 3.

the data again show the normal behavior of the unique propagation step. In the treated control cellulose (Fig. 2), reaction P₂ was considered to represent this abnormal behavior, by comparison of the shape of this plot with other plots, although the apparent energy of activation is not quite as low. It is assumed that the latter part of the decomposition consists of a continuous propagation, depolymerization type of reaction, as discussed in the theory. The portion where it undergoes some abnormal weight loss of the sample may be disregarded for the present discussions. The observed energy of activation for the propagation reaction could be assigned as 48-54 kcal/mole for cotton cellulose (mercerized) and 54-55 kcal/mole for the treated control cellulose.

Energies of activation were found to be unusually high in the last four samples. The calculated energies of activation are 82-86 kcal/mole for absorbent cotton, 80-87 kcal/mole for the corresponding ball-milled absorbent cotton, 95 kcal/mole for the dewaxed, kiered cotton, and 73-74 kcal/mole for the microcrystalline cellulose.

The values reported in the literature^{1-5, 10-12} for the latter part of the cellulose pyrolytic reaction (pseudo first-order type) ranged from 33 to 56 kcal/mole.

In a recent publication on DTA and TGA of cellulose pyrolysis, Akita and Kasa,¹³ reported that the energy of activation for α cellulose was 43-52 kcal/mole, and the average energy of activation for the ammonium phos-

phate-treated cellulose was 32 kcal/mole. They did not, however, mention anything about the difference between the initial and the later stages of the kinetics.

Kinetics of the Initiation Reaction

The initial decomposition data were analyzed by the equation:

$$\log (-dW_r/dt) = -(E_{app}/2.303RT) + C \quad (35)$$

where C is a constant. This equation represents both eqs. (14) and (21), and therefore the energy of activation for the initiation reaction could be determined from the value of apparent energy or E_{app} . Figure 4 represents the plot for samples 1-4 (Table I). The initial data of the treated control cellulose (samples 3 and 4) show a good fit to two straight lines and accordingly two energies of activation were obtained. The other samples (1 and 2) show only a single straight line.

The initiation portion of the reactions for the other four samples is plotted in Figure 5. In the case of these samples somewhat lower energies of activation were found at the very beginning of decomposition (initial slope shown in Fig. 5). The energies of activation for all the samples (except 2 and 4 of Table I) are tabulated in Table III. It may be seen from Figures 1-3 that a sharp transition of initial kinetics to a latter type (pseudo first-order type) is not evident. In an extreme case, in sample 3, the decomposition of 4-88% fits with eq. (35) and 7-91% (Table II) also fits with eq. (17). This is somewhat confusing, but not unrealistic. Apparently,

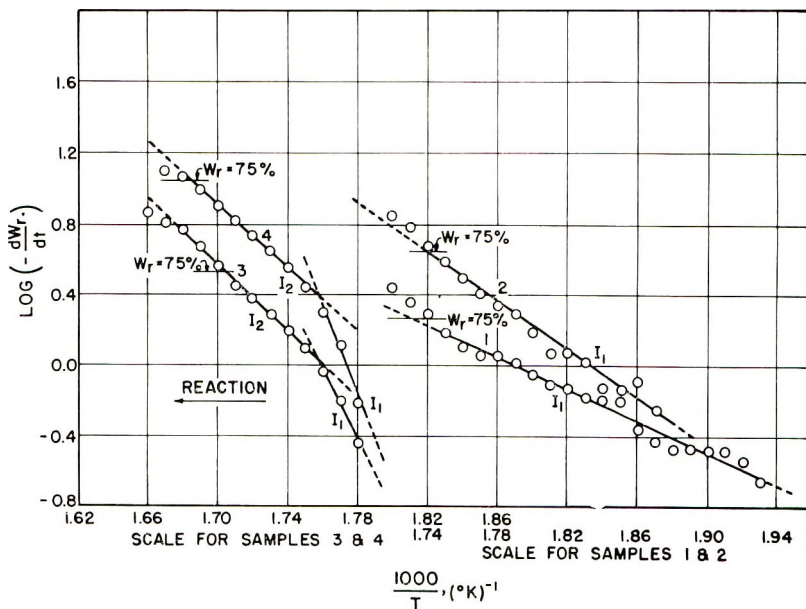


Fig. 4. Application of initiation kinetics to samples 1-4 eqs. (14) and (21).

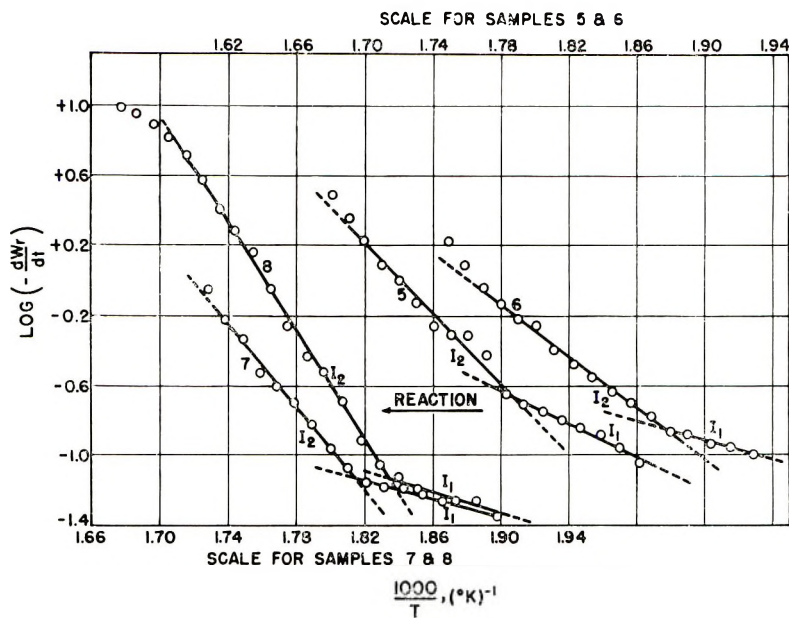


Fig. 5. Application of initiation kinetics to samples 5-8 by eqs. (14) and (21).

the initial kinetics of the pseudo zero-order type as shown by the above equation transforms gradually to the pseudo first-order type. Because of the close proximity of the values of the energy of activation in the two cases the data show very good fit with both equations. In so far as the transition region is concerned, from this analysis no definite assignment could be made. However, the apparent energies of activation for two types of reactions could be obtained by analyzing the data with the aid of the above

TABLE III
Ranges of Decomposition and Apparent Energies of Activation
of the Initial Decomposition (Zero-Order Type)

Cotton sample	Approximate range of decomposition, %	Apparent energy of activation, kcal/mole
Commercial yarn (mercerized)	0-43	34
Same, treated control	0-4	100
	4-88	50
Absorbent cotton	0-2	22
	2-13	45
Absorbent cotton, vibration ball-milled	0-0.3	12
	0.3-14	34
Dewaxed, kiered	0-0.4	10
	0.4-2	51
Microcrystalline	0-0.3	10
	0.3-20	69

two equations, as discussed above. A similar situation could also be observed in the cellulose samples 1 and 2. Therefore, in this analysis no attempt was made to determine the exact region of transformation.

Now it has been realized that more sophisticated assumptions concerning the initial reaction, as discussed in the theory, could not be checked with the present set of data unless the experimental technique is modified and more precise data are obtained. As long as the major portion of the data of the initial part of the decomposition shows straight lines in a plot of $\log(-dW_r/dt)$ versus $1/T$, it is reasonable to assume that the initial decompositions follow the kinetics discussed under case I or II. In the case of the control cellulose (samples 1 and 2) and the treated control cellulose (samples 3 and 4) (ignoring the first 4% decomposition of the latter sample) the apparent energies of activation obtained were 34 and 50 kcal/mole. If a stationary steady state is assumed as described in case II, the apparent activation energies are equal to the energy of activation for the initiation reaction, E_i (i.e., the energy for the glucosidic bond scission). If, however, the stationary steady state is not assumed, the apparent energy of activation would be equal to $E_p + 1.05E_i$, which indicates a negative value for E_i since $E_p > E_{app}$ in the above cases. Therefore, a stationary steady state assumption seems to be more logical.

With the exception of the treated control (samples 3 and 4) relatively low energies of activation were found at the very beginning of decomposition. For the absorbent cotton (sample 5) it was 22 kcal/mole. For the corresponding ball-milled sample (sample 6) it was 12 kcal/mole. For both the dewaxed, kiered (sample 7) and the microcrystalline cellulose (sample 8) it was 10 kcal/mole. This activation energy for the very early stages of reaction might be representing a specific decomposition step, but in all these cases it corresponds to only 2% or less of the sample weight. Therefore, these data have been disregarded in the subsequent discussions.

It is hard to explain the reason for getting an extremely high energy of activation for the initial 4% decomposition of the treated control cellulose (samples 3 and 4). However, the following explanation may be pertinent: During the start of the decomposition the chain reaction initiates, but a time lag occurs for the attainment of the stationary state. During this period eq. (14), derived under case I, would be effective. If the activation energy for the propagation reaction of this sample is 54 kcal/mole (Table II) and that for the initiation reaction is 50 kcal/mole, then it is expected that the apparent energy before the attainment of the stationary state would be $E_p + 1.05E_i$ or 106 kcal/mole. Thus, the calculated value of E_{app} is very close to that obtained experimentally. In the other four samples, presumably, the time lag was practically negligible and therefore this stage of the reaction was not obtained.

In view of the above discussions the energies of activation for the initiation reaction, i.e., the energy of activation for glucosidic bond scission are obtained as 34 kcal/mole for the control cellulose (samples 1 and 2) and 50 kcal/mole for the treated control cellulose (samples 3 and 4). Table IV

summarizes the average values of E_p and E_i as obtained from the present analysis.

We would like to point to an interesting observation that the energy of activation for the initiation reaction seems to have a tendency to increase with the chemical treatment of cellulose. It was found that E_i for the treated control cellulose (samples 3 and 4) is higher than that of the untreated one (samples 1 and 2). Perhaps this suggests that a "treated" cellulose may undergo somewhat selective chain scission. Chemical treatment destroys some of the vulnerable decomposition (or degradation) sites and therefore a further heat treatment leads to a random scission. It is known¹⁴ that the activation energy for a selective degradation is lower than that of a random scission in some polymers.

TABLE IV
Energies of Activation for the Initiation Step (E_i) and the
Propagation Step (E_p) of Cellulose Decomposition

Samples	Energies of activation, kcal/mole	
	Initiation (E_i)	Propagation (E_p)
Control cellulose, mercerized	34	48-54
Treated control cellulose	50	54-55
Absorbent cotton	45	82-86
Absorbent cotton, vibratory ball-milled	34	80-86
Dewaxed, kier boiled cotton	51	95
Microcrystalline cellulose (Avicel PH)	69	73-74

However, a more intensive study will be necessary to reveal the effects of chemical and mechanical treatment on the energy of activation for the chain scission of the native cellulose.

The values of E_p and E_i both, in many instances, are in contradiction with those obtained from our isothermal study, reported earlier. This discrepancy may be partly attributed to the limitations of a few general assumptions. In this context, the following discussions are pertinent:

An important aspect of the thermal decomposition of cellulose or polymers, in general, needs attention which is concerned with the application of the Arrhenius equation. The Arrhenius equation, $k = A \exp \{-E/RT\}$, has been found to be applicable to chemical reactions in solutions and gases. The classical theoretical equations were later developed^{15,16} based on (1) molecular collisions and (2) transition state theory. According to the former theory $k = ZT^{1/2} \exp \{-E/RT\}$, where Z is the frequency factor.

In a polymer decomposition reaction it is unlikely that the decomposition proceeds by a collision mechanism. According to the transition state theory the decomposition of cellulose (or any polymer) molecules can be represented by the following equation.



where $[B^*]$ is the transition state of B, and B_1 and L are the decomposition products. The above equation can be written in the form of the partition function of the molecules as

$$\frac{[B^*]}{[B]} = \frac{F^*}{F_B} \exp \{ -E_0/RT \}$$

where F^* denotes the complete partition function for the transition state and F_B is the complete partition function for the initial ground state.

Since the number of atoms in the molecule in the transition state is equal to that in the ground state, the specific rate constant can be expressed¹⁷ to a first approximation as

$$k = KT/hf_v \exp \{ -E_0/RT \}$$

where k is the specific rate constant, h is Planck's constant, K is Boltzmann's constant, and f_v is the partition function for the vibrational degree of freedom. Since f_v is independent of temperature, the equation can be expressed as $k = ZT \exp \{ -E_0/RT \}$, where Z is a constant.

Unlike in the Arrhenius equation, the first factor is dependent on temperature in the above equation. Presumably, in a thermogravimetric kinetic expression the above equation would be more appropriate. To our knowledge, all the thermogravimetric expressions developed so far are based on the Arrhenius equation. Also, in our present approach the same equation has been applied although the possible limitation of the equation has been realized. The expressions derived in this paper become more complicated and in some cases unsolvable if the above equation is used instead of the Arrhenius equation.

Finally, it will be necessary to resolve the basic differences between isothermal and temperature-programmed studies which lead to different values of energy of activation. It is also important to clarify the course of the abnormal weight loss which resulted in an intermediate low activation energy during the propagation reaction as discussed above.

Appreciation is expressed to P. Harbrink for assistance with the thermogravimetric measurements; to G. Pittman for preparation of the figures; and to the American Viscose Corporation for the microcrystalline cellulose.

Use of a company or product name by the Department does not imply approval or recommendation of the product to the exclusion of others which may also be suitable.

References

1. S. L. Madorsky, V. E. Hart, and S. Straus, *J. Res. Nat. Bur. Stand.*, **56**, 343 (1956).
2. W. K. Tang and W. K. Neill, in *Thermal Analysis of High Polymers (J. Polym. Sci. C, 6)*, B. Ke, Ed., Interscience, New York, 1964, p. 65.
3. P. K. Chatterjee and C. M. Conrad, *Text. Res. J.*, **36**, 487 (1966).
4. P. K. Chatterjee, *J. Appl. Polym. Sci.*, in press.
5. A. E. Lipska and W. J. Parker, *J. Polym. Sci.*, **10**, 1439 (1966).
6. J. H. Flynn and L. A. Wall, *J. Res.*, **70A**, 487 (1966).
7. C. D. Doyle, *J. Appl. Polym. Sci.*, **6**, 639 (1962).
8. P. K. Chatterjee, *J. Polym. Sci. A*, **3**, 4253 (1965).

9. E. S. Freeman and B. Carroll, *J. Phys. Chem.*, **62**, 394 (1958).
10. R. M. Esteve, Jr., H. M. Gollis, and R. Garcia, Progress Reports Nos. 12 and 13, Q. M. Contract No. DA 44-109-QM-1414, University of Rhode Island, Kingston, R. I.
11. E. J. Murphy, *J. Polym. Sci.*, **58**, 649 (1962).
12. C. M. Conrad and P. Harbrink, paper presented at the 154th Meeting of the American Chemical Society, Chicago, Ill., Sept. 10-15, 1967. *Text. Res. J.*, **38**, 366 (1968).
13. K. Akita and M. Kase, *J. Appl. Polym. Sci.*, **5**, 833 (1967).
14. H. H. G. Jellinek and Ming Dean Luh, paper presented to Division of Polymer Chemistry, 153rd American Chemical Society Meeting, Miami Beach, Fla., April 1967.
15. S. Glasstone, K. J. Laidler, and H. E. Eyring, *The Theory of Rate Processes*, McGraw-Hill, New York, 1941, p. 153.
16. K. J. Laidler, *Chemical Kinetics*, McGraw-Hill, New York, 1950, p. 56.
17. F. A. Frost and R. G. Pearson, *Kinetics and Mechanism*, Wiley, New York, 2nd ed., 1963, p. 96.

Received January 10, 1968

Revised March 19, 1968

Preparation and Properties of Poly(phosphonatoalanes)*

DONALD L. SCHMIDT and EDWARD E. FLAGG,
The Dow Chemical Company, Midland, Michigan 48640

Synopsis

Two general types of poly(phosphonatoalanes), $[-Al(X)O-P(O)(R)O-]_n$ ($X = Cl$ or F , $R =$ alkyl or aryl) and $[-Al(OP(O)R_2)O-P(O)(R')O-]_n$, were prepared and studied. Poly[chloro(phosphonato)alanes] are infusible and have low molecular weights ($n = 4-11$). Polyfluoro(phosphonato)alanes are fusible and also have low molecular weights, but under certain conditions grow to higher polymers ($n = 30-45$). Poly[phosphinato(phosphonato)alanes] are fusible and are prepared with high molecular weights ($n = 83-340$).

INTRODUCTION

Poly(phosphonato)alanes[†] have been prepared¹ by the reaction of the diester or acid chloride of methylphosphonic acid, $CH_3PO(OH)_2$, with aryl or alkoxy alanes, $Al(OR)_3$, or by the reaction of methyl or vinyl phosphonic acids with tris(triethylsiloxy)alane. These reactions do not readily go to completion and the resulting polymers are ill-defined and of low molecular weight. These difficulties have been circumvented in our laboratory by reacting etherated alanes (aluminum hydrides) or diethylfluoroalane, $FAl(C_2H_5)_2$, with phosphonic acids at Dry Ice temperatures. These very fast reactions proceed to essentially 100% completion to form new polymers with elimination of hydrogen or alkanes.

The first type of polymer with the empirical formula $[-Al(X)O-P(O)(R)O-]_n$, $X = Cl$ or F , was prepared by reacting phosphonic acids with $ClAlH_2 \cdot 2(THF)_2$ or $FAl(C_2H_5)_2$ in tetrahydrofuran (THF):



where $X = Cl$ or F , $Y = H$ or C_2H_5 , $R =$ alkyl or aryl.

The second type of polymer was prepared by the sequential reaction of phosphonic and phosphinic acids with alane or alkyl alanes.

* Presented in part at the 154th American Chemical Society Meeting, Chicago, Illinois, September 1967.

† The nomenclature is simplified by using the substituted alane (AlH_3) convention, i.e., $[-Al(F)O-P(O)(CH_3)O-]_n$ is poly[fluoro(methylphosphonato)alane]. Aluminum (III) is the only common ion, and the use of the normal convention for bridging groups leads to very complex names.

TABLE I
Properties and Analyses of Polymers of Type $[-Al(X)O-P(O)(R)O-]_n \cdot [m(THF)]_n$

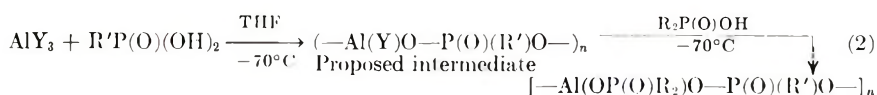
Poly- mer No.	R	X	Moles THF per monomer <i>m</i>	Anal calcd			Anal found			Mp, °C	Mol wt (THF) primary solution ^a	Mol wt (THF) after redissolving	Stability TGA, °C ^b		
				C, %	H, %	Al, %	P, %	C, %	H, %					Al, %	P, %
I	CH ₃	Cl	0.08	9.77	2.26	16.63	19.09	9.30	2.40	16.63	19.15	Inf ^c	—	2100 (<i>n</i> = 7.5)	590
II	C ₁₁ H ₅	F	0.10	11.42	2.60	—	21.04	10.21	2.26	—	20.85	360-400	Insol	—	620
III	C ₆ H ₅	Cl	0.65	38.92	3.87	10.17	11.67	38.90	4.03	9.74	11.50	Inf	—	2300 (<i>n</i> = 8.7)	590
IV	C ₆ H ₅	F	0.60	41.12	4.03	11.00	12.62	40.45	4.07	10.60	12.30	440-500	1160 (<i>n</i> = 4.7)	Insol	695
V	C ₈ H ₁₇	Cl	0.10	38.53	6.85	10.30	11.83	39.05	7.20	10.82	11.75	Inf	—	2900 (<i>n</i> = 11)	410
VI	C ₈ H ₁₇	F	0.35	42.86	7.57	10.24	11.76	42.60	7.76	10.05	12.05	340-360	2660 (<i>n</i> = 11)	4700 (<i>n</i> = 18)	420
VII	C ₈ H ₁₇ C ₁₂ H ₂₅	F	0	40.35	7.19	11.33	13.00	40.47	7.27	11.22	12.92	340-360	—	Insol	420
		F	0.45	50.72	8.85	8.25	9.48	49.90	8.70	8.00	9.50	230-280	2100 (<i>n</i> = 6.5)	5200-6500 ^d (<i>n</i> = 16-20)	380

^a The solvents used for diluting these solutions were obtained by collecting the solvent (on a vacuum line) from a portion of the primary reaction solution.

^b Thermal stabilities were determined by TGA in a nitrogen atmosphere using a heating rate of 10°C/min. The values correspond to the temperature at which the unsolvated polymers began to lose weight.

^c Infusible.

^d Molecular weights of polymers from subsequent reactions were 10,000 (*n* = 31) and 14,500 (*n* = 45).



This paper describes the preparation and properties of the two polymeric systems.

EXPERIMENTAL

All reactions were carried out in a dry nitrogen atmosphere and the tetrahydrofuran (THF) was distilled from sodium-biphenyl complex. Diethylfluoroalane, in heptane, was obtained from Texas Alkyls Inc. Etherated alane and bis(tetrahydrofuran)chloroalane were prepared by previously reported methods.² Gel-permeation chromatograms were obtained with a Waters Associates apparatus with THF as the solvent. Infrared spectra were recorded on Beckman IR 9 and IR 11 instruments. Fluorolube mulls were used for the 3800-1330 cm^{-1} region; Nujol mulls were used below 1330 cm^{-1} . The x-ray powder diffraction patterns were obtained by using $\text{CuK}\alpha$ radiation with a Debye-Scherrer camera having a 7.16 cm radius. Differential thermal analysis (DTA) was carried out by use of a duPont 900 Differential Analyzer. Ebulliometric molecular weights, $\bar{M}_n < 10^4$, were obtained as previously described.² Membrane osmometer measurements, $\bar{M}_n > 10^4$ were obtained in THF by using a Mechrolab Model 501 membrane osmometer, and the values reported were obtained by extrapolation to infinite dilution. Elemental analyses were performed in our laboratories and are reported in Tables I, II, and III. Fluoride ion concentration was determined in a hot water-polymer mixture by titrating with thorium nitrate according to the procedure of Eger and Yarden.³

Preparation and Properties of the Acids

The phosphonic and phosphinic acids were purified by repeated recrystallization. All acids were white solids whose thermal stability, hydrophobicity, and acidity depended on the number and nature of the hydrocarbon substituents. In general,^{4,5} the thermal stability, acidity, and water solubility decreases with increasing alkyl content.

n-Octyl and *n*-dodecylphosphonic acids were prepared by the reaction of alkyl bromides with either a trialkyl phosphite or sodium salt of a dialkyl-phosphite, followed by hydrolysis.^{4,6}

ANAL. Calcd for *n*-octylphosphonic acid, $\text{C}_8\text{H}_{19}\text{PO}_3$: C, 49.47%; H, 9.86%; P, 15.95%. Found: C, 49.39%; H, 9.82%; P, 16.00%; mp 102.5°C (lit.⁶ 99.5-100.5°C). Calcd for *n*-dodecylphosphonic acid, $\text{C}_{12}\text{H}_{27}\text{PO}_3$: C, 57.58%; H, 10.87%; P, 12.37%. Found: C, 57.85%; H, 10.87%; P, 11.91%; mp 100°C (lit.⁶ 100.5-101.5°C).

Methyl⁶ and phenylphosphonic acids⁵ are commercially available from Hooker Chemical and Aldrich Chemical Companies.

TABLE II
Properties and Analyses of Polymers of Type $[-Al(OP(O)R''R''O)-P(O)(R'O)-]_n$

Polymer No.	R''	R'''	R'	Anal. calcd			Anal. found			Mp, °C ^a		
				C, %	H, %	Al, %	P, %	C, %	H, %		Al, %	P, %
VIII	CH ₃	CH ₃	CH ₃	16.83	4.24	12.61	--	16.40	4.13	12.32	--	400-430
IX	C ₆ H ₅	C ₆ H ₅	CH ₃	46.17	3.87	7.98	--	47.47	3.97	7.14	--	430-500
X ^b	C ₆ H ₅ ^c	CH ₃	C ₈ H ₁₇	51.12	7.45	--	13.87	51.00	7.60	--	13.70	350-405
XI ^b	C ₆ H ₁₃	C ₆ H ₁₃	C ₈ H ₁₇	53.10	9.56	--	13.69	52.80	9.66	--	13.45	320-348
XII ^b	C ₁₂ H ₂₅	C ₁₂ H ₂₅	C ₈ H ₁₇	61.91	10.88	--	9.98	61.80	10.81	--	9.78	250-312
XIII	C ₆ H ₅ CH ₂ ^d	C ₄ H ₉	C ₁₂ H ₂₅	56.77	8.52	5.55	12.72	56.90	8.52	5.13	12.70	220-235
XIV	C ₆ H ₅ CH ₂ ^e	C ₇ H ₁₅	C ₁₂ H ₂₅	59.08	8.96	5.10	11.72	59.48	8.84	4.98	11.85	220-230

^a Melting points were obtained by both a melting point block and by DTA.

^b Polymers X, XI, XII form partially soluble gels in THF.

^c Calculated for one THF molecule per monomer unit. The polymer was devolatilized only a short time.

^d The initial molecular weight in THF was 1380 ($n = 2.7$); after four days the molecular weight increased to 166,000 ($n = 340$).

^e The initial molecular weight was 3780 ($n = 11.5$). After devolatilization and redissolving in THF, the molecular weight increased to 27,000 ($n = 83$).

TABLE III
Properties and Analyses of Polymers of Type $[-Al(OP(O)R_2)OP(O)(C_6H_7)O-]_n$

Polymer No.	Phosphinate ligands OP(O)R ₂	Ligand ratio	Anal. calcd			Anal. found			MP, °C	Properties
			C, %	H, %	Al, %	C, %	H, %	Al, %		
XV	OP(O)(C ₆ H ₁₃) ₂ and OP(O)(CH ₃)(C ₆ H ₅)	1:1	50.84	8.29	--	50.50	8.10	8.10	340-360	Insol (THF), hard
XVI	OP(O)(C ₆ H ₁₃) ₂ and OP(O)(C ₁₂ H ₂₅) ₂	2:1	56.60	10.23	--	56.30	10.21	10.21	280-310	semibrittle Semisol (THF), semisoft, semiflexible

ANAL. Calcd equiv wt for methylphosphonic acid, CH_3PO_3 : 96.0, 48.0. Found: 96.0, NDE;* mp 106°C (lit.⁶ $104\text{--}105^\circ\text{C}$). Calcd equiv wt for phenylphosphonic acid $\text{C}_6\text{H}_5\text{PO}_3$: 158.1, 79.1. Found: 159, NDE; mp 163.5° (lit.⁶ $161\text{--}162^\circ\text{C}$).

Dimethylphosphinic acid was prepared by the peroxide oxidation of tetramethyl diphosphine disulfide, the main product from the reaction of methyl magnesium bromide and thiophosphoryl chloride.⁷

ANAL. Calcd for $\text{C}_2\text{H}_7\text{PO}_2$: C, 25.82%; H, 7.58%; P, 33.29%. Found: C, 25.53%; H, 7.36%; P, 33.08%; mp 88.5°C (lit.⁷ $88.5\text{--}90.5^\circ\text{C}$).

Symmetrical phosphinic acids, di-*n*-hexyl and di-*n*-dodecyl, were prepared by treating the appropriate Grignard reagent with di-*n*-butyl phosphite and oxidizing the intermediate di-*n*-alkyl phosphine oxide.⁸

ANAL. Calcd for di-*n*-hexylphosphinic acid, $\text{C}_{12}\text{H}_{27}\text{PO}_2$: C, 61.5%; H, 11.6%; P, 13.2%. Found: C, 61.6%; H, 11.3%; P, 13.4%; mp $78.5\text{--}79.5^\circ\text{C}$ (lit.⁸ $78\text{--}79^\circ\text{C}$). Calcd for di-*n*-dodecylphosphinic acid, $\text{C}_{24}\text{H}_{51}\text{PO}_2$: C, 71.59%; H, 12.77%; P, 7.69%. Found: C, 71.80%; H, 12.97%; P, 7.78%; mp $94.4\text{--}94.8^\circ$ (lit.⁸ $93.8\text{--}94.4^\circ\text{C}$).

Unsymmetrical phosphinic acids, $\text{C}_6\text{H}_5\text{CH}_2(\text{C}_4\text{H}_9)\text{PO}(\text{OH})$ and $\text{C}_6\text{H}_5\text{CH}_2(\text{C}_7\text{H}_{15})\text{PO}(\text{OH})$,[†] resulted from the treatment of dialkyl alkyl phosphonites with benzyl chloride and subsequently hydrolyzing the phosphinate esters.⁹

ANAL. Calcd. for benzyl(*n*-butyl)phosphinic acid, $\text{C}_{11}\text{H}_{17}\text{PO}_2$: C, 62.25%; H, 8.07%; P, 14.59%. Found: C, 62.34%; H, 8.14%; P, 14.64%; mp 98°C (lit.⁹ $97\text{--}98^\circ\text{C}$). Calcd for benzyl(*n*-heptyl)-phosphinic acid, $\text{C}_{14}\text{H}_{23}\text{PO}_2$: C, 65.95%; H, 9.10%; P, 12.25%. Found: C, 66.12%; H, 9.12%; P, 12.18%; mp 92.9°C .

Methylphenylphosphinic acid¹⁰ was graciously sent to us by Dr. B. P. Block through the intercession of the Office of Naval Research. Diphenylphosphinic acid¹⁰ is commercially available from Aldrich Chemical Company.

ANAL. Calcd equiv wt for methylphenylphosphinic acid, $\text{C}_7\text{H}_9\text{PO}_2$: 156.1. Found: 156; mp 135°C (lit.¹⁰ $134.5\text{--}135.5^\circ\text{C}$). Calcd equiv wt for diphenylphosphinic acid, $\text{C}_{12}\text{H}_{11}\text{PO}_2$: 218.2. Found: 215; mp 192.5°C (lit.⁵ 191°C).

Preparation of $[\text{—Al}(\text{Cl})\text{O—P}(\text{O})(\text{R})\text{O—}]_n$

The preparation of poly[chloro(phosphonato)alanes] requires the reaction of $\text{AlH}_2\text{Cl}\cdot 2(\text{THF})$ and $\text{RP}(\text{O})(\text{OH})_2$ in a 1:1 mole ratio. For a typical example, $[\text{—Al}(\text{Cl})\text{O—P}(\text{O})(\text{C}_8\text{H}_{17})\text{O—}]_n$ was prepared by slowly adding 0.003 mole of $\text{AlH}_2\text{Cl}\cdot 2(\text{THF})$ to a stirred solution of 0.003 mole *n*-octylphosphonic acid in 1500 ml THF at Dry Ice temperature. After addition, the solution was allowed to warm to room temperature; the solvent was removed under reduced pressure and the product dried under high vacuum for 24 hr. Quantitative yields were obtained.

* No definite end-point detected.

† This acid was prepared by R. E. Ridenour of our laboratory; no reference was found in the literature.

Preparation of $[-\text{Al}(\text{F})\text{O}-\text{P}(\text{O})(\text{R})\text{O}-]_n$

Method A. Preparation of poly[fluoro(phosphonato)alanes] requires the reaction of $\text{FAl}(\text{C}_2\text{H}_5)_2$ and $\text{RP}(\text{O})(\text{OH})_2$ in a 1:1 mole ratio. For a typical example, $[\text{Al}(\text{F})\text{O}-\text{P}(\text{O})(\text{C}_8\text{H}_{17})\text{O}-]_n$ was prepared by slowly adding 0.003 mole of $\text{FAl}(\text{C}_2\text{H}_5)_2$ (heptane solution) in 500 ml THF to a stirred solution of 0.003 mole of $\text{C}_8\text{H}_{17}\text{P}(\text{O})(\text{OH})_2$ in 1500 ml THF at Dry Ice temperature. After addition, the solution was allowed to warm to room temperature; the solvent was removed under reduced pressure and the product dried under high vacuum for six hrs. A quantitative yield was obtained having 0.35 THF molecule per monomer unit. A portion of this material retained 0.10 THF molecule per monomer unit after remaining on the vacuum line three days. A nonsolvated product was obtained after heating at 200°C for an additional 3 hr under vacuum. Infrared analysis of the volatile material indicated the presence of only THF.

Method B. This method requires the reaction of equal molar amounts of phosphonic acid and etherated alane $[\text{AlH}_3 \cdot 0.33(\text{C}_2\text{H}_5)_2\text{O}]$ followed by addition of hydrogen fluoride. For a typical example, 0.005 mole of phenylphosphonic acid in 500 ml THF was slowly added to a stirred solution of 0.005 mole of etherated alane in 2000 ml of THF at Dry Ice temperature. After the addition was completed, 0.005 mole of hydrogen fluoride was added. The product was isolated in the same manner as in procedure A.

Preparation of $[\text{Al}(\text{OP}(\text{O})\text{R}_2)\text{O}-\text{P}(\text{O})(\text{R}')\text{O}-]_n$

The preparation of poly[phosphinato(phosphonato)alanes] requires the sequential reaction of equal molar amounts of phosphonic acid, etherated alane, and phosphinic acid. For a typical reaction, 0.002 mole of *n*-octylphosphonic acid in 400 ml THF was slowly added to a stirred solution of 0.002 mole of etherated alane in 1000 ml of THF at Dry Ice temperature. After the initial addition was completed, 0.002 mole of di-*n*-hexylphosphinic acid was added. The reaction was allowed to warm from Dry Ice temperature to ambient temperature. The reaction mixture was refluxed for 3 hrs, and the solvent was removed under reduced pressure. The product was dried under high vacuum for 24 hrs, and quantitative yields were obtained.

DISCUSSION

The reaction of alanes or substituted alanes with Brönsted acids to yield bis(tetrahydrofuran)haloalanes and bis(tetrahydrofuran)fluorohaloalanes has been studied.^{2,11} This concept has now been extended to the preparation of poly[halo(phosphonato)alanes]. The reaction of alanes with phosphonic acids proceeds smoothly when carried out at low temperature (-70°C); at higher temperatures (-30°C) well defined products are seldom obtained. The fluoro(phosphonato)alanes were also prepared by the reaction of a 1:1 mole ratio of acid and etherated alane followed by

anhydrous HF; however, the use of diethylfluoroalane is the most convenient procedure.

The polymeric poly[halo(phosphonato)alanes] (Table I) retain small amounts of THF, depending on the length of time the samples were kept on the vacuum line. Heating the polymers at 200°C under vacuum completely removes the THF. With the exception of fluoro(methylphosphonato)alane, (II, Table I), the polymers are soluble when a critical amount of THF is retained. For example, poly[fluoro(*n*-octylphosphonato)alane] is soluble in THF when solvated with at least 0.35 mole of THF per monomer unit but becomes insoluble when 0.1 mole of solvent remained. In general, the solubility increases, and the melting point decreases as the size of the substituted alkyl group attached to the phosphorus atom increases. The chloro materials are less fusible, more soluble,

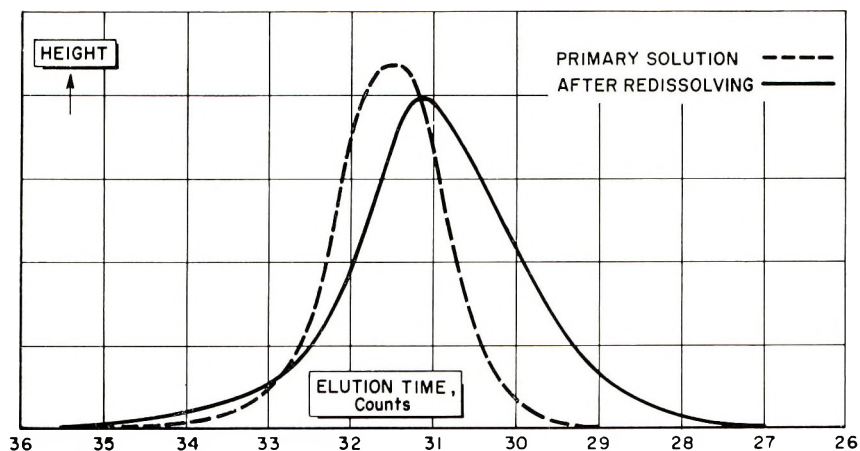


Fig. 1. Gel-permeation chromatographs of poly[fluoro(*n*-dodecylphosphonato)alane] (VII).

and hydrolytically less stable than the corresponding fluoro-substituted polymers because of the Al—Cl bond. A solution of the chloro-*n*-octyl derivative, (V), produced a gel when exposed to the atmosphere, presumably by crosslinking through the reaction of Al—Cl bonds with water.

The fluoro(phosphonato)alanes showed unusual resistance to water. After polymers VI and VII were heated at 100°C for 63 hr in water, only 0.8 and 0.4% of the fluoride was detected in the homogeneous solution. No change in physical appearance of the polymers was observed during this test.

Molecular weights of polymers VI and VII (Table I) were determined in the primary reaction solution. The materials obtained by careful solvent removal were then redissolved in THF and molecular weights remeasured. An increase in degree of polymerization (DP) took place after redissolution. This difference is clearly evident in the gel-permeation chromatographs (Fig. 1) of poly[fluoro(*n*-dodecylphosphonato)alane] (VII). An increase

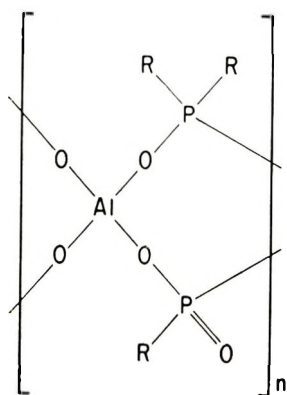
in molecular weight was not observed for the poly[chloro(phosphonato)alanes] (I, III, and V).

Poly[phosphinato(phosphonato)alanes] (Tables II and III) can easily be desolvated under vacuum at room temperature. The polymers with small R groups are insoluble in THF, but if the size of the attached R groups is increased or if unsymmetrical phosphinic acids are used, the solubilities increase. The "soluble" polymers tend to become insoluble upon standing in solution at ambient temperature. The molecular weight of mixed phosphinato polymer XIII was 1350 immediately after preparation. After four days, the molecular weight increased to 16.6×10^4 ; upon further standing, precipitation occurred. The solution of polymer XIV had a molecular weight of 3780 before devolatilization; after carefully removing the solvent under vacuum, 80% of the polymer could be redissolved and the soluble portion had a molecular weight of 27×10^3 . This polymer fraction had an identical elemental analysis as the original, and more insoluble material was isolated when the above procedure was repeated. In general, increasing the size of R groups decreases the melting point and increases the flexibility of the polymer. Using two phosphinic acids (Table III) markedly increases the flexibility of the resulting material. Phosphinato(phosphonato)alanes are hydrolytically stable at elevated temperatures and are quite resistant to both aqueous acids and bases. Thus, a thin film of polymer XV (Table II) showed no visual signs of hydrolysis when heated under pressure in water at 150°C for 22 hr; no weight loss or gain was detected, and the elemental analysis was identical before and after the water treatment.

With the exception of I and II (Table I), which are amorphous, the chloro- and fluoro(phosphonato)alanes typically give x-ray diffraction patterns with several broad bands. The phosphinato(phosphonato)alanes (Tables II and III) are much more crystalline; the x-ray diffraction pattern of VIII gave 27 sharp lines after annealing. As the size of the R group increases, the number of lines decreases.

Chloro(phosphonato)alanes have low molecular weights in solution but the desolvated solids are insoluble and infusible. They are probably highly crosslinked because the higher coordinate states of aluminum can be satisfied by interchain bonding in the solid state. The desolvated fluoro(phosphonato)alanes are fusible which suggests they are less crosslinked. Since the Al—F—Al bridge has been demonstrated to be reasonably strong (F bridging much stronger than Cl),¹¹ it is possible that the coordinate states of aluminum in these polymers are satisfied by intrachain fluorine-bridged bonding. Phosphinato(phosphonato)alanes (Table II and III) are fusible and in some cases soluble, which is consistent with a linear rather than crosslinked polymer. The phosphinate P=O moiety probably forms a coordinate intrachain double-bridged eight-membered ring structure (I) similar to structures proposed for polymeric metal phosphinates.¹²⁻¹⁴ It should be noted that the >P=O group of phosphonates can also form coordinate or ionic bonds, especially in the solid state.

The polymerization reaction resulting from the addition of phosphinic



I

acid to alanes apparently does not follow a simple condensation or addition mechanism. Initially phosphonatoalanes have low molecular weights ($n = 3-11$) which are consistent with cyclics or short chains. Poly[chloro(phosphonato)alanes] do not increase in molecular weight, but poly[fluoro(phosphonato)alane] polymers grow when the solvent is carefully removed. Poly[phosphinato(phosphonato)alanes] continue to grow in THF solutions. This increase in molecular weight may be associated with chain branching as well as linear chain growth. The relative growth of the different polymers depends upon the ability of the substituents on aluminum to compete with the solvent for coordination sites. Kinetic and mass action effects favor the formation of solvent-aluminum bonds, but, thermodynamically, the Al—O—P—O and Al—F—Al bonds are stronger. Simple entropy considerations suggest that the phosphinate moieties should be more effective in bridging than the fluoro moiety; the polymerization of phosphinato(phosphonato)alanes in solution supports this conclusion. A reduction in solvent concentration should favor the formation of both types of bridges.

Infrared spectra of the polymers have been obtained. Chloro- and fluoro(phosphonato)alanes generally give one broad band in the $1100-1150\text{ cm}^{-1}$ region resulting primarily from P—O stretching vibrations. The phosphinato(phosphonato)alanes have strong P—O antisymmetric and symmetric bands in the regions of $1140-1160\text{ cm}^{-1}$ and $1080-1090\text{ cm}^{-1}$. Comparisons of the infrared data of both types of polymers with infrared and Raman data for $\text{CH}_3\text{P}(\text{O})(\text{ONa})_2$ ¹⁵ and $(\text{CH}_3)_2\text{P}(\text{O})\text{ONa}$ ¹⁶ suggest that the P—O bonds are equivalent. Discussion of the spectral data for these polymers, as well as other related Al—O—P and Sn—O—P polymers, will be published¹⁷ in a separate communication in order to present systematically the case for equivalent P—O bonds. In addition to infrared spectral studies, other work is now in progress to elucidate the structure of the above mentioned polymers.

The comparative thermal stabilities measured by thermal gravimetric analysis (TGA) indicate that methyl and phenyl groups attached to phosphorus are more stable than higher alkyl groups. The chloro and fluoro(phosphonato) alanes are more stable than the phosphinato(phosphonato)-

alanes which usually decompose between 350 and 500°C. Fluoro(methylphosphonato)alane, II, is stable to 620°C, while dimethylphosphinato(methylphosphonato)alane, VIII, begins to decompose near 500°C.

SUMMARY AND CONCLUSIONS

Tractable poly(phosphonatoalanes) have been prepared that have moderately high molecular weights. The fast, facile reaction of alanes and Brønsted acids insure the formation of Al—O—P bonds, although the presence of rings or short chains is suggested by the initial low molecular weights. Polymer growth can take place in solution as exemplified by the increase in DP of the poly[phosphinato(phosphonato)alanes]. This probably involves displacement reactions of phosphinato-, phosphonato-, and solvent ligands at the coordinate sites of the aluminum ions. The growth of the polymers in solution probably reflects the relative bridging strength [$-\text{OPR}_2(\text{O})>-\text{F}>-\text{Cl}$] of the pendant moieties. The physical and chemical properties of the solids can be explained by the participation of $-\text{Cl}$, $-\text{F}$, and all phosphoryl ($>\text{P}=\text{O}$) groups in coordinate or ionic bonding. Multiple bonding of this type is enhanced by the removal of coordinated solvent molecules. These data support the conclusion that polymerization is dependent upon the solvent concentration, the degree of solvation, temperature, and reaction time.

This work was supported in part by the Office of Naval Research. We are indebted to Mr. R. B. Nunemaker and associates for analyses and Mr. L. E. Swim, Mr. E. T. Wagoner, and C. D. Chow for molecular weight, TGA, and gel-permeation chromatograph studies. We are also indebted to Dr. T. Alfrey for his valuable discussions and suggestions.

References

1. A. A. Zhdanov, K. A. Andrianov, A. A. Kasokova, and T. S. Baksheyeva, *Polym. Sci. USSR*, **6**, 1038 (1964).
2. D. L. Schmidt and E. E. Flagg, *Inorg. Chem.*, **6**, 1262 (1967).
3. C. Eger and A. Yarden, *Anal. Chem.*, **28**, 512 (1956).
4. P. C. Crofts and G. M. Kosolapoff, *J. Amer. Chem. Soc.*, **75**, 3379 (1953).
5. G. M. Kosolapoff, *Organophosphorus Compounds*, Wiley, New York, 1950, pp. 143-171.
6. G. M. Kosolapoff, *J. Amer. Chem. Soc.*, **67**, 1180 (1945).
7. H. Rienhardt, D. Bianchi, and D. Mölle, *Chem. Ber.*, **90**, 1656 (1957).
8. R. H. Williams and L. A. Hamilton, *J. Amer. Chem. Soc.*, **77**, 3411 (1966).
9. M. Sander, *Chem. Ber.*, **93**, 1220 (1960).
10. A. J. Saraceno and B. P. Block, *Inorg. Chem.*, **3**, 1699 (1964).
11. E. E. Flagg and D. L. Schmidt, paper presented at the 156th American Chemical Society Meeting (Abstracts), Atlantic City, September 1968.
12. S. H. Rose and B. P. Block, *J. Polym. Sci. A-1*, **4**, 573 (1966).
13. S. H. Rose and B. P. Block, *J. Polym. Sci. A-1*, **4**, 583 (1966).
14. S. H. Rose and B. P. Block, *J. Amer. Chem. Soc.*, **87**, 2076 (1966).
15. R. A. Nyquist, *J. Mol. Structure*, in press.
16. R. A. Nyquist, *J. Mol. Structure*, in press.
17. R. A. Nyquist, D. L. Schmidt, E. E. Flagg, and R. E. Ridenour, to be published.

Received March 18, 1968

Revised May 2, 1968

Polymerization of Acrylamide and Methacrylamide Photoinitiated by Azidopentamminecobalt(III) Chloride

L. V. NATARAJAN and M. SANTAPPA, *Department of Physical
Chemistry, University of Madras, Madras, India*

Synopsis

The kinetics of polymerization of acrylamide and methacrylamide, photoinitiated by azidopentamminecobalt(III) chloride in homogeneous aqueous acid medium was studied systematically. Monochromatic wavelengths 365, 405, and 435 m μ were employed for irradiation. Polymerization proceeded without any induction period, and the reaction was followed by measurements of rate of monomer disappearance (bromometrically), rate of complex disappearance (spectrophotometrically), and the chain lengths of the polymer formed (viscometrically). The dependences of the rate of polymerization on variables like light intensity, light absorption fraction by the complex, wavelength, monomer concentration, hydrogen ion concentration, nature of the acid used (HClO₄, HNO₃, and H₂SO₄), etc., were studied. The rate of polymerization of acrylamide depended on the unit power of monomer concentration and on the square root of light absorption fraction k_t and light intensity I . The rate of methacrylamide polymerization was proportional to the unit power of monomer concentration and fractional powers of 0.25 and 0.30 of k_t and I , respectively. A kinetic reaction scheme is proposed and discussed in the light of the experimental results, and it has been concluded that (1) the primary photochemical act is an electron transfer reaction from the azide ion to Co(III) in the complex, (2) initiation of polymerization is by azide radical, (3) termination is by mutual destruction of polymer radicals.

INTRODUCTION

Only a few quantitative studies¹⁻⁴ have been reported on the photobehavior of the cobalt(III) ammine complexes. Absorption of light by the complexes led to transfer of an electron from the ligand to the central cobalt(III) followed by the decomposition of the complex yielding ligand radicals. Cobaltous ion formation from a number of cobalt(III) complexes was shown by Adamson,¹ Linhard,² Endicott and Hoffman,³ and Klein and Moeller.⁴ Significant concentration of radicals produced during photolysis of pentamminecobalt(III) complexes implied the possibility of photoinitiation of vinyl polymerization. The photoinitiating capacity of the azidopentamminecobalt(III) chloride was first reported by the present authors.⁵ Recently Delzenne⁶ also observed photoinitiation of acrylamide polymerization by some pentamminecobalt(III) complexes. Free radicals formed during the irradiation of the complexes with light of $\lambda < 400$ m μ

corresponding to the charge transfer band of the complexes initiated polymerization. In this paper we report a detailed and systematic kinetic study of polymerization of acrylamide and methacrylamide photosensitized by azidopentamminecobalt(III) chloride at different wavelengths ($\lambda = 365, 405, 435 \text{ m}\mu$) with a view to elucidate the nature of the primary process, subsequent dark reactions, and initiation and termination of polymerization.

EXPERIMENTAL

Optical Arrangement

Two types of light sources were used; a high pressure mercury vapor lamp (250 W; Mazda ME/D box type fitted with glass windows, supplied by B. T. H. Co., U.K.) and a bulb-type ultraviolet lamp (125 W, Mazda MBW/U, also supplied by B. T. H. Co., purity of $365 \text{ m}\mu$ being better than 99%). The light from the lamp, condensed and rendered parallel by a biconvex lens, was allowed to pass through a series of filter combinations⁷ to isolate the required monochromatic wavelengths. To obtain light of $\lambda = 365 \text{ m}\mu$, the 125 W lamp was used without any filters. The reaction cell (4.6 cm light path, 4.6 cm diameter) was a cylindrical vessel (capacity 75 ml) fused at both ends with flat, optically clear, quartz plates and had two outlet tubes of standard B-14 cones for deaeration of the system.

Preparation of the Complex

Azidopentamminecobalt(III) chloride prepared by the method of Linhard and Flygare² was >99% pure as checked by spectrophotometry ($\log \epsilon$ at $303 \text{ m}\mu = 3.93$; Linhard's² value was 3.94). The cobalt(III) content of the azido complex determined by the method of Palmer⁸ was 22.65% (theoretical 22.9%).

Reagents

Acrylamide (American Cyanamid Co.), recrystallized⁹ from warm chloroform solution was a white, crystalline solid (mp 84.5°C). Methacrylamide (Rohm and Haas) purified by crystallization from benzene-ethanol mixture (4:1 by volume) and dried under vacuum for about 12 hr was a white, crystalline solid, mp 109.8°C . Potassium ferrioxalate, used for actinometry, was prepared¹⁰ from potassium oxalate and ferric chloride and purified by recrystallization from water. Perchloric acid (E. Merck, G. R., ca. 60% HClO_4), sulfuric acid (AnalaR, B. D. H., ca. 36*N*) and nitric acid (AnalaR, B. D. H.) were employed. Solvents like methanol, ethanol, chloroform benzene, and acetone were distilled immediately before use, and middle cuts were used. Nitrogen, freed from traces of oxygen by Fieser's¹¹ solution was passed through to deaerate the reaction system.

Estimations

The purity and concentrations of the monomer were estimated by the usual bromometry.¹² A typical experiment was as follows. The re-

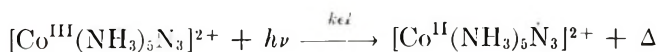
action mixture containing azido complex ($\sim 2 \times 10^{-4}$ mole/l.); monomer (~ 0.1 mole/l.); acid (HClO_4 , $\text{pH} \approx 2$) and neutral salt (~ 0.1 mole/l. NaClO_4) was taken in the reaction cell and deaerated for about 45 min in the dark. The reaction cell was then mounted in a thermostat at $35 \pm 0.01^\circ\text{C}$ (maintained by a toluene regulator and hot-wire vacuum switch relay, Gallenkamp) in the path of the monochromatic light and irradiated for about 5–15 min, depending on the type and concentration of monomer. The rate of monomer disappearance was followed by pipetting out aliquots of the reaction solution before and after irradiation and estimating the monomer concentration by bromometry. The rate of disappearance of the azido complex was followed by the change in absorbancy of the reaction solution (measured in a U.V. spectrophotometer; Hilger & Watts Uvispek, H 700) after irradiation and reference to a Beer's law calibration curve (optical density OD versus concentration of the azido complex at $\lambda = 303 \text{ m}\mu$). The light intensity of the mercury vapor lamp was measured by potassium ferrioxalate actinometry.¹⁰ The polyacrylamide formed in the irradiated system was precipitated by addition of methanol to the latter and purified by reprecipitation by adding methanol to aqueous solution of the polymer. The viscosities of 0.1% solutions of polyacrylamide in 1.0*M* sodium nitrate were measured in an Ubbelohde viscometer (Polymer Consultants Corporation, U.K.) thermostatted at $30 \pm 0.01^\circ\text{C}$ in a viscometric bath designed for precision viscometry (Krebs Electrical and Manufacturing Co., New York). From the intrinsic viscosities $[\eta]$, the number-average molecular weight of the polymer \bar{M}_n was calculated by using the Mark-Houwink relationship:⁹

$$[\eta] = 6.8 \times 10^{-4} \bar{M}_n^{0.66} \quad (1)$$

KINETIC SCHEME

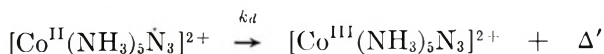
The following kinetic scheme appears to explain all the experimental results.

Light Absorption:



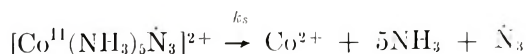
Here, k_i is the light absorption fraction by the complex, I is the light intensity, Δ refers to the excess energy which may be dissipated to the surrounding medium.

Dark Back Reaction:



where Δ' refers to the excess energy.

Decomposition of the Complex:



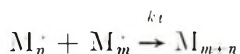
Initiation:



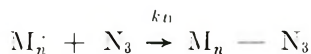
Propagation:



Mutual Termination:



Termination by $\overset{\cdot}{\text{N}}_3$:



Termination by Complex:



RESULTS AND DISCUSSION

Initiation of vinyl polymerization by azidopentamminecobalt(III) chloride under deaerated conditions was only photochemical in nature. Induction periods (~ 10 min) were observed with the presence of dissolved O_2 in the system. The steady-state maximum rate was observed to be dependent on the type of monomer; monomer concentration, complex concentration, and wavelength of light. In the case of acrylamide, for example, the maximum steady rate ($\sim 4.0 \times 10^{-5}$ mole/l.-sec) was attained in about 10 min with 20–30% conversions of acrylamide of low concentration (~ 0.1 mole/l.) and [complex] $\sim 2 \times 10^{-4}$ mole/l. (Fig. 1) at $\lambda = 365 \text{ m}\mu$; for higher [M] (~ 0.35 mole/l.) under the same conditions ($\lambda = 365 \text{ m}\mu$, [complex] $\approx 2 \times 10^{-4}$ mole/l.) the maximum steady rate of $\sim 3.8 \times 10^{-4}$ mole/l.-sec (Fig. 2) was reached in 5 min with conversions of 25–35%. Almost all the experiments were carried out at low acrylamide concentrations (~ 0.2 mole/l.), and the conversions were restricted to be within 35%. A few experiments where [M] was varied, the time of irradiation was reduced to 5 min. In the case of methacrylamide the maximum steady rate ($\sim 2.5 \times 10^{-5}$ mole/l.-sec) was attained in about 5 min, and conversions were less than 10%. In most of the experiments the conversions of the complex were of the order of $\approx 40\%$. Polymerization was also noticed in diffused daylight and in sunlight. Most of the experiments were conducted in perchloric acid and some in sulfuric and nitric acid to study the effect of anions. The pH was kept at approximately 2 in all polymerization experiments; for $\text{pH} > 4$ photolysis would lead to precipitation of cobalt(III) hydroxide. All experiments were done under deaerated conditions and at constant ionic strength ($\mu = 0.1$). The effects of variation of light absorption fraction, light intensity, monomer concentration, hydrogen ion concentration, acid medium, wavelength of light, tempera-

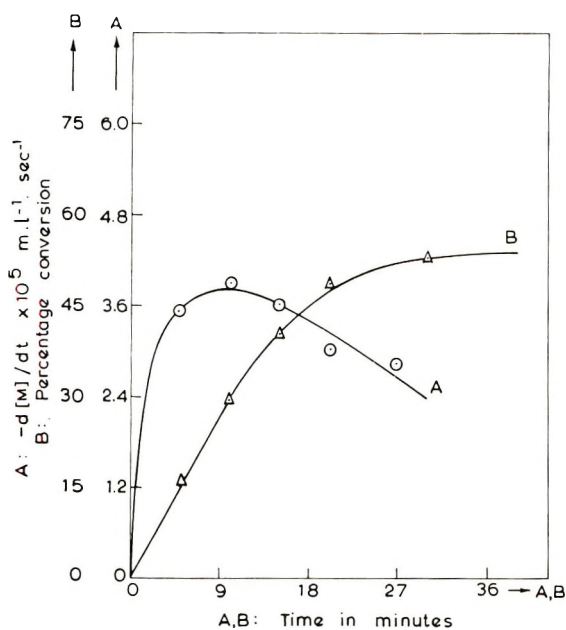


Fig. 1. Steady-state attainment: (a) plot of $-d[M]/dt$ vs. time; (b) percentage conversion vs. time. $[M] = 0.11$ mole/l, $k_e = 0.85$.

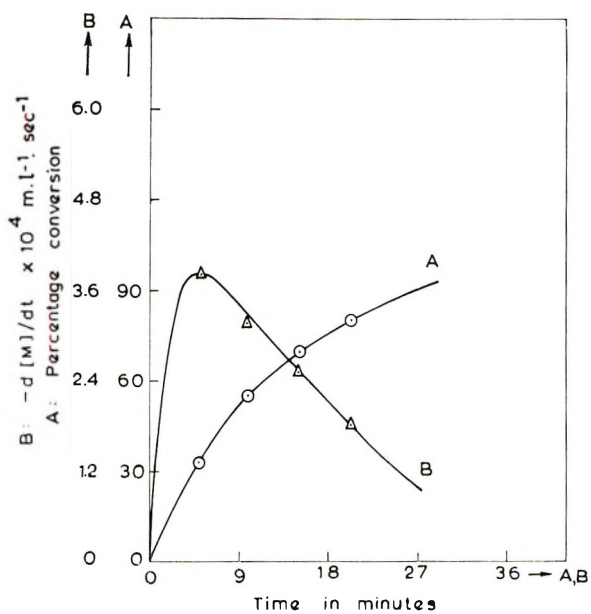


Fig. 2. Steady-state attainment: (a) plot of $-d[M]/dt$ vs. time; (b) percentage conversion vs. time. $[M] = 0.35$ mole/l, $k_e = 0.80$.

ture, ionic strength, etc., on the measurable, rate of monomer disappearance, chain length of polymer were studied in detail. Under our experimental conditions irradiation of the azido complex (without monomer) led only to redox decomposition giving N_3 , Co^{2+} , and NH_3 and there was no photoaquation, as evidenced by the absence of any aquated product, i.e., $[Co(NH_3)_5H_2O]^{3+}$ during irradiation.

Rate of Monomer Disappearance ($-d[M]/dt$)

Making the usual assumptions for stationary-state kinetics for micro and macro radicals and also constancy of k_p and k_t with chain length, the expressions for the rate of monomer disappearance under conditions of N_3 initiation and mutual termination would be:

$$-d[M]/dt = (k_p/k_t^{1/2})[M] \left(\frac{k_s k_e I}{k_s + k_d} \right)^{1/2} \quad (2)$$

It was observed that the rate of monomer disappearance was proportional to (a) unit power of monomer concentration for both acrylamide and methacrylamide (Figs. 3), (b) square root of the incident light intensity (Fig. 4) (c) the one-half power of light absorption fraction (Fig. 5) for acrylamide. These results clearly indicated that with acrylamide, termination was only mutual type. Termination by azide radical would require dependence of $[M]^2$ on rate, not observed by us. The dependence of $-d[M]/dt$ on $k_e^{0.25}$ and $I^{0.30}$ with methacrylamide observed by us indicated that termination

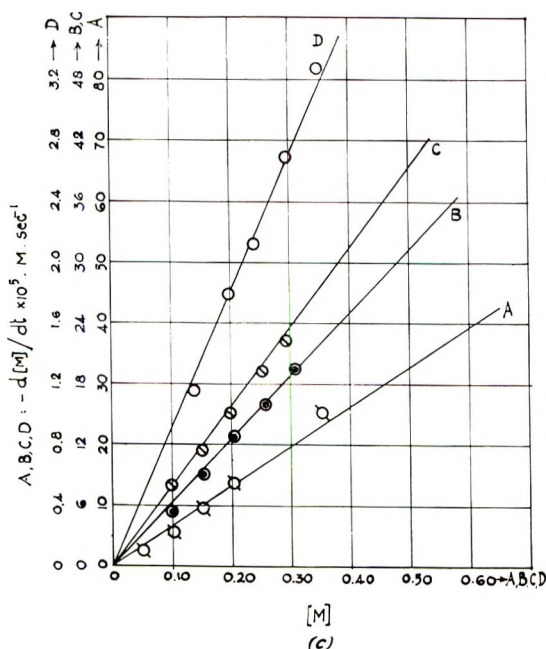


Fig. 3. Plots of $-d[M]/dt$ vs. $[M]$: (A) acrylamide, 405 $m\mu$; (B) acrylamide, 365 $m\mu$; (C) acrylamide, 435 $m\mu$; (D) methacrylamide, 435 $m\mu$. $k_e = 0.85$.

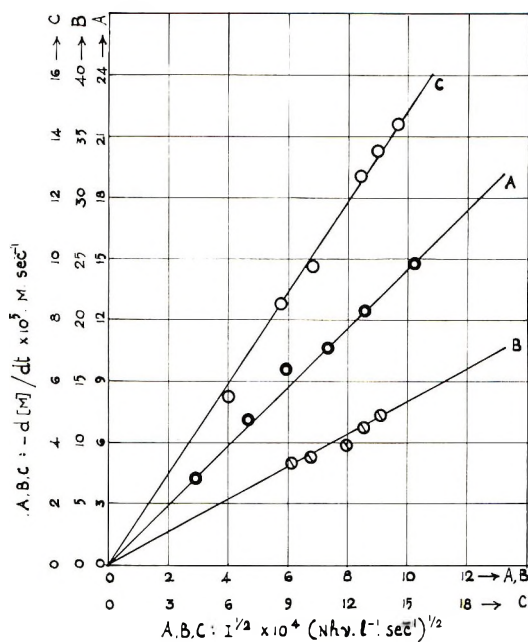


Fig. 4. Plots of $-d[M]/dt$ vs. $I^{1/2}$: (A) acrylamide, 365 $m\mu$; (B) acrylamide, 405 $m\mu$; (C) acrylamide, 435 $m\mu$. $k_t = 0.85$; $[M] = 0.25$ mole/l.

was probably a mixed type, i.e., termination by azide radical plus mutual termination. Toppet and co-workers,¹³ studying the dye-sensitized photopolymerization of acrylamide observed that the rate depended on $I^{0.35}$ and $[\text{sensitizer}]^{0.50} \rightarrow 0$ and suggested that termination was by primary radicals. Venkata rao and Santappa¹⁴ also obtained for $-d[M]/dt$ powers of ~ 0.35 for both I and k_t in the photopolymerization of methacrylamide by uranyl ions, and mixed termination involving primary radicals and mutual type was suggested. According to Dainton,¹⁵ the propagation velocity of methacrylamide was much less than that of acrylamide due to the steric strain conferred on the former by the substitution of a methyl group adjacent to the double bond. The probability of primary radicals like \dot{N}_3 interacting with polymethacrylamide radicals would be higher than that for interaction of two sterically unfavorable polymethacrylamide radicals for mutual termination. Therefore, termination by \dot{N}_3 seems to be plausible. The experimental results did not correspond to termination by complex molecule, which would require a dependence of k_t and I on $-d[M]/dt$. For photopolymerization of acrylamide by chloropentamminecobalt(III) complex, Delzenne⁶ observed a deviation from the square root dependence for the complex concentration and light intensity on the rate. By varying the concentration of chloro complex from 5×10^{-4} to 1×10^{-2} mole/l., Delzenne⁶ observed a fall in the value from 0.5 for the exponent of the complex concentration with increase of the latter as well as a decrease in r_p . This was explained by the oxidative termination of polymer radicals by

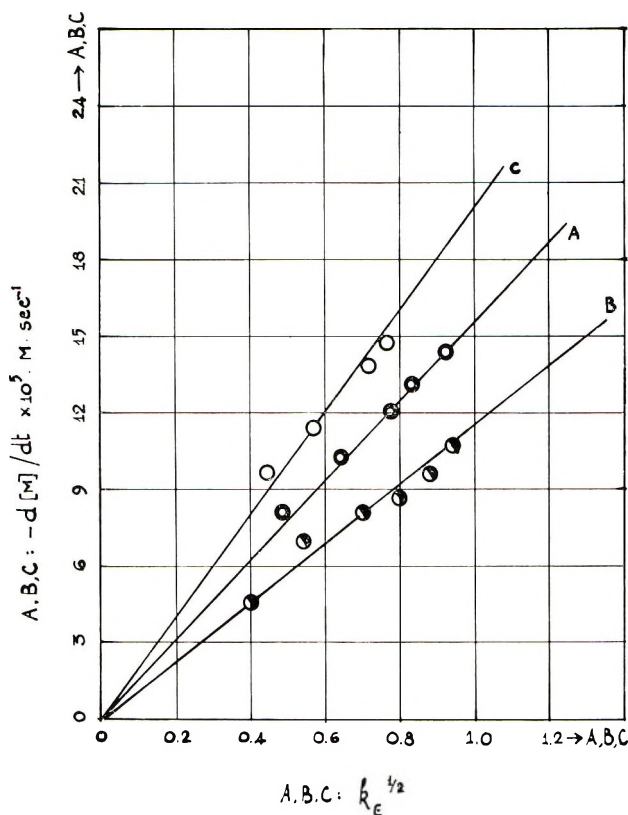


Fig. 5. Plots of $-d[M]/dt$ vs. $k_t^{1/2}$: (A) acrylamide, 365 $m\mu$; (B) acrylamide, 405 $m\mu$; (C) acrylamide, 435 $m\mu$. $[M] = 0.25$ mole/l.

complex molecules similar to that of linear termination by metals ions. It may be mentioned here that the experimental conditions employed by Delzenne⁶ were entirely different from ours; very high $[M]$ ($[M] = 4.2$ mole/l.) and polychromatic light being used, and chain lengths and the rates of complex disappearance having been not computed by the former. Polymerization of acrylamide by azido complex did not reveal termination by complex molecule under our experimental conditions, since the rate was strictly proportional to $k_t^{0.5}$ and $I^{0.5}$. Linear termination by complex molecule observed by Delzenne⁶ was perhaps due to high concentration of complex and monomer used; on the other hand, it was necessary to restrict the complex concentration to a low value of $\sim 7 \times 10^{-4}$ mole/l. in our experiments, and therefore linear termination in our work was unlikely. The polymerization of acrylamide at three different wavelengths (365, 405, and 435 $m\mu$) revealed dependences of $[M]$, $k_t^{0.5}$, and $I^{0.5}$ on rates. The values of $k_p/k_t^{1/2}$ evaluated were constant for different wavelengths (Table I). The effect of varying the acid concentration, initially added azide ion, cobaltous ion, and ionic strength had negligible effects on the rates. Varying the type of acid medium ($HClO_4$, HNO_3 , H_2SO_4) did not have any effect,

the rates of monomer disappearance being strictly proportional to unit power of monomer concentration and to one-half powers of k_t and I in all the acid media. The values of $k_p/k_t^{1/2}$ were the same with varying acid media (Table I).

Rate of Complex Disappearance ($-d[C]/dt$)

The rate of complex disappearance under conditions of \dot{N}_3 initiation and mutual termination would be:

$$-d[C]/dt = (k_s/(k_s + k_d))k_t I \quad (3)$$

The net quantum yield for complex disappearance, ϕ_c , would be equal to $k_s/(k_s + k_d)$. The rate of complex disappearance was found to be proportional to first powers of k_t and I and independent of monomer concentration for both the monomers (Figs. 6 and 7). This was true for all the wavelengths and different acid media.

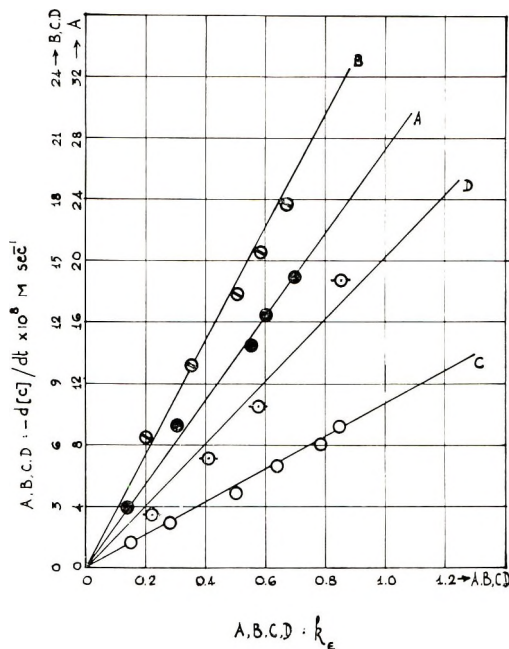


Fig. 6. Plots of $-d[C]/dt$ vs. k_t : (A) acrylamide, 365 $m\mu$; (B) acrylamide, 405 $m\mu$; (C) acrylamide, 435 $m\mu$; (D) methacrylamide, 435 $m\mu$.

Quantum Yields ϕ_c

The primary photochemical reaction is the transfer of an electron from the coordinatively bound azide ligand to the central cobalt(III) followed by the homolytic fission of the cobalt azide bond to produce azide radical. The formation of azide radical was evident from the nitrogen evolution which occurred as a result of $N_3 \rightarrow 3/2 N_2 \uparrow$, in the absence of monomer in our

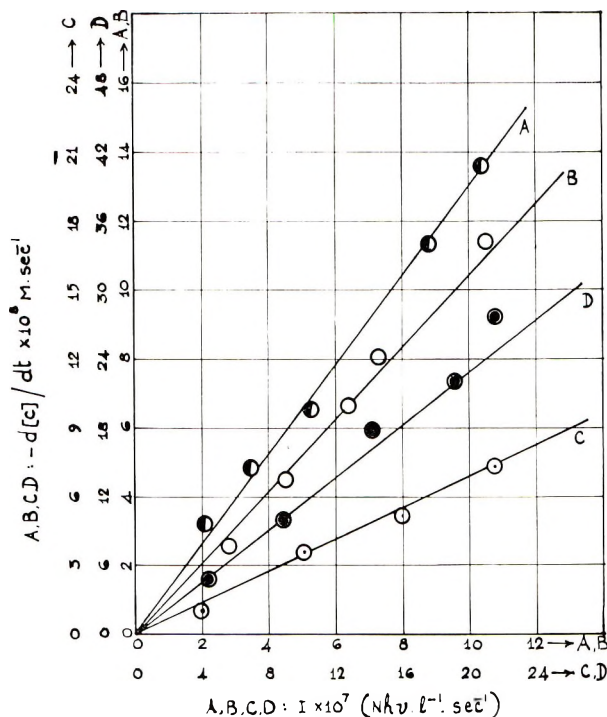


Fig. 7. Plots of $-d[C]/dt$ vs. I : (A) acrylamide, 365 $m\mu$; (B) acrylamide, 405 $m\mu$; (C) acrylamide, 435 $m\mu$; (D) methacrylamide, 435 $m\mu$.

irradiated system.^{16,17} The dominance of the Franck-Rabinowitch¹⁸ cage effect in preventing the separation of the fragments produced was evident from the low quantum yield ϕ_c (Table I) obtained at different wavelengths. The predominance of the cage effect would depend upon the magnitude of the term Δ which would decrease with increasing wavelength of incident light intensity; at longer wavelengths, the energy with which the two species [pentamminecobalt(II) complex and \dot{N}_3] collide with the solvent molecules would be less and the species may not be able to shear the solvent cage. The assumption of the cage effect which demands that the quantum yields should decrease with increase of wavelength of incident light appeared to be validated by ϕ_c , decreasing with increasing wavelength (Table 1), the lower values of ϕ_c implying $k_d > k_s$. The absence of variation of values of ϕ_c (Table I) in various acid media ($HClO_4$, HNO_3 , and H_2SO_4) showed that the acid medium did not play any role in the primary photochemical reaction.

Chain Lengths n

On the basis of mutual termination the expression for chain length would be:

$$n = k_p/k_t^{1/2}[M]/\{(k_s + k_d)/k_s k_c I\}^{1/2} \quad (4)$$

TABLE I
Rate Constants $k_p/k_t^{1/2}$ for Acrylamide

Wavelength λ , m μ	Medium	$k_p/k_t^{1/2}$, l ^{1/2} -mole ^{-1/2} -sec ^{-1/2}		Average $k_p/k_t^{1/2}$, l ^{1/2} mole ^{-1/2} -sec ^{-1/2}	ϕ_c
		$[-d[M]/dt \text{ vs. } [M]]$	$[-d[M]/dt \text{ vs. } I^{1/2}]$		
405	HClO ₄	2.17	1.98	2.05	0.13
365	HClO ₄	1.71	1.90	1.83	0.18
435	HClO ₄	1.88	1.92	1.89	0.12
435	HNO ₃	1.86	2.01	1.94	0.12
435	H ₂ SO ₄	1.70	1.94	1.86	0.12

Chain lengths were found to be proportional to the first power of monomer concentration and inversely proportional to the square root of k_t and I (Fig. 8). It may be seen that the experimental results do not agree with the other modes of termination, i.e., by azide radical or complex molecule.

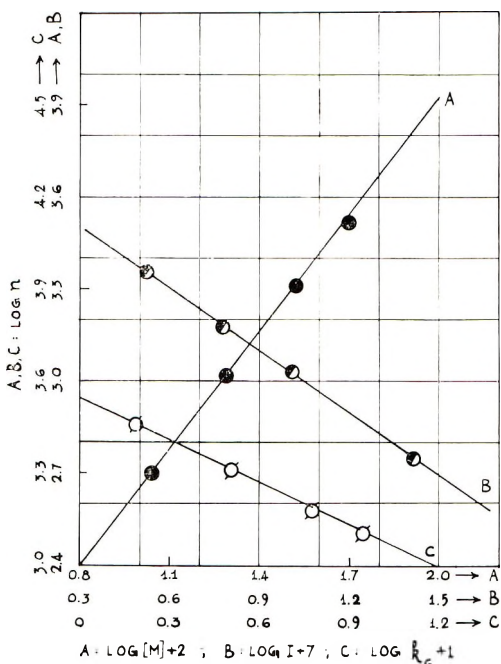


Fig. 8. Plots of $\log n$ vs. \log variables for acrylamide, 365 $m\mu$: (A) $\log n$ vs. $\log [M]$; (B) $\log n$ vs. $\log I$; (C) $\log n$ vs. $\log k_t$.

Azide radical termination would require a square dependence on monomer concentration and inverse dependence of k_t and I , whereas termination by complex would require zero exponent values for k_t and I .

Rate Constants $(k_p/k_t)^{1/2}$

The rate constants $k_p/k_t^{1/2}$ were evaluated from slopes of the plots of $-d[M]/dt$ versus $k_t^{1/2}$ or $I^{1/2}$ or $[M]$ and assuming $k_s/(k_s + k_d) = \phi_c = (-d[C]/dt)/k_t I$. Our values of $k_p/k_t^{1/2}$ (Table I) were same within limits of experimental errors as expected for different wavelengths. (Dainton⁹ obtained a value of 4.2 for polyacrylamide with hydrogen peroxide as photoinitiator at $\lambda = 365 m\mu$ in aqueous solution.)

Grateful acknowledgement is made to the Council of Scientific and Industrial Research, New Delhi, for the award of a Junior Research Fellowship and to the University of Madras for the award of Stipendary Studentship to one of us (L.V.N.) during the course of this work.

References

1. A. W. Adamson, *Discussions Faraday Soc.*, **29**, 163 (1960).
2. M. Linhard and H. Z. Flygare, *Z. Anorg. Allgem. Chem.*, **262**, 328 (1950).
3. J. F. Endicott and M. Z. Hoffman, *J. Amer. Chem. Soc.*, **87**, 3348 (1965).
4. D. Klein and C. W. Moeller, *Inorg. Chem.*, **4**, 394, 398 (1965).
5. L. V. Natarajan and M. Santappa, *J. Polym. Sci. B*, **5**, 357 (1967).
6. G. A. Delzenne, in *International Symposium on Macromolecular Chemistry (J. Polym. Sci. C, 16)*, O. Wichterle and B. Sedlacek, Eds., Interscience, New York, 1967, p. 1027.
7. E. J. Bowen, *Chemical Aspects of Light*, Oxford Univ. Press, London, 1946, p. 279.
8. W. G. Palmer, *Experimental Inorganic Chemistry*, Cambridge Univ. Press, 1959, p. 534.
9. F. S. Dainton and M. Tordoff, *Trans. Faraday Soc.*, **53**, 499 (1957).
10. C. A. Parker and C. G. Hatchard, *Proc. Roy. Soc. (London)*, **A235**, 518 (1956).
11. L. F. Fieser, *J. Amer. Chem. Soc.*, **46**, 2639 (1924).
12. G. Mino and S. Kaizermann, *J. Polym. Sci.*, **38**, 393 (1959).
13. S. Toppett, G. A. Delzenne, and G. Smets, *J. Polym. Sci. A*, **2**, 1539 (1964).
14. K. Venkatarao and M. Santappa, *J. Polym. Sci. A-1*, **5**, 637 (1967).
15. F. S. Dainton and W. D. Sisley, *Trans. Faraday Soc.*, **59**, 1369 (1963).
16. S. A. Penkett and A. W. Adamson, *J. Amer. Chem. Soc.*, **87**, 2514 (1965).
17. M. G. Evans, M. Santappa, and N. Uri, *J. Polym. Sci.*, **7**, 243 (1951).
18. J. Franck and E. Rabinowitch, *Trans. Faraday Soc.*, **30**, 120 (1934).

Received March 26, 1968

Revised May 4, 1968

Isomerization of *cis*-1,4-Polybutadiene by $\text{RhCl}_3 \cdot 3\text{H}_2\text{O}$

FRANTISEK HRABAK, *Institute of Macromolecular Chemistry,
Czechoslovak Academy of Sciences, Prague, Czechoslovakia*

Synopsis

The isomerization of *cis*-1,4-polybutadiene by RhCl_3 in aqueous emulsion was studied. The reaction was found to be slowed down by air and by base but not by quinone and was independent of the polymer solvents. Quinone did not suppress polymer gel formation. The results obtained suggest a nonradical mechanism of these reactions.

INTRODUCTION

The isomerization of *cis*-1,4-polybutadiene to the *trans*-1,4 structure has been observed when aqueous emulsions of *cis*-polybutadiene in benzene¹ or dimethylformamide-benzene² were treated by Rh salts. However, no data concerning the course of the reaction under these conditions have been published. To elucidate this structural transformation, the influence of a radical inhibitor, of temperature, and of solvents on the isomerization of polybutadiene by $\text{RhCl}_3 \cdot 3\text{H}_2\text{O}$ was studied.

EXPERIMENTAL

Materials

cis-1,4-Polybutadiene 1203 was used. After reprecipitation from benzene solution with 2-propanol it contained 94-96% *cis*, 2.5-3% *trans* and 2.5-3% vinyl structures. The dry polymer in 1-g portions was sealed in evacuated glass ampules. The solvents used had the following refractive indices (n_D^{20}) after distillation: benzene 1.5016, toluene 1.4971, *m*-xylene 1.4977, 1-chloropentane 1.4125. The carbon disulfide was Matheson Coleman & Bell Spectroquality Reagent. Sodium lauryl sulfate was commercial Duponol ME. Solid sodium decylbenzene sulfonate was recovered from 30% aqueous solution (Santomerse SX) by dilution with methanol, precipitation of iron with aqueous ammonia, and evaporation of the filtrate.

Methods

Solutions of *cis*-polybutadiene in the appropriate solvents were emulsified in water (total volume 50 ml) and stirred with a magnetic stirrer in a two-necked volumetric flask reactor. One neck, normally closed with a stan-

ard taper glass stopper, served for withdrawal of the samples with a pipet while nitrogen was passed in through the other during sampling. The reactor was immersed in a glass water bath. The samples of emulsion were coagulated by methanol, and the precipitate was immediately dissolved in carbon disulfide. After standing over a small amount of anhydrous CaCl_2 for 1–2 hr the solution was placed on a KBr disk, the CS_2 was evaporated in a stream of dry nitrogen, and the polybutadiene film was dried in the vacuum of an oil pump. The spectrum of the film was measured on a Perkin-Elmer Model 337 spectrophotometer. The characteristic absorbances for the *trans*-1,4, vinyl, and *cis*-1,4 structures in polymer were measured at 970, 915, and 740 cm^{-1} . The spectra of the nonvolatile components of the emulsion system, RhCl_3 , and sodium decylbenzene sulfonate, recorded from KBr pellet showed no characteristic absorbance at these frequencies.

Following Hampton,³ the total absorbance at a particular frequency [$E = \log(I_0/I)$] was considered to consist of the absorbances of the KBr crystal [$E_c = \log(I_0/I_c)$] and of the polybutadiene film [$E_f = \log(I_0/I_f)$]. Hence the absorbance of the polybutadiene film was expressed as the difference between the total absorbance and that recorded from the KBr crystal [$E_f = \log(I_c/I)$]. In the calculations according to Silas et al.,⁴ the absorbance area within the frequency range 835–635 cm^{-1} was measured planimetrically. By analogy with the previous method the absorbance area of the polybutadiene film $E_{f(835-635)}$ was expressed as the difference between total absorbance area, $E_{(835-635)}$ and that for the KBr crystal, $E_{c(835-635)}$.

RESULTS

To check both methods^{3,4} of calculation, the absorbances of two polybutadiene films of different thickness were measured and the contents of the various unsaturated groupings was calculated. The results are shown in Table I. The results calculated according to Hampton³ differed less for

TABLE I
Calculation of the Proportion of Unsaturated Groupings in the Original Polybutadiene by the Methods of Hampton³ and of Silas et al.⁴

$E_{970} - E_c$	$E_{915} - E_c$	$E_{740} - E_c$	$(E - E_c)_{835-635}$	<i>trans</i> , %	Vinyl, %	<i>cis</i> , %	Ref- erence
0.107	0.107	0.455	0.156	2.6	2.7	94.7	3
				1.9	2.6	95.5	4
0.331	0.332	1.33	0.415	2.8	2.9	94.2	3
				2.5	3.2	94.3	4

the two films than those obtained by the second method.⁴ Further confirmation of the reproducibility of the data obtained by Hampton's procedure is given by the results shown in Table II. However, it will be noted that the results become unreliable for high absorbances [in Table II, the sample

TABLE II
Influence of Rh Salts on the Proportion of Unsaturated Groupings in Emulsion I

Rh salt	Temperature, °C	Reaction time, hr	Absorbance				<i>trans</i> , %	Vinyl, %	<i>cis</i> , %
			$E_{970} - E_c$	$E_{915} - E_c$	$E_{740} - E_c$				
Rh(NO ₃) ₃ ·2H ₂ O	40	0.25	0.076	0.077	0.385	2.4	2.6	95.0	
	40	22	0.278	0.277	1.134	2.8	2.8	94.4	
	40	30	0.178	0.177	0.710	2.9	2.9	94.2	
RhCl ₃ ·3H ₂ O	40	48	0.395	0.395	1.340	3.7	3.6	92.7	
	40	1	0.224	0.224	0.940	2.6	2.8	94.6	
	40	41	0.116	0.118	0.566	2.0	2.3	95.7	
RhCl ₃ ·3H ₂ O + HCOOH	60	61	0.108	0.108	0.471	2.5	2.6	94.9	
	60	84	0.138	0.138	0.582	2.6	2.7	94.7	
	60	107	0.091	0.091	0.398	2.5	2.6	94.9	

TABLE III
Isomerization of *cis*-Polybutadiene at 70°C. in Emulsion 2

No.	Emulsifier	Solvent	Reaction time, hr	Treatment of sample ^a	<i>trans</i> , %	Vinyl, %	<i>cis</i> , %
1	Lauryl sulfate	<i>m</i> -Xylene	14	A	3.3	2.9	93.8
			14	A reprecip. from C ₆ H ₆ A and B	3.2	2.8	94.0
			27.5	A and B	22.7	3.9	73.4
2	Decylbenzene sulfonate	<i>m</i> -Xylene	42	A	3.5	2.7	93.8
			14	A	3.5	2.7	93.8
			27.5	A reprecip. from C ₆ H ₆ and left for 72 h. A and B	24.0	4.5	71.5
3	Decylbenzene sulfonate	Toluene	27.5	A and B	18.7	3.6	77.7
			49 ^b	A reprecip. from C ₆ H ₆	3.6	2.7	93.7
			72 ^b	A + NH ₄ OH	4.6	2.7	92.7
			21	A	2.8	2.7	94.5
			21	A + HCl and B	6.0	2.7	91.3
			21	A + NH ₄ OH and B	2.3	2.4	95.3
			72	A + HCOOH	2.8	2.8	94.4
4	Decylbenzene sulfonate	Amyl chloride	72	A + HCOOH and B	5.6	2.9	91.5
			72	A + NaOH and B	2.7	2.4	94.9
			16.5	A	2.5	2.5	95.0
			46 ^b	A	3.6	3.1	93.3
			71 ^b	A + NaOH and B	3.9	3.2	92.9

^a Treatments: A, coagulated by CH₃OH; B, precipitate kept under N₂ for 24 hr.

^b Isomerization in precipitate verified.

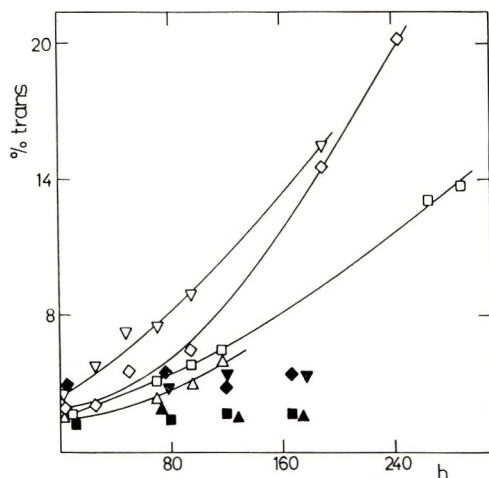


Fig. 1. Polybutadiene isomerization in films from CS_2 solutions of samples 2 and 4 in Table III: (Δ , \blacktriangle) 2-49; (∇ , \blacktriangledown) 2-72; (\square , \blacksquare) 4-46; (\diamond , \blacklozenge) 4-71; (Δ , ∇ , \square , \diamond) fresh solutions; (\blacktriangle , \blacktriangledown , \blacksquare , \blacklozenge) CS_2 solutions dried over CaCl_2 for 336 hr.

with $\text{Rh}(\text{NO}_3)_3$ after 48 hr reaction]. Hampton's method of calculation is simpler than that of Silas et al.,⁴ while the results obtained by the two procedures do not differ substantially, provided the absorbances were not too high. For this reason only the first method was used in further calculations.

The first experiments were carried out in the following emulsion system (emulsion 1): 95 g benzene, 5 g polybutadiene, 150 g H_2O , 4.32 g lauryl sulfate, 0.1 g $\text{RhCl}_3 \cdot 3\text{H}_2\text{O}$ or 0.123 g $\text{Rh}(\text{NO}_3)_3 \cdot 2\text{H}_2\text{O}$. Oxygen was not removed from the reaction mixtures. At 40°C no isomerization occurred with either $\text{Rh}(\text{NO}_3)_3 \cdot 2\text{H}_2\text{O}$ or $\text{RhCl}_3 \cdot 3\text{H}_2\text{O}$ during two days as demonstrated by the data in Table II, nor was there any change in the proportion of the different unsaturated groupings when the temperature of the reaction was raised to 60°C for 43 hr more. The addition of formic acid (0.5 g/5 g of polybutadiene) had no effect.

In further experiments, higher concentrations of $\text{RhCl}_3 \cdot 3\text{H}_2\text{O}$ and emulsifier were used. The isomerizations were carried out at 70°C in the emulsion 2: 95 g *m*-xylene (or toluene, 1-chloropentane, benzene), 5 g polybutadiene, 150 g H_2O , 6.48 g lauryl sulfate (or 7.2 g decylbenzene sulfonate), 1.5 g $\text{RhCl}_3 \cdot 3\text{H}_2\text{O}$. The results of these experiments are given in Table III. They show the isomerization is very slow in both aromatic and aliphatic solvents in the presence of atmospheric oxygen. The isomerization proceeded faster in coagulated polybutadiene, with the exception of the samples prepared by latex coagulation in the presence of a base. The acceleration of the isomerization in the precipitate suggests its sensitivity to oxygen.

For the samples marked with superscript b (Table III), isomerization in the precipitate was verified. The films from these samples were left on the KBr crystals and the proportion of different unsaturated groupings was

measured after several time intervals. The results are shown in Figure 1. The longer the polybutadiene had been exposed to the catalyst in the emulsion, the faster was the isomerization of the polybutadiene film on the KBr crystals. The films on the KBr crystals became hard and only swelled but did not dissolve in benzene.

Unlike the solid films on the KBr crystals, solutions of the polymers in CS₂ did not undergo isomerization. After the films from fresh solutions of samples 2-49, 2-72, 4-46, 4-71 had been prepared on KBr crystals (open symbols in Fig. 1) the residual solutions were kept over anhydrous CaCl₂ for 336 hr, samples were again placed on KBr crystals, and the proportions of

TABLE IV
Course of Isomerization in Inert Atmosphere, Air and with Quinone

No.	Temperature, °C	Reaction medium	Time, hr	<i>trans</i> , %	Vinyl, %	<i>cis</i> , %	Note
1	70	C ₆ H ₆	118	10	2.5	87.5	Partly gel
2	70	C ₆ H ₅ CH ₃	69	8.1	4.3	87.6	Gel
3	70	C ₆ H ₆ , with quinone	77	14.3	5.4	80.3	Gel
4	70	C ₆ H ₅ CH ₃	68 ^a	2.7	2.7	94.6	In CS ₂
			120 ^a	3.0	3.1	93.9	Colorless soln.
			167 ^a	4.4	4.0	91.6	Colorless soln.
			209 ^a	4.4	3.3	92.3	Colorless soln.
			282	12.9	3.3	83.8	Brown CS ₂ soln.
			330				Gel
5	40	C ₆ H ₆	72	2.2	2.5	95.3	In CS ₂
			109	2.4	2.5	95.1	Soluble
			150	4.1	3.8	92.1	Partly gel

^a Experiments in air; all other experiments in inert atmosphere.

the unsaturated groupings in the films were measured after various time intervals. The results (filled symbols in Fig. 1) suggest no isomerization in the CS₂ solutions during the 336-hr drying period and no isomerization in the films prepared from these dried solutions. It can be inferred that the polybutadiene isomerization in the films from fresh CS₂ solutions may have been caused by Rh salts incorporated in the polybutadiene while no such salts would remain in thoroughly dried CS₂ solutions.

In further experiments the course of isomerization in an inert atmosphere (N₂) and with an inhibitor (quinone) was investigated. The experiments were carried out in the emulsion 2 with decylbenzene sulfonate as emulsifier. If the isomerization was to be carried out in inert atmosphere, the initial charge was frozen and evacuated on an oil pump. Then the reactor

was filled with nitrogen and placed in a thermostat. The proportions of the individual unsaturated groupings were measured at various time intervals. The results (Table IV) show that the rate of isomerization is greater in the inert atmosphere than in air. If the temperature was lowered from 70 to 40°C, the rate of isomerization decreased considerably, but the gel formed at a relatively low degree of isomerization.

TABLE V
Polybutadiene Isomerization in Films on KBr Crystals

Sample	Time on KBr crystals, hr	<i>trans</i> , %	Vinyl, %	<i>cis</i> , %
4-68	124	3.4	2.6	94.0
	174	4.2	2.8	93.0
	218	4.9	2.8	92.3
4-209	72	7.5	3.3	89.2
	121	9.8	4.5	85.7
	166	11.6	5.4	83.0
4-282	50	47.3	4.3	48.4
	96	50.7	6.7	42.6

The samples from the experiments 4 in Table IV were used to evaluate the dependence of the isomerization rate in polybutadiene films on the duration of reaction between polybutadiene and RhCl₃ in emulsion. For this purpose the films from experiment 4 were left on the KBr crystals, and the contents of the *cis*, vinyl, and *trans* structures in polymer were measured at various time intervals. The results (Table V) show that the greater the reaction time in emulsion, the greater the rate of isomerization on the KBr crystal. These results confirmed those given in Figure 1.

CONCLUSIONS

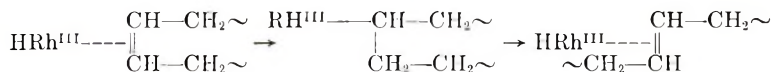
The results can be summarized as follows.

- (1) No isomerization occurred with 2% Rh salt (referred to polybutadiene) at 40 and 60°C in air, even after addition of formic acid (Table II).
- (2) Only slow isomerization occurred with 30% RhCl₃·3H₂O at 70°C in air. No difference in the rate of isomerization was observed with toluene, *m*-xylene and amyl chloride as solvents (Table III).
- (3) The rate of isomerization increased in an inert atmosphere (Table IV). However, in air the Rh salt is also bound to the polybutadiene chains. This is seen from the increasing rate of isomerization in films with the increasing time of the previous exposure in emulsion (Fig. 1, Table V).
- (4) Isomerization did not occur in the precipitate if the latex with Rh salt was coagulated in the presence of a base (Table III).

- (5) The isomerization was not inhibited by quinone, though it was slowed down by atmospheric oxygen (Table IV).
- (6) At some degree of isomerization the polybutadiene formed a gel. Gel formation was not inhibited by quinone (Table IV).

The mechanism of *cis-trans* polybutadiene isomerization by RhCl_3 is apparently different from the radical mechanism of the sensitized photochemical and γ -ray-induced isomerization of polybutadiene explained by Golub.^{5,6} While the sensitized isomerization proceeds in air, though under a deep degradation of polybutadiene, the isomerization of polybutadiene by RhCl_3 is inhibited in air. The insensitivity of the RhCl_3 isomerization and gel formation to quinone (Table IV) excludes a radical mechanism for these reactions as well. The course of polybutadiene isomerization by RhCl_3 is rather reminiscent of the reaction between TiCl_4 and natural rubber described by Ferri.⁷ The product coagulated from a solution of natural rubber in benzene by TiCl_4 was highly crosslinked and contained Ti and Cl.

No definite reaction scheme can be proposed for the polybutadiene isomerization by RhCl_3 on the basis of these results. However, the inhibition of this reaction by base is similar to the effect observed by Cramer⁸ in the isomerization of low molecular weight olefins. Intermediate formation of an Rh(III) hydride was assumed to occur in the isomerization of butenes by RhCl_3 , the concentration of the hydride being lowered by bases. The reaction scheme for the isomerization of butenes, considering both addition and elimination of rhodium hydride,⁸ seems to be analogically applicable to the *cis-trans* isomerization of polybutadiene:



According to this scheme, some migration of the double bonds ought to be possible due to the possible elimination of a hydrogen atom from two adjacent carbon atoms. The inhibition of polybutadiene isomerization by atmospheric oxygen might be understandable in connection with an unstable hydride intermediate.

The facts that the gel formation proceeded in the presence of the quinone, that the Rh salt was removed from the CS_2 solutions of polybutadiene after drying over CaCl_2 , and other experimental observations suggest that the isomerized polybutadiene chains are crosslinked by means of the Rh salt molecules.

The measurements were carried out at the Institute of Polymer Science, the University of Akron, Ohio, USA. The work was sponsored by the Goodyear Company. I should like to express my thanks to Prof. M. Morton, director of the Institute of Polymer Science, who directed my attention to this topic.

References

1. R. E. Rinehart, H. P. Smith, H. S. Witt, and H. Romeyn, Jr., *J. Amer. Chem. Soc.*, **84**, 4145 (1962).
2. C. E. H. Bawn, D. G. T. Cooper, and A. M. North, *Polymer*, **7**, 113 (1966).
3. R. R. Hampton, *Anal. Chem.*, **21**, 923 (1949).
4. R. S. Silas, J. Yates, and V. Thornton, *Anal. Chem.*, **31**, 529 (1959).
5. M. A. Golub, *J. Polym. Sci.*, **25**, 373 (1957).
6. M. A. Golub, *J. Amer. Chem. Soc.*, **81**, 54 (1959).
7. C. Ferri, *Helv. Chim. Acta*, **20**, 1393 (1937).
8. R. Cramer, and R. V. Lindsey, *J. Amer. Chem. Soc.*, **88**, 3534 (1966).

Received February 8, 1968

Revised May 7, 1968

Modification of Poly(vinyl Chloride). X. Crosslinking of Poly(vinyl Chloride) with a Soft Segment of an Elastomer Containing Thiol Groups

YOSHIRO NAKAMURA and KUNIO MORI, *Department of Applied
Chemistry, Iwate University, Morioka, Japan*

Synopsis

To obtain poly(vinyl chloride) (PVC) of excellent toughness, a new method of crosslinking PVC is proposed in which PVC is crosslinked with the soft segment in an elastomer such as liquid Thiokol. The reaction can be accomplished by immersing PVC-Thiokol blends in liquid ammonia at 20–30°C. A similar reaction occurs in aqueous ammonia when hexamethylphosphoramide is used as an activator. Characteristics of the crosslinked PVC thus obtained and of the controls of a similar uncrosslinked composition (PVC-Thiokol LP-8, 100:5 by weight) were as follows: tensile strength, 7.3 and 4.8 kg/mm²; elongation at break, 30 and 2.5%; Young's modulus, 3.5×10^4 and 2.9×10^4 kg/cm²; tensile impact, 88 and 15 kg-cm/cm³, respectively. The crosslinked PVC as plasticized with dioctyl phthalate (DOP) and the control blend (PVC-Thiokol LP-8-DOP, 100:10:10 by weight), respectively, showed tensile strengths of 5.9 and 4.8 kg/mm², elongations at break of 44 and 24%, Young's moduli of 2.5×10^4 and 1.6×10^4 kg/cm², and tensile impact strengths of 62 and 120 kg-cm/cm³. As the crosslinkage through the soft segments increases up to about 5%, the elongation at break, Young's modulus, and tensile impact, in addition to the tensile strength, are improved. This is different from the results so far observed with the crosslinked amorphous polymers and is characteristic of the products of crosslinking through the soft segment. The experimental results are discussed in this paper.

INTRODUCTION

The shock resistance of poly(vinyl chloride) (PVC) has been improved by blending elastomers such as ABS and MBS rubbers. However, in regard to the tensile strength or zero-strength temperature, the improved PVC is inferior to the original PVC as the elastomer is contained in the former.

The object of this paper is to present a new method for improving the shock resistance property of PVC without lessening such properties as the tensile strength or zero-strength temperature. The new method is based on the principle of crosslinking rigid polymers with the soft segment contained in the elastomers.¹

When PVC was crosslinked with liquid Thiokol as in the present studies, the product, compared with the original PVC, showed higher tensile

strength, zero-strength temperature, and elongation at break, as well as excellent shock resistance.

In the case of crosslinked elastomers such as vulcanized rubbers, the elongation and shock resistance tend to decrease with the increase of the crosslink density, though the tensile strength, zero-strength temperature, and Young's modulus tend to increase. This was not the case with the modified PVC obtained in the present studies.

The crosslinking of PVC with liquid Thiokol was not accelerated by morpholine, which had been found to accelerate the crosslinking of PVC with dithiol compounds such as ethanedithiol, Thiokol A, or with trithiocyanuric acid.² In the present studies, liquid ammonia was found to accelerate the crosslinking with liquid Thiokol, and this led us to perform the present work successfully. No other polar solvents tested, e.g., dimethylformamide and dimethyl sulfoxide, showed any accelerating action. So far as is known, no previous report has shown that the reaction of PVC with Thiokol can be accelerated by liquid ammonia.

EXPERIMENTAL

Materials

The elastomers used were various types of Thiokol LP (liquid dithiol compounds) and ethanedithiol. Five types of Thiokol LP were supplied from Thiokol Chemical Corp., and were used without purification. Table I shows their molecular weights and structures. Ethanedithiol was prepared as reported previously.²

TABLE I
Molecular Weights and Structures of Thiokol LP

Type of thiokol	MW	Structure
LP-2	4000	Branched
LP-32	4000	Linear
LP-3	1000	Branched
LP-33	1000	Linear
LP-S	500-700	Linear

The rigid polymer used was Geon 101-EP, a PVC homopolymer having a degree of polymerization of 1450. Dioctyl phthalate was used as the plasticizer, and organic tin compounds and metal stearate were used as stabilizers against coloration at elevated temperatures. All these additives were commercial products. Dimethylformamide, dimethyl sulfoxide, hexamethylphosphoramide (HMPA), and tetrahydrofuran (THF), reagent grade, were purified by fractional distillation under atmospheric or reduced pressure. Liquid ammonia was prepared from ammonia tank in the autoclave.

Method of Blending and Crosslinking

PVC and Thiokol LP or ethanedithiol were blended in a two-roller mill, with heating at 120–150°C for 10 min in the presence or absence of the additives. The recipes are shown in Table II.

TABLE II
Typical Blending Recipes

	Parts by wt
PVC (Geon 101-EP)	100
Thiokol LP or ethanedithiol	5
Diethyl phthalate	0–10
KS-40 ^a or KS-20 ^b	0–1

^{a, b} Organic thiotin compound and dibutyltin laurate, respectively (Kyodo Yakuhin Co.).

A 5-g portion of the colorless, blended sheets, about 0.3 mm thick, and 30 ml. of liquid ammonia or 28% aqueous ammonia saturated with sodium chloride were charged in a stainless steel autoclave of 100 ml capacity and maintained at 20 or 50°C for 60 min. Reducing the pressure after cooling, the whitened sheets were taken out, washed with water, and allowed to stand at room temperature for 60 min to remove the ammonia gas absorbed. The sheets were then heated for 30 min in an air bath at 100°C to make the cloudiness of the sheets disappear. The resulting sheets were colorless, transparent, and infusible and insoluble in boiling THF.

Analysis and Instruments

The resulting sheets, usually about 0.2 g, were extracted with THF in a Soxhlet apparatus overnight. The remaining swollen gel was surface-dried and quickly enclosed in a weighing tube to weigh. The gel was then dried by vacuum-pumping in a desiccator at room temperature for at least 18 hr.

The percentage of THF-insoluble material is given from the ratio of the weight of the dried gel and the weight of the original sample. The swelling ratio Sw is reported as the ratio of the swollen weight to the weight of the dried gel. The composition of the dried gel was determined from the chlorine and sulfur content by the Schöniger method.³

The unextracted sheets, about 0.3 mm thick were stamped into test dumbbells, 25 × 50 mm overall and 5 mm wide at the neck. The stress-strain curves were obtained with a recording Autograph P-100 at the drawing rate of 5 mm/min at 20°C. The tensile impact was similarly determined at the drawing rate of 500 mm/min. The zero-strength temperature and elongation at break were measured with a Toyoseiki tensile heat distortion apparatus (ASTM D1637 – 59T) under the specified stress of 15 kg/cm² at the heating rate of 2°C/min. The folding endurance was determined with MIT type testing machine (ASTM D643 – 43) at 25°C

under the specified stress of 25 kg/cm² for the specimens, 0.3–0.35 mm thick. The shrinkage test for the specimens 0.3 mm thick was followed by BS 1763-1956 at 150 ± 2°C for 15 min. The infrared spectra were recorded with Shimadzu IR 27 spectrophotometer in a potassium bromide disk.

RESULTS AND DISCUSSION

Blending

The calculated solubility parameter⁴ of liquid Thiokols and of ethanedithiol is about 7.9, which is approximately equal to that of PVC. Therefore, blending of PVC with liquid Thiokols, except those of high molecular weight such as LP-2 or LP-32, or with ethanedithiol can easily be carried out with or without addition of the plasticizer.

Conditions of Crosslinking

In the polar solvents such as dimethylformamide, HMPA, and dimethyl sulfoxide, the dithiol compounds do not react with PVC over a wide range of temperature (up to 150°C). But, as shown in Figures 1 and 2, a crosslinking reaction occurs when PVC–dithiol blends are immersed in liquid ammonia at 20–60°C, and insoluble and infusible sheets are obtained. When the blends are immersed in the medium at higher temperatures, the resulting sheets are more easily colored on aging at 150°C (Table III). From Figures 1–3, it can be concluded that the optimum condition for the crosslinking of PVC sheets of about 0.3 mm thick and containing 5 parts of Thiokol LP-3 in liquid ammonia is to treat them at 20°C for 60 min.

The crosslinking reaction also occurs in 28% aqueous ammonia when HMPA is added as an activator (Fig. 4). However, with HMPA, the resulting PVC discolors more rapidly on aging at 150°C. For the crosslinking of PVC sheets about 0.3 mm thick and containing 5 parts of

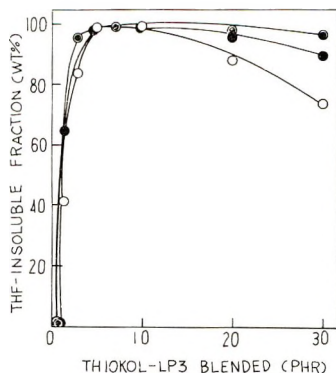


Fig. 1. Effect of Thiokol LP-3 blended and immersion temperature on the PVC crosslinking reaction: (○) 20°C; (●) 40°C; (●) 60°C. PVC–Thiokol blends, 0.3 mm thick, immersed in liquid ammonia for 60 min.

TABLE III
Shrinkage and Effect of the Stabilizer on Discoloration in Aging at 150°C

Blend	Stabilizer added in PVC blends, phr	Immersion temperature, °C ^a	THP-insolubles, %	Shrinkage, %	Color after aging at 150°C ^b		
					15 min.	30 min.	45 min.
PVC-Thiokol, 100:5 ^c	0	Not immersed	0	13	0	1	2
	0	50	99.9	1.8	3	4	4
	0	20	94.2	2.1	2	3	4
	1 (KS-40) ^d	20	78.3	2.5	0	1	2
PVC-Thiokol, 100:10 ^e	0	Not immersed	0	27.3	0	1	2
	1 (KS-40)	30	43.7	4.0	0	1-2	3
	1 (KS-20) ^f	30	89.2	6.6	1	2	3

^a Blends were immersed in liquid ammonia for 60 min.

^b 0, colorless; 1, pale brownish yellow; 2, pale brown; 3, brown; 4, black.

^c PVC-Thiokol LP-8 blends (100:5 parts by wt).

^d Organic thioin compound (Kyodo Yakuhin Co.).

^e PVC-Thiokol LP-8 blends (100:10 parts by wt) containing 10 parts of DOP

^f Dibutyltin laurate (Kyodo Yakuhin Co)

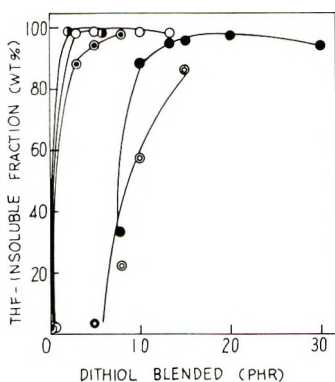


Fig. 2. Effect of the dithiol compound on the PVC crosslinking reaction: (○) LP-8; (●) LP-33; (●) LP-2; (⊙) LP-32; (◌) ethanedithiol. PVC-dithiol blends, 0.3 mm thick, immersed in liquid ammonia for 60 min at 50°C.

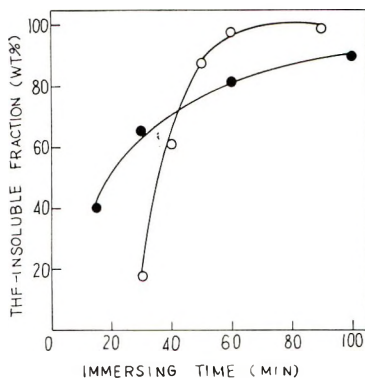


Fig. 3. Effect of immersion time on the PVC crosslinking reaction: (○) PVC-Thiokol LP-3 blends (100:5 by weight), 0.3 mm thick, immersed in liquid ammonia at 20°C; (●) PVC-Thiokol LP-3 blends (100:10 by weight) containing 30 parts hexamethylphosphoramide, 0.35 mm thick, immersed in 28% aqueous ammonia at 60°C.

Thiokol LP-3 and 30 parts of HMPA in aqueous ammonia, it seems most favorable to immerse the sheets in the medium at 60°C for 120 min (Figs. 3 and 4).

Liquid ammonia similarly accelerated the crosslinking of PVC-ethanedithiol blends or of PVC-Thiokol blends plasticized with some plasticizer (Figs. 2 and 5). A stabilizer such as metal stearate inhibited the crosslinking reaction, but no inhibition was observed with the organic tin compound (Table III).

The sulfur content in the residual gel of THF extraction is less than that in the original blends (Table IV). This may be due to the dissolution of the unreacted Thiokol into THF during extraction or into liquid ammonia during the reaction. The latter case is avoidable by saturating the liquid ammonia with sodium chloride.

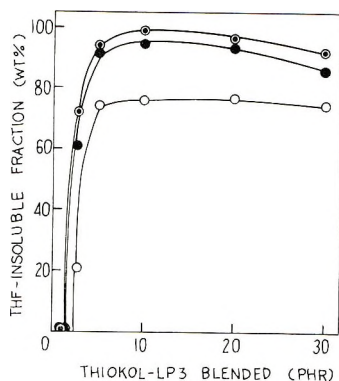


Fig. 4. Effect of Thiokol LP-3 blended and immersion temperature on the PVC crosslinking reaction: (○) 40°C; (●) 60°C; (⊙) 100°C. PVC-Thiokol blends containing 30 parts hexamethylphosphoramide, 0.3 mm thick, immersed in 28% aqueous ammonia for 120 min.

Crosslinking Reaction

The permeation of ammonia into PVC-Thiokol blends is facilitated by Thiokol which is compatible with PVC and liquid ammonia. Table IV shows that about one molecule of Thiokol combines with PVC to liberate two molecules of hydrogen chloride. The crosslinking reaction, dehydrochlorinated condensation, seems to occur through ionization of C-Cl and S-H due to the inductive effect of liquid ammonia of high polarity. Although the formation of crosslinkage through the addition of Thiokol to

TABLE IV
Relationship Between Hydrogen Chloride Liberated and Thiokol Combined with PVC on Immersion of the Blends in Liquid Ammonia

Original blends		THF-insoluble fraction of the uncross-linked PVC			
Thiokol blended with PVC, phr	S content, %	HCl liberated, mmole/- 100 g PVC ^a	THF-insolubles, %	S content, %	Thiokol combined, mmole/- 100 g. PVC ^b
0	0	0.28	0	0	0
5	1.82	5.24	98.1	1.02	2.32
10	3.47	10.20	98.2	2.08	4.81
10 ^c	3.47	0	0	No crosslinking occurs	
20	6.37	11.50	95.8	2.76	6.70

^a From PVC-Thiokol LP-3 blends, 0.3 mm thick, on immersion in liquid ammonia for 60 min at 60°C.

^b From the S content in the THF-insoluble fraction on the basis of the condition: one molecule of Thiokol condenses with PVC, liberating two molecules of HCl.

^c 10 parts of Thiokol LP-3 blended with 100 parts of dehydrochlorinated PVC^{5,6} and these blends were only heated in air bath for 60 min at 50°C.

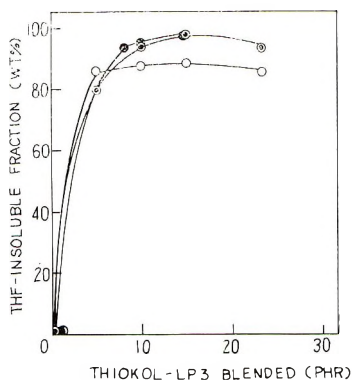


Fig. 5. Influence of plasticizer on the PVC crosslinking reaction: (●) tricresyl phosphate; (⊙) dioctyl phthalate; (○) trimellitate (Trimex T-10, Kao Soap Co.). PVC-Thiokol blends containing 10 parts of plasticizer, 0.3 mm thick, immersed in liquid ammonia for 60 min at 20°C.

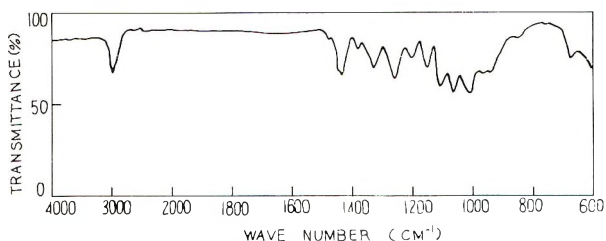


Fig. 6. Infrared spectrum of crosslinked PVC. Sample is THF-insoluble fraction of the crosslinked PVC prepared by immersion of PVC-Thiokol LP-3 blends (100:5 by weight) in liquid ammonia for 60 min at 30°C.

$>C=C<$ in PVC is possible,^{5,6} the results in Table IV show that this can be neglected.

In Figure 6 are illustrated the infrared absorption spectra of the THF-insoluble fraction obtained from the PVC-Thiokol blend after treatment in liquid ammonia. Four strong bands assigned to the ether linkage appear in the region of 1020–1150 cm^{-1} , this indicating that PVC and Thiokol has reacted.

Structure of Crosslinked PVC

Table V shows the average chain length between the crosslinks; M_c is evaluated from the values of V_2 in the Flory-Rehner equation,⁷ and M'_c , from the sulfur content in the THF-insoluble fraction on the basis of combination of Thiokol with PVC at certain intervals. In the system of PVC-Thiokol-HMPA-aqueous ammonia, the values of M_c and M'_c are approximately equal. In the system of PVC-Thiokol-liquid ammonia, however, M'_c is smaller than M_c when the Thiokol content is 10% or more. It appears probable that not all Thiokol blended participates in the crosslinking but some in the formation of side chains.

TABLE V
Average Molecular Weight Between Crosslinks Calculated from the Swelling Ratio or Sulfur Content in THF-Insoluble Fraction^a

Thiokol blended with PVC, phr	Thiokol combined with PVC, mole/(CH—CH) Cl × 100	Swelling ratio S_w	M'_c	V_2	M_c
5	0.140	4.87	44,700	0.1426	46,900
5 ^b	0.145	4.51	43,100	0.1541	42,000
10	0.188	4.43	33,200	0.1581	40,400
10 ^b	0.300	3.58	20,800	0.1990	19,500
30	0.405	4.20	15,420	0.1704	28,900
30 ^b	0.416	3.15	15,200	0.2300	14,200

^a Crosslinking performed by immersing PVC-Thiokol LP-3 blends in liquid ammonia for 60 min at 60°C.

^b Crosslinking also performed in 28% aqueous ammonia.

Properties of Crosslinked PVC

Stress-Strain Curves. Figure 7 shows typical stress-strain curves traced from the autograph chart. The curves *a* and *b*, respectively, refer to the control blends with and without addition of the plasticizer. A marked change in the stress-strain curves can be observed after crosslinking PVC with Thiokol with or without adding the plasticizer (curves *c* and *d*). The high modulus of *c* and *d* curves indicates that the crosslinking of PVC with Thiokol results in the improvement of PVC in regard to its toughness.

As shown in Figure 8 (*A* and *B*), the crosslinked PVC has peak tensile strength of 5.1–7.5 kg/mm² when 5–10% Thiokol is added. Further

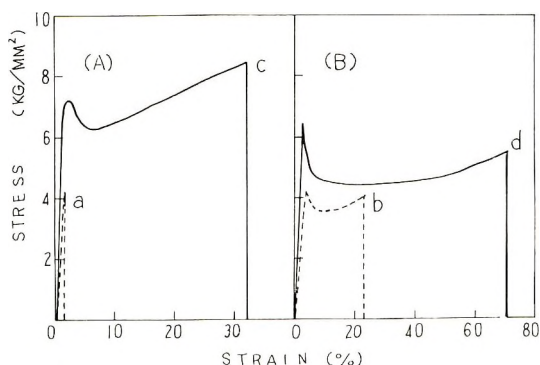


Fig. 7. Stress-strain relationship of (—) crosslinked PVC and (---) controls of the same composition: (A) PVC-Thiokol LP-8 blends (100:5 by weight); (B) PVC-Thiokol LP-8-dioctyl phthalate (100:5:10 by weight). Crosslinking was performed by immersing the blends in liquid ammonia for 60 min at 30°C.

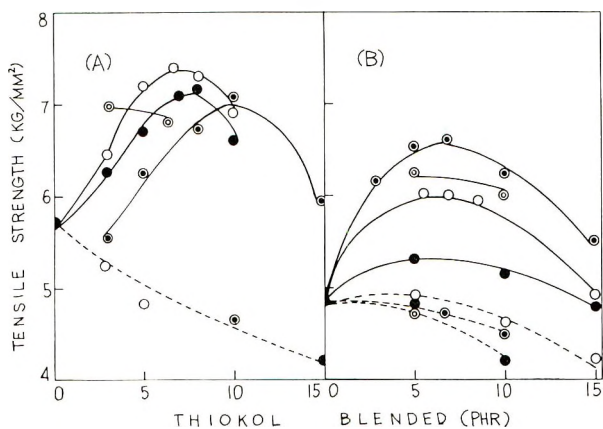


Fig. 8. Relationship between tensile strength and Thiokol blended: for (A) PVC-Thiokol blends and (B) PVC-Thiokol blends containing 10 parts of dioctyl phthalate: (O) LP-8; (◐) LP-3; (●) LP-33; (◑) ethanedithiol; (---) controls. Cross-linking was performed by immersion of the blends in liquid ammonia for 60 min at 30°C; tests were at 15°C.

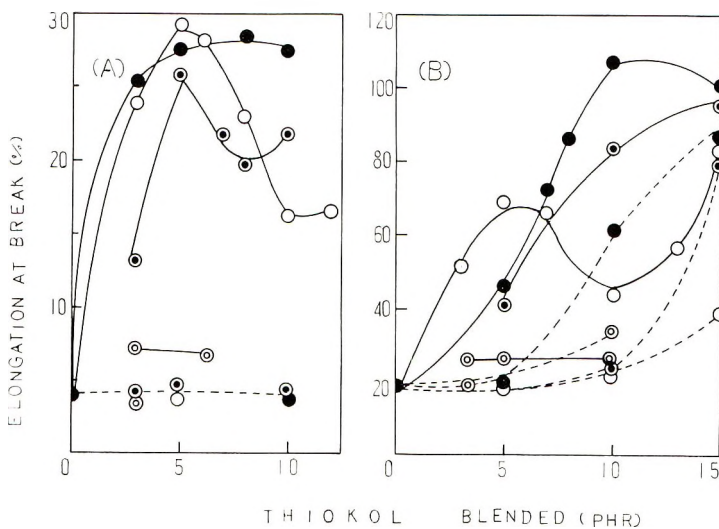


Fig. 9. Relationship between elongation at break and Thiokol blended. For symbols and conditions see Figure 8.

addition of Thiokol reduces the tensile strength. Similar tendencies are observed with the elongation, Young's modulus, folding endurance, and tensile impact (Figs. 9-12). The structure (chain length and branching) of the Thiokol blended significantly affects the shape of the curves.

In general, as the crosslink density increases in amorphous polymers, the elongation and swelling by solvents decrease, whereas the rigidity and zero-

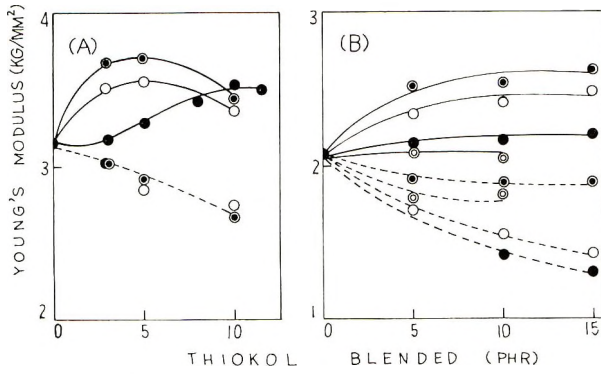


Fig. 10. Relationship between Young's modulus and Thiokol blended. For symbols and conditions see Figure 8.

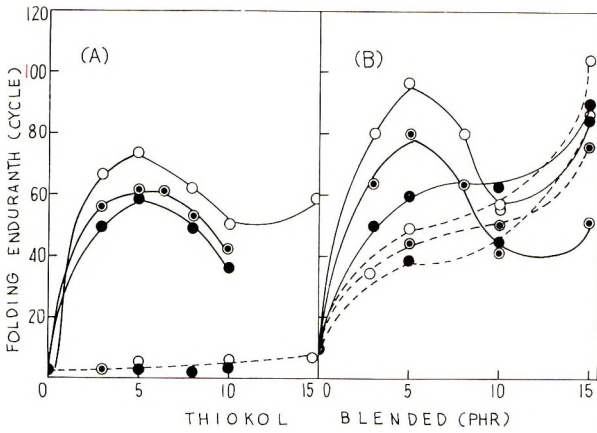


Fig. 11. Relationship between folding endurance and Thiokol blended. Specimens were 0.3-0.35 mm thick. For symbols and conditions see Figure 8.

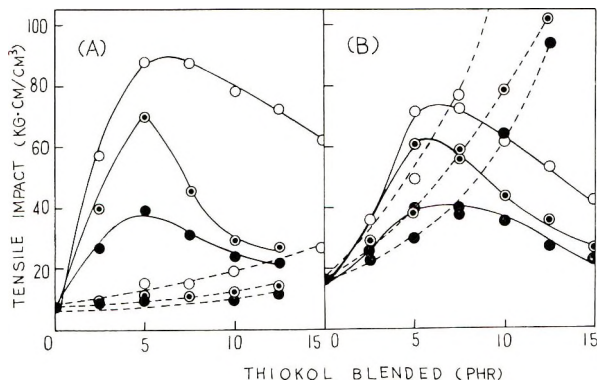


Fig. 12. Relationship between tensile impact strength and Thiokol blended. For symbols and conditions see Figure 8.

strength temperature increase. It is significant that, when PVC is cross-linked with the soft segment in liquid Thiokol, the elongation, zero-strength temperature, and tensile impact, in addition to the tensile strength, increase.

Folding Endurance and Tensile Impact. The crosslinked PVC containing no plasticizer shows considerably high folding endurance and tensile impact compared with the uncrosslinked controls (Figs. 11 and 12). With plasticizer, however, the crosslinked PVC is not remarkably improved in these properties as compared to the controls of the same composition.

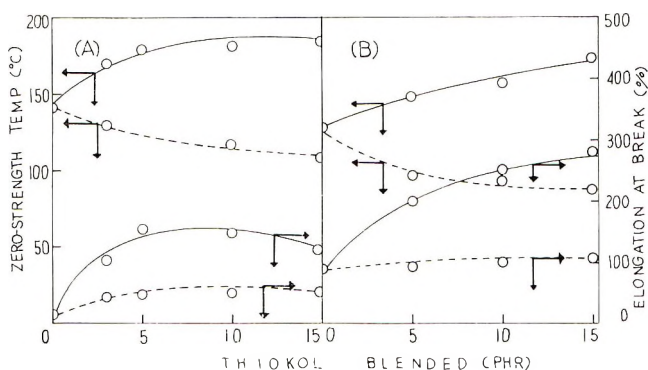


Fig. 13. Relationship between zero-strength temperature, elongation at break, and Thiokol LP-8 blended for (A) PVC-Thiokol blends; (B) PVC-Thiokol blends with 10 parts dioctyl phthalate.

Zero-Strength Temperature and Elongation. In Figure 13 are shown the elongation at break and the corresponding zero-strength temperatures of the crosslinked PVC and of the uncrosslinked controls. The addition of Thiokol up to about 5–10% results in an increase both in the elongation and in the zero-strength temperature.

Thermal Stability. The crosslinked PVC gives better dimensional stability at elevated temperatures as shown in Table III.

The crosslinked PVC is discolored (brown) on aging at 150°C more rapidly than the uncrosslinked controls. This may be avoided by immersing the samples in liquid ammonia at lower temperatures, 10–20°C., with the addition of the organic tin compound as the stabilizer. A slight decrease in the crosslinking efficiency is observed when an excess amount of the stabilizer is used. Metal stearate cannot be used as the stabilizer because, as mentioned already, the crosslinking reaction is markedly inhibited.

Thanks are given to Mr. K. Miyagi, Mr. M. Nishinomiya, Mr. Y. Chiba, and Mr. T. Yamada for their assistance in the experimental work.

References

1. Y. Nakamura, *Enkabiniru to Polima*, **7**, 11 (1967).
2. Y. Nakamura, *Kobunshi Kagaku*, **22**, 646 (1965).
3. W. Schöniger, *Microchim. Acta*, **1955**, 123.
4. P. S. Small, *J. Appl. Chem.*, **3**, 71 (1948).
5. K. Takemoto, *Kogyo Kagaku Zasshi*, **62**, 1934 (1959).
6. M. J. Hunter, *Ind. Eng. Chem.*, **40**, 1350 (1948).
7. P. J. Flory, *J. Chem. Phys.*, **18**, 108 (1950).

Received May 16, 1968

Kinetics of High-Intensity Electron-Beam Polymerization of a Divinyl Urethane

S. S. LABANA, *Applied Research Laboratory,
Ford Motor Company, Dearborn, Michigan 48121*

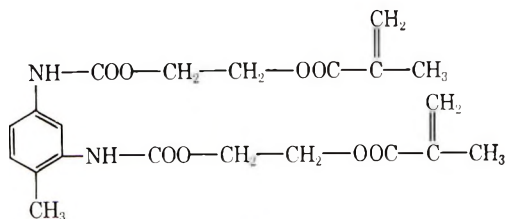
Synopsis

The kinetics of high-intensity electron beam-induced polymerization of di(2'-methacryloxyethyl)-4-*m*-phenylenediurethane during the network formation has been studied up to complete gelation and up to 56% conversion of unsaturation. From experimentally determined gel fractions, rate of disappearance of unsaturation, kinetic chain length, and intensity dependence, it is proposed that the polymerization takes place in a swollen network where the growing chains undergo unimolecular termination, and where gel-gel reaction is prohibited. The rate expression derived is: $\ln[\alpha(1-g)^{0.546}] = \ln \alpha_0 - 2.51k_p k_t / k_b$, where α is the total unsaturation and g is the gel fraction. The value of k_p/k_t is found to be 2.1 and that of G_B , the free radical yield per 100 eV absorbed, to be 16; these high values are ascribed to the high viscosity of the polymerizing system.

INTRODUCTION

The kinetics of radiation-initiated addition polymerizations of divinyl monomers during gel formation have received little attention: A statistical treatment is reported^{1,2} for crosslinking of unsaturated polyesters with an average of 11.6 double bonds per molecule, although the approach is inapplicable to polyester molecules with fewer than four double bonds.³ Network polymerization of polyester acrylates are described⁴⁻⁶ with respect to the mechanism of autoacceleration and the relation between the apparent reactivity and structure of polyesters, but kinetics beyond the autoacceleration stage are not presented. Copolymerization and gel formation of styrenated unsaturated esters are reported under a variety of radiation conditions, and the results for low-intensity x-rays are explained in terms of homogeneous free-radical reactions,⁷ although at the higher intensities the concepts of activated radicals and discrete volume elements are invoked.⁸

This paper describes the kinetics of the electron beam-initiated polymerization of the divinyl monomer, di(2'-methacryloxyethyl)-4-methyl-*m*-phenylenediurethane (I) during gel formation and up to 56% conversion of unsaturation.



I

EXPERIMENTAL

Materials

Monomer 2-hydroxyethyl methacrylate, from Rohm and Haas Company, was purified by vacuum distillation through a 10×1 in. column packed with glass helices, bp $58^\circ\text{C}/0.2$ mm, η_D^{25} 1.4505. Toluene diisocyanate (4-methyl-*m*-phenylene diisocyanate) mp 20 – 22°C , from Mathieson, Coleman and Bell, was used as received.

Di(2'-methacryloxyethyl)-4-methyl-*m*-phenylenediurethane was prepared by adding 4-methyl-*m*-phenylene diisocyanate (0.23 mole) to 2-hydroxyethyl methacrylate (0.5 mole) at a rate to maintain the temperature of the reaction mixture at 42 – 45°C . After the addition, the mixture was stirred at 45°C until infrared analysis showed complete reaction. The product was then dissolved in chloroform, washed four times with water, and the chloroform solution dried over anhydrous magnesium sulfate. Removal of the solvent gave a semisolid material ($T_g = 4^\circ\text{C}$, as determined by DTA method) which crystallized from 2-butanone to a white solid, mp 95°C .

The density of the monomer, measured by float-sink technique using mixtures of benzene and carbon tetrachloride, was found to be 1.031 g/ml at 25°C . The density of the gel was similarly found to be 1.248 g/ml.

The infrared spectrum showed the expected peaks at 3280, 1735, 1710, 1635, 1620, 1603, 945, 812, and 763 cm^{-1} . The ultraviolet absorption spectrum in ethanol solution showed peaks at $210\text{ m}\mu$ ($\epsilon = 8000$) and $242\text{ m}\mu$ ($\epsilon = 4000$).

ANAL. Calcd for $\text{C}_{21}\text{H}_{26}\text{N}_2\text{O}_8$: C, 58.01%; H, 6.04%; N, 6.47%. Found: C, 58.04%; H, 6.00%; N, 6.48%.

Polymerizations and Gel Fraction Measurements

A film of the monomer cast from acetone solution onto a sodium chloride plate was dried for 4 hr under 0.01 mm vacuum, then covered with a 0.025-mm thick Teflon film and clamped in an infrared cell mount. The cell assembly was evacuated at 0.01 mm for 1 hr then maintained in a nitrogen atmosphere for an additional hour. In case the material crystallized out, it was melted by gentle warming and cooled rapidly in a stream of nitrogen.

Polymerizations were conducted in the liquid state. After a small amount of polymer was formed, the material showed no tendency to crystallize, and the film remained transparent. The sample was irradiated with a 270-kV electron beam in a nitrogen atmosphere at a dose rate of 3.3 ± 0.2 Mrad/sec. The total dose absorbed was measured by using blue cellophane.⁹ The rate of polymerization was followed by noting the rate of disappearance of the "olefinic" 945 and 812 cm^{-1} peaks in the infrared, with the use of a Teflon film in the reference beam, and calculating absorbance from the peak height by the baseline technique.¹⁰ Both peaks yield the same rate data. The intensity of the aromatic absorption peak at 763 cm^{-1} was constant during the polymerization and hence served as an internal standard. Conversions were reproducible to $\pm 3\%$.

For gel fraction determinations, a weighed amount of monomer (about 0.5 g) was irradiated as a thin film on aluminum foil under a nitrogen atmosphere. The coated foil was rolled into a cylindrical shape and placed in a double thimble made of 100-mesh Monel wire cloth inside and 200 mesh wire cloth outside. The soluble fraction was extracted for 150 hr in a Soxhlet apparatus with acetone containing 1% ethyl mercaptan as inhibitor. The thimble with its contents was then dried to constant weight under vacuum at 65°C. The gel fraction was calculated from the weight loss after extraction. Gel fractions were reproducible to $\pm 7\%$.

RESULTS AND DISCUSSION

When exposed to a high-intensity electron beam, the diurethane (I) polymerizes rapidly; chain growth is accompanied by gel formation. Conversion of unsaturation versus time and dose, together with gel fraction data, are given in Table I and plotted in Figures 1 and 2.

TABLE I
Conversion of Unsaturation and Gel Fractions
as a Function of Time and Dose

Time, sec	Total dose, Mrad	Conversion, %	Gel fraction
0.1	0.33	15	0.05
0.3	0.99	23	0.15
0.6	1.98	28	0.26
1.2	3.96	35	0.49
1.8	5.94	40	0.62
2.4	7.92	44	0.72
3.0	9.90	47	0.79
3.6	11.88	49	0.85
4.2	13.86	51	—
4.8	15.84	53	0.94
5.4	17.82	55	—
6.0	19.80	56	1.00
7.2	23.76	57	—
8.4	27.72	58	—
9.6	31.68	59	—
10.8	35.64	60	—

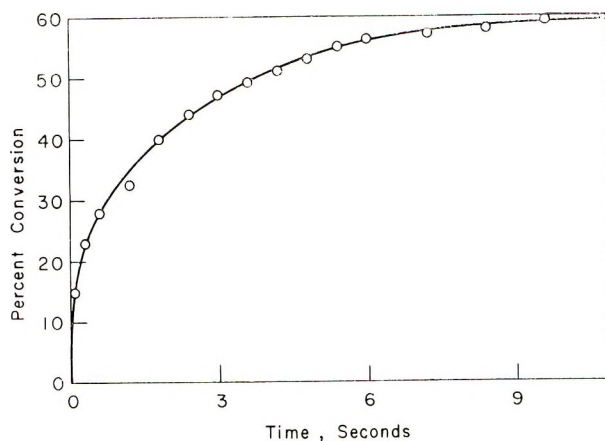


Fig. 1. Disappearance of unsaturation of I with 277 kV electron beam at 3.3 Mrad/sec.

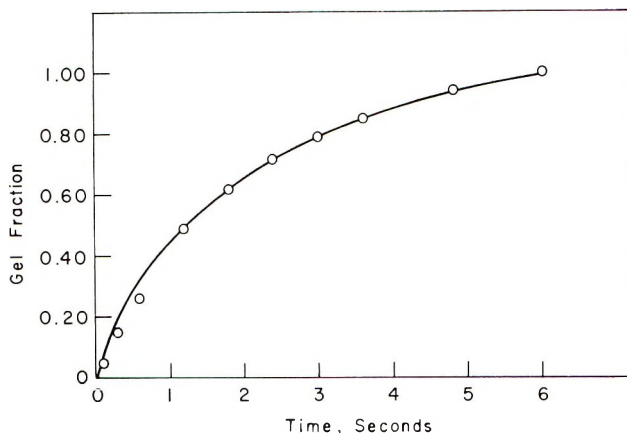


Fig. 2. Gel formation during polymerization of I with 277 kV electron beam at 3.3 Mrad/sec.

Rates were proportional to the intensity in the range of 0.8–3.3 Mrad/sec and independent of incremental exposure lengths; conversion depended only on the total dose absorbed. This is shown by additional conversion data given in Table II.

The residual unsaturation in the isolated gel changes only slightly with conversion (Table III), indicating that the reaction of gel radicals with gel double bonds is slow in comparison to the overall rate of polymerization; this slow reaction is attributed to the immobility of the gel radicals. The tight structure of the gel is shown by the absence of significant swelling in solvents like acetone, ethanol, and dimethylformamide.

The soluble polymer formed is of a low degree of polymerization (DP), presumably due to the high initiation rate. Thus, the molecular weight of the soluble polymer, extracted at 35% conversion (gel fraction = 0.5)

TABLE II
Conversion of Unsaturation as a Function of Time and Dose at Different Dose Rates

Dose rate, Mrad/sec	Time, sec	Total dose, Mrad	Conversion, %
0.83	0.2	0.17	8
	0.4	0.33	15
	1.2	1.00	22
	2.4	1.99	28
	4.8	3.98	34
1.66	9.6	7.97	45
	0.1	0.17	8
	0.2	0.33	16
	0.6	1.06	23
	1.2	1.99	28
	2.4	3.98	35
	4.8	7.97	44

TABLE III
Absorbance at 812 cm^{-1} in the Extracted Gel
Normalized to Equal Peak Height at 763 cm^{-1}

Exposure time, sec	Total dose, Mrad	Absorbance
0.6	1.98	0.490
1.2	3.96	0.470
1.8	5.94	0.480
2.4	7.92	0.460
3.0	9.90	0.460

and measured cryoscopically in dioxane, is 1900, which corresponds to a DP of 4.

Kinetic Scheme

It is assumed that: initiation by high-energy radiation takes place randomly in the sol and gel phases, polymerization takes place in network swollen with monomer, and termination is unimolecular. The kinetic scheme of eqs. (1)–(7) then is proposed for the polymerization of I:

Initiation:



Propagation:



Termination:



In these equations, g is the gel fraction, and therefore $(1 - g)$ is the sol fraction; \dot{S} and \dot{G} are a sol and a gel radical, respectively; S and G are double bonds in the sol and gel phases; k_i , k_p , and k_t are initiation, propagation, and termination rate constants, respectively. This approach is similar to that taken by Burlant and Hinsch^{7,8} and neglects any transfer mechanism.

Assuming steady-state conditions for reactive free radicals, eqs. (8) and (9) describe the concentrations of reactive radicals in the sol and gel phases:

$$d[\dot{S}]/dt = k_i(1 - g) - k_p[\dot{S}][G] - k_t[\dot{S}] = 0 \quad (8)$$

$$d[\dot{G}]/dt = k_i(g) + k_p[\dot{S}][G] - k_t[\dot{G}] = 0 \quad (9)$$

When eqs. (8) and (9) are solved for $[\dot{S}]$ and $[\dot{G}]$, there is obtained

$$[\dot{S}] = \frac{k_i(1 - g)}{k_p[G] + k_t} \quad (10)$$

$$[\dot{G}] = \frac{k_i(k_p[G]/k_t + g)}{k_p[G] + k_t} \quad (11)$$

The term $k_p[G]/k_t$ approximates an average kinetic chain length n . The rate of propagation, R_p , from the above is given by:

$$R_p = 2k_p[\dot{S}][S] + k_p[\dot{S}][G] + k_p[\dot{G}][S] \quad (12)$$

and the rate of termination, R_t , is:

$$R_t = k_t([\dot{S}] + [\dot{G}]) \quad (13)$$

which then leads to:

$$n = R_p/R_t = \frac{2k_p[\dot{S}][S] + k_p[\dot{S}][G] + k_p[\dot{G}][S]}{k_t([\dot{S}] + [\dot{G}])} \quad (14)$$

Equation (14) can be rewritten:

$$n = \frac{k_p([S] + [G])[\dot{S}]}{k_t([\dot{S}] + [\dot{G}])} + \frac{k_p[S](\dot{S} + \dot{G})}{k_t([\dot{S}] + [\dot{G}])} \quad (15)$$

since $[\dot{S}]$ is lost both by conversion to \dot{G} and by termination, while \dot{G} is lost only by the termination process, $[\dot{S}]$ is expected to be much less than $([S] + [\dot{G}])$. The first term in eq. (15) can, therefore, be neglected; and for an average value of n (around 4), where $[G] = [S]$, it reduces to:

$$n = k_p[G]/k_t \quad (16)$$

Substituting for $k_p[G]/k_t$ in eqs. (3) and (4) yields:

$$[\dot{S}] = k_t(1 - g)/[(n + 1)k_t] \quad (17)$$

$$[\dot{G}] = k_t(n + g)/[(n + 1)k_t] \quad (18)$$

If total unsaturation is represented by α , i.e., if

$$\alpha = [S] + [G] \quad (19)$$

then

$$[S] = (1 - g)\alpha \quad (20)$$

and

$$[G] = g\alpha \quad (21)$$

Rewriting eq. (21) and differentiating both sides with respect to time yields

$$\frac{1}{g} \frac{dg}{dt} = \frac{1}{[G]} \frac{d[G]}{dt} - \frac{1}{\alpha} \frac{d\alpha}{dt} \quad (22)$$

Based on the proposed mechanism, we can write

$$\frac{d[G]}{dt} = k_p[\dot{S}][G](n - 2) + k_p[\dot{G}][S](n - 1) \quad (23)$$

where a soluble chain is incorporated in the gel phase at an average DP of n . When a sol radical of n monomer units carrying $(n - 1)$ double bonds reacts with a gel double bond, there is a net gain of $(n - 2)$ double bonds in the gel phase. Similarly when a gel radical adds to a sol unit consisting of n monomer units and containing n double bonds, the gain in the gel phase is $(n - 1)$ double bonds.

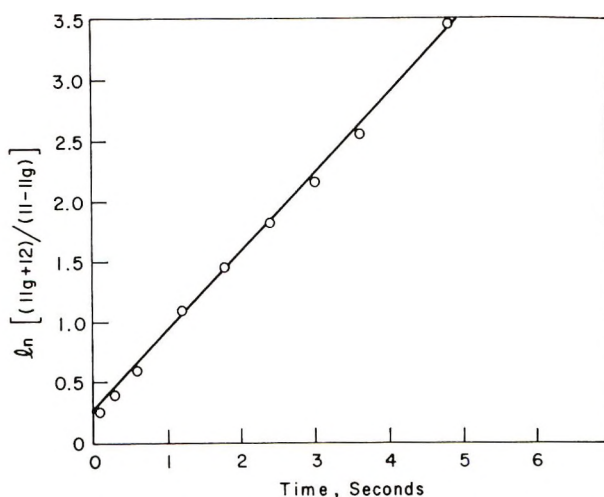


Fig. 3. Plot of $\ln[(11g + 12)/(11 - 11g)]$ vs. time according to eq. (28)

Substituting the values for $[\dot{S}]$ and $[\dot{G}]$ from eqs. (17) and (18) and for $[S]$ and $[G]$ from eqs. (20) and (21), eq. (23) becomes:

$$d[G]/dt = \left\{ k_p k_i / [(n+1)k_t] \right\} [(n-2)(1-g)g + (n-1)(n-g)(1-g)]\alpha \quad (24)$$

The rate of the disappearance of the total unsaturation is given by:

$$-d\alpha/dt = 2k_p[\dot{S}][S] + k_p[\dot{S}][G] + k_p[\dot{G}][S] \quad (25)$$

Introducing values of $[S]$, $[G]$, $[\dot{S}]$, and $[\dot{G}]$ from eqs. (17), (18), (20), and (21) into eq. (25) leads to:

$$-d\alpha/dt = [(n+2)/(n+1)](k_p k_i / k_t)(1-g)\alpha \quad (26)$$

On substituting for $d[G]/dt$ and $d\alpha/dt$ from eqs. (24) and (26) in eqs. (22) and simplifying, there is obtained:

$$dg/dt = \left\{ \frac{k_p k_i}{[(n+1)k_t]} \right\} [(n^2 - n) - (n^2 - 4n + 1)g - (3n - 1)g^2] \quad (27)$$

On substituting the experimentally found value of 4 for n and integrating, eq. (27) yields

$$\ln[(11g + 12)/(11 - 11g)] = 4.6At + \ln K_0 \quad (28)$$

or

$$g = (11K_0 e^{4.6At} - 12)/(11K_0 e^{4.6At} + 11) \quad (29)$$

where $A = k_p k_i / k_t$, and $\ln K_0$ is the constant of integration.

According to eq. (27), the present treatment can be evaluated by plotting $\ln[(11g + 12)/(11 - 11g)]$ against time using the experimental values of g ; a straight line is predicted with a slope of $4.6A$ and an intercept of $\ln K_0$. Figure 3 shows that, in fact, a straight line is obtained up to complete gelation of the material.

The above treatment can also be used to describe the rate of disappearance of unsaturation as functions of time and gel fraction. On substituting for g from eq. (29) and using the value (obtained from Fig. 3) of 1.35 for K_0 , when $n = 4$, eq. (26) becomes:

$$-d\alpha/dt = 2.51A\alpha/(K_0 e^{4.6At} + 1) \quad (30)$$

which on integration gives:

$$\alpha = K[1 + K_0 e^{4.6At}]^{0.545} e^{-2.51At} \quad (31)$$

where K is a constant.

From eq. (29) we have:

$$K_0 e^{4.6At} = [(11g + 12)/(11 - 11g)] \quad (32)$$

Combining eqs. (31) and (32) and simplifying:

$$\ln[\alpha(1-g)^{0.545}] = K_\alpha - 2.51At \quad (33)$$

where K_α is constant.

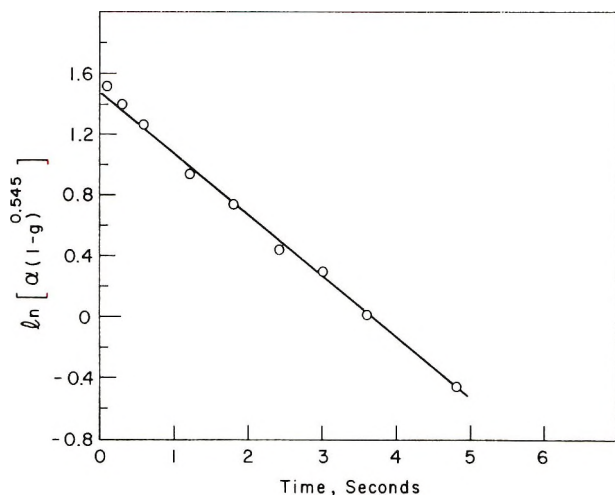


Fig. 4. Plot of $\ln[\alpha(1 - g)^{0.545}]$ vs. time according to eq. (34).

Now on using the known limits, i.e., $t = 0$, $g = 0$, and $\alpha = \alpha_0$ (α_0 being the initial unsaturation), eq. (33) becomes:

$$\ln[\alpha(1 - g)^{0.545}] = \ln \alpha_0 - 2.51At \quad (34)$$

Again according to eq. (34) a straight line should be obtained if $\ln[\alpha(1 - g)^{0.545}]$ is plotted against time. Such a linear plot, shown in Figure 4, indicates the reasonableness of the present scheme up to 56% conversion of unsaturation and complete gelation.

From the intercept on the ordinate in Figure 4, α_0 is found to be 4.50 mole/l., which is slightly lower than the value of 4.75 mole/l. for double bonds calculated by using the measured density of the monomer. This small discrepancy does not necessarily suggest any error in the theoretical concept but perhaps small (<5%) amount of polymerization at the beginning of the kinetic run.

Kinetic Parameters

The value of A , i.e., $k_p k_i / k_t$, is calculated from the slopes of the straight lines in Figures 3 and 4 to be $14.4 \pm 0.5 \times 10^{-2} \text{ sec}^{-1}$. The ratio k_p/k_t , obtained from eq. (16) by substituting the value of 4 for n and 1.89 mole/l. for $[G]$, is 2.1. This then gives a value for k_i of 6.8×10^{-2} mole/l.-sec. The free radical yield, G_R (the number of initiating radicals formed per 100 Ev of energy absorbed) calculated from this value of k_i is 16.

It is to be noted that the degree of polymerization n is held constant in this kinetic scheme, an assumption which may not be strictly valid. However, small changes in the value of n have little effect, as it appears both in the numerators and the denominators of the kinetic equations, and therefore tends to cancel out; this can be readily seen in eq. (26).

The value of k_p/k_t found in the present study is greater by a factor of 10^5 than the value generally encountered in conventional polymerization of monomers, such as methyl methacrylate, and is attributed to reduction in k_t due to the high viscosity of the polymerizing medium; in fact, termination rate constants decrease by a factor of 10^5 – 10^6 during the hardening of polyester acrylates.¹¹

A value of k_t can be estimated roughly from the growing chain concentration in the volume element swept out by a polymer radical: If the polymer radical has a sphere of mobility of 50 Å radius—a reasonable value for $DP = 4$ —then the volume accessible to this radical is $\frac{4}{3}\pi(50)^3 \times 10^{-27}$ l., and the total volume accessible to one mole of radicals is $\frac{4}{3}\pi(50)^3 \times 10^{-27} \times 6.02 \times 10^{23}$ or 326 l. The total free radicals formed by radiation in this volume is $326k_i$. The rate of termination R_t then is given by:

$$R_t = 326k_i([\dot{S}] + [\dot{G}]) \quad (35)$$

The rate of termination from the kinetic scheme is:

$$R_t = k_t([\dot{S}] + [\dot{G}]) \quad (36)$$

From eqs. (34) and (35), there is obtained:

$$k_t = 326k_i \quad (37)$$

Using 6.8×10^{-2} mole/l.-sec as the value for k_i gives k_t to be 22. Since $k_p/k_t = 2.1$, k_p in the present study is then 46, a value quite comparable to 54 noted for the propagation rate constant of methyl methacrylate at 70% conversion.¹²

The free-radical yield G_R of 16 is comparable to G_R value of 12 observed for methyl methacrylate at radiation dose rate of less than one rad per second. But with the increase in dose rate, G_R decreases in all monomers; for example, in case of methyl methacrylate G_R falls to 1.5 as the dose rate is increased to 296 rad/sec.¹³ The decrease in G_R at high intensities is generally explained by decrease in the efficiency of chain initiation owing to greater increase in radical-radical interaction. In the present work such a decrease in G_R is not observed because of low rate of radical-radical interaction in the viscous medium, a view consistent with very low value of k_t given above.

We express our appreciation to Drs. S. Gratch, W. J. Burlant, and E. Aronoff for helpful discussions during the course of this work.

References

1. A. Charlesby, *Proc. Roy. Soc. (London)*, **A241**, 495 (1957).
2. A. Charlesby, V. Wycherley, and T. T. Greenwood, *Proc. Roy. Soc. (London)*, **A244**, 54 (1958).
3. W. J. Burlant and J. Hirsch, *J. Polym. Sci.*, **61**, 303 (1962).
4. G. V. Korolev and A. A. Berlin, *Vysokomol. Soedin.*, **4**, 1654 (1962); *Polym. Sci. USSR*, **4**, 500 (1963).

5. G. V. Korolev and N. N. Tvorogov, *Vysokomol. Soedin.*, **6**, 1006 (1964); *Polym. Sci. USSR*, **6**, 1107 (1967).
6. G. V. Korolev, B. R. Smirnov, L. A. Zhiltsova, L. I. Makhonina, N. N. Tvorogov, and A. A. Berlin, *Vysokomol. Soedin.*, **A9**, 9 (1967); *Polym. Sci. USSR*, **9**, 8 (1967).
7. W. Burlant and J. Hinsch, *J. Polym. Sci.*, **A2**, 2135 (1964).
8. W. Burlant and J. Hinsch, *J. Polym. Sci.*, **A3**, 3587 (1965).
9. E. J. Henley and D. Richman, *Anal. Chem.*, **28**, 1580 (1956).
10. R. T. Conley, *Infrared Spectroscopy*, Allyn and Bacon, Boston, 1966, p. 210.
11. G. V. Korolev, B. R. Smirnov, and A. B. Volkhovitinov, *Vysokomol. Soedin.*, **4**, 1660 (1962); *Polym. Sci. USSR*, **4**, 506 (1963).
12. P. Hayden and H. Melville, *J. Polym. Sci.*, **43**, 201 (1960).
13. A. Chapiro, *J. Chim. Phys.*, **47**, 764 (1950).

Received April 26, 1968

Revised May 20, 1968

Extrathermodynamic Approach to the Study of the Adsorption of Organic Compounds by Macromolecules

CORWIN HANSCH and FRIEDERIKE HELMER, *Department of
Chemistry, Pomona College, Claremont, California 91711*

Synopsis

By using substituent constants and regression analysis, an analysis has been made of the binding of derivatives of aniline and acetanilide to nylon and rayon, the experimental data of Ward and Upchurch being used. The amount of organic compounds bound from an aqueous solution by these two types of synthetic macromolecules is shown to be related to the octanol-water partition coefficients P . In the case of the aniline derivatives, where the basicity of the compounds varied considerably, a good model describing binding results from the linear combination of the two parameters related to free energy, i.e., $\log P$ and ΔpK_a . The latter term is the difference between pK_a for aniline and a particular derivative. For the neutral acetanilides a simple linear free-energy relation between $\log P$ and $\log K$ is found. Of special note is the fact that the dependence of binding of these two classes of compounds to two classes of synthetic macromolecules as indicated by the coefficient with the $\log P$ term very closely parallels that found for a variety of biopolymers. The mechanism of hydrophobic binding seems to be the same in both the synthetic and natural polymers.

The adsorption of organic compounds by various substances, solid or liquid, has long been of interest to different groups of scientists. We have been concerned with the problem from the biochemical and pharmacological points of view.^{1,2} For the purpose of correlating chemical structure with the interaction of organic compounds with biopolymers, we have been exploring the extrathermodynamic approach³ employing thermodynamically-based substituent constants.^{4,5} Our working hypothesis has been that as a first approximation, the free-energy change (ΔF_{BR}°) in a standard biological response which could be attributed to a single chemical or physical reaction (such as binding to a macromolecule) can be factored⁶ as follows:

$$\Delta F_{BR}^\circ = \Delta F_{L/H}^\circ + \Delta F_{elect}^\circ + \Delta F_{steric}^\circ \sim \ln k_{BR} \quad (1)$$

In eq. (1), $\Delta F_{L/H}^\circ$ represents that portion of the free-energy change which can be attributed to hydrophobic bonding,^{7,8} ΔF_{elect}° represents the electronic contribution, and ΔF_{steric}° represents the spatial demands of reactants and products on the free-energy change. k_{BR} is a rate or equilibrium constant for the rate-limiting chemical or physical reaction which ultimately

causes an observed biological response. The effect of substituents on the free-energy change of a reference molecule can be represented as in eq. (2):

$$\delta_X \Delta F_{\text{BR}}^\circ = \delta_X \Delta P_{\text{L./H}}^\circ + \delta_X \Delta F_{\text{elect}}^\circ + \delta_X \Delta F_{\text{steric}}^\circ \sim \delta_X \log k_{\text{BR}} \quad (2)$$

One can use constants from model systems in a Hammett-type approach to evaluate the effect of substituents on k_{BR} :

$$\log k_{\text{BR}} \equiv \log 1/C_X = k\pi_X + \rho\sigma_X + k' E_{\text{SX}} + k'' \quad (3)$$

In eq. (3) C_X is the molar concentration of compound with substituent X producing an equivalent biological response such as ED_{50} or LD_{50} in a fixed time interval under standard conditions. The constants k , ρ , k' , and k'' are fixed for a given system and are evaluated by the method of least squares. $\pi = \log P_X - \log P_{\text{H}}$, where P_X is the octanol-water partition coefficient⁴ for a given derivative and P_{H} that for a parent compound and E_s is the Taft steric parameter. The parameters shown in eq. (3) are simply representative. Others could easily be formulated. In particular, E_s has been designed⁹ for intramolecular effects but may be of use in intermolecular interactions.¹⁰ In certain instances, higher order forms of eq. (3), such as eq. (4), can be expected to give better correlations.¹¹

$$\log k_{\text{BR}} = \log 1/C = a\pi + \rho\sigma + bE_s + c(\rho\sigma) + d(\pi E_s) + e(\sigma E_s) + f(\pi\sigma E_s) + g \quad (4)$$

The work at hand is a much less complex case, where instead of working with biological response determined by k_{BR} , the binding constant between small organic compounds and macromolecules is under consideration. This of course could be the simple physical equilibrium constant which could be the rate-determining factor in a biochemical inhibitory process.¹¹ For this reason we have been studying the use of eqs. such as (3) and (4) for correlating the binding of small molecules to biopolymers.¹²⁻¹⁴ Equation (5) illustrates

$$\log 1/C = 0.751 \log P + 2.301 \quad \begin{array}{l} n = 42 \\ r = 0.960 \\ s = 0.159 \end{array} \quad (5)$$

an example where a nonspecific binding, presumably hydrophobic in nature, is well correlated using partition coefficients (P) from the octanol-water reference system. In eq. (5), C is the molar concentration of organic compound¹⁵ necessary to produce a one-to-one complex with bovine serum albumin by equilibrium dialysis.¹³ The number of organic molecules studied is represented by n , r is the correlation coefficient, and s is the standard deviation from regression. The 42 different compounds correlated by eq. (4) include weakly basic aromatic amines, aliphatic alcohols and ketones, and bulky molecules such as 1-hydroxyadamantane and camphor-quinone.

Linear free-energy relationships between binding in other systems and $\log P$ are given in eqs. (6)–(10).

Binding of miscellaneous organic compounds by bovine hemoglobin:¹³

$$\log 1/C = 0.713 \log P + 1.512 \quad \begin{array}{l} n = 17 \\ r = 0.950 \\ s = 0.160 \end{array} \quad (6)$$

Binding of alcohols by ribonuclease:¹⁰

$$\log K = 0.504 \log P - 1.560 \quad \begin{array}{l} n = 4 \\ r = 0.999 \\ s = 0.012 \end{array} \quad (7)$$

Binding of RCOO^- by bovine serum albumin:¹⁰

$$\log K = 0.594\pi - 6.514 \quad \begin{array}{l} n = 5 \\ r = 0.966 \\ s = 0.213 \end{array} \quad (8)$$

Binding of Barbiturates by homogenized rabbit brain:¹¹

$$\log \% \text{ bound} = 0.526 \log P + 0.467 \quad \begin{array}{l} n = 4 \\ r = 0.992 \\ s = 0.056 \end{array} \quad (9)$$

Binding of penicillins by human serum:¹⁶

$$\log (B/F) = 0.488\pi - 0.628 \quad \begin{array}{l} n = 79 \\ r = 0.924 \\ s = 0.134 \end{array} \quad (10)$$

In eqs. (7) and (8), K is a binding constant. In eq. (10), B refers to per cent bound and F to per cent free. Although the methods of expressing binding in eqs. (5)–(10) are not all comparable with each other, the slopes of the equations are essentially covered by the rather narrow range of $0.6 \pm .1$. The more or less uniform slopes for a wide variety of molecules binding to such a varied group of biopolymers indicates a common mechanism of binding which, for convenience, one can call hydrophobic. No special electronic or steric terms (other than those contained in the octanol-water model) have been included.

The purpose of this report is to apply the above approach to the binding of organic compounds by synthetic polymers. There is considerable theoretical as well as practical advantage to be gained from quantitative correlation of chemical structure and binding and the great diversity of synthetic polymers provides interesting models for study. For our present purpose, the exceptional data of Ward and Upchurch¹⁷ provide an interesting case for analysis. From the data in Table I we have derived eqs. (11)–(14) for the binding of anilines to nylon and rayon. All of the anilines studied

$$\log K_{\text{nylon}} = 0.635 \log P - 7.384 \quad \begin{array}{l} n = 17 \\ r = 0.719 \\ s = 0.495 \end{array} \quad (11)$$

TABLE IA
Adsorption of Substituted Anilines on Nylon and Cellulose Triacetate

Compound	log P	ΔpK_a	log K_N		log K_R		$ \Delta \log K_N $	Obs.	Calcd. ^b	$ \Delta \log K_R $
			Obs.	Calcd. ^a	Obs.	Calcd. ^b				
Aniline	0.90	0.00	-7.155	-7.206	-6.569	-6.486	0.05	-6.569	-6.486	0.08
2-Methylaniline ^c	1.40	0.19	-7.000	-6.825	-6.357	-6.150	0.18	-6.357	-6.150	0.21
4-Methylaniline	1.39	-0.54	-7.301	-7.009	-6.283	-6.283	0.29	-6.301	-6.283	0.02
<i>N</i> -Methylaniline	1.66	-0.27	-6.620	-6.763	-6.036	-6.072	0.14	-6.036	-6.072	0.04
4-Chloroaniline ^c	1.77	0.60	-6.167	-6.474	-5.481	-5.850	0.31	-5.481	-5.850	0.37
2-Chloroaniline	1.59	1.94	-6.200	-6.276	-5.712	-5.730	0.08	-5.712	-5.730	0.02
<i>N</i> -Ethylaniline ^c	2.16	-0.53	-6.495	-6.491	-5.958	-5.813	0.00	-5.958	-5.813	0.15
2-Nitroaniline ^c	1.23	4.87	-6.041	-5.809	-5.547	-5.440	0.23	-5.547	-5.440	0.11
<i>N,N</i> -Dimethylaniline	2.31	-0.48	-6.284	-6.378	-5.674	-5.714	0.09	-5.674	-5.714	0.04
3,4-Dichloroaniline ^c	2.81	1.80	-5.365	-5.493	-4.992	-5.014	0.13	-4.992	-5.014	0.02
4-Nitroaniline	1.39	3.56	-5.958	-6.018	-5.469	-5.570	0.06	-5.469	-5.570	0.10
<i>N</i> -Butylaniline ^c	3.16	-0.37	-5.848	-5.783	-5.184	-5.178	0.07	-5.184	-5.178	0.01
2,4-Dinitroaniline ^c	1.51	3.98	-5.712	-5.836	-5.248	-5.424	0.12	-5.248	-5.424	0.18
<i>N</i> -Phenylaniline ^c	3.03	3.68	-4.783	-4.892	-4.620	-4.554	0.11	-4.620	-4.554	0.07
<i>N</i> -Benzylaniline ^c	3.59	0.36	-5.461	-5.319	-4.710	-4.791	0.14	-4.710	-4.791	0.08
2,5-Dichloroaniline ^c	2.57	3.05	-5.423	-5.352	-4.951	-4.942	0.07	-4.951	-4.942	0.01
2,3-Dichloroaniline ^c	2.57	3.05	-5.462	-5.352	-5.143	-4.942	0.11	-5.143	-4.942	0.20

^a Calculated by using eq. (13).

^b Calculated by using eq. (14).

^c Calculated values assuming additivity of π of log P .

TABLE IB
Adsorption of Substituted Acetamides on Nylon and Cellulose Triacetate

Compound	log <i>P</i>	σ^s	log <i>K_N</i>		log <i>K_R</i>		Δ log <i>K_R</i>
			Obs.	Calcd. ^b	Obs.	Calcd. ^c	
Acetanilide	1.16	0.000	-6.678	-6.357	-6.495	-6.270	0.23
4-Hydroxyacetanilide ^d	0.55	-0.363	-6.602	-6.777	-6.886	-6.781	0.11
4-Aminoacetanilide	-0.07	-0.660	-7.222	-7.205	-7.301	-7.300	0.00
4-Chloroacetanilide	1.86	0.227	-5.925	-5.872	-5.578	-5.685	0.11
4-Nitroacetanilide	1.40	0.780	-5.992	-6.190	-5.662	-6.079	0.41
4-Bromoacetanilide	2.18	0.232	-5.762	-5.651	-5.482	-5.417	0.07
3,4-Dichloroacetanilide	2.62	0.600	-5.218	-5.347	-5.166	-5.048	0.12

^a Values from the compilation of H. H. Jaffé.

^b Calculated by using eq. (18).

^c Calculated by using eq. (19).

^d Calculated values assuming additivity of π and log *P*.

$$\log K_{\text{nylon}} = 0.669(\pm 0.12) \log P + 0.242(\pm 0.05) \Delta pK_a - 7.808(\pm 0.27)$$

$$\begin{aligned} n &= 17 \\ r &= 0.974 \\ s &= 0.167 \end{aligned} \quad (12)$$

$$\log K_{\text{rayon}} = 0.582 \log P - 6.727$$

$$\begin{aligned} n &= 17 \\ r &= 0.789 \\ s &= 0.367 \end{aligned} \quad (13)$$

$$\log K_{\text{rayon}} = 0.607(\pm 0.10) \log P + 0.174(\pm 0.04) \Delta pK_a - 7.033(\pm 0.24)$$

$$\begin{aligned} n &= 17 \\ r &= 0.970 \\ s &= 0.150 \end{aligned} \quad (14)$$

by Ward and Upchurch were included in the derivation of the eqs. (11)–(14) except 2-nitro-4-chloroaniline for which no pK_a value could be found. Ward and Upchurch showed from a study of adsorption isotherms that the amount of solute in micromoles absorbed per gram of adsorbent, (X/m), was related to the equilibrium concentration C as follows:

$$X/m = KC^{1/n}$$

Since the adsorption on nylon and the cellulose triacetate was linear, $n = 1$, Ward and Upchurch selected an arbitrary equilibrium concentration ($0.2 \times 10^{-4}M$) and used the X/m value at this concentration as a numerical expression for k . Comparison of eq. (11) with eq. (12) and eq. (13) with eq. (14) indicates that the electronic role of the substituent is quite important. The parameter, ΔpK_a , is defined as:

$$\Delta pK_a = pK_a(\text{aniline}) - pK_a(\text{substituted aniline})$$

Thus it is analogous to the Hammett σ constant, and a positive coefficient with the ΔpK_a term means that electron-withdrawing substituents increase binding. The mechanistic interpretation of this would seem to be that as the lone pair electrons are made less available for interaction with water, the anilines become more hydrophobic and are more tightly bound to the nylon. This effect of electron withdrawal on hydrophobicity has been previously noted. The inclusion of an additional term in $\log P \cdot \Delta pK_a$ [such as the interaction terms of eq. (4)] in eqs. (12) and (14) did not result in a significant reduction in the variance. The figures in parentheses are the 95% confidence intervals.

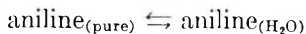
Ward and Upchurch¹⁷ showed that binding of the anilines to nylon was in part correlated with their water solubility. From their data we have formulated eqs. (15) and (16) for comparison with eqs. (12) and (14). In eqs. (15) and

$$\log K_{\text{nylon}} = 0.638 \log 1/S - 7.338 \quad \begin{aligned} n &= 17 \\ r &= 0.866 \\ s &= 0.357 \end{aligned} \quad (15)$$

$$\log K_{\text{rayon}} = 0.554 \log 1/S - 6.622 \quad \begin{array}{l} n = 17 \\ r = 0.898 \\ s = 0.263 \end{array} \quad (16)$$

(16), S represents the molar solubility in 2% ethanol. Equation (15) rationalizes 75% of the variance in the data ($r^2 = 0.75$) while eq. (12) accounts for 95% of the variance. Equation (16) accounts for 81% of the variance while eq. (14) explains 94%.

What are the reasons for the improved correlations obtained with the additional $\text{p}K_a$ term? In effect, $\log 1/S$ is a partitioning term. It is an equilibrium constant for the case:



We have shown¹⁹ that there is indeed a high correlation between $\log 1/S$ for liquids and $\log P$ as illustrated in eq. (17).

$$\log 1/S = 1.214 \log P - 0.850 \quad \begin{array}{l} n = 140 \\ r = 0.955 \\ s = 0.344 \end{array} \quad (17)$$

While there is a good linear relation between $\log 1/S$ and $\log P$ for liquids, we have found¹⁸ that such correlations do not usually obtain for solids. More than simple nonspecific partitioning is involved in the ΔG of transfer of a molecule from its highly oriented position in the crystal to that in solution. Thus, while simple partitioning is probably the main process involved in binding of anilines from water to rayon or cellulose acetate, $\log 1/S$ is not the best free-energy related term to use as a model for evaluating the binding.

The importance of the $\Delta \text{p}K_a$ term in eqs. (12) and (14) arises from the fact that $\log P$ values are for the un-ionized form of the anilines.⁴ Of particular interest are the coefficients associated with $\log P$ terms in eqs. (12) and (14). These are quite close to those in eqs. (5)–(10) and bring out the surprisingly narrow range of dependence of binding to macromolecules of a wide range on $\log P$.

Ward and Upchurch also reported on the binding of substituted acetanilides. From these data we have formulated eqs. (18) and (19). Although

$$\log K_{\text{nylon}} = 0.691(\pm 0.23) \log P - 7.157(\pm 0.37) \quad \begin{array}{l} n = 7 \\ r = 0.961 \\ s = 0.203 \end{array} \quad (18)$$

$$\log K_{\text{rayon}} = 0.837(\pm 0.26) \log P - 7.241(\pm 0.42) \quad \begin{array}{l} n = 7 \\ r = 0.967 \\ s = 0.227 \end{array} \quad (19)$$

binding was reported for 14 derivatives, we are able to treat only 7 because of the lack of suitable parameters for the interaction of *ortho* substituents and *N*-substituents; that is, we cannot calculate $\log P$ from the parent molecule. Special electronic interaction does not appear to occur since the addition of an electronic term (σ) to eq. (18) or (19) does not improve the

correlation. This is to be expected since the lone pair electrons are already so delocalized in the amide bond that they have relatively little tendency to react with water or the polymer.

Comparisons with $\log 1/S$ are made in eqs. (20) and (21). Again, it is clear

$$\log K_{\text{nylon}} = 0.573 \log 1/S - 7.436 \quad \begin{array}{l} n = 7 \\ r = 0.818 \\ s = 0.424 \end{array} \quad (20)$$

$$\log K_{\text{rayon}} = 0.758 \log 1/S - 7.715 \quad \begin{array}{l} n = 7 \\ r = 0.897 \\ s = 0.391 \end{array} \quad (21)$$

from a comparison of eq. (18) with eq. (20) and of eq. (19) with eq. (21) that $\log P$ is a much more suitable parameter than $\log 1/S$. Ward and Upchurch also reported on the binding of a set of carbamates. However, suitable constants are not available to treat these data.

The above results do indicate that the extrathermodynamic method using physico-chemical parameters³ can be used to rationalize the binding of small molecules by synthetic as well as natural macromolecules. It is our belief that through the use of equations such as eq. (3) or eq. (4) based on the models of eqs. (1) and (2) one can, via regression analysis, obtain considerable information about intermolecular interactions. In particular, this approach should be of help in elucidating in quantitative terms some of the details of the dyeing process.

This work was supported by NIH grant GM-07492.

References

1. C. Hansch and T. Fujita, *J. Amer. Chem. Soc.*, **86**, 1616 (1964).
2. C. Hansch, *Ann. Repts. Med. Chem.*, **1966**, 347.
3. J. E. Leffler and E. Grunwald, *Rates and Equilibria of Organic Reactions*, Wiley, New York, 1963.
4. T. Fujita, J. Iwasa, and C. Hansch, *J. Am. Chem. Soc.*, **86**, 5175 (1964).
5. C. Hansch and S. M. Anderson, *J. Org. Chem.*, **32**, 2583 (1967).
6. C. Hansch and E. W. Deutsch, *Biochim. Biophys. Acta*, **112**, 381 (1966).
7. W. Kauzmann, *Advan. Protein Chem.*, **14**, 37 (1959).
8. G. Némethy, *Angew. Chem.*, **6**, 195 (1967).
9. M. Newman, *Steric Effects in Organic Chemistry*, Wiley, New York, 1956, p. 556.
10. C. Hansch, *Farmaco*, **23**, 293 (1968).
11. C. Hansch and S. M. Anderson, *J. Med. Chem.*, **10**, 745 (1967).
12. C. Hansch, E. W. Deutsch, and R. N. Smith, *J. Am. Chem. Soc.*, **87**, 2738 (1965).
13. C. Hansch, K. Kiehs, and G. L. Lawrence, *J. Amer. Chem. Soc.*, **87**, 5770 (1965).
14. K. Kiehs, C. Hansch, and L. Moore, *Biochemistry*, **5**, 2602 (1966).
15. F. Helmer, K. Kiehs, and C. Hansch, *Biochemistry*, in press.
16. A. E. Bird and A. C. Marshall, *Biochem. Pharmacol.*, **16**, 2275 (1967).
17. T. M. Ward and R. P. Upchurch, *J. Agr. Food Chem.*, **13**, 334 (1965).
18. C. Hansch and F. Helmer, unpublished data.
19. C. Hansch, J. E. Quinlan, and G. Lawrence, *J. Org. Chem.*, **33**, 347 (1968).

Received April 15, 1968

Revised May 20, 1968

Thermal Degradation of Copolymers of Methyl Methacrylate and Methyl Acrylate. I. Products and General Characteristics of the Reaction

N. GRASSIE and B. J. D. TORRANCE,* *Chemistry Department,
The University of Glasgow, Glasgow, Scotland*

Synopsis

The technique of thermal volatilization analysis (TVA), applied to methyl methacrylate-methyl acrylate copolymers having molar composition ratios 112/1, 26/1, 7.7/1, and 2/1, has demonstrated that the stabilization of poly(methyl methacrylate) by copolymerized methyl acrylate is due to inhibition of the depolymerization initiated at terminally unsaturated structures, probably by direct blockage by methyl acrylate units. The molecular weight of the copolymers decreases rapidly during degradation, suggesting that a random scission process is involved. The products of degradation consist of the monomers, carbon dioxide, chain fragments larger than monomer, and a permanent gas fraction which is principally hydrogen. Infrared and ultraviolet spectral measurements suggest that the residual polymer, which is colored, incorporates carbon-carbon unsaturation. The complete absence of methanol among the products is surprising in view of its abundance among the products of degradation of poly(methyl acrylate). These observations have been accounted for qualitatively in terms of acceptable polymer behavior.

A recent series of papers¹⁻⁴ has been concerned with the study of degradation processes in copolymers. In a summary of this and previous work⁵ it was shown that this kind of investigation not only helps to clarify the degradation processes which occur in the homopolymers of the constituent monomers but also to demonstrate the mechanism whereby a small amount of a comonomer may influence the stability of a polymer either favorably or adversely.

Acrylates are used commercially in this way to stabilize poly(methyl methacrylate). The small concentrations used have no significant influence on the useful physical properties of the parent polymer. The mechanism of this stabilization and the way in which the acrylate units influence the ultimate breakdown process have not been reported upon. This and the following paper⁶ represent the first stage of a study of the degradation properties of methacrylate-acrylate systems and continue the wider systematic investigation of degradation reactions in copolymers.

* Present address: Research Department, Courtaulds Ltd., Coventry England.

EXPERIMENTAL

Preparation of Copolymers

Methyl methacrylate (MMA) (I.C.I. Ltd.) and methyl acrylate (MA) (B.D.H. Ltd.) were purified by standard methods involving washing with caustic soda solution to remove inhibitor, washing with distilled water to remove residual caustic soda, drying over anhydrous calcium chloride, and distilling under vacuum, the first and last 10% being eliminated. Thereafter the monomers were stored in the dark at -18°C until used. The polymerization initiator, 2,2'-azoisobutyronitrile was purified by recrystallization from methanol.

The reactivity ratios, $r_a = 1.8$, $r_b = 0.35$ (where A is MMA; B is MA), previously determined by nuclear magnetic resonance spectroscopic methods,⁷ were used to calculate the proportions of the monomers required to prepare polymers of appropriate composition. The monomers, purified as above, were distilled twice more under vacuum before distilling into dilatometers, containing 0.075% (w/v) of initiator, which were sealed off under vacuum. Copolymerizations were carried to approximately 5% conversion in a thermostat at 65°C . The resulting copolymers were precipitated three times from chloroform solution by methanol, dried in a vacuum oven at 50°C for 24 hr and ground to a fine powder (120 mesh). Copolymers with MMA and MA in the molar ratios 112/1, 26/1, 7.7/1, and 2/1 were thus prepared.

Degradation Techniques

Degradations were carried out in the apparatus illustrated in Figure 1. Samples of the powdered copolymers (2–4 mg) were spread evenly on the bottom of glass tube A, which was a Quickfit FG 35 flange with the end sealed and flattened. It was heated by immersion in an electrically heated and thermostatted Wood's metal bath. The temperature of the inside surface of the degradation tube was calibrated against the bath temperature by checking the melting points of pellets of pure tin, bismuth and antimony (232 , 271 , and 327°C respectively). The water-cooled copper coil B, protected the grease of the flange from the heat of the bath.

The volume of the section bounded by taps T_1 , T_2 , and T_3 , including the Macleod gauge, and of the reaction vessel to T_1 were measured by the standard method of expanding a known volume of gas, in a reservoir attached to the apparatus, into these sections in turn and observing the change in pressure. The total volume to T_2 and T_3 was of the order of 325 ml, varying with the various tubes, A, which were used from time to time.

Permanent gases formed during degradation were estimated from the increase in pressure observed during degradation with T_2 closed and C immersed in liquid nitrogen. They were analyzed for carbon monoxide, hydrogen, and methane by methods previously described.⁸ With C at -78°C the additional pressure was due to carbon dioxide which was

checked by absorption on soda asbestos (B.D.H. Ltd., microanalytical reagent) in D. Products not volatile at -78°C but volatile at room temperature were distilled into the calibrated capillary E and stored at -18°C . They consisted of the monomers and were analyzed by standard gas-liquid chromatography techniques by use of a Perkin-Elmer Fractometer. Methanol was sought in this fraction but never found. Products involatile at room temperature, which had condensed on the area of the reaction

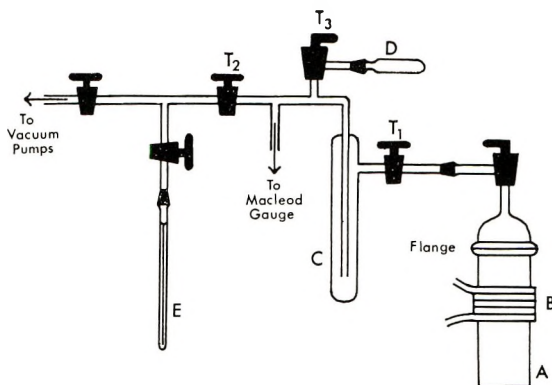


Fig. 1. Degradation apparatus.

vessel cooled by B, were estimated by weighing the reaction vessel before and after their removal by solvent.

Thermal volatilization analyses were carried out on equipment which has already been described in detail by McNeill.⁹

Molecular Weights

Number-average molecular weights were measured by using a Mechrolab high-speed membrane osmometer. The molecular weights of the poly(methyl methacrylate) (PMMA) and the 112/1, 26/1, 7.7/1 and 2/1 copolymers were 82×10^4 , 60×10^4 , 60×10^4 , 42.5×10^4 , and 37×10^4 , respectively.

Spectroscopic Measurements

Infrared spectra were obtained by using a Perkin-Elmer 237 spectrophotometer. Materials of lower MA content were used in the form of a film mounted between brass rings to prevent warping. For copolymers of higher acrylate contents and for degradation residues, films were deposited on NaCl plates from chloroform solution, the last traces of solvent being removed by heating at 50°C in a vacuum oven for 24 hr.

Ultraviolet spectra were obtained by using a Unicam model SPS00 spectrophotometer with the polymer either in the form of film or in chloroform solution.

RESULTS AND DISCUSSION

Thermal Volatilization Analysis

Thermal volatilization analysis thermograms for 25-mg samples of PMMA and the four copolymers are compared in Figure 2. Below 200°C the evolution of occluded volatile material is observed as the polymer melts and softens. At higher temperatures there are two obvious trends in the characteristics of evolution of volatile products of degradation as the MA content of the copolymer is increased. First, the peak in the vicinity of 280°C progressively decreases. Second, the maximum of the main peak moves to higher temperatures. It is obvious from these thermograms that volatilization occurs at an appreciable rate at temperatures above 260°C, so that the temperature range 260–300°C may be most convenient for isothermal studies.

The volatilization thermogram for PMMA, in Figure 2, has previously been accounted for^{9,10} in terms of the known degradation properties of this material. The lower temperature peak is the result of depolymerization initiated at unsaturated terminal structures. The peak at higher temperature is the result of depolymerization initiated by random scission of the polymer molecules.

In the light of previous work on the influence of comonomers on the degradation properties of PMMA²⁻⁴ there are two possible explanations of the progressive decrease in the amount of chain terminally initiated depolymerization as the MA content of the copolymer is increased. The first

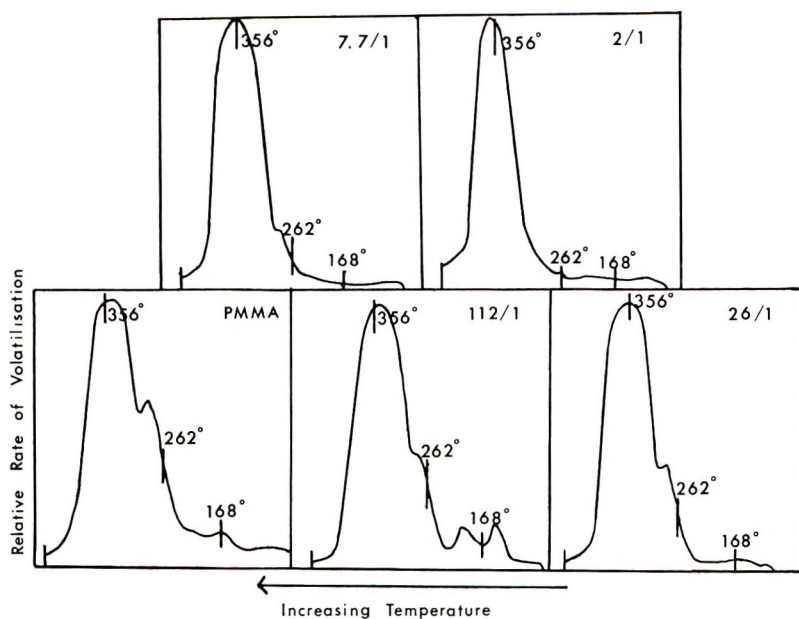


Fig. 2. Thermal volatilization analysis thermograms of poly(methyl methacrylate) and methyl methacrylate-methyl acrylate copolymers.

TABLE I
 Composition of Volatile Products of Degradation

Polymer	Composition, % by weight of total volatiles					
	CO ₂	Permanent gases	Methanol	MMA	MA	Chain fragments
PMMA	—	—	—	>96	—	—
112/1	Trace	—	—	>96	—	Trace
26/1	<1	Trace	—	93	0.8	5
7.7/1	>1	0.1	—	87	2.5	10
2/1	3	0.4	—	64	7.0	25
PMA ^a	7.5	1	15	—	0.76	75

^a Data of Madorsky.¹³

and most obvious explanation is that, as in MMA copolymers with acrylonitrile,³ units of the second monomer block the passage of chain depolymerization. Blocking of this kind is certainly not complete since monomeric MA does appear among the reaction products. The constant ratio throughout the range of copolymer compositions studied, of one MA unit in four being liberated as monomer (see Table I) may be some measure of the blocking efficiency in the temperature range of the randomly initiated reaction. The blocking efficiency at the lower temperature at which the terminally initiated reaction occurs should be very much greater as in acrylonitrile copolymers.⁴

It is not possible to make quantitative deductions from monomer ratio data alone, however, since the MA-terminated radical which results from this kind of blocking must ultimately undergo some further reaction which may complicate the situation.

The second explanation of the suppression of the terminally initiated reaction is that, as in the copolymerization of MMA and styrene,^{2,11} the presence of the second monomer favors combination rather than disproportionation as the termination step. In this way the proportion of terminally unsaturated structures is drastically reduced even in copolymers containing quite small proportions of styrene. An assessment of this possibility cannot be made for the MMA-MA system, however, since the relevant copolymerization data are not available. The tendency for the high temperature peak to move to higher temperatures with increasing MA content favors the first theory. Thus it can be accounted for in terms of a progressive decrease in the amount of monomer produced per initiation. This chain or zip length for depolymerization should not vary with copolymer composition if the second theory applies to the complete exclusion of the first.

Thus it is clear that the progressive suppression of the low temperature peak in the volatilization thermograms in Figure 2 can be accounted for qualitatively in terms of blocking by MA units, although some contribution to the effect by a decrease in the proportion of unsaturated chain ends formed during copolymerization cannot be entirely eliminated.

Changes in Molecular Weight

Figure 3 illustrates the changes which occur in the molecular weight of the 26/1 copolymer during degradation in the temperature range 282–326°C. The other copolymers behave similarly. Although this behavior is characteristic of a random scission process it cannot be taken as evidence in favor of the random initiation reaction discussed above, since the large chain fragments which are seen in Table I to be a major product of degradation of the copolymers must be formed in transfer reactions of the type which also lead to chain scission during the thermal degradation of poly-(methyl acrylate) (PMA).

All the copolymers remain completely soluble, even after extensive degradation, which contrasts with the tendency to gel formation in PMA.¹²

A close association between chain scission and the production of carbon dioxide is demonstrated in the following paper.⁶

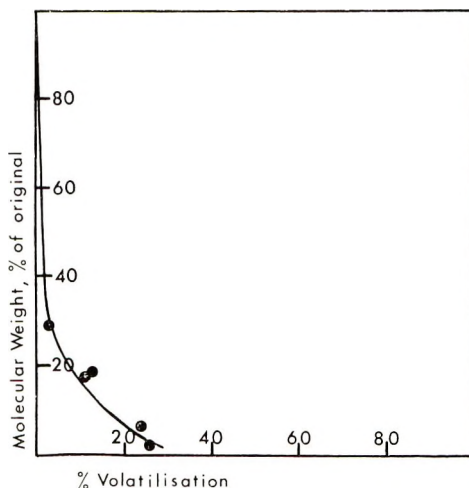


Fig. 3. Molecular weight changes during degradation of 26/1 methyl methacrylate-methyl acrylate copolymer.

Volatile Products of Degradation

The compositions of the volatile products of degradation of the copolymers and the two homopolymers are compared in Table I. Each of the results quoted represents an average of 3–5 experiments carried to relatively high extents of volatilization in the temperature range 260–300°C. The permanent gas fraction is found to consist of hydrogen with traces of methane and carbon monoxide.

The yields of chain fragments, carbon dioxide, and permanent gases are approximately as one would predict from the copolymer compositions and the behaviors of the homopolymers. There are, however, at least two major deviations between the pattern of products predicted in this way and

the actual experimental results. First, no methanol is obtained from any of the copolymers in spite of the high yield from PMA. Thus, because the yield of carbon dioxide is proportional to the MA content, it seems that carbon dioxide and methanol are produced in two completely separable reactions. This is perhaps surprising, since the methanol and carbon dioxide must both be associated with decomposition of the ester group in the MA unit. Secondly, MA is obtained from the copolymers in large amounts than might be expected from the behavior of PMA. This was previously

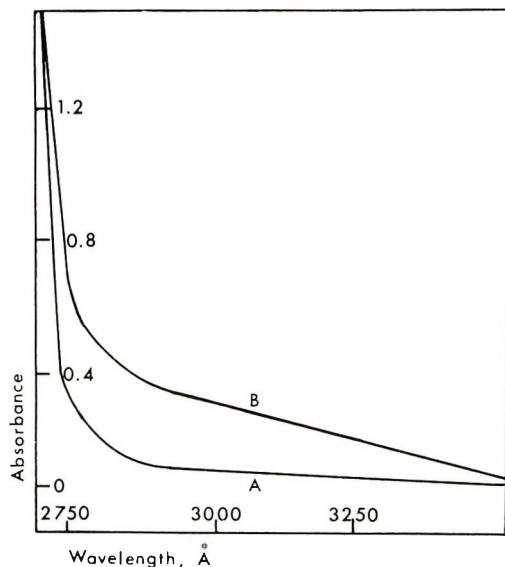


Fig. 4. Ultraviolet absorption spectra of 2/1 methyl methacrylate-methyl acrylate copolymer in chloroform solution: (A) undegraded; (B) after 50% volatilization.

observed by Strassburger and his colleagues.¹⁴ It is obvious from the data in Table I that a fairly constant ratio of about 1 in 4 of the MA units in the 26/1, 7.7/1 and 2/1 copolymers are liberated as monomer. The amount produced from the 112/1 copolymer was too small to be detected.

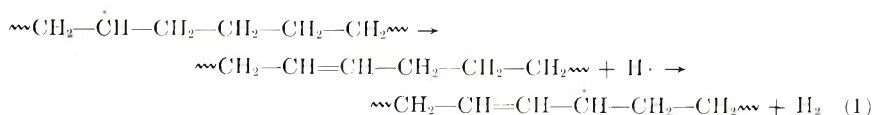
Unsaturation in the Residual Copolymer

At higher extents of degradation, residual copolymer is colored yellow. For comparable extents of volatilization the depth of color increases with increasing MA content of the copolymer. Ultraviolet spectra show an increase in absorbance in the 2750–3750 Å region, as illustrated in Figure 4. Table II shows the color to be expected and the wavelength of absorption for various lengths of carbon-carbon conjugation which suggests that conjugated sequences up to six units in length are present in the colored material. The development of absorption at 1630 cm^{-1} in the infrared spectrum of degraded polymer, as in Figure 5, is confirmation of the appearance of ethylenic structures.

TABLE II
Color and Absorption Maxima for Conjugated Ethylenic Structures

Length of conjugation	Color	Absorption maximum, Å
4	Pale yellow	2960
5	Pale yellow	3350
6	Yellow	3600
8	Orange	4150

The development of ethylenic conjugation is reminiscent of the degradation behavior of polyvinyl esters which liberate the corresponding acid in a chain process which progresses along the polymer molecule. The ability of polymers to develop this kind of conjugation, presumably by the liberation of hydrogen, has been demonstrated for polyethylene¹⁵ and polystyrene¹⁶ under high energy and ultraviolet irradiation, respectively. It has been suggested¹⁷ that once a radical is produced on the polymer chain the reaction may proceed in these polymers by a mechanism strictly analogous to the radical mechanism which has been proposed for the degradation of poly(vinyl chloride):¹⁸



A comparable reaction in MMA-MA copolymers would involve the evolution of one or more of the products hydrogen, methane, and methyl formate

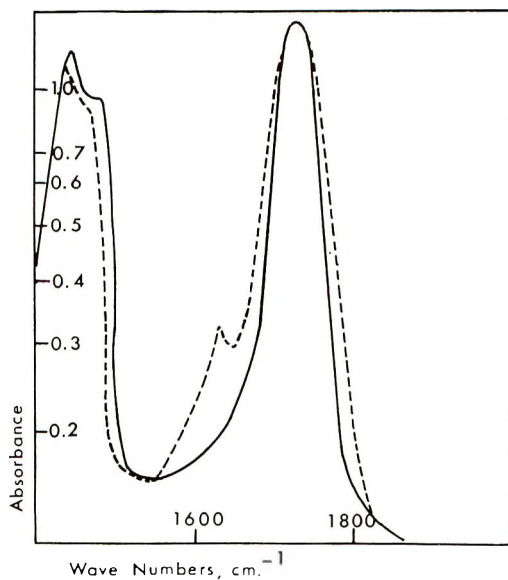
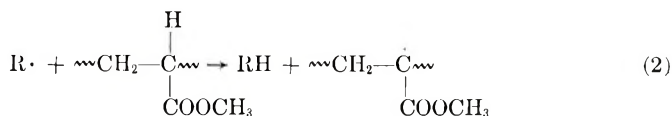


Fig. 5. Infrared absorption spectra of films of 2/1, methyl methacrylate-methyl acrylate copolymer: (—) undegraded; (---) after 50% volatilization.

and could account for at least some of the hydrogen and methane which have been shown above to appear among the volatile products. In the present instance, the initial radicals would be produced in the kind of transfer reactions which lead to large volatile fragments and chain scission in the degradation of PMA [eq. (2)].



Absence of Methanol among the Reaction Products

The complete absence of methanol from the volatile products of degradation of all four copolymers is an unexpected feature of the reaction in view of its prominence among the products from PMA. It would appear that while methanol production is a property of long sequences of methyl acrylate units, it is not a property of isolated units and in this connection it is clearly of interest to obtain information about the distribution of MA units in the various copolymers under discussion. Harwood¹⁹ has shown how the sequence distribution of monomer units in copolymers can be predicted provided reactivity ratios and monomer mixture or copolymer composition are known. By using Harwood's methods, the data in Table III have been calculated for the four copolymers. The first five columns in Table III are self-explanatory. The data in the last column represent

TABLE III
Data on Sequence Distribution in the Copolymers

Copolymer composition (MMA-/MA)	MMA- MMA bonds in copolymer, %	MMA-MA bonds in copolymer, %	MA-MA bonds in copolymer, %	Fraction <i>z</i> of MA in middle units of MA triads	<i>z</i> × % Ma in copolymer
112/1	98.234	1.762	0.004	0.000020	0.000017
26/1	92.675	7.25	0.075	0.0004	0.0015
7.7/1	77.95	21.1	0.95	0.0069	0.08
2/1	42.3	48.8	8.9	0.073	2.43

the relative percentage concentrations of MA units in the middle of MA triads whose immediate environment is thus comparable with the environment of a MA unit in a PMA molecule.

In order to be able to discuss the whole question of methanol production in a completely satisfactory way it will clearly be necessary to study copolymers covering the whole composition range. However, the fact that no detectable amounts of methanol were obtained from any of the copolymers under discussion allows a few observations to be made. For example, it is clear that methanol production is not even a property of pairs of MA units since measurable amounts of methanol would have been produced

from the 2/1 copolymer, 8.9% of whose chain linkages are between pairs of methyl acrylate units. Only 2.43% of all chain units are in an environment comparable with the PMA chain environment. Thus by comparison with PMA (Table I) one would expect methanol to comprise about 0.36% of the total products which is at the limit of the analytical methods used. These results therefore indicate that sequences of at least three MA units are necessary for the evolution of methanol. This conclusion is in accord with the thermal degradation behavior of ethylene-MA copolymers.²⁰ Thus block copolymers produce methanol in the quantities expected from the MA content while random copolymers produce very much less.

Apparently conflicting results have been reported for pyrolysis-gas-liquid chromatography studies on MMA-MA copolymers¹⁴ when it was found that a 4/1 copolymer yielded methanol. However, in the preparation of this copolymer the conversion of the monomer mixture was carried to 100% so that in the later stages of the copolymerization virtually pure PMA was being formed. It was also reported, however, that an equivalent mixture of the two homopolymers gave a much higher yield of methanol than a copolymer of the same overall composition.

Production of Methyl Acrylate and Chain Fragments

Although the principal products of degradation of PMA and PMMA are so different, the reactions have been explained in terms of a single chain depolymerization mechanism in which there are two competing steps, namely depropagation and intramolecular transfer. In PMMA the former predominates so that high yields of monomer are obtained, while in PMA the latter predominates to give long chain fragments as the principal product. It is clear from Table I that as one would expect, a high proportion of the MM in the copolymers is accounted for as monomer among the products. Table I also shows that the yields of MA and chain fragments both increase in proportion to the concentration of MA in the copolymers. The constant ratio, throughout the copolymer composition range studied, of one MA unit in four being liberated as monomer is therefore a measure of the relative probabilities of depropagation and transfer occurring at a long chain radical terminated by a MA unit. In copolymers containing higher proportions of MA in which a higher proportion of the MA units will occur in groups, depropagation will be inhibited as in PMA, and these relationships will undoubtedly break down.

Production of Carbon Dioxide

Carbon dioxide is not produced in significant quantities during the thermal degradation of PMMA. On the other hand, the data in Table I demonstrate that the yields of carbon dioxide from the copolymers are approximately in proportion to the MA content so that liberation of carbon dioxide may be a property of individual MA units. In view of a possible association of chain scission with MA units it seems that carbon dioxide might also be closely associated with chain scission. It is also clear that

since chain scission plays such a vital part in this degradation process its mechanism will have to be clarified if a satisfactory picture of the overall reaction is to be given. It has therefore been found convenient to devote the following paper⁶ to carbon dioxide production and chain scission leading to a discussion of mechanism and kinetics.

CONCLUSIONS

The high rates of monomer production from PMMA due to chain terminal initiation are suppressed in the copolymers due to the blocking of the depropagation process by the MA units. Thus degradation occurs in the copolymers only at temperatures at which PMMA molecules devoid of terminal unsaturation degrade. This involves random scission followed by depropagation. When depropagation reaches an isolated unit of MA, there is competition among depropagation, intramolecular transfer, and intermolecular transfer which results in MA monomer, large chain fragments and chain scission, respectively. Depropagation is unlikely to occur from a radical chain end which comprises a sequence of more than one MA unit so that only the transfer processes can occur. During the course of the reaction the copolymers become yellow, the rate of coloration being greater the greater the MA content of the copolymer. This has been associated with the formation of carbon-carbon conjugation in the chain backbone. It seems possible that hydrogen and methane, which appear as minor products of the reaction are being liberated from adjacent units in the polymer molecules in a chain reaction which is initiated by the intermolecular transfer process mentioned above and which is therefore in competition with chain scission.

The fact that methanol does not appear among the volatile products of degradation of any of the copolymers demonstrates that at least three adjacent units of MA are necessary in the polymer chain for its formation.

This research work has been sponsored by the United States Air Force under Contract AF 61(052)-883 through the European Office of Aerospace Research, OAR, United States Air Force.

We also record our thanks to Messrs. R. Smith and G. Perrit who carried out molecular weight measurements and gave general technical assistance.

References

1. N. Grassie and E. M. Grant, *European Polym. J.*, **2**, 255 (1966).
2. N. Grassie and E. Farish, *European Polym. J.*, **3**, 305 (1967).
3. N. Grassie and E. Farish, *European Polym. J.*, **3**, 619 (1967).
4. N. Grassie and E. Farish, *European Polym. J.*, **3**, 627 (1967).
5. N. Grassie, S.C.I. Monograph, No. 26, *Advances in Polymer Sciences and Technology*, Soc. Chem. Ind., London, 1967, p. 191.
6. N. Grassie and B. J. D. Torrance, *J. Polym. Sci. A-1*, **6**, 3515 (1968).
7. N. Grassie, B. J. D. Torrance, J. D. Fortune, and J. D. Gemmell, *Polymer*, **6**, 653 (1965).
8. N. Grassie and R. S. Roche, *Makromol. Chem.*, **112**, 16 (1968).
9. I. C. McNeill, *J. Polym. Sci. A-1*, **4**, 2479 (1966).

10. I. C. McNeill, *European Polym. J.*, **4**, 21 (1968).
11. J. C. Bevington, H. W. Melville, and R. P. Taylor, *J. Polym. Sci.*, **14**, 463 (1954).
12. G. G. Cameron and D. R. Kane, *J. Polym. Sci. B*, **2**, 693 (1964).
13. S. L. Madorsky, *J. Polym. Sci.*, **11**, 491 (1953).
14. J. Strassburger, G. M. Brauer, M. Tryon, and A. F. Forziati, *Anal. Chem.*, **32**, 454 (1960).
15. S. Ohnishi, S. Sugimoto, and I. Nitta, *J. Polym. Sci. A*, **1**, 605 (1963).
16. N. Grassie and N. A. Weir, *J. Appl. Polym. Sci.*, **9**, 999 (1965).
17. N. Grassie, *Pure Appl. Chem.*, in press.
18. R. R. Stromberg, S. Straus, and B. G. Achhammer, *J. Polym. Sci.*, **35**, 355 (1959).
19. H. J. Harwood, *Angew. Chem.*, **4**, 394 (1965).
20. K. J. Bombaugh, C. E. Cook, and B. H. Clampitt, *Anal. Chem.*, **35**, 1834 (1963).
21. N. Grassie, in *Chemical Reactions of Polymers*, E. M. Fettes, Ed., Interscience, New York, 1964, p. 565.

Received January 26, 1968

Thermal Degradation of Copolymers of Methyl Methacrylate and Methyl Acrylate. II. Chain Scission and the Mechanism of the Reaction

N. GRASSIE and B. J. D. TORRANCE,*
*Chemistry Department, The University of Glasgow,
Glasgow, Scotland*

Synopsis

It has been established that one molecule of carbon dioxide is produced for each chain scission during degradation of methyl methacrylate-methyl acrylate copolymers with molar compositions in the ratios 112/1, 26/1, 7.7/1, and 2/1. Thus the relatively simple measurement of the production of carbon dioxide can be used to determine the extent of chain scission. In this way the relationships between chain scission and volatilization, zip length, copolymer composition, and the production of permanent gases have been established. The rate of chain scission is proportional to a power of the methyl acrylate content of the copolymer less than 0.5, from which it has been concluded that a significant proportion of the initial production of radicals and the subsequent attack of these radicals on the polymer chains is at random and not specifically associated with the methyl acrylate units. A mechanism for the overall thermal degradation process in this copolymer system is presented in the light of these observations.

It was suggested in the previous paper¹ that there may be a link between the chain scission and the production of carbon dioxide which occur during thermal degradation of methyl methacrylate-methyl acrylate (MMA-MA) copolymers. In the present paper it is demonstrated that over the range of copolymer compositions studied one molecule of carbon dioxide is liberated for each chain scission. It is therefore possible to use carbon dioxide production as a measure of chain scission and thus to study the relationship between chain scission and certain other features of the reaction in a very much more sensitive way and to larger extents of reaction than is possible by use of the more conventional measurement of molecular weight.

EXPERIMENTAL

The polymers referred to and the experimental methods applied in the present work are those described in the previous paper.¹

* Present address: Research Department, Courtaulds Ltd., Coventry, England.

RESULTS AND DISCUSSION

Chain Scission and Carbon Dioxide Production

A typical series of curves for the production of carbon dioxide over a range of temperatures is illustrated in Figure 1. During the initial period of low reaction rate, which is more pronounced the lower the temperature, the copolymer retains its powdery appearance and has clearly not attained the temperature of the reaction vessel. The point of transition to the higher rate can be seen to be associated with the conversion of the polymer to a transparent film. This may be loosely termed melting. The mobility of the "molten" polymer thereafter will ensure that its temperature rises rapidly to that of the reaction vessel and the subsequent high rate may be taken as a reliable measure of the rate at the temperature quoted. By heating copolymer samples slowly it was confirmed by visual observation that the "melting points" are all in the range 240–260°C whereas pure PMMA "melted" at 160–170°C.

It has previously been shown² that the number of chain scissions N which has occurred per molecule of copolymer is given by eq. (1),

$$N = [M_0(1 - x)/M] - 1 \quad (1)$$

in which M_0 and M are the original molecular weight and the molecular weight at an extent of volatilization x , respectively. In Figure 2 chain scissions per molecule of polymer calculated in this way are plotted against molecules of carbon dioxide produced per molecule of polymer at a variety of temperatures for various extents of degradation of the four copolymers (see Table 1, columns 5 and 6). The straight line in Figure 2 has been drawn with a slope of 45°. It is obvious that within experimental error

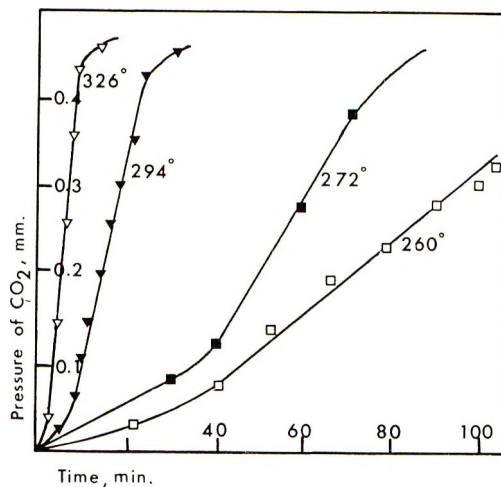


Fig. 1. Production of carbon dioxide during degradation of 7.7/1 methyl methacrylate-methyl acrylate copolymer.

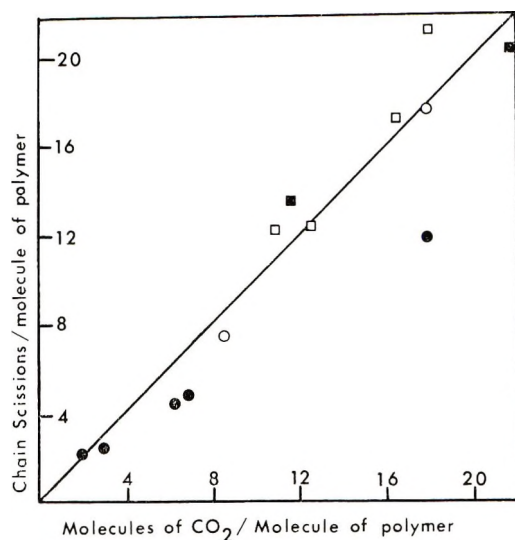


Fig. 2. Relationship between carbon dioxide production and chain scission during degradation of methyl methacrylate-methyl acrylate copolymers: (○) 112/1; (●) 26/1; (□) 7.7/1; (■) 2/1.

TABLE I
Summary of Carbon Dioxide-Chain Scission Data

Copolymer	Degradation temperature, °C	Volatilization, %	MW of residue	Scissions/molecule	Molecules CO ₂ /molecule
112/1	294	6.6	66,000	7.46	8.2
	282	22.5	—	—	7.2
26/1	294	31.5	58,000	6.21	11.6
	282	26.0	15,000	28.6	24.5
	282	62.0	—	—	52.4
	282	79.5	—	—	66
	294	2.3	175,000	2.34	2.8
	294	23.6	40,000	11.8	17.6
	272	—	190,000	2.2	1.9
	294	12.5	115,000	4.8	6.0
7.7/1	326	11.0	110,000	4.68	6.6
	282	16.4	27,000	12.1	10.5
	282	25.0	23,600	12.5	12.4
	282	31.4	13,000	21.3	17.8
	294	17.3	20,000	17.5	16.1
	294	32.2	—	—	18.0
	294	50.3	—	—	30.0
	326	74.7	—	—	35.5
2/1	294	13.9	15,000	20.3	22.0
	310	5.3	24,000	13.6	11.2
	310	15.4	16,800	17.7	17.7
	310	27.3	—	—	35.5
	310	45.2	—	—	48.0
	310	53.4	—	—	60.0

and over the range of experimental conditions represented in Figure 2, each chain scission in all four copolymers is associated with the production of one molecule of carbon dioxide. Beyond about 45% volatilization there is some deviation from this relationship, but this is due to the fact that polymer molecules are then disappearing from the system in appreciable quantities by complete unzipping so that eq. (1) no longer applies. Since the molecular weight decreases so rapidly during degradation and since the measurement of low molecular weight is inaccurate owing to diffusion effects in the osmometer, the measurement of the production of carbon dioxide is very much more reliable at all but the lowest extents of degradation. For this reason, all chain scission data quoted in the following sections of this paper were calculated from carbon dioxide production data.

Volatilization, Chain Scission, and Zip Length

The previous paper¹ has shown the reaction to consist essentially of chain scission followed by three competing reactions, namely, depropagation to monomer, intramolecular transfer giving large chain fragments, and intermolecular transfer which may lead to further chain scission or, to a lesser extent, to conjugated unsaturation in the polymer backbone. It seems, therefore, that there should be at least a qualitative correlation between the number of monomer units liberated per chain scission, the zip length, and copolymer composition and the pattern of products described in the previous paper.

On plotting representative data from Table I as in Figure 3, it is clear that over a large part of the reaction a constant amount of volatilization occurs per chain scission for each copolymer, which is consistent with the reaction mechanism outlined above. From the slopes of plots, as in Figure 3,

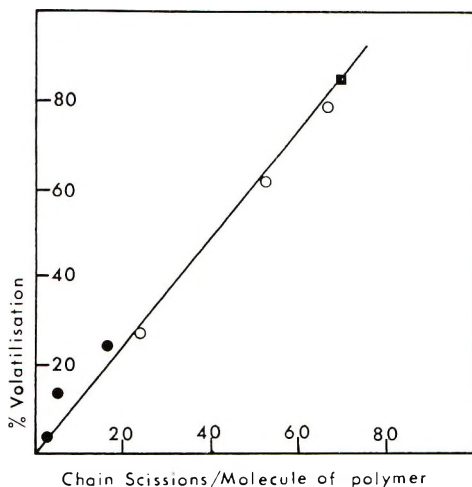


Fig. 3. Relationship between volatilization and chain scissions during degradation of 26/1 methyl methacrylate-methyl acrylate copolymers: (O) 282°C; (●) 294°C; (■) 326°C.

TABLE II
Zip Lengths

Copolymer	Slope <i>A</i>	Initial MW, M_0	MW lost/ scission ($M_0A/100$)	Average wt of monomer unit <i>B</i>	Zip length ($M_0A/100B$)
112/1	2.9	600,000	17,320	100	173
26/1	1.22	600,000	7,320	99.5	74
7.7/1	1.68	425,000	7,150	97.2	74
2/1	0.88	370,000	3,260	95.3	34

the zip length for each copolymer can be calculated as in Table II. Although there may be considerable experimental error in these values of zip length, they are undoubtedly correct to within 10%.

Table III in the previous paper indicates that in the 112/1 copolymer the proportion of adjacent MA units is extremely small, and indeed there must be relatively few MA units even in the close vicinity of each other. Thus there should be expected to be relatively little intramolecular transfer and this is confirmed by the absence of any significant amount of chain fragments. In the previous paper it was shown that approximately one in four of the methyl acrylate units are liberated as monomer so it may be assumed that at least for single MA units there is a 1 in 4 chance that depropagation will pass through them. For the 112/1 copolymer this will lead to an average zip length of approximately 150 $[112 + (112/4) + (112/4^2) + \dots]$ which is in satisfactory agreement with the value of 173 in Table II.

As the MA content of the copolymers is increased so that a greater proportion of the MA units form adjacent sequences, monomer production is increasingly suppressed and intramolecular transfer with the production of chain fragments plays an increasing part. Since the zip length values in Table II become proportionately greater compared with the monomer ratios in the copolymers and since the zip length includes chain fragments based as it is on total weight loss, it is obvious that a radical terminated by a sequence of MA units is very much more likely to undergo intramolecular than intermolecular transfer. The present experimental data only allow these qualitative observations to be made. A more quantitative analysis will only be possible when a precise analysis of the chain fragments can be carried out.

Chain Scission and Copolymer Composition

In view of the possibly important part which MA units may play in the chain scission process it is important to investigate the dependence of rate of chain scission upon MA content as a step towards the establishment of the overall reaction mechanism. The rates of carbon dioxide evolution after "melting" of the polymer (see Fig. 1) were taken as a measure of rate of chain scission. Owing to the considerable potential experimental error and the possibility of the sample size influencing mea-

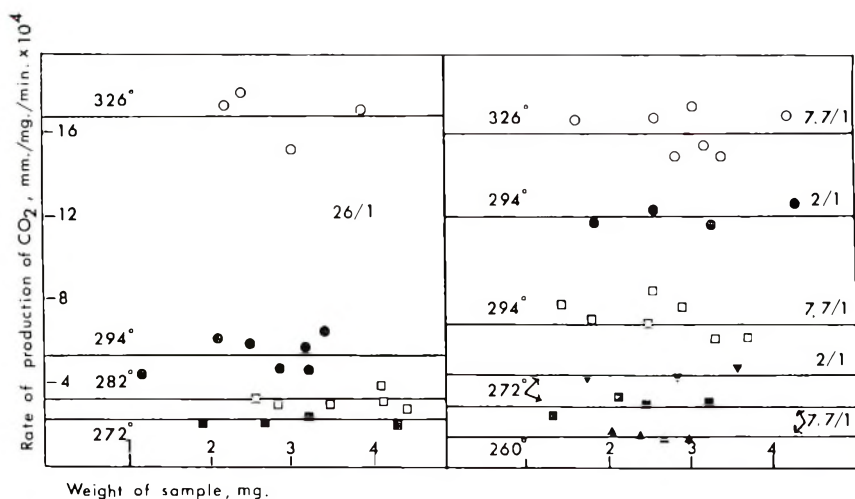


Fig. 4. Dependence of rate of production of carbon dioxide on size of polymer sample for methyl methacrylate-methyl acrylate copolymers.

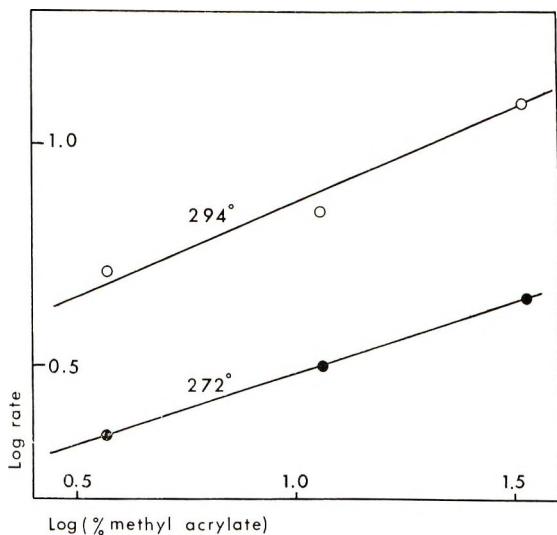


Fig. 5. Relationship between rate of chain scission and methyl acrylate content for methyl methacrylate-methyl acrylate copolymers.

sured rates, rates of carbon dioxide production were measured for samples of various sizes for each copolymer. Results are illustrated in Figure 4, which demonstrates no consistent trend with sample size. The horizontal lines indicate average values of rate. Figure 5 illustrates the relationship between rate and MA content for the 26/1, 7.7/1, and 2/1 copolymers at 294 and 272°C. The slopes of the straight lines through these points are 0.42 and 0.33 respectively. Although the limited number of experimental data makes the probable error fairly high, taking the two sets of data to-

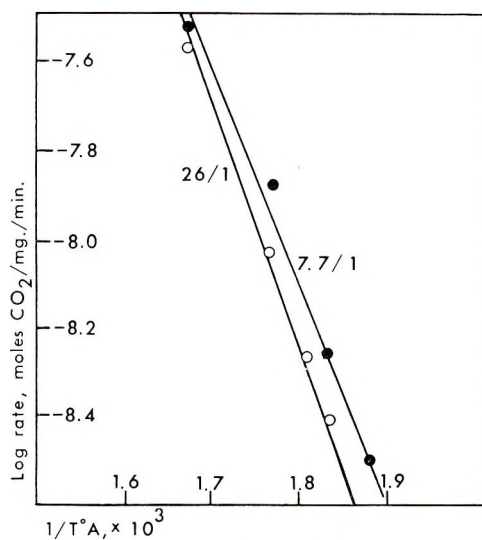


Fig. 6. Arrhenius plot of chain scissions during degradation of methyl methacrylate-methyl acrylate copolymers.

gether it may reasonably be claimed that the rate of chain scission is proportional to less than the half power of the MA content of the copolymer.

Activation Energy for Chain Scission

The data for the 26/1 and 7.7/1 copolymers in Figure 4 are represented in Figure 6 in the form of an Arrhenius plot from which a value of 23.5 ± 2 kcal/mole may be deduced for the energy of activation of chain scission. This is also the value for the energy of activation for volatilization, since volatilization has been shown to be a linear function of chain scission for each copolymer. It is low compared with the values for the initial volatilization of PMMA³ and PMA⁴ which are 32 and 34 Kcal/mole, respectively. Both the low exponent in the relationship between rate of chain scission and MA content and this low value of energy of activation are evidence in favor of the involvement of chain scission as an integral part of a radical chain process.

Chain Scission and the Production of Permanent Gases

It was reported in the previous paper that permanent gases, particularly hydrogen, are produced during the reaction although in quantities very much less than carbon dioxide. It was also suggested that these permanent gases might be associated with the coloration which occurs, the radical resulting from intermolecular transfer acting as a center of initiation for two competing reactions, the first resulting directly in chain scission and the second in the evolution of hydrogen and methane in a chain process similar to that which has been suggested for the liberation of hydrogen chloride from poly(vinyl chloride).⁵ If these conclusions are correct, they should

provide a basis for the explanation of any relationship which exists between carbon dioxide and permanent gas production.

The data in Table III demonstrate that for a wide range of degradation temperatures and extents of reaction, the ratio of chain scissions to permanent gas production is constant for each copolymer but that the proportion of permanent gases increases with the MA content of the copolymer.

TABLE III
Chain Scissions and Permanent Gases

Copolymer	Degradation temperature, °C	Vola-tilization, %	Chain scissions/ molecules of permanent gas	Average ratio
26/1	200	1	20	20
	220	2	25	
	294	85	18	
	294	85	17	
	326	80	20	
7.7/1	326	80	12	12
	326	1	12	
2/1	294	50	8	8
	310	52	7	
	310	60	8	

This is in accordance with the mechanism outlined above. Thus the constant value for each copolymer demonstrates the close association of chain scission and permanent gas production throughout the whole course of the reaction. Also, because permanent gas production and coloration are associated with MA rather than MMA units, the chain reaction in which permanent gases are liberated is more likely to occur, the greater the probability that the transfer radical finds itself in the vicinity of MA units; that is, the greater the MA content of the copolymer.

Mechanism and Kinetics of Chain Scission

In order to gain further information about the site of the initial chain scission and of the intermolecular transfer process with which chain scission and carbon dioxide production are associated, these two processes may be regarded as the initiation and propagation steps of a chain reaction whose rate is measured by the rate of chain scission.

In view of the fact that the degradation reaction occurs in the copolymers at the same temperature as the randomly initiated phase of the degradation of PMMA, random initiation seems the most likely initiation process in this chain reaction. Thus the rate of initiation would be independent of the MA content of the copolymer and given by

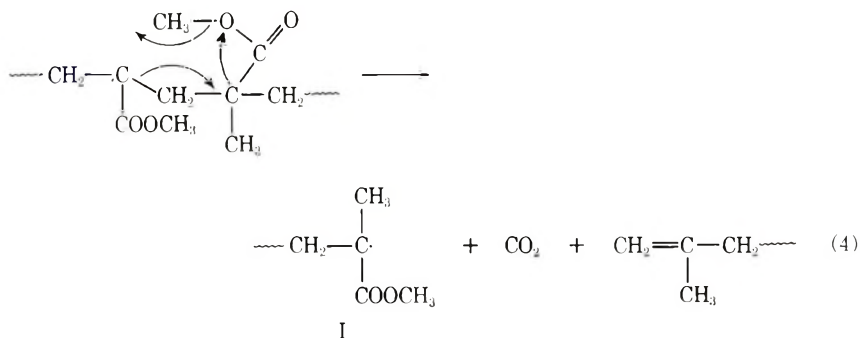
$$\text{rate of initiation} = k_i[M_n] \quad (2)$$

in which k_i is the rate constant for initiation and $[M_n]$ the concentration of the copolymer which may be taken as constant throughout the range of copolymer composition studied.

The propagation step might reasonably be expected to involve the abstraction of a tertiary hydrogen atom from a methyl acrylate unit by a polymer radical, $P\cdot$, thus

$$\text{rate of propagation} = k_p [P\cdot][MA] \quad (3)$$

Chain scission and the production of carbon dioxide can be explained in terms of reaction of the resulting radical in a six-membered ring mechanism [eq. (4)].



The radical I will liberate monomer and chain fragments and ultimately carry on propagation of the chain scission process by abstracting a further tertiary hydrogen atom.

In accordance with experimental findings, one molecule of carbon dioxide is produced per chain scission in this mechanism if it can be assumed that the chain length is appreciable such that the number of initiation steps which occurs without production of carbon dioxide is negligible compared with the number of propagation steps. It may also be noted that a unit of MMA is formed in each act of scission which could explain the small proportion of MMA which is found among the volatile products of degradation of PMA.^{6,7}

Termination might reasonably be expected to occur by mutual destruction of pairs of radicals, so that

$$\text{rate of termination} = k_t [P\cdot]^2 \quad (5)$$

On applying stationary-state kinetics to this mechanism it can easily be demonstrated that the rate of chain scission should be proportional to the first power of the MA content of the copolymer, which is not in accordance with the experimental values of less than 0.5.

It is possible, however, that initiation may be specifically associated with MA units and that the propagation step is random rather than specifically at MA units. Termination, on the other hand, may be associated with the hydrogen and methane loss reaction:

MA content is increased such that MA units occur increasingly in groups, then reaction (4) becomes significant and, by comparison with reaction (5), proves to be much faster than reaction (3). Although tertiary hydrogen atoms are undoubtedly more reactive in transfer processes than methylene hydrogen atoms, the very much higher concentration of the latter in the copolymers ensures that reaction (5) is predominantly a random process.

Although for any given copolymer the relative amounts of reactions (6) and (7) remain constant throughout the reaction, reaction (7) becomes relatively more important as the proportion of MA in the copolymer is increased. This is not surprising, since the principal permanent gaseous product, hydrogen, is to be expected from the MA units only, according to the mechanism proposed.

This research work has been sponsored by the United States Air Force under Contract AF 61 (052)-883 through the European Office of Aerospace Research, OAR, United States Air Force.

We also record our thanks to Messrs. R. Smith and G. Peritt who carried out molecular weight measurements and gave general technical assistance.

References

1. N. Grassie and B. J. D. Torrance, *J. Polym. Sci. A-1*, in press.
2. N. Grassie and E. M. Grant, *European Polym. J.*, **2**, 255 (1966).
3. N. Grassie, *Chemistry of High Polymer Degradation Processes*, Butterworths, London, 1956.
4. S. L. Madorsky, *J. Polym. Sci.*, **11**, 491 (1953).
5. R. R. Stromberg, S. Straus, and B. G. Achhammer, *J. Polym. Sci.*, **35**, 355 (1959).
6. S. Straus and S. L. Madorsky, *J. Res. Nat. Bur. Stand.*, **50**, 165 (1953).
7. G. G. Cameron, unpublished communication.

Received January 26, 1968

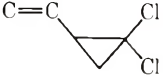
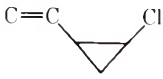
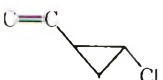
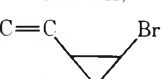
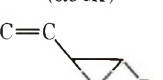
isomer was extremely readily polymerized in comparison with the *trans* isomer which gave no polymer. This paper reports the results of further experiments on the cationic polymerization of 1,1-dichloro-2-vinylcyclopropane (I) and the *cis* and *trans* isomers of 1-chloro-2-vinylcyclopropane (II) together with the isomers of 1-bromo-2-vinylcyclopropane (III).

Results

Cationic polymerizations with such Lewis acids as SnCl_4 , AlCl_3 , and AlBr_3 were carried out in a sealed tube under a nitrogen atmosphere and were homogeneous even in bulk. Powdery, white, soluble polymers were obtained from *cis*-II and *cis*-III in 30–40% yield. The same conditions gave no polymer from I and *trans*-II, and gave a small amount of polymer from *trans*-III in lower yield than *cis*-III. Solution polymerizations of *cis* isomers gave a polymer in lower yields than bulk. The related data of bulk polymerization are summarized in Table I.

The halogen contents of the polymers (Table I) indicate that almost no dehalogenation took place during the polymerization process (calcd for $\text{C}_5\text{H}_7\text{Cl}$: Cl, 34.56%; calcd for $\text{C}_5\text{H}_7\text{Br}$: Br, 54.35%). The presence of cyclopropyl group was shown in every one of the polymers from the infrared absorptions at 1030–1040 cm^{-1} and the NMR signals at 0–1.0 ppm.

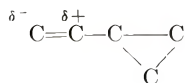
TABLE I
Results of Polymerization

Monomer	Initiator	Initiator, mole-%	Polymerization		Polymer	
			Temp, °C	Time, days	Yield, %	Halogen content, %
 (I)	SnCl_4	3.9	-50	2	—	
	SnCl_4	2.7	-78	2	—	
	SnCl_4	47.3	-78	3	—	
	SnCl_4	115.4	-78	3	—	
 (<i>cis</i> -II)	SnCl_4	8.6	-50	2	32	
	SnCl_4	3.3	-78	2	40	32.86
 (<i>trans</i> -II)	SnCl_4	3.0	-78	2	—	
	SnCl_4	8.5	-78	2	—	
 (<i>cis</i> -III)	SnCl_4	2.3	-50	5	35	53.32
	AlCl_3	0.4	-50	6	1.3	
	AlBr_3	0.6	-50	6	4.9	
 (<i>trans</i> -III)	SnCl_4	1.0	-50	6	Trace	
	AlBr_3	0.4	-50	7	Trace	

Although these data showed the structure of the polymers to be of the 1,2-type, similar to the cationic polymerization of other vinylcyclopropanes,^{1,2} 1,5-type and some other saturated types of polymers are also found. In the case of the polymer of *cis*-III obtained with SnCl_4 , in addition to the 78% of 1,2 units, the presence of 1,5 and unidentified structures were shown by the calculation of the integral data of NMR signals. The amount of 1,5-type structural unit was 14% by NMR spectroscopy and 13% by determination of number of double bonds by using the Rosenmund-Kuhnhehn reagent.⁴ The unknown structure might be a cyclobutyl compound, as suggested by Ketley et al.⁵

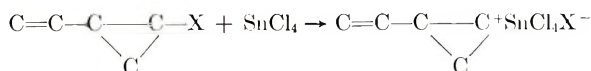
Discussion

In the polymerization of vinylcyclopropanes, some experimental results indicate² that the cyclopropyl ring cannot be opened by direct addition of radical or cation. Moreover, the investigation⁶ of the effect of the cyclopropyl group in hydroboration postulated that the cyclopropyl group is more electron-releasing than other alkyl groups and that vinylcyclopropane is polarized:



These facts support the presumption that in the cationic polymerization of vinylcyclopropane, cations react with the double bond of the monomers to give cyclopropylcarbinyl cation.

Then consider halogen derivatives reacting with Lewis acids in the initiation step:



The difficulty of formation of this cyclopropyl cation, because of ring strain, and the ease with which it undergoes rearrangement if formed,⁷⁻⁹ eliminated the possibility of the initiation of polymerization by such a cyclopropyl cation. Using a large amount of catalyst with (I) also gave no polymer (Table I). It is shown that the failure of polymerization is not caused by preferential reaction of SnCl_4 with chlorine. Therefore, in the polymerization of halogen derivatives, polymerization must be initiated by the proton formed by the reaction of Lewis acids with adventitious water. Then a substituted cyclopropylcarbinyl cation must be formed during the initiation and propagation steps.

The electronegative effect of two chlorines on the cyclopropane ring considerably negates the electron-donating character of cyclopropyl group. Such an interpretation is valid for the failure of cationic polymerization of (I). However, so far as isomers of 1-halo-2-vinylcyclopropanes are concerned, the electronic effect of halogen on the double bond is probably equivalent for *cis* and *trans* isomers. Therefore, the position of the halogen affects the polymerizability by steric hindrance.

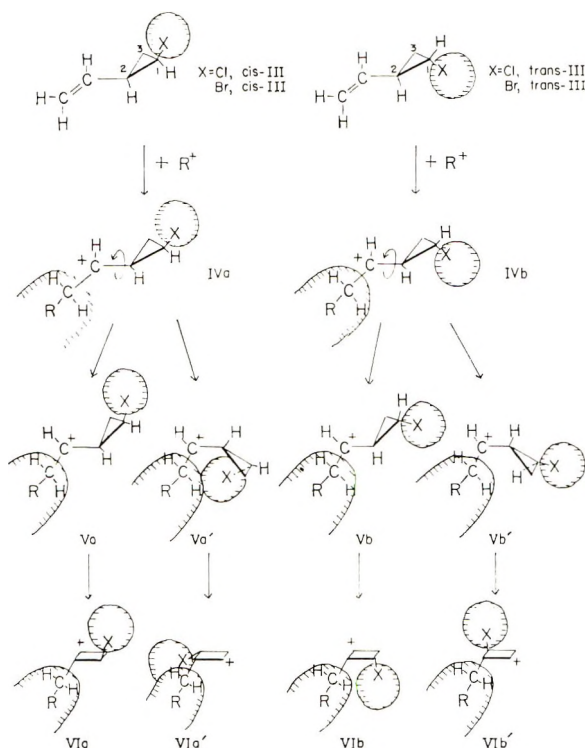


Fig. 1. Steric conformation of *cis* and *trans* halo-2-vinylcyclopropane during cationic polymerization. R^+ denotes initiator fragment or active polymer end.

Steric conformation of *cis* and *trans*-1-halo-2-vinyl cyclopropanes in the process of cationic polymerization is as shown in Figure 1. The monomers react with a cationic initiator fragment in the initiation step or react with an active polymer end in the propagation step to form cyclopropylcarbinyl cations, (IVa) and (IVb).^{*} Recent investigations¹⁰⁻¹² on this cation have shown that the maximum cyclopropyl ring can be achieved with the bisected conformation. Thus, the cyclopropyl ring lies in a plane which is perpendicular to the plane of the $\text{RCH}_2-\text{C}^+-\text{H}$ system in (IVa) and (IVb). Two conformations having such orientation are in each isomer. In Figure 1, they are shown as (Va) and (Va') from *cis* isomer, and (Vb) and (Vb') from *trans* isomer. Addition of the next monomers to these cations causes 1,2-type polymers. Then, it must be considered that the halogen atoms and RCH_2 group occupy a large space and, moreover, there is a large counterion near the carbonium ion. In order that the vinyl group with large substituents, such as vinylcyclopropanes, may approach the carbonium cation, the system must have considerable free space around the cation. It is observed from molecular models that (Va') from the *cis* isomers has the most preferred conformation for this hypothesis.

* The peculiarity of this cation was described in the preceding paper.²

The presence of a small amount of 1,5-type compound and cyclobutyl structural units showed the ring to be cleaved. The following discussion is based on assumption that the ring is opened at the C_1-C_2 bond, which is more probable than C_2-C_3 cleavage. In the cation, $R-C-C=C-C-C^+X$, that gives the 1,5-type structural unit, the effect of the original stereo isomers disappears. As shown in Figure 1, in the cyclobutyl cations, (VIa) and (VIa') from *cis* isomers, (VIb) and (VIb') from *trans* isomers, the steric effect also becomes equivalent. However, conformation (Va') must be more readily rearranged to 1,5-type or cyclobutyl cation than (Va), (Vb), and (Vb') in view of its steric conformation.

As above, the failure of polymerization of *trans*-II and *trans*-III can be interpreted in terms of steric hindrance of the halogen in the *trans* position. Also the failure of cationic polymerization of (I) may be due to steric hindrance rather than the electron-withdrawing effect of the chlorine atom.

Experimental

The monomer, 1,1-dichloro-2-vinylcyclopropane (I), was prepared as previously described.¹ Details of synthesis and assignment of stereoisomers of 1-chloro-2-vinylcyclopropane (*cis*-II and *trans*-II) has already been described.² The isomers of 1-bromo-2-vinylcyclopropane (*cis*-III and *trans*-III) were prepared according to the procedure of Seyferth et al.;¹³ *cis*-III, bp 127.5°C/760 mm Hg, n_D^{25} 1.4967; *trans*-III, bp 115.5°C/760 mm Hg, n_D^{25} 1.4885.

The purification of initiators and solvents, the polymerization and polymer purification, and the spectrographic analysis of the polymers were as previously described.¹ Determination of halogen was carried out with the use of a modified type combustion flask.¹⁴

The author wishes to express her gratitude to Prof. I. Moritani of the Osaka University for his guidance during the work.

References

1. T. Takahashi and I. Yamashita, *Kogyo Kagaku Zasshi*, **68**, 869 (1965).
2. T. Takahashi, *J. Polym. Sci. A-1*, **6**, 403 (1968).
3. C. E. Schildknecht, *Ind. Eng. Chem.*, **50**, 107 (1958).
4. K. W. Rosenmund and W. Kuhnhehn, *Z. Nahr. Genussm.*, **46**, 154 (1923).
5. A. D. Ketley, A. J. Berlin, and L. P. Fisher, *J. Polym. Sci. A-1*, **5**, 227 (1967).
6. S. Nishida, I. Moritani, K. Ito, and K. Sakai, *J. Org. Chem.*, **32**, 939 (1967).
7. P. Mayo, Ed., *Molecular Rearrangements I*, Wiley, New York, 1963, p. 254-259.
8. H. C. Brown, R. S. Fletcher, and R. B. Johannesen, *J. Amer. Chem. Soc.*, **73**, 212 (1951).
9. H. C. Brown and M. Borkowski, *J. Amer. Chem. Soc.*, **74**, 1894 (1952).
10. C. U. Pittman, Jr. and G. A. Olah, *J. Amer. Chem. Soc.*, **87**, 2998 (1965).
11. N. C. Deno, J. S. Liu, L. O. Turner, D. N. Lincoln, and R. E. Fruit, Jr., *J. Amer. Chem. Soc.*, **87**, 3000 (1965).
12. H. C. Brown and J. D. Cleveland, *J. Amer. Chem. Soc.*, **88**, 2051 (1966).
13. D. Seyferth, H. Yamazaki, and D. L. Alleston, *J. Org. Chem.*, **28**, 703 (1963).
14. S. Ota, *Japan Analyst*, **15**, 689 (1966).

Received May 1, 1968

Anionic Copolymerization of 1,1-Diphenylethylene and 2,3-Dimethylbutadiene*

HEIMEI YUKI, KOICHI HATADA, and TADANORI INOUE,
*Department of Chemistry, Faculty of Engineering Science, Osaka
University, Toyonaka, Osaka, Japan*

Synopsis

1,1-Diphenylethylene (M_2) and 2,3-dimethylbutadiene (M_1) were copolymerized with *n*-butyllithium in tetrahydrofuran. The rate of consumption of each monomer was followed by the change of high resolution NMR spectra of the reaction mixture. The copolymerization proceeded alternately, if the ratio of initial monomer concentrations, $[M_2]_0/[M_1]_0$, was sufficiently larger than unity. By assuming the rate constant k_{22} to be zero, the constants k_{21} were obtained from the consumption rates of the monomers. In the alternating copolymerization, 2,3-dimethylbutadiene was incorporated into the copolymer only as the 1,4-structure, while the 1,2-structure was predominant in homopolymerization.

INTRODUCTION

Alternating copolymers have been prepared by an anionic mechanism from the combinations of a monomer (M_2), such as 1,1-diphenylethylene or stilbene which can not homopolymerize easily, and a comonomer (M_1), such as styrene, butadiene, isoprene, or 2,3-dimethylbutadiene when the initial concentration of M_2 is sufficiently larger than that of M_1 .¹ The possibility of the formation of an alternating copolymer from styrene and 1,1-diphenylethylene was discussed in connection with a kinetic study of the anionic copolymerization of these two monomers in THF with sodium counterion at 25°C.² An alternating copolymer of α -stilbazole and 2-vinylpyridine has also been prepared by use of an anionic initiator.³

In this paper, the investigation of the anionic copolymerization of 1,1-diphenylethylene and 2,3-dimethylbutadiene in tetrahydrofuran by using *n*-butyllithium as an initiator will be reported. The copolymerizations were followed by the high resolution NMR spectra of the reaction mixtures.

EXPERIMENTAL

Materials

1,1-Diphenylethylene was prepared by the dehydration of diphenylmethyl carbinol according to Allen.⁴ The crude product was treated with Na-K

* Presented at the International Symposium on Macromolecular Chemistry, Tokyo, 1966.

alloy at about 60°C under nitrogen pressure for several hours and distilled under reduced nitrogen pressure. To the main fraction, a small amount of *n*-butyllithium solution in *n*-hexane was added in portions, with stirring, until the deep red color of 1,1-diphenylethylene anion persisted. Then the fraction was redistilled under reduced nitrogen pressure; bp, 115°C/3 mm Hg, n_D^{20} 1.6085. The purified 1,1-diphenylethylene was stored in a sealed ampule under nitrogen pressure at -20°C.

2,3-Dimethylbutadiene was synthesized by the dehydration of pinacol as described by Allen.⁵ The product was purified by a fractional distillation under nitrogen pressure; bp 69.2°C/760 mm Hg n_D^{25} 1.4362. The purified 2,3-dimethylbutadiene was thoroughly dried with (*i*-Bu)₃Al and distilled *in vacuo* before use.

n-Butyllithium was prepared in cyclohexane according to Ziegler's method⁶ from *n*-butyl chloride and metallic lithium.

Tetrahydrofuran was refluxed and distilled over calcium hydride and redistilled over lithium aluminum hydride under high vacuum before use.

n-Hexane was purified in the usual manner,⁷ dried, and stored over calcium hydride. This was mixed with a small amount of *n*-butyllithium dissolved in *n*-hexane and distilled under high vacuum before use.

Nitrogen and argon were purified by being passed through *n*-butyllithium dissolved in Nujol and then through a column packed with molecular sieves 4A cooled to -78°C in a Dry Ice-acetone bath.

Polymerization

The monomers and tetrahydrofuran were charged in an ampule with the use of a vacuum system, which had been flushed with dry argon. To the monomer solution, a solution of *n*-butyllithium was added with a hypodermic syringe under argon pressure at 21.5°C. The ampule was immediately sealed off. After the desired reaction time at 21.5°C the polymerization was stopped by adding a small amount of methanol, and the polymer was precipitated by pouring the mixture into a large amount of methanol. After standing overnight, the polymer was collected by filtration, washed with methanol, and dried *in vacuo* at room temperature.

The polymerization was followed by NMR spectroscopy. A part of the reaction mixture was transferred into an NMR sample tube with a hypodermic syringe immediately on the addition of *n*-butyllithium to the monomer solution and the tube was sealed. This was done under an atmosphere of dry argon. The NMR measurements were carried out at 21.5°C and at 100 Mcps with a JNM-4H-100 spectrometer (Japan Electron Optics Lab.), cyclohexane, the solvent of *n*-butyllithium used, being used as an internal reference. The scanning time of the spectral region of 9 ppm was 2.5 min; this did not affect the results of measurements because of the slow rate of the polymerization.

Infrared Spectra

The infrared spectra of polymer were obtained with a JASCO IR-S spectrometer on the thin film cast on a rock salt plate from solution in carbon tetrachloride.

Solution Viscosity

The solution viscosity of the polymer was determined in toluene at 30.0°C with the use of an Ostwald viscometer.

RESULTS

Polymerization of 2,3-Dimethylbutadiene

The polymerization of 2,3-dimethylbutadiene was carried out in tetrahydrofuran at 21.5°C with the addition of a known amount of benzene as a spectral reference. The reaction was followed by NMR spectroscopy. In Figure 1 are shown the NMR spectra of 2,3-dimethylbutadiene, of the reaction mixture under the polymerization of this diene, and of the polymer obtained. With the polymerization of 2,3-dimethylbutadiene, the peaks

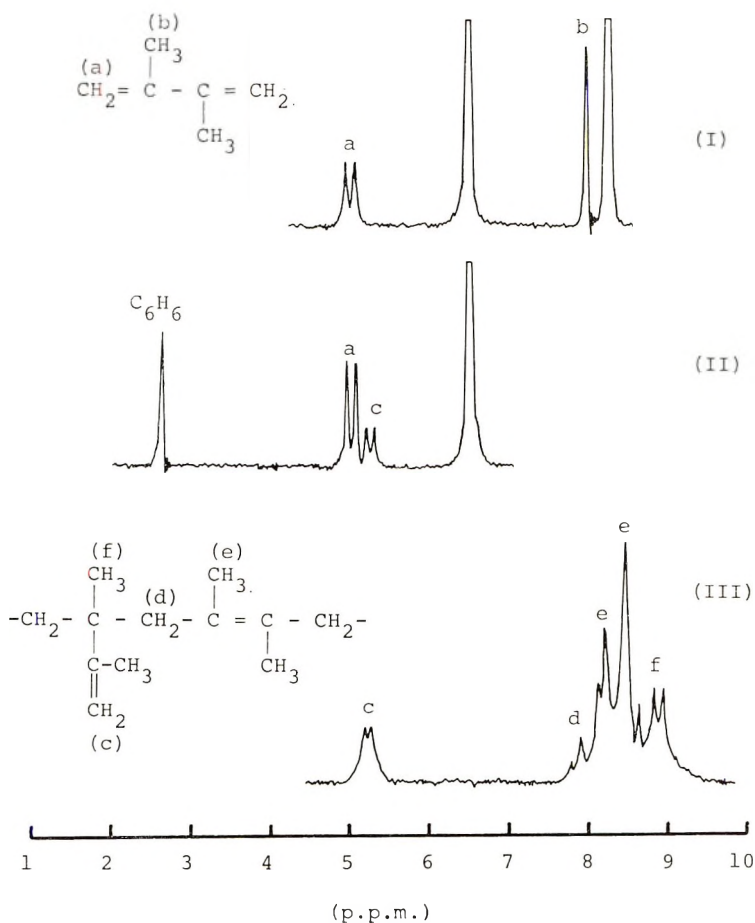


Fig. 1. NMR spectra: (I) 2,3-dimethylbutadiene in THF; (II) reaction mixture of 2,3-dimethylbutadiene and *n*-BuLi in THF containing a small amount of benzene; (III) the resultant polymer in CCl_4 .

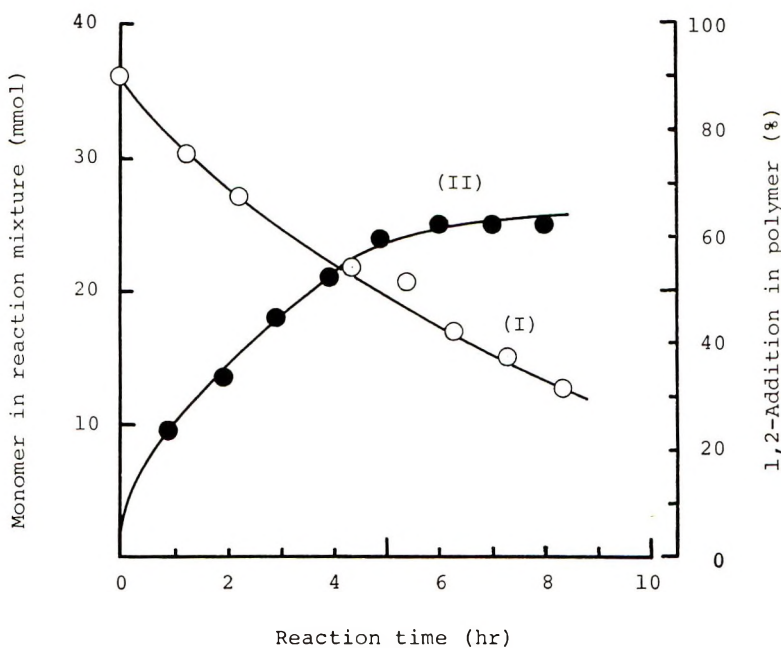


Fig. 2. Anionic polymerization of 2,3-dimethylbutadiene by *n*-BuLi in THF: (I) monomer consumption vs. time; (II) occurrence of 1,2 addition vs. time. Monomer, 36 mmole; *n*-BuLi, 0.4 mmole; total volume, 16 ml; temperature, 21.5°C.

(a) at 5.01 and 5.10 ppm due to the methylene protons of the monomer gradually vanished, and new peaks appeared at 5.25 and 5.31 ppm and at above 7.5 ppm. The rate of polymerization was followed by the change in the relative intensity of methylene signals in the monomer against the signal of benzene added as a reference. The signals (c) at 5.25 and 5.31 ppm were attributed to the methylene protons of the side-chain vinylidene group of the polymer produced by 1,2 addition of the monomer. The rate of occurrence of the 1,2 addition was also followed by the increase of the intensities of these two peaks.

Figure 2 shows the decrease in monomer concentration and the increase in the fraction of 1,2 addition with the polymerization time. The fraction of 1,2 addition in the polymerization increased with time in the earlier stages of the reaction and became constant later.

It was confirmed from the NMR spectra of the reaction mixture of 1,1-diphenylethylene and *n*-butyllithium in tetrahydrofuran that the homopolymerization of 1,1-diphenylethylene did not occur to any appreciable extent under the same conditions.

Copolymerization of 2,3-Dimethylbutadiene and 1,1-Diphenylethylene

The copolymerization of 1,1-diphenylethylene (M_2) and 2,3-dimethylbutadiene (M_1) were carried out at various ratios of the initial monomer

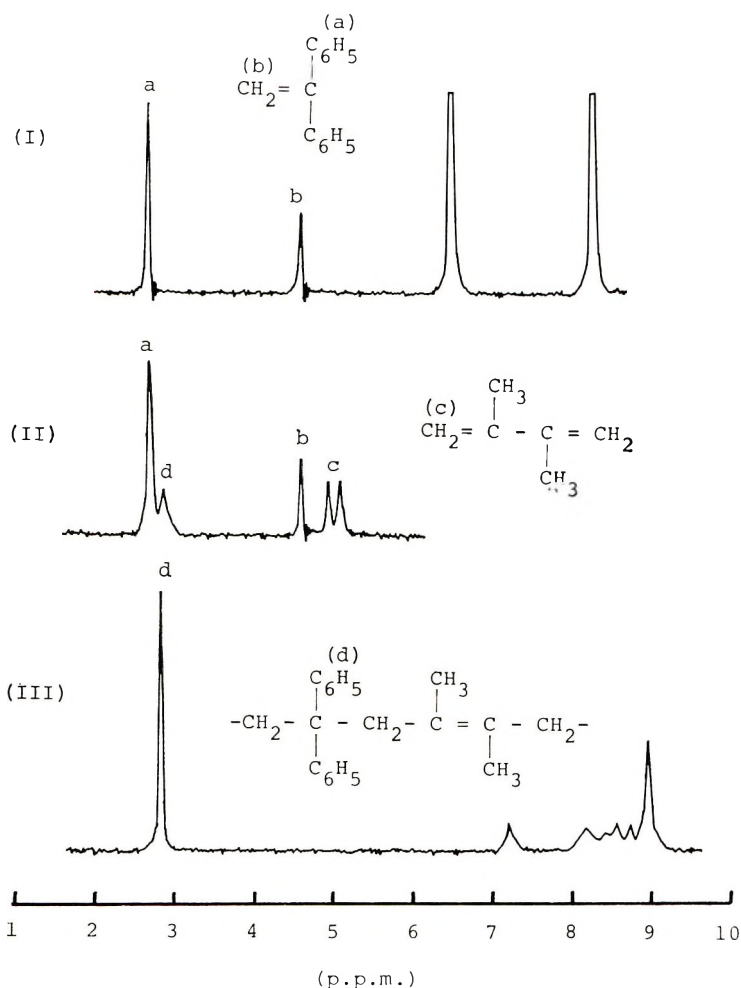


Fig. 3. NMR spectra: (I) 1,1-diphenylethylene in THF; (II) reaction mixture of 2,3-dimethylbutadiene, 1,1-diphenylethylene, and *n*-BuLi in THF; (III) the resultant polymer in CCl_4 .

concentrations, $[M_2]_0/[M_1]_0$, and followed by NMR spectroscopy. Figure 3 shows the NMR spectra of 1,1-diphenylethylene of the reaction mixture under the copolymerization of 1,1-diphenylethylene and 2,3-dimethylbutadiene and of the copolymer obtained. In the course of copolymerization the signals of the methylene protons in 1,1-diphenylethylene and 2,3-dimethylbutadiene vanished gradually and that of the phenyl protons in 1,1-diphenylethylene shifted from 2.71 to 2.90 ppm. It must be noted that no peaks appeared at about 5.25 and 5.31 ppm. This indicates that there was no vinylidene methylene caused by the 1,2-addition of the diene in the copolymer. The rate of consumption of each monomer was followed with the change of the relative intensity of methylene signal in each monomer against the sum of those of the phenyl protons in 1,1-diphenylethylene and

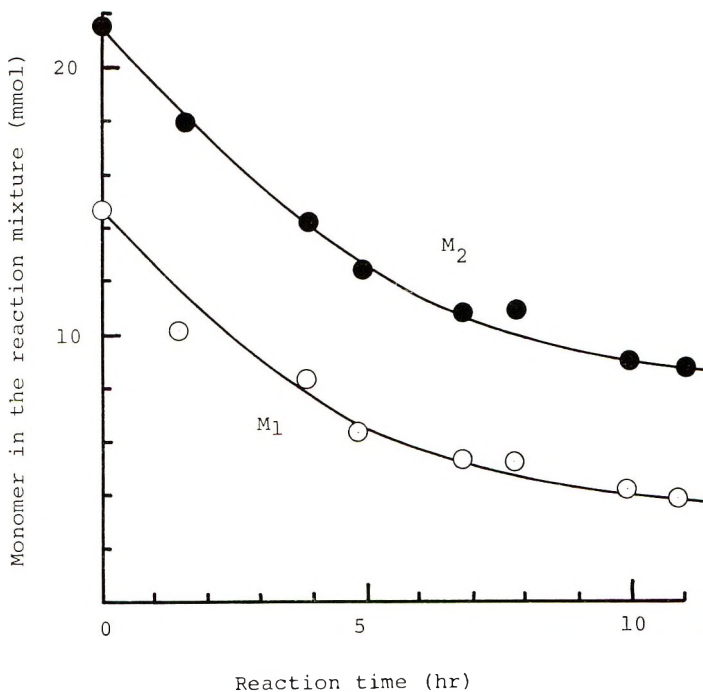


Fig. 4. Monomer consumption vs. reaction time at $[M_2]_0/[M_1]_0 = 1.48$ for anionic copolymerization of 2,3-dimethylbutadiene (M_1) and 1,1-diphenylethylene (M_2). Total amount of monomer, 36 mmole; n -BuLi, 0.4 mmole; solvent, THF; total volume, 16 ml; temperature, 21.5°C.

in copolymer, which must not be changed with the reaction. The results of the copolymerization at $[M_2]_0/[M_1]_0 = 1.48$ are shown in Figure 4, for example.

The relationships between the consumptions of the two monomers in the copolymerizations at various ratios of $[M_2]_0/[M_1]_0$ are shown in Figure 5. The linear relationships having a slope of unity showed that the copolymerization proceeded alternately at $[M_2]_0/[M_1]_0 = 1$ and in the earlier stage of the polymerization at other ratios of $[M_2]_0/[M_1]_0$. At a smaller initial concentration of M_2 than of M_1 the deviation from the straight line, caused by sequences rich in M_1 , was observed at a later stage of the reaction. At the ratio $[M_2]_0/[M_1]_0 = 1.48$, the plot also deviates concavely at the later stage, but it is not certain at the present time whether the deviation was caused by the possibility of the addition of 1,1-diphenylethylene to 1,1-diphenylethylene anion or other reasons including NMR measurement. Even the dimer of 1,1-diphenylethylene was not obtained by the homopolymerization of this monomer under the same conditions, although it has been reported⁸ that 1,1-diphenylethylene could be polymerized by metallic sodium at 100–110°C in bulk.

On the other hand, a series of copolymerizations were carried out at 30°C with varying reaction times at ratios of $[M_2]_0/[M_1]_0 = 1.55$, and the solu-

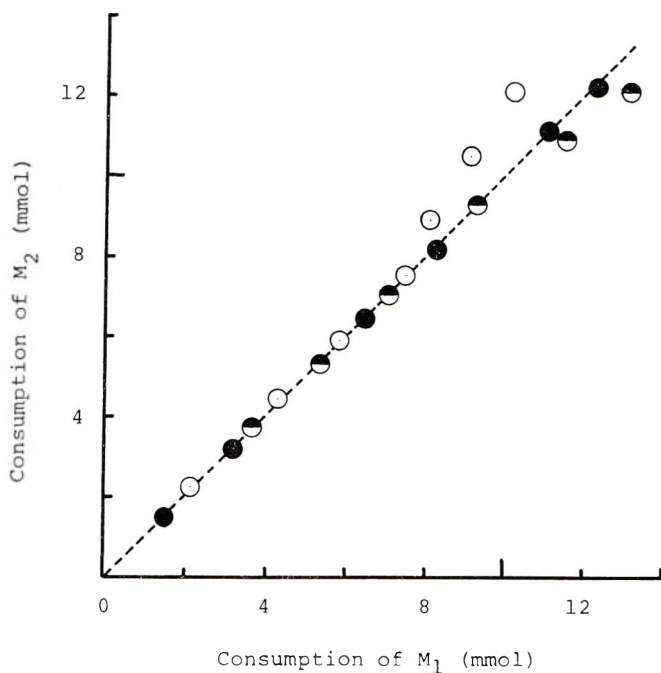


Fig. 5. Consumption of M_2 vs. consumption of M_1 for anionic copolymerization of 2,3-dimethylbutadiene (M_1) and 1,1-diphenylethylene (M_2): (○) $[M_2]_0/[M_1]_0 = 1.48$; (●) $[M_2]_0/[M_1]_0 = 1.03$; (◐) $[M_2]_0/[M_1]_0 = 0.668$. Total amount of monomer, 36 mmole; n -BuLi, 0.4 mmole; solvent, THF; total volume, 16 ml; temperature, 21.5°C.

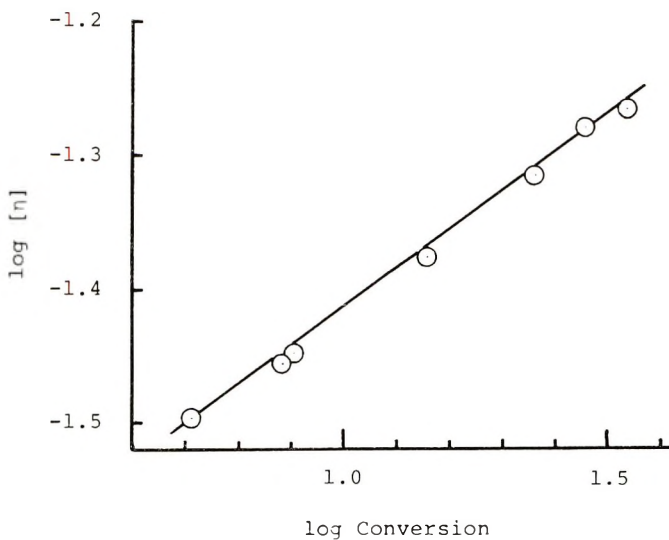
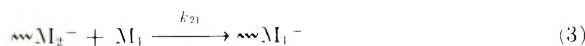
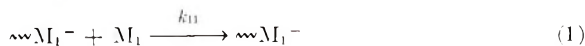


Fig. 6. Plot of $\log [\eta]$ vs. \log conversion for anionic copolymerization of 2,3-dimethylbutadiene (M_1) and 1,1-diphenylethylene (M_2). M_1 , 2.97 mmole; M_2 , 4.60 mmole; n -BuLi, 0.153 mmole; THF, 15 ml; temperature, 30°C. Viscosity was measured for toluene solution at 30°C.

tion viscosities of the copolymers obtained were determined in toluene at 30°C. In Figure 6 $\log [\eta]$ is plotted against \log conversion. The linear relationship between the two suggests that neither termination nor chain transfer is included in this copolymerization.

DISCUSSION

The results above mentioned showed that the anionic copolymerization of 1,1-diphenylethylene and 2,3-dimethylbutadiene proceeds without termination and chain transfer, and alternately at least in the earlier stage of the reaction. For the propagation reactions (1)–(4),

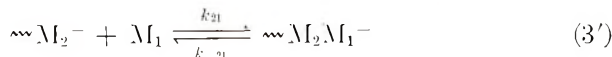


the rates of monomer consumptions are represented by eqs. (5) and (6).

$$-d[M_1]/dt = k_{11}[M_1^-][M_1] + k_{21}[M_2^-][M_1] \quad (5)$$

$$-d[M_2]/dt = k_{12}[M_1^-][M_2] + k_{22}[M_2^-][M_2] \quad (6)$$

Ureta et al.² have reported that the addition of styrene to 1,1-diphenylethylene anion is reversible in the anionic copolymerization of these two monomers, where the rate constants are $k_{21} = 0.5\text{--}0.7$ l/mole-sec and $k_{-21} = 13$ sec⁻¹. The addition of 2,3-dimethylbutadiene to 1,1-diphenylethylene anion may also be reversible in the copolymerization of these monomers. If so, the reaction (3) and eq. (5), respectively, must be written as



and

$$-d[M_1]/dt = k_{11}[M_1^-][M_1] + k_{21}[M_2^-][M_1] - k_{21}[M_2 M_1^-] \quad (5')$$

However, reaction (2) may be very fast to prevent not only the reaction (1), i.e., $k_{12} \gg k_{11}$, but also the reverse reaction in (3'). We may assume that the reversibility of the reaction (3') does not affect so much the results, and eq. (5') can be rewritten in the form of eq. (5).

From the alternating character of the copolymerization $k_{22} = 0$ and $k_{12} \gg k_{11}$ will be assumed, and the following relationships can be derived.

$$-d[M_1]/dt = -d[M_2]/dt \quad (7)$$

$$k_{21}[M_2^-][M_1] = k_{12}[M_1^-][M_2] \quad (8)$$

The lack of termination leads to

$$C = [M_1^-] + [M_2^-] \quad (9)$$

where C is the concentration of n -butyllithium used. From eqs. (5), (8), and (9) the eq. (10) is obtained

$$-d \ln [M_1]/dt = k_{21}C/(1 + k_{21}[M_1]/k_{12}[M_2]) \quad (10)$$

The alternating character in the copolymerization of 1,1-diphenylethylene and 2,3-dimethylbutadiene can be explained by the high reactivity of 1,1-diphenylethylene toward an anion owing to the high resonance stabilization of its anion, in spite of the lack of homopolymerizability, and by the lower reactivity of 2,3-dimethylbutadiene due to the inductive effect of methyl groups in this monomer. This interpretation also suggests that the addition of 1,1-diphenylethylene anion to 2,3-dimethylbutadiene must be very slow. So we can assume $k_{12} \gg k_{21}$ and the eq. (10) can be rewritten in the form of eq. (11),

$$-d \ln [M_1]/dt = k_{21}C \quad (11)$$

which shows the first-order reaction with respect to the monomer M_1 . Integration of eq. (11) gives eq. (12).

$$\ln [M_1]_0/[M_1] = k_{21}Ct \quad (12)$$

Actually, the rate of consumption of monomer M_1 in the copolymerization fitted a first-order plot as shown in Figure 7. In this figure the results of homopolymerization of monomer M_1 are also plotted. The rate constants

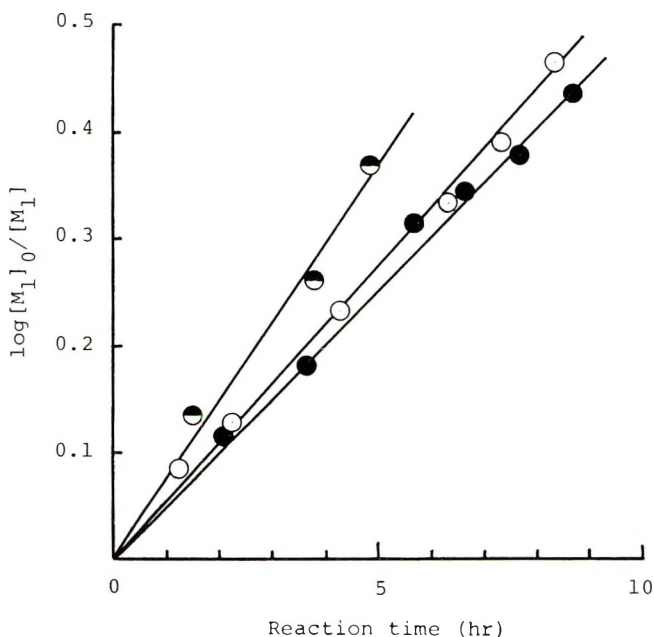


Fig. 7. First-order plots of M_1 consumption for anionic copolymerization of 2,3-dimethylbutadiene (M_1) and 1,1-diphenylethylene (M_2): (●) $[M_2]_0/[M_1]_0 = 1.48$; (●) $[M_2]_0/[M_1]_0 = 1.03$; (○) $[M_2]_0/[M_1]_0 = 0$.

k_{11} and k_{21} were obtained from the slope of these straight lines. The data thus obtained are summarized in Table I, together with the rate constants reported in the literature.⁹⁻¹¹ The orders of magnitude of k_{11} and k_{21} obtained here seem to be reasonable from the chemical structures of 2,3-dimethylbutadiene and 1,1-diphenylethylene.

TABLE I
Rate Constant in Anionic Copolymerization (THF)

Monomers ^a		k_{11} , l/mole-sec	k_{21} , l/mole-sec
M_1	M_2		
Butadiene	Styrene	1.8(Li, 30°C) ^b	3.27×10 (Na, 25°C) ^c
Isoprene	Styrene	1.4×10^{-1} (Li, 30°C) ^d	1.7×10 (Na, 25°C) ^c
2,3-DMB	Styrene	1.4×10^{-3} (Li, 22°C) ^e	4.8×10^{-1} (Na, 25°C) ^c
2,3-DMB	1,1-DPE	1.4×10^{-3} (Li, 22°C) ^e	$1.3 \sim 1.8 \times 10^{-3}$ (Li, 22°C) ^e

^a 2,3-DMB = 2,3-dimethylbutadiene; 1,1-DPE = 1,1-diphenylethylene.

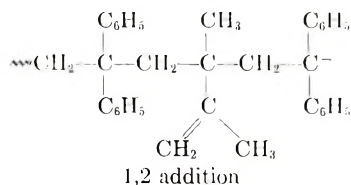
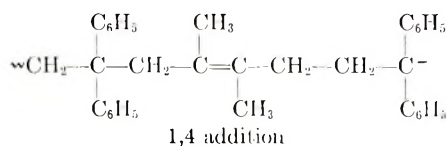
^b Data of Morton et al.⁹

^c Data of Shima et al.¹¹

^d Data of Morton and Fetters.¹⁰

^e This work.

It was shown that no 1,2 addition of 2,3-dimethylbutadiene occurred in the copolymerization, while it took place in the homopolymerization of this monomer. The 1,4 addition of 2,3-dimethylbutadiene must be forced by the steric hindrance which may be encountered in the 1,2 addition in the alternating copolymerization.



A similar situation can be seen in the form of alternating copolymer of 1,1-diphenylethylene and α -methylstyrene. These monomers could not be copolymerized with anionic initiators in spite of the copolymerizability between 1,1-diphenylethylene and styrene.

The authors are very grateful to Mr. Y. Terawaki for the measurements of NMR spectra.

References

1. H. Yuki, K. Kosai, S. Murahashi, and J. Hotta, *J. Polym. Sci. B*, **2**, 1121 (1964).
2. E. Ureta, J. Smid, and M. Szwarc, *J. Polym. Sci. A-1*, **4**, 2219 (1966).
3. G. Natta and U. Nardio, *Makromol. Chem.*, **83**, 161 (1965).
4. C. F. H. Allen and S. Converse, in *Organic Synthesis*, Coll. Vol. I, H. Gilman and A. H. Blatt, Eds., Wiley, New York, 1956, p. 226.
5. C. F. H. Allen and A. Bell, in *Organic Synthesis*, Coll. Vol. III, E. C. Horning, Ed., Wiley, New York, 1955, p. 312.
6. K. Ziegler and H. G. Gellert, *Ann.*, **567**, 179 (1950).
7. A. Weissberger, E. S. Proskauer, J. A. Riddock, and E. E. Toops, Jr., *Organic Solvents*, 2nd Ed., Interscience, New York, 1955, p. 311.
8. K. Kuwata, S. Ishida, and K. Hirota, *Nippon Kagaku Zasshi*, **80**, 25 (1959).
9. M. Morton, E. E. Bostick, R. A. Livigni, L. J. Fetters, *J. Polym. Sci. A*, **1**, 1735 (1963).
10. M. Morton and L. J. Fetters, *J. Polym. Sci. A*, **2**, 3311 (1964).
11. M. Shima, J. Smid, and M. Szwarc, *J. Polym. Sci. B*, **2**, 735 (1964).

Received February 8, 1968

Revised May 20, 1968

Syntheses of Aromatic Polyketones and Aromatic Polyamide

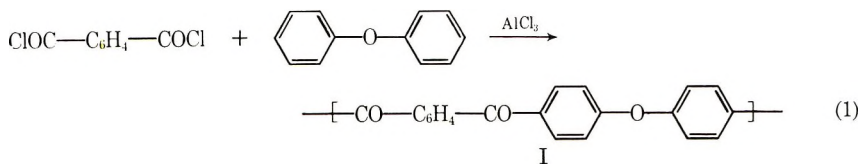
Y. IWAKURA, K. UNO, and T. TAKIGUCHI,
*The Department of Chemistry, Faculty of Engineering,
 University of Tokyo, Bunkyo-ku, Tokyo, Japan*

Synopsis

High molecular weight aromatic polyketones were prepared from *p*- and *m*-phenoxybenzoic acid in polyphosphoric acid by heating the reaction mixture at 100°C. High molecular weight aromatic polyamide was derived from the polyketone obtained through Schmidt reaction or Beckmann rearrangement. The polyamide obtained by Schmidt reaction was found to have some regularity in an arrangement of its repeating units. The thermal stability of the polyketone and the polyamide were good.

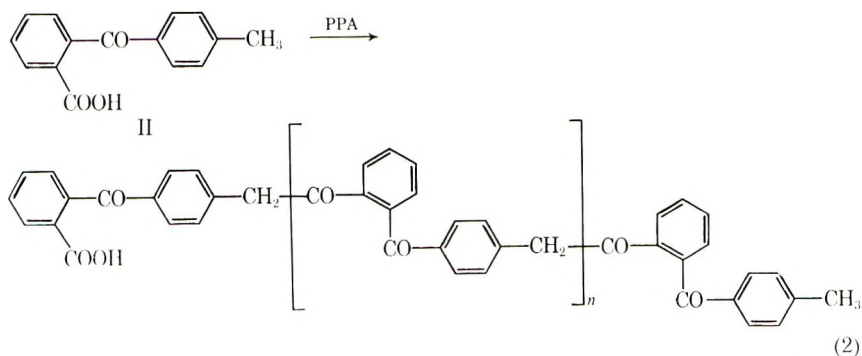
INTRODUCTION

In our laboratory, extensive studies on the synthesis of heat-resistant polymers in polyphosphoric acid (PPA) have been carried out.¹ Aromatic polyketones were expected to show heat-resistant properties by virtue of having a conjugated system in main chain, but very little was known about them. The *meta* and *para* aromatic polyketones (I) prepared from isophthaloyl chloride and diphenyl ether [eq. (1)] through Friedel-Crafts reaction were found to have low viscosities because of the low solubility in the reaction mixture.²



Ketocarboxylic acid (II) was known to give polyketone in PPA (see structure atop next page). In this case, however, the reaction was found to proceed between carboxylic acid and the methyl group. Moreover, the degree of polymerization was only 5-7.³

The present paper describes the syntheses of high molecular weight aromatic polyketones from phenoxybenzoic acids in PPA, and further, the preparation of polyamide from polyketone through Schmidt reaction.



RESULTS AND DISCUSSION

Formation of Polyketone

In previous studies on the preparation of polyoxadiazoles and polybenzimidazoles,^{4,5} dicarboxylic acids were found to react easily with nucleophilic reagents such as hydrazine and diaminobenzidine in PPA and sulfuric acid (oleum) as well as carboxylic acid derivatives such as acid chlorides, nitriles, acid amides, and so on. Therefore, the reaction of aromatic dicarboxylic acids such as phthalic acid, isophthalic acid, and aliphatic dicarboxylic acids with diphenyl ether in PPA to yield polyketones was examined. The reaction, however, gave no polymer under conditions similar to those described in Table I.

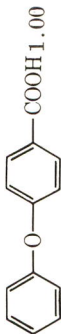
Aromatic carboxylic acids which have phenoxy group in the *para* or *meta* position to the carboxyl group were synthesized and a self-polycondensation action in PPA were examined. The results are summarized in Table I.

In the infrared absorption spectra of the products, the absorptions due to carboxylic acid around 2700 and 1700 cm^{-1} disappeared completely, and a new absorption characteristic of aromatic ketone appeared at 1650 cm^{-1} . Consequently, the resulting polymers may be considered to be polyketones. The analytical data for the polymer also supported the formation of polyketone.

In a Friedel-Crafts reaction, it is well known that the attack of an electrophile on substituted benzene occurs at sites both *para* and *ortho* to the electron-donating substituent. It is reported that in the preparation of polysulfone from *p*-phenoxybenzenesulfonic acid in PPA, both *para* and *ortho* derivatives were formed, as shown by the NMR spectrum of the polysulfone obtained.⁶ The NMR spectrum of the polyketone (I-2, Table I) measured in concentrated sulfuric acid at elevated temperature gave only two doublets at 9 cps coupling constant, and no other signals were observed, as shown in Figure 1.

This result shows the presence of only two kinds of protons which are *ortho* to each other. The signal appearing in the lower magnetic field could be assigned to the proton *ortho* to carbonyl by analogy with the NMR

TABLE I
Synthesis of Polyketone

No.	Monomer	Wt mono- mer, g	Wt PPA, g	Temp, °C	Time, hr	Yield, %	η_{inh}^a	PMT, °C	Anal.			
									Calcd		Found	
									C, %	H, %	C, %	H, %
I-1		1.00	20	160	23	96	0.16					
I-2	"	1.00	20	130	23	98	0.36	355	79.54	4.11	78.85	4.30
I-3	"	1.00	20	110	23	98	0.53	360				
I-4		1.00	20	110	14	98	0.45	350	79.54	4.11	79.05	4.31

^a Viscosity measured in concentrated sulfuric acid, 0.2 g/100 ml, at 25°C.

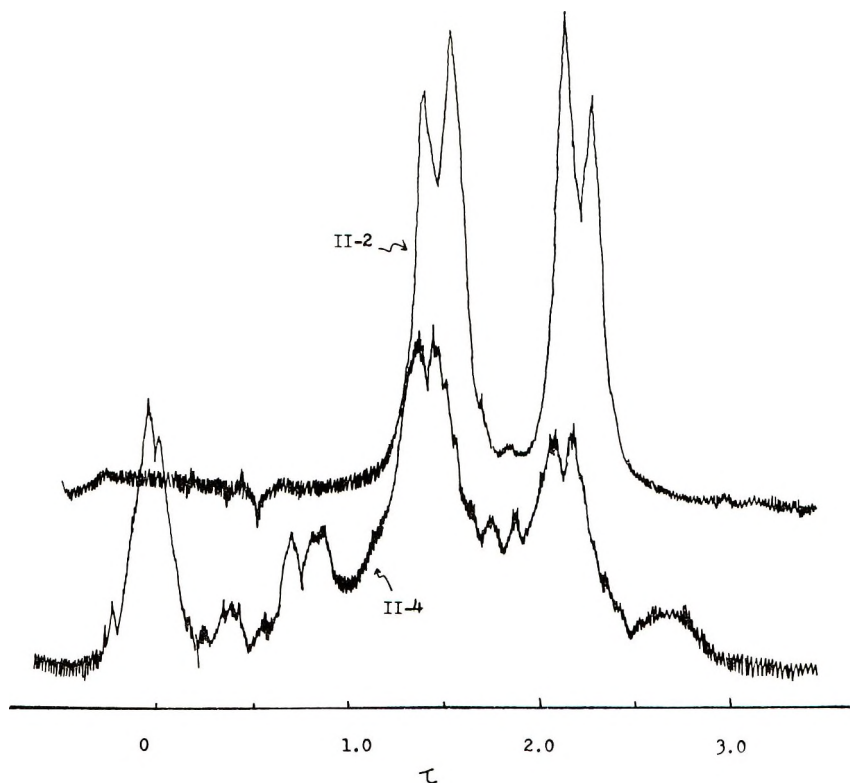
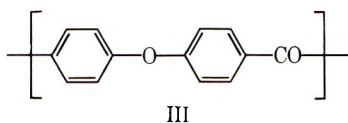


Fig. 1. NMR spectra of polyketones I-2 and I-4.

spectrum of *p*-methoxybenzoic acid. Therefore, the polyketone obtained here would be considered to be linear and have only one kind of structural unit (III).



On the other hand, polyketone I-4 (Table I) gave a more complicated spectrum.

Formation of Polyamide from Polyketone

Amides are known to be prepared from ketones by Schmidt reaction. The polyketone so obtained was then subjected to a reaction with sodium azide in PPA and sulfuric acid to give polyamide. The results are shown in Table II. The infrared spectrum of the polymer formed showed characteristic absorptions around 3300, 1650, and 1530 cm^{-1} . Results of elemental analysis (Table II) show that a temperature of 50°C and a reaction period of 9 hr is enough to give the amide, but 30°C and 4 hr could not convert the ketone to amide completely.

TABLE II
Reaction of Polyketone with Sodium Azide

No.	Wt polyketone, g.	Wt Na ₂ N ₃ , g.	Solvent	Temp, °C	Time, hr	Yield, %	η_{inh}	PMT, °C	Anal.					
									Calcd			Found		
									C, %	H, %	N, %	C, %	H, %	N, %
II-1	1.2 ^a	0.38	Oleum	35-45	3	1.19	0.44	205	73.92	4.30	6.63	73.62	4.11	2.49
II-2	1.0 ^b	0.32	PPA	50	9	0.94	1.25	255	73.92	4.30	6.63	73.10	4.35	6.47
II-3	5.0 ^b	1.44	PPA	50	7.5	0.56								

^a $\eta_{inh} = 0.44$.

^b The polyketone was prepared from the indicated weight of 4-phenoxybenzoic acid in PPA, and the resulting polyketone was subjected to subsequent Schmidt reaction in PPA without isolating the polymer.

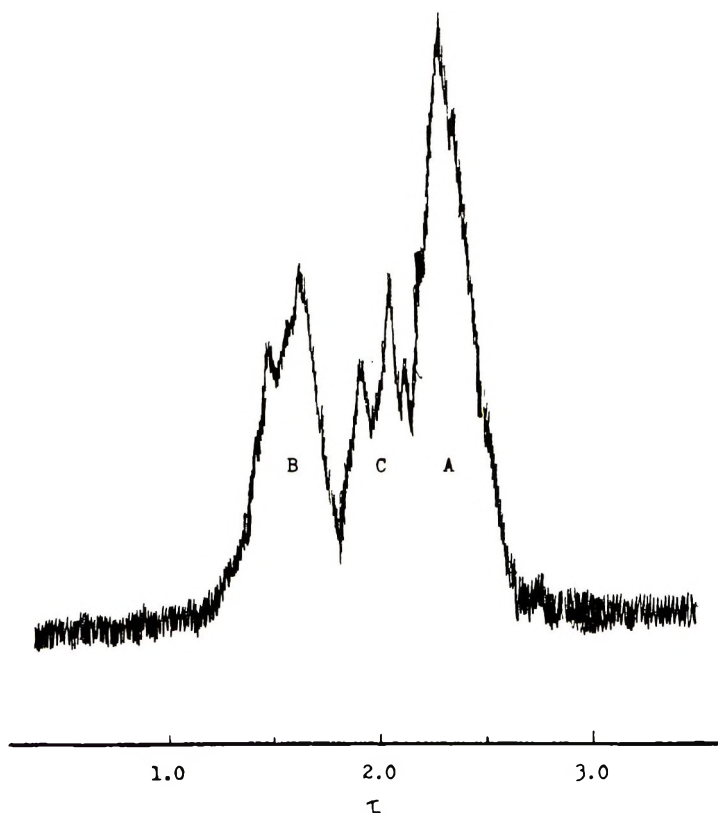
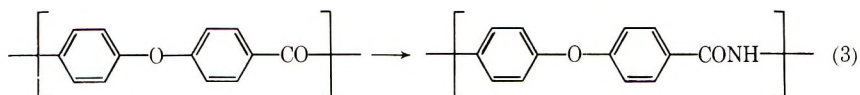


Fig. 2. NMR spectrum of polyamide II-2.

Viscosities of the polymers obtained did not decrease. In polymer II-2, rather, an increase in viscosity was observed. The NMR spectrum of polymer II-2 is shown in Figure 2.

Signals of the polymer seem to be divided into three parts: A, B, and C. The areas of the signals B and C were nearly the same and about one half of that of A. The chemical shifts of A and B were nearly the same as those of polyketone in Figure 1. The NMR results seem to correspond to a change of the ketone to amide as shown in eq. (3), if the signal of C is attributed to protons *ortho* to the amino group.



To elucidate the structure of the polyamide further, polyamide II-2 was hydrolyzed by boiling it in aqueous hydrogen chloride. The hydrolysis of the polymer was slow. On boiling the polymer for 60 hr, about 60% of the polymer was recovered. The infrared spectrum of the polymer recovered was essentially the same as that of original polymer. This

of the amount of the amino acid. However, the actual molar ratio of diamine, dicarboxylic acid, and amino acid was approximately 3:2:20 in mole. Therefore, the amide group formed at first seems to give some influence to the direction of next rearrangement. X-ray diffraction patterns of polyketone I-2 and polyamide II-2 are shown in Figure 3.

The polyketone is essentially amorphous, but the polyamide seems to be partially crystalline. If the direction of the rearrangement in Schmidt reaction were quite random, the polyamide obtained would be rather amorphous. Therefore, actual crystallinity of the polyamide obtained may support the above assumption.

Beckmann rearrangement through oxime is also well known as an another amide formation reaction from ketone. As the aromatic polyketone obtained here was insoluble in almost all organic solvents, the reaction of it with hydroxyl amine and the succeeding rearrangement were examined in PPA and sulfuric acid, and the results are shown in Table III.

TABLE III
Reaction of Polyketone with Hydroxylamine

No.	Wt polyketone, g	Wt NH ₂ OH·- HCl, g	Solvent	Temp, °C	Time, min	Yield, %	η_{inh}
III-1	0.70 ^a	0.248	PPA 12 g	100 135	60 45	0.47	0.12
III-2	0.50 ^a	0.177	H ₂ SO ₄ 4 ml	100 130	25 20	0.50	0.16
III-3	0.50 ^a	0.177	"	100 130	15 10	0.50	0.15

^a $\eta_{inh} = 0.44$.

The infrared absorption spectra of the products indicated that the polymer obtained in PPA had some amide linkage which was suggested by absorptions at 3300 and 1530 cm^{-1} . But the polymer obtained in sulfuric acid had no amide linkage. Viscosities of the polymers in both cases became very small. Therefore, a chain degradation reaction seemed to occur prior to the rearrangement.

Properties of Polyketone and Polyamide

The polyketones obtained here were insoluble in almost all organic solvents, but the polyamide was soluble in some organic solvents. The qualitative solubility of the polyamide II-2 is shown in Table IV.

Thermal behavior of polyketone and polyamide was examined by thermogravimetric analysis; results are shown in Figure 4.

A weight loss in these polymers was observed above 435°C, both in nitrogen and in air. This result shows sufficient thermal stability of both polymers.

TABLE IV
Solubility of Polyamide II-2

Solvent	Solubility ^a
Concentrated sulfuric acid	+++
Dichloroacetic acid	+++
Formic acid	—
<i>m</i> -Cresol	+++
Dimethyl sulfoxide	++
<i>N</i> -Methylpyrrolidone	+
Dimethyl formamide	—
Hexamethyl phosphoramide	—

^a Solubility: (+++) soluble easily, able to form film cast from the solution; (++) soluble on heating; (+) partially soluble; (—) insoluble.

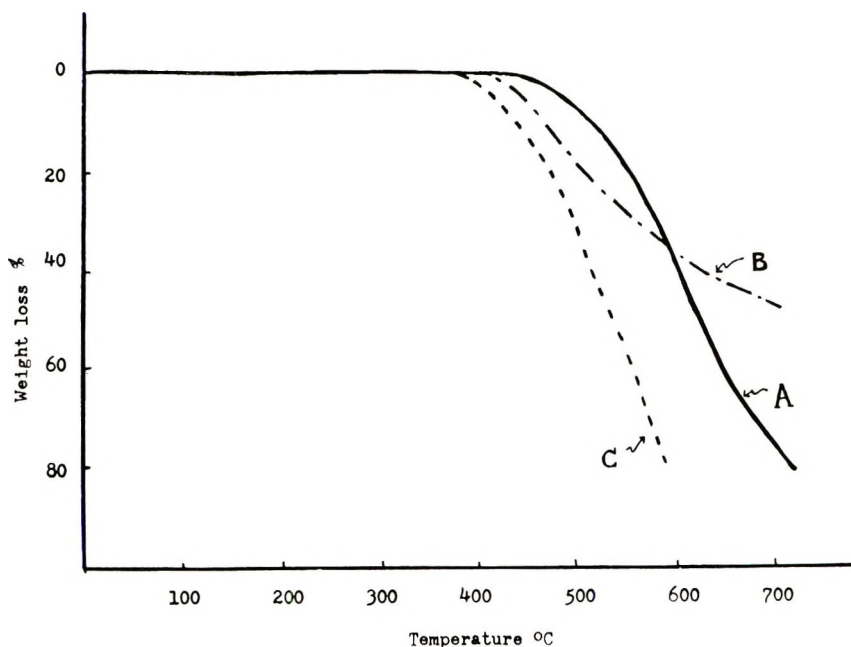


Fig. 4. Results of thermogravimetry. (A) polyketone I-2 in N_2 ; (B) polyamide II-2 in N_2 ; (C) polyamide II-2 in air.

EXPERIMENTAL

Materials

4-Phenoxybenzoic Acid. 4-Phenoxybenzoic acid was prepared according to Tomita⁷ by oxidizing 4-phenoxytoluene with potassium permanganate; mp 160–161.5°C (lit.⁷ 160°C).

3-Phenoxybenzoic Acid. This compound was synthesized from 3-phenoxytoluene similarly as the 4-phenoxy compound; mp 145°C (lit.⁸ 145°C).

Solvents. Solvents used were commercially available. Sulfuric acid was 98% analytical grade and PPA was 116%.

Polymerization to Polyketone

A typical example will be described. In a two-necked 50-ml flask equipped with stirrer and thermometer was placed 20 g of PPA and 1.00 g of well ground 4-phenoxybenzoic acid. The flask was heated with stirring at a definite temperature for a given time. On pouring the reaction mixture in ice water, white polymer precipitated. After filtration, the polymer was dipped in diluted aqueous sodium bicarbonate solution, washed with water, and dried. The polymer yield was 0.9 g.

Amidation Reaction

Schmidt Reaction A. A mixture of 7 ml of concentrated sulfuric acid, 0.5 g of oleum, 1.2 g of polyketone, and 0.38 g of sodium azide was heated at 35°C for 4 hr. The reaction mixture became red-orange. After cooling the reaction mixture, it was poured into ice water and the polymer precipitated was collected. The polymer produced was dipped in aqueous sodium bicarbonate solution, washed with water, and dried; the yield was 1.19 g; the polymer melting point was 205°C.

Schmidt Reaction B. A mixture of 1.00 g of 4-phenoxybenzoic acid and 23 g of PPA was heated at 100°C for 14 hr with stirring. After cooling of the reaction mixture, 0.320 g of sodium azide was added during 15 min. The mixture was heated again to 50°C for an additional 9 hr. The resulting polymer was isolated similarly as above. The yield was 0.940 g, polymer melting point 255°C.

Beckmann Rearrangement

To a mixture of 0.700 g of polyketone and 13 g of PPA was added 0.248 g of hydroxylamine hydrochloride at 90°C for 15 min. After addition of the salt, the reaction mixture was heated at 100°C for 60 min and for an additional 45 min at 130°C. Isolation and purification of the polymer was similar to above; the yield was 0.419 g.

Hydrolysis of the Polyamide

A mixture of 100 ml of concentrated hydrochloric acid and 1.500 g of the polyamide was refluxed for 60 hr. The undissolved polymer was collected by filtration, washed with hot water, and dried, yielding 920 mg of material. The filtrate and hot water which was used for washing were combined and concentrated to 20 ml. On cooling the residual solution, white crystals precipitated. The crystals (4,4'-dicarboxydiphenyl ether) were recrystallized from water, yielding 55 mg. The filtrate was made alkaline by adding potassium hydroxide and extracted with ether. From the ethereal solution, 4,4'-diaminodiphenyl ether, 62 mg was obtained. The alkaline aqueous solution was acidified again by hydrochloric acid and concentrated

under reduced pressure and extracted with methanol. From the methanol solution 4-amino-4'-carboxydiphenyl ether 450 mg was isolated.

References

1. S. Inoue, Y. Imai, K. Uno, and Y. Iwakura, *Makromol. Chem.*, **95**, 236 (1966).
2. H. W. Bonner, U.S. Pat. 3,065,205 (1962).
3. S. D. Ron and M. Schwarz, *J. Amer. Chem. Soc.*, **79**, 3020 (1955).
4. Y. Iwakura, K. Uno, and S. Hara, *J. Polym. Sci. A*, **3**, 45 (1965).
5. Y. Iwakura, K. Uno, and Y. Imai, *J. Polym. Sci. A*, **2**, 2615 (1964).
6. Y. Iwakura, K. Uno, and T. Takiguchi, *J. Soc. Org. Synth. Chem. Japan*, **25**, 797 (1967).
7. M. Tomita, Y. Okajima, K. Yoshida, and H. Nariyuki, *J. Pharm. Soc. Japan*, **70**, 42 (1950).
8. G. Lork and F. H. Kempter, *Monatsh. Chem.*, **67**, 23 (1935).

Received December 21, 1967

Revised May 1, 1968

Polyhydrazides. I.

N-Alkylated Polyhydrazides from Diesters and Hydrazine

YOSHIO IWAKURA, KEIKICHI UNO, SHIGEYOSHI HARA,*
and SHIGERU KUROSAWA, *Department of Synthetic Chemistry,
Faculty of Engineering, University of Tokyo, Bunkyo-ku, Tokyo, Japan*

Synopsis

N-Alkylated polyhydrazides containing 1,3,4-oxadiazole linkages in them were prepared by solution polycondensation of dicarboxylic acid diesters with hydrazine in fuming sulfuric acid or polyphosphoric acid. Their preparation, characterization, and some physical properties are described.

INTRODUCTION

The study reported previously¹ has indicated that high molecular weight poly-1,3,4-oxadiazoles can easily be prepared by solution polycondensation of dicarboxylic acids or their simple derivatives, such as amides and nitriles, and hydrazine sulfate in fuming sulfuric acid or polyphosphoric acid. Fuming sulfuric acid (oleum) and polyphosphoric acid (PPA) were used as not only condensing agents but also solvents of the polycondensation. In the course of this investigation, when dialkyl esters were used as the dicarboxylic acid derivatives, the resulting polymers showed behavior different from that of poly-1,3,4-oxadiazoles, and these polymers were found to be *N*-alkylated polyhydrazides.

The solution polycondensation of terephthaloyl chloride and alkylhydrazine was reported to give *N*-alkylated polyhydrazide by Frazer and Wallenberger.² This is the only paper that described the preparation of *N*-alkylated polyhydrazide.

In this paper, the polycondensation of various dialkyl esters of dicarboxylic acids with hydrazine salts and the characterization of the resulting polymers will be described.

RESULTS AND DISCUSSION

Solution Polycondensation

Tables I and II show the results of the polycondensation of terephthalic acid diesters with hydrazine in oleum and in PPA, respectively. In

* Present address: Teijin Limited, Tokyo, Japan.

TABLE I
Polycondensations of Terephthalic Acid Diesters and Hydrazine Sulfate in Fuming Sulfuric Acid

No.	Monomers			Wt oleum, g ^a	Reaction conditions			Polymer	
	Diester	Wt diester, g	Wt hydrazine sulfate, g		Temp, °C	Time, hr	Yield, g	η_{inh}^b	
								H ₂ SO ₄	<i>m</i> -Cresol
PI-1	Dimethyl	7.7	6.2	100	85	2	6.9	0.05	1.47
PI-2	Diethyl	4.4	3.3	50	100	2	2.9	1.61	Insol. ^c
PI-3	Di- <i>n</i> -propyl	1.25	0.8	13	85	3	0.8	0.08	Insol.
PI-4	Diisopropyl	1.25	0.8	13	130	5	0.7	0.06	Insol.
PI-5	Diphenyl	2.0	1.0	20	130	5	1.0	1.49	Insol.
PI-6	Dibenzyl	1.7	0.7	13	110	1.5	2.7	0.12	Insol.
					85	3			
					130	4			

^a Oleum: 30% SO₃-fuming sulfuric acid.

^b Measured at a concentration of 0.2 g/100 ml at 30°C.

^c The polymer was insoluble in organic solvents.

TABLE II
Polycondensations of Terephthalic Acid Diesters and Hydrazine Salts in Polyphosphoric Acid

No.	Monomers		Wt hydrazine salt, g	Wt PPA, g ^a	Reaction conditions		Polymer		
	Diester	Hydrazine salts			Temp, °C	Time, hr	Yield, g	η_{inh}^b	
								H ₂ SO ₄	<i>m</i> -Cresol
PII-1	Dimethyl	Sulfate	3.2	50	140	6	3.3	—	0.03
PII-2	Dimethyl	Dihydrochloride	2.5	50	140	3	3.4	—	0.15
PII-3	Diethyl	Sulfate	3.2	50	140	3	4.1	—	0.60
PII-4	Diethyl	Dihydrochloride	2.5	50	160	6	3.7	0.04	0.85
PII-5	Di- <i>n</i> -propyl	Dihydrochloride	1.2	25	140	3	1.5	0.29	Insol.
PII-6	Diisopropyl	Dihydrochloride	1.2	25	170	4	1.6	0.68	Insol.
PII-7	Diphenyl	Sulfate	1.6	25	170	4	1.9	0.28	Insol.
PII-8	Diphenyl	Dihydrochloride	1.3	25	160	6.5	1.8	0.28	Insol.
PII-9	Dibenzyl	Sulfate	0.7	15	140	15	1.7	0.18	Insol.
					160	15			

^a PPA: 116% Polyphosphoric acid.

^b See Table I.

TABLE III
Polycondensations of Isophthalic Acid Diesters and Hydrazine Salts in Fuming Sulfuric Acid or Polyphosphoric Acid

No.	Monomers			Reaction solvent ^a	Wt. solvent, g	Reaction conditions		Polymer			
	Diester	Wt di-ester, g	Hydrazine salt			Wt hydra-zine, g	Temp, °C	Time, hr	Yield, g	η_{inh}^b	
								H ₂ SO ₄	<i>m</i> -Cresol		
PIII-1	Dimethyl	1.9	Sulfate	1.4	30	Oleum	85	3	1.8	0.06	1.15
							130	4			
PIII-2	Diethyl	4.4	Sulfate	2.9	50	Oleum	85	3	2.9	0.20	Insol. ^b
							130	10			
PIII-3	Diphenyl	3.2	Sulfate	1.4	25	Oleum	85	3	1.6	0.84	Insol.
							130	7			
PIII-4	Dimethyl	1.9	Dihydro-chloride	1.3	25	PPA	140	3	1.7	—	0.16
							170	13.5			
PIII-5	Diethyl	4.4	Dihydro-chloride	2.5	50	PPA	140	3	3.6	—	0.46
							170	6			
PIII-6	Di- <i>n</i> -propyl	2.5	Dihydro-chloride	1.2	25	PPA	140	3	1.6	0.47	Insol.
							170	4			
PIII-7	Diphenyl	3.2	Dihydro-chloride	1.3	35	PPA	140	3	2.3 ^c	—	—
							170	13			

^a See Tables I and II.

^b See Table I.

^c Most of the diester remained unreacted.

TABLE IV
 Polycondensation of Dimethyl Ester of *trans*-1,4-Cyclohexanedicarboxylic Acid (CHM) or Sebacic Acid (SM)
 and Hydrazine Sulfate in Polyphosphoric Acid

No.	Diester	Wt diesters, g	Wt hydrazine sulfate, g	Wt PPA, g	Reaction conditions		Polymer		
					Temp, °C	Time, hr	Yield g	PAIT, °C	η_{inh}^a
PIV-1	CHM	5.4	2.9	50	140	3	3.8	270	1.16
PIV-2	SM	4.6	3.1	50	140	2	3.9	200	1.90

^a Measured at a concentration of 0.2 g/100 ml in *m*-Cresol at 30°C.

TABLE V
Self-Polycondensation of Terephthalic Acid Monoethyl Ester
Monohydrazide in PPA or in Oleum

No.	Wt monomer, g	Reaction medium	Wt reaction medium, g	Reaction conditions		Polymer	
				Temp, °C	Time, hr	Yield, g	η_{inh}^a
PV-1	1.0	PPA	15	140	3	0.7	0.28
PV-2	0.8	Oleum	11	85	3	0.6	1.15
				139	1		

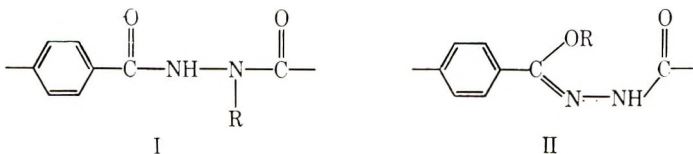
* Measured at a concentration of 0.2 g/100 ml in 10% SO₃-fuming sulfuric acid at 30°C.

Table III, the results of the polycondensation of isophthalic acid diesters with hydrazine salts in oleum or in PPA are listed. The results from diesters of nonaromatic dicarboxylic acid and hydrazine sulfate are described in Table IV. In Table V are shown the results of the self-polycondensation of monoethyl ester monohydrazide of terephthalic acid in oleum and in PPA.

When fuming sulfuric acid was used as a solvent and a condensing agent, soluble polymers were obtained only from dimethyl esters (PI-1 and PIII-1), where the word "soluble" means soluble in dichloroacetic acid. On the other hand, with PPA, soluble polymers were obtained both from dimethyl esters (PII-1, PII-2, PIII-4, PIV-1, and PIV-2) and from diethyl esters (PII-3, PII-4, and PIII-5). However, with diphenyl isophthalate, most of it remained unreacted. When the self-polycondensation was carried out in polyphosphoric acid, the obtained polymer (PV-1) was partly soluble in dichloroacetic acid.

Structures of Polymers

Figure 1 shows the infrared spectra of the soluble polymers (PI-1 and PII-4). They gave strong amide absorption bands at 3250, 1680–1650, 1525, and 1300 cm⁻¹, and they also showed absorption bands at 3000–2800, 1470–1460, and 1380 cm⁻¹ characteristic of methyl and ethyl groups. In addition to the above, the weak absorption bands of 1,3,4-oxadiazole structure were observed. The above result of the infrared spectra may suggest the presence of structures I or II in the soluble polymers along with a small extent of 1,3,4-oxadiazole units.



Results of elemental analyses shown in Table VI also support such a structure. Then, in order to make it clear which of the presumed structures is correct, the following experiments, were carried out.

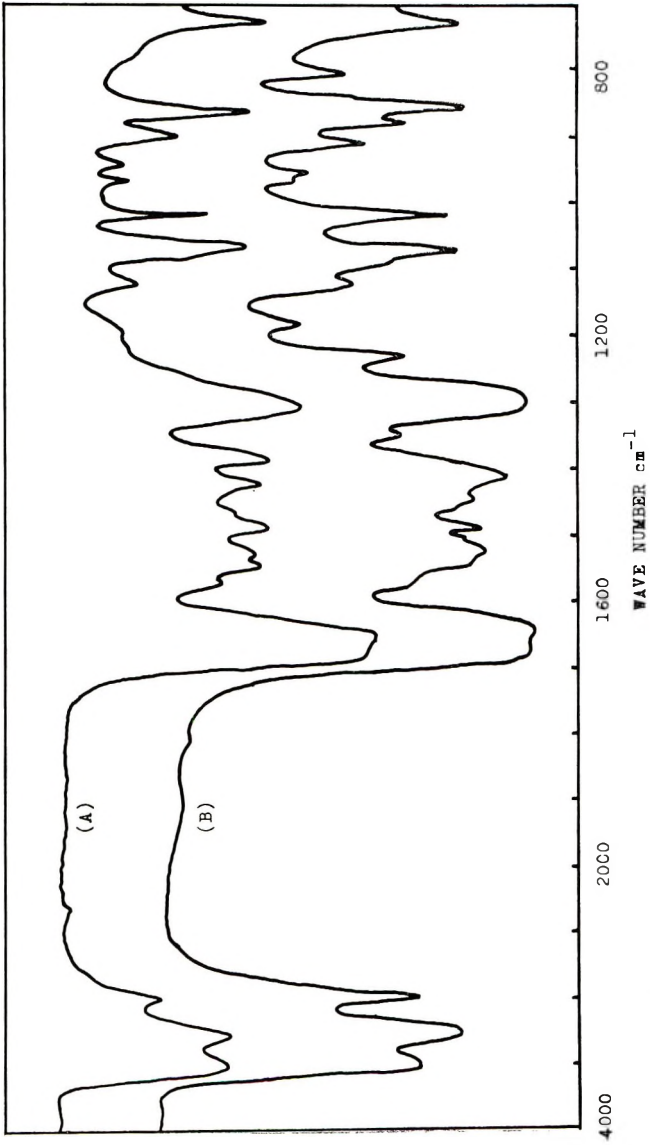
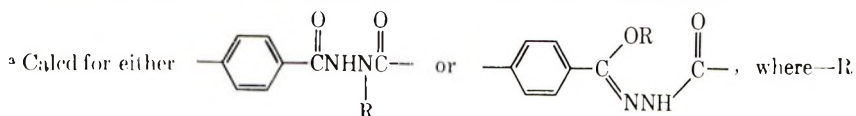


Fig. 1. Infrared spectra of the soluble polymers: (A) PI-I film; (B) PII-4 film.

TABLE VI
 Nitrogen Analyses

Polymer	N, %	
	Calcd ^a	Found
PI-1	15.90 ^b	15.73
PII-3	14.73 ^c	14.65
PIII-1	15.90 ^b	16.40
PIII-5	14.73 ^c	15.28

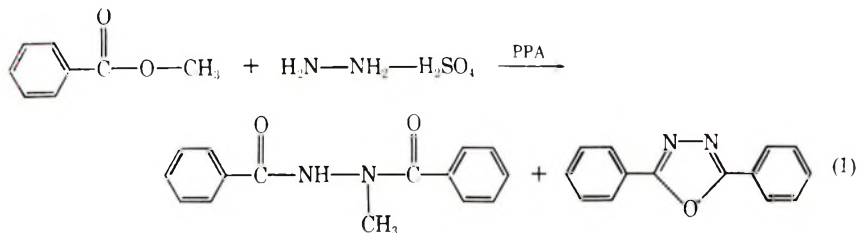


is —CH₃, —C₂H₅.

^b Calcd for R = CH₃.

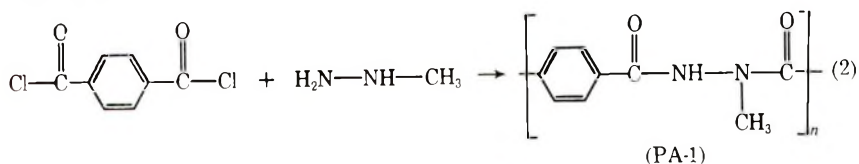
^c Calcd for R = C₂H₅.

Model Reaction. On the condensation reaction of methyl benzoate with hydrazine sulfate in polyphosphoric acid, the mixture of *N*-methyl-*N,N'*-dibenzoylhydrazine and 2,5-diphenyl-1,3,4-oxadiazole resulted almost quantitatively [eq. (1)].



The result of this model reaction should support structure I, and also explains the existence of phenylene-1,3,4-oxadiazole unit in the polymer chain. Moreover, as shown in Figure 2A, *N*-methyl-*N,N'*-dibenzoylhydrazine gave an infrared absorption spectrum very similar to that of PI-1.

Comparison with Authentic Polymer. Authentic poly-*N*-methylterephthallylhydrazide (PA-1) was prepared from terephthaloyl chloride and methylhydrazine by the use of an interfacial polycondensation procedure [eq. (2)].



The infrared spectrum of PA-1, shown in Figure 2B, coincides well with that of PI-1 shown in Figure 1A, except that the infrared spectrum of PA-1 has no absorption band characteristic of the 1,3,4-oxadiazole linkage. This fact also supports the structure I.

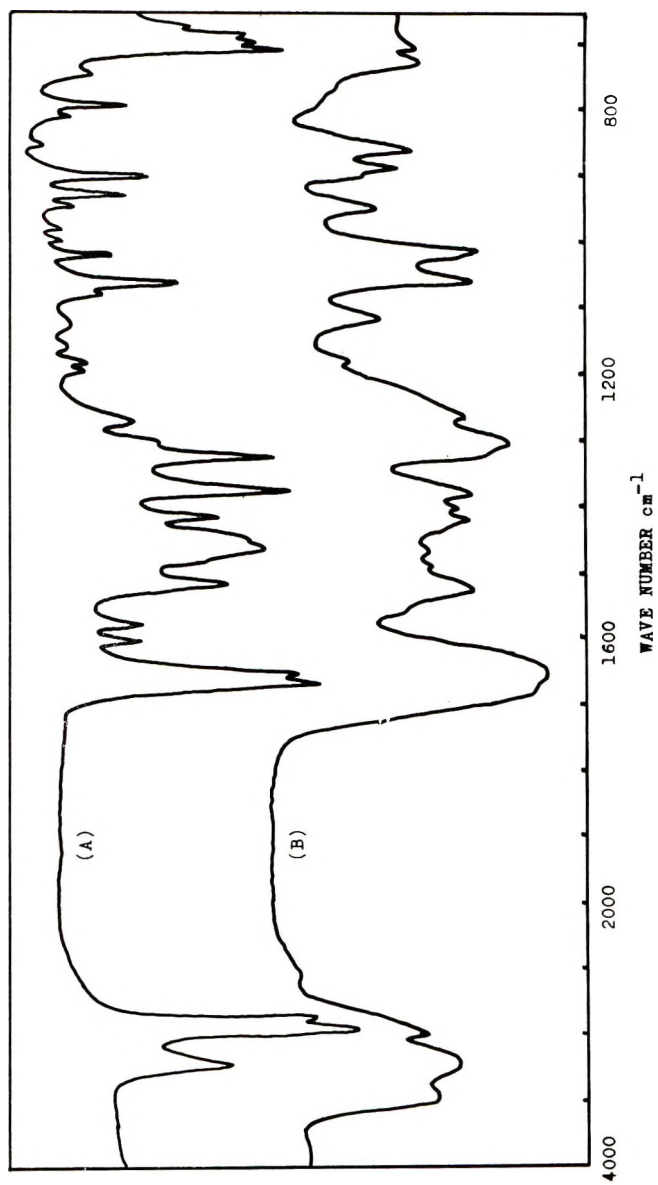


Fig. 2. Infrared spectra: (A) *N*-methyl-*N,N'*-dibenzoylhydrazine in Nujol; (B) authentic poly-*N*-methylterephthalylhydrazide film.

The infrared spectra of insoluble polymers obtained were of the same form as those of polyphenylene-1,3,4-oxadiazoles.¹ But when the attained molecular weight of the polymer was very low, for example, in the case of PI-3 and PI-4, strong absorption bands characteristic of ester groups were observed. On the other hand, polymers of much higher molecular weight (PII-7 and PII-8) gave a weak absorption band at 1730–1715 cm^{-1} .

Physical Properties of Polymers

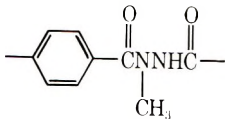
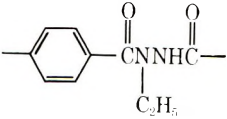
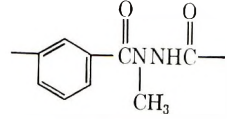
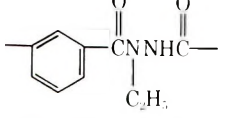
Since the soluble polymers obtained here have both hydrazide linkages and 1,3,4-oxadiazole units, these polymers are essentially copolymers. The properties of these copolymers, therefore, are thought to change with the variation of the ratio of 1,3,4-oxadiazole unit to hydrazide unit, and some characteristic properties for the soluble polymers are described qualitatively below.

N-Alkylated polyhydrazides (alkyl = methyl, ethyl) obtained here were soluble in such organic solvents as dimethyl sulfoxide, dimethylformamide, dimethylacetamide, *N*-methylpyrrolidone, formic acid, and dichloroacetic acid at room temperature or on warming. Tough films could be cast from those solutions of the polymers.

The x-ray diffraction diagrams measured by the powder method with the use of Ni-filtered $\text{CuK}\alpha$ radiation indicated that all *N*-alkylated polyhydrazides obtained here were amorphous.

Melting temperatures of these polyhydrazides are listed in Table VII. On being kept at their respective melting temperatures, the polymers

TABLE VII
Melting Temperatures (PMT) of Polymers

Polyhydrazide	PMT, °C ^a
PI-1 	330–340
PII-3 	310–320
PIII-1 	280–290
PIII-5 	265–275

^a PMT was measured on the hot stage.

solidified immediately and became infusible. Figure 3 shows the thermogravimetric analysis curves for polyhydrazides. Unsubstituted polyisophthalylhydrazide showed a clear and abrupt weight loss due to cyclodehydration above 280°C. Similar weight losses were observed in the curves of *N*-alkylated polyhydrazides above their melting temperatures, but not so sharply. These weight losses would correspond to the cyclization and subsequent degradation. After being kept for 7 hr under reduced

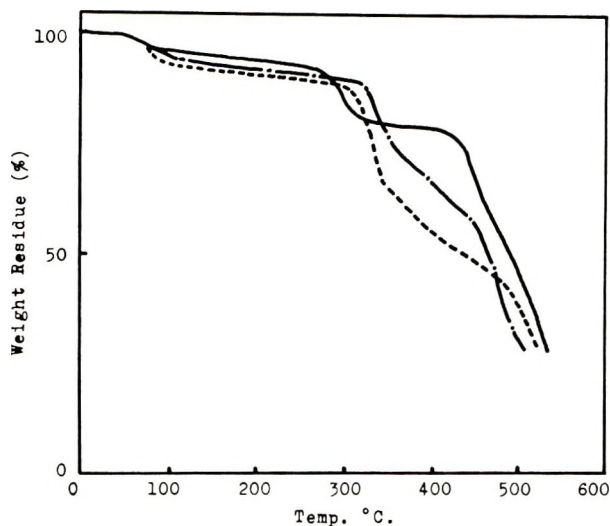
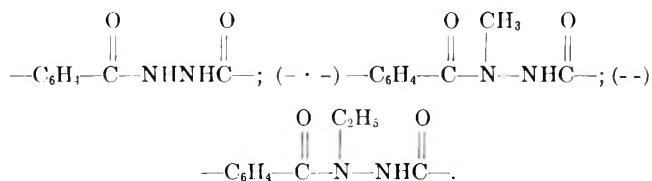


Fig. 3. Thermogravimetric analysis curves for polyhydrazides in air: (—);



pressure at 300°C, as shown in Figure 4, PI-1 gave an infrared spectrum very similar to that of poly-*p*-phenylene-1,3,4-oxadiazole, though it still gave a considerable amount of amide absorption bands. These facts may indicate that *N*-alkylated polyhydrazides can thermally be converted to poly-*p*-phenylene-1,3,4-oxadiazole. However, the conversion to oxadiazole is a little more difficult than that of unsubstituted polyhydrazide.

EXPERIMENTAL

Materials

Hydrazine salts, diesters of terephthalic and isophthalic acid, and other reagents used here were obtained commercially or prepared by the usual methods. They were purified by recrystallization or distillation.

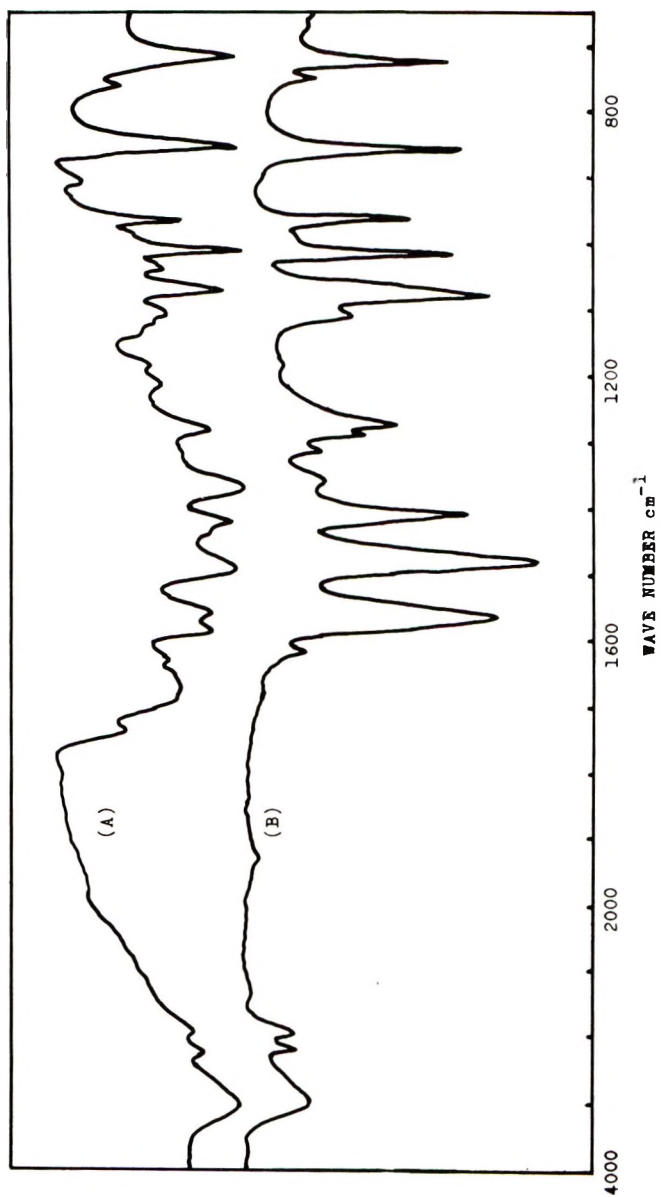


Fig. 4. Infrared spectra: (A) PI-1 in KBr (after being heated for 7 hr at 300°C); (B) 'insoluble' polymer film PI-5.

Fuming sulfuric acid (30% SO₃) and 116% polyphosphoric acid, were commercially available and were used without further purification.

Model Compound

The authentic *N*-methyl-*N,N'*-dibenzoylhydrazine was prepared from methylhydrazine and benzoyl chloride by the method of Brüning;³ mp 142.5–143°C (lit.³ mp 143°C).

Model Reaction

To 100 g of 116% polyphosphoric acid were added 13.6 g of methyl benzoate and 6.5 g of hydrazine sulfate. The reaction mixture was heated to 140°C and kept at this temperature for 8 hr under mechanical stirring and then poured into 1 liter of ice water. The precipitate was filtered, washed several times with water, and dried. The product weighed 12 g. The infrared spectrum of this precipitate was perfectly equal to that of the mixture of *N*-methyl-*N,N'*-dibenzoylhydrazine and 2,5-diphenyl-1,3,4-oxadiazole. The latter component was isolated from the mixture by fractional recrystallization from water-ethanol solution, as it was less soluble than the former component. It weighed 2 g and melted at 136–136.5°C (lit.⁴ mp 138°C). About 10 g of crude *N*-methyl-*N,N'*-dibenzoylhydrazine was obtained from the filtrate. It was purified by recrystallization from ethanol. It melted at 143.5–144°C (lit. mp 143°C,³ 145°C⁵).

Authentic Polymer

An authentic poly-*N*-methylterephthallylhydrazide was prepared as described below.

In a mixer was placed a solution of 3 g of methylhydrazine sulfate, 3.5 g of sodium hydroxide and 100 ml of ice water. To the vigorously stirred solution was added, all at one time, 4 g of terephthaloyl chloride dissolved in 30 ml chloroform. The reaction mixture was stirred for 10 min. Then, the precipitated polymer was filtered, washed with water, and dried under reduced pressure at 50°C. The yield was 1.7 g. The polymer obtained was partially insoluble in dimethyl sulfoxide probably due to crosslinking. The soluble part was used as the authentic sample for the comparison of the infrared spectra.

ANAL. Calcd for (C₉H₈N₂O₂)_n: C, 61.36%; H, 4.58%; N, 15.90%. Found: C, 61.11%; H, 4.81%; N, 15.70%.

Solution Polycondensation

Typical examples of the preparation of poly-*N*-alkyl-terephthallylhydrazides from diesters and hydrazine are described below.

Poly-*N*-methylterephthallylhydrazide (PI-1). Dimethyl terephthalate (7.7 g) and hydrazine sulfate (6.2 g) were heated in 30% SO₃-fuming sulfuric acid (100 g) to 85°C and kept for 2 hr at this temperature, and then this mixture was again heated to 110°C and kept for 3 hr at this

temperature. It gradually became viscous as the polycondensation reaction proceeded. The solution was poured into 1 liter of ice water with vigorous stirring. The precipitated polymer was filtered, dipped in running water for 3 days to remove sulfuric acid and dried under reduced pressure at 50°C. The product weighed 6.9 g. The polymer had an inherent viscosity of 1.71 (0.2% in *m*-cresol at 30°C), and an inherent viscosity of 0.05 (0.2% in 95% sulfuric acid at 30°C). It melted gradually between 330 and 340°C.

ANAL. Calcd for $(C_9H_8N_2O_2)_n$: N, 15.90%. Found: N, 15.73%.

Poly-*N*-ethylterephthalyhydrazide (PII-4). Diethyl terephthalate (4.4 g) and hydrazine dihydrochloride (2.5 g) were heated in 116% polyphosphoric acid (50 g) slowly to 140°C and kept at this temperature for 3 hr. The temperature was again raised to 160°C and kept for 4 hr at this temperature. After cooling to 80°C, the viscous solution was poured into 1 liter of ice water with vigorous stirring. The precipitate was dipped in running water for 3 days, and dried under reduced pressure at 50°C. The yield was 3.7 g. The inherent viscosity in *m*-cresol was 0.85 (0.2%) and that in 95% sulfuric acid was 0.04 (0.2%). The polymer melted at 310–320°C slowly.

References

1. Y. Iwakura, K. Uno, and S. Hara, *J. Polym. Sci. A*, **3**, 45 (1965).
2. A. H. Frazer and F. T. Wallenberger, *J. Polym. Sci. A*, **2**, 1147 (1964).
3. G. v. Brünig, *Ann.*, **253**, 12 (1889).
4. R. Stölle, *J. Prakt. Chem.*, **69**, 157 (1904).
5. A. Michaelis and E. Handanck, *Ber.*, **41**, 3289 (1908).

Received April 15, 1968

Revised May 31, 1968

Polyhydrazides. II.

***N*-Methylated Polyhydrazides by Direct Solution Polycondensations of Methylated Hydrazines and Dicarboxylic Acid Components**

YOSHIO IWAKURA, KEIKICHI UNO, SHIGEYOSHI HARA,*
and SHIGERU KUROSAWA, *Department of Synthetic Chemistry,
Faculty of Engineering, University of Tokyo, Bunkyo-ku, Tokyo, Japan*

Synopsis

N-Methylated polyhydrazides were prepared from methylated hydrazines and terephthalic acid or dimethyl terephthalate, and from terephthalic acid, hydrazine sulfate, and dimethyl sulfate by the solution polycondensation method in fuming sulfuric acid or polyphosphoric acid.

INTRODUCTION

In a series of studies on solution polycondensation with fuming sulfuric acid (oleum) or polyphosphoric acid (PPA) as a solvent, it has been reported¹ that polyphenylene-1,3,4-oxadiazoles were obtained from benzenedicarboxylic acids or their simple derivatives and hydrazine salts. However, *N*-alkylated polyhydrazides were formed when dialkyl esters of dicarboxylic acids were used as dicarboxylic acid components.² It was, therefore, expected that, when *N*-substituted hydrazines were used instead of hydrazine, *N*-substituted polyphenylenehydrazides would easily be obtained without further cyclization.

On the other hand, in the course of the investigation of the polycondensation between dimethyl terephthalate and hydrazine salts, it was of interest to know whether high molecular weight *N*-methylated polyhydrazide could be obtained from terephthalic acid and methylhydrazine in oleum or in PPA. Accordingly, in order to obtain some information on the reaction scheme of the polycondensation of dimethyl terephthalate and hydrazine, the investigations described in this paper were undertaken.

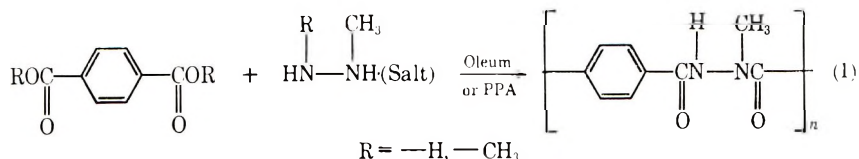
This paper describes the preparation of *N*-methylated polyhydrazides by solution polycondensation in oleum or PPA from terephthalic acid or dimethyl terephthalate and methylated hydrazines and from terephthalic acid with hydrazine sulfate or dimethyl sulfate.

* Present address: Teijin Limited, Tokyo, Japan.

RESULTS AND DISCUSSION

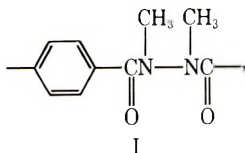
Polyhydrazides

The results of polycondensations are summarized in Tables I and II. *N*-Methylated polyhydrazide was prepared by the direct solution polycondensation of methylhydrazine or *N,N'*-dimethylhydrazine and terephthalic acid or dimethyl terephthalate in oleum or PPA [eq. (1)].

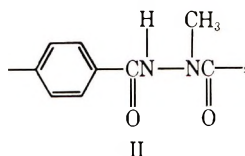


The molecular weights of *N*-methylated hydrazides obtained were not so high, but this polymer formation reaction was confirmed to proceed in fairly good yield.

When *N,N'*-dimethylhydrazine was used as a hydrazine component, the resulting polymer was expected to have the recurring unit I:



but the actual structure was quite different from this. The infrared spectrum and elemental analyses suggested that the structure of the polymer obtained was identical with that of poly-*N*-methylterephthalylhydrazide, II:



The formation of such a structure is presumably due to a new demethylation reaction. This demethylation reaction will be discussed later.

Fuming sulfuric acid was superior to polyphosphoric acid for the preparation of *N*-methylated polyhydrazides. PPA is known to give a higher molecular weight PPA easily on elimination of water from a low molecular weight PPA at a high temperature. Such a property of PPA, i.e., the presence of water eliminated, would cause the low molecular weights of polyhydrazides obtained in PPA. On polycondensation reaction in this system, the molar ratio of terephthalic acid and the hydrazine component seemed not to significantly affect the inherent viscosities of the polymers obtained. Similar results were obtained in the preparation of polyoxadiazoles from dicarboxylic acids and hydrazine salts.¹ Such a

TABLE I
Preparations of *N*-Methylated Polyhydrazide from Methylated Hydrazine

No.	Monomer A 	Hydrazine component B ^a	Molar ratio of monomers, A/B	Reaction solvents	Reaction conditions		Polymer		
					Temp, °C	Time, hr	Yield, % ^b	η_{inh}^c	PMT, °C ^d
PI-1	OH	MHS	1	Oleum	80	2	78	0.20	300
PI-2	OH	MHS	2	Oleum	100	2	84	0.41	320
PI-3	OH	MHS	2	PPA	100	8	80	0.11	275
PI-4	OCH ₃	MHS	2	Oleum	120	2	84	0.40	300
PII-1	OH	DNH	1	Oleum	150	28	27	0.15	300
PII-2	OH	DMH	2	Oleum	100	10	67	0.17	300
PII-3	OH	DMH	2.6	Oleum	80	2	82	0.18	300
PII-4	OH	DMH	2	PPA	100	10	30	0.10	260
PII-5	OCH ₃	DMH	2	Oleum	120	2	83	0.23	290
PII-6	OCH ₃	DMH	2	PPA	150	28	—	—	—

^a MHS = methylhydrazine sulfate; DMH = *N,N'*-dimethylhydrazine dihydrochloride.

^b Calculation based on theoretical yield for complete polycondensation.

^c In *m*-cresol at a concentration of 0.2 g/100 ml at 30°C.

^d Polymer melt temperature on hot stage.

TABLE II
 Polycondensation of Terephthalic Acid and Hydrazine Sulfate in the Presence of Dimethyl Sulfate in Oleum^a

No.	Wt terephthalic acid, g	Wt hydrazine sulfate, g	Wt dimethyl sulfate, g	Reaction conditions		Polymer		
				Temp, °C	Time, hr	Yield, g	η_{inh}^b	PMT, °C
PIII-1	1.7	2.0	3.8	125	0.5	1.7	0.86	Infusible ^c
PIII-2	1.7	1.5	3.8	135	1.5	1.7	0.92	Infusible ^c
PIII-3	1.7	1.5	4.2	135	2.5	1.6	0.64	320

^a Oleum (30% SO₃ fuming sulfuric acid), 50 g.

^b Obtained in dichloroacetic acid at a concentration of 0.2 g/100 ml, at 30°C.

^c Infusible below 500°C but degraded gradually above 320°C.

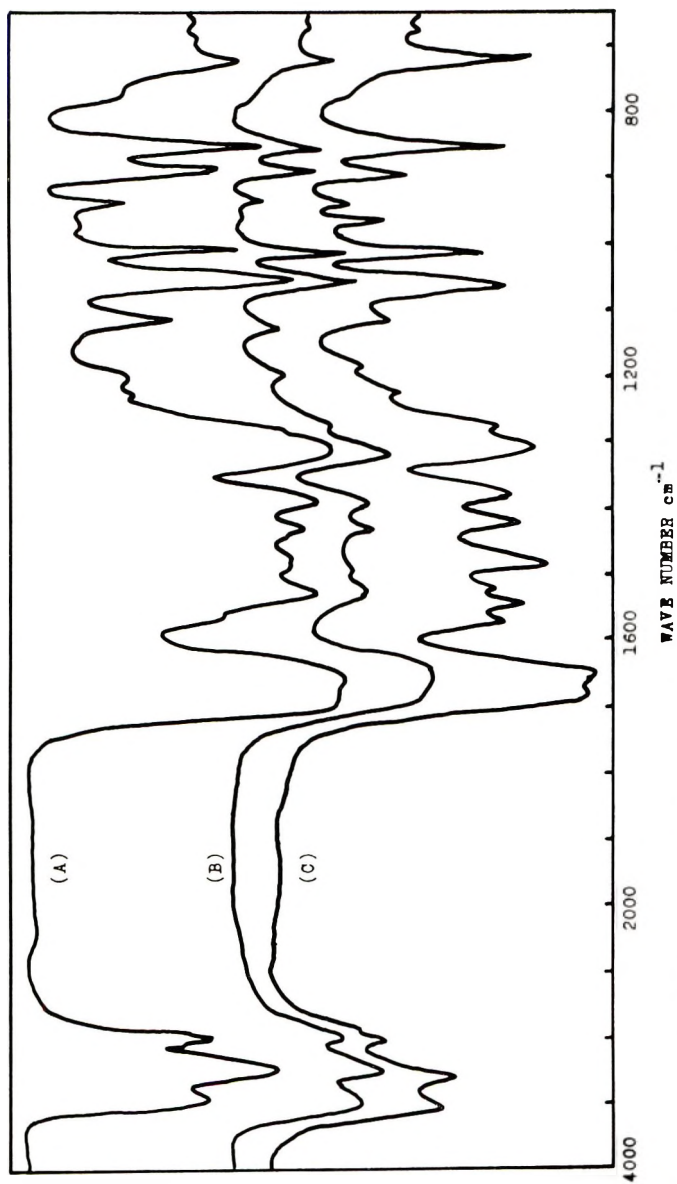
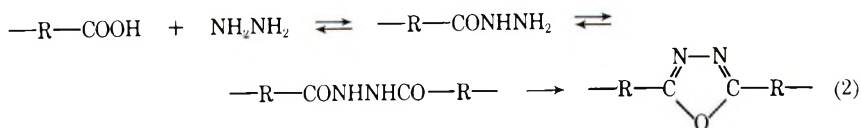


Fig. 1. Infrared spectra of polymers: (A) PI-2 film; (B) PI-1 film; (C) PIII-2 film.

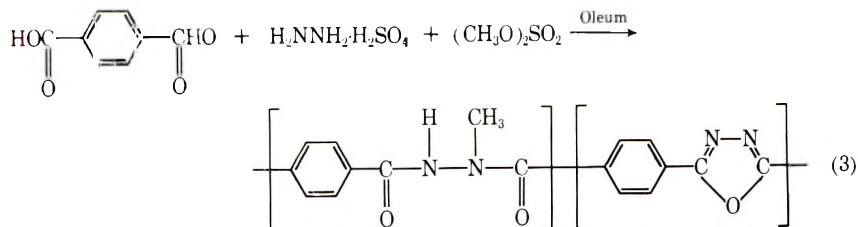
phenomenon has been considered to occur as a result of the apparent irreversible formation of oxadiazole ring from hydrazide as shown in eqs. (2):



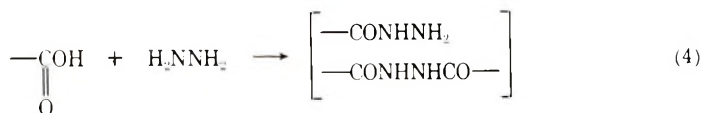
However, the results obtained here would suggest that the diacyl type compound is also very stable in this system, and almost all of the compounds go to the right-hand side of the equilibrium eqs. (2) to form diacyl hydrazine.

The infrared spectra of PI and PII, as shown in Figure 1, agreed well with that of the authentic poly-*N*-methylterephthalyhydrazide.²

On the polycondensation of terephthalic acid with hydrazine sulfate in the presence of dimethyl sulfate, a polymer having a different structure from poly-1,3,4-oxadiazole, was obtained. The results are listed in Table II. All polymers obtained by this method showed high inherent viscosities. The infrared spectrum of the polymer gave absorptions characteristic of hydrazide in addition to the absorptions of the 1,3,4-oxadiazole ring. The polymer obtained was soluble in dichloroacetic acid. Therefore the polymer would be composed of 1,3,4-oxadiazole and *N*-methylhydrazide units as shown in eq. (3).

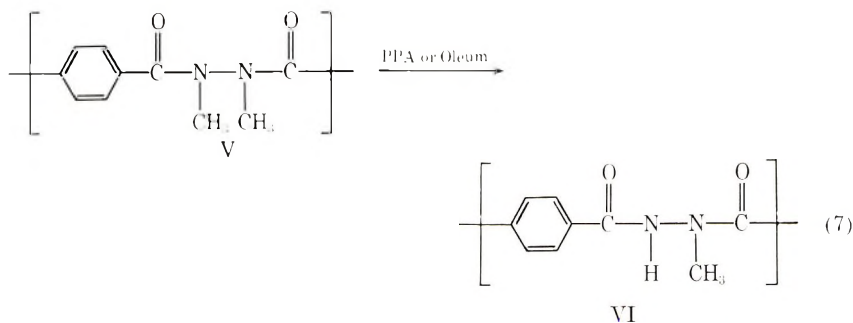
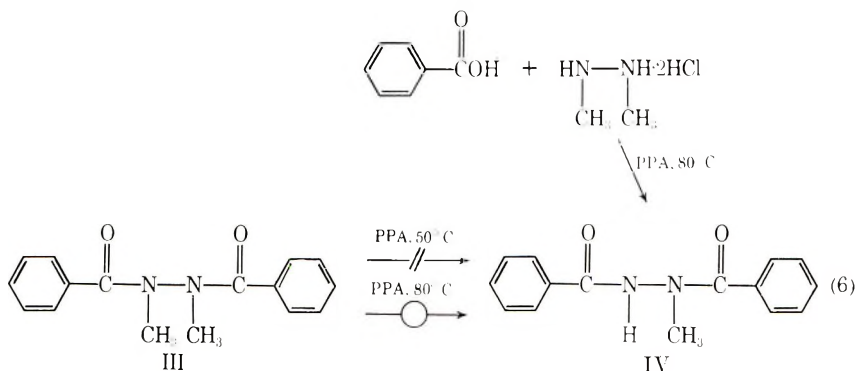
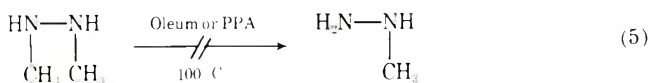


Dimethyl sulfate is well known to be useful as methylating agent of hydrazide³ and amide.⁴ *N,N'*-Dimethyl-*N,N'*-dibenzoylhydrazine was prepared through the methylation of *N,N'*-dibenzoylhydrazine by dimethyl sulfate. ϵ -Caprolactam and dimethyl sulfate reacted to give both *N*-methylated and *O*-methylated products. In addition, a cyclic hydrazide such as 1,2-phthaloylhydrazine was found to be methylated on the nitrogen atom by dimethyl sulfate in PPA to give 1-methyl-1,2-phthaloylhydrazine. However, in oleum, this hydrazine was not methylated in spite of the strong methylating ability of dimethyl sulfate. On the other hand, in the reaction of terephthalic acid, hydrazine, and dimethyl sulfate in oleum, *N*-methylated hydrazide linkage was formed. In this reaction, monohydrazide and a diacylhydrazine would be formed as an intermediate [eq. (4)].



Therefore, it would be reasonable to consider that the hydrazide formed is partially methylated by dimethyl sulfate and partially dehydrated to form 1,3,4-oxadiazole. The methylation and the demethylation would proceed as competitive reactions.

Along with the above experiments, some new and curious types of behavior of alkylated hydrazine were noted in strongly acidic media as PPA or oleum. When *N,N'*-dimethylhydrazine was heated alone at 100°C in oleum or PPA, this dimethylhydrazine was recovered unchanged quantitatively [eq. (5)]. However, heating of *N,N'*-dimethylhydrazine in PPA in the presence of benzoic acid at 80°C gave only *N*-methyl-*N,N'*-dibenzoylhydrazine (IV) instead of *N,N'*-dimethyl-*N,N'*-dibenzoylhydrazine (III). The hydrazide (III) prepared from *N,N'*-dimethylhydrazine and benzoyl chloride was converted to the hydrazide (IV) when heated at 80°C in PPA, but not at 50°C [eq. (6)]. Poly-*N,N'*-dimethylterephthalyldiazide was also converted to demethylated polymer, poly-*N*-methylterephthalyldiazide, at 100°C in fuming sulfuric acid or PPA [eq. (7)].



These experimental facts indicate that the demethylation reaction takes place by interaction of such a solvent as oleum or PPA after the formation of hydrazide linkage.

It is concluded that both the methylation of the N atom of hydrazine and the cleavage of the C-N bond of *N,N'*-dimethylhydrazine occur after the formation of hydrazide linkages, but the mechanism of the interaction of the solvent remains unresolved.

EXPERIMENTAL

Materials

Methylated hydrazines, terephthalic acid, and dimethyl terephthalate were obtained commercially and purified by the usual methods. Oleum (30% SO₃ fuming sulfuric acid) and 116% polyphosphoric acid (PPA), which were available commercially, were used without further purification.

N-Methyl-*N,N'*-dibenzoylhydrazine

Authentic Compound. This compound was prepared from methylhydrazine and benzoyl chloride by the method of Brünning⁵ and recrystallized from methanol; mp 143–144°C (lit.⁵ mp 143°C).

Model Reaction. Benzoic acid (3.0 g) and *N,N'*-dimethylhydrazine dihydrochloride (1.4 g) were heated in 116% polyphosphoric acid (60 g) at 80°C for 5 hr. After cooling, the mixture was poured into 500 g of ice water. The precipitate was filtered, washed with water and then with methanol, and dried. It weighed 2.7 g. The infrared spectrum of this compound was identical with that of authentic *N*-methyl-*N,N'*-dibenzoylhydrazine. It was recrystallized from methanol; mp 141.5–142.5°C.

N,N'-Dimethyl-*N,N'*-dibenzoylhydrazine

This was prepared from *N,N'*-dimethylhydrazine and benzoyl chloride by the method of Know and Köhler⁶ and recrystallized from water-methanol (1:1); mp 85–86°C (lit.⁶ mp 85°C).

Authentic Poly-*N,N'*-dimethylterephthalyhydrazide

This polymer was prepared by the use of an interfacial polycondensation method similar to that described in an earlier paper² from *N,N'*-dimethylhydrazine and terephthaloyl chloride.

Methylation of 1,2-Phthaloylhydrazine by Dimethyl Sulfate

1,2-Phthaloylhydrazine (1.62 g) and dimethyl sulfate (1.89 g) were heated in polyphosphoric acid (40 g) at 130°C for 5 hr. After cooling, the solution was poured into ice water. The precipitate was separated and washed with 200 ml of water. After drying it weighed 1.65 g. The infrared spectrum of this compound was identical with that of the authentic 1-methyl-1,2-phthaloylhydrazine which was prepared from phthalic anhydride and methylhydrazine in polyphosphoric acid. It was recrystallized from water and melted at 227–230°C (lit.⁷ mp 239–240°C).

ANAL. Calcd for C₉H₈O₂N₂: C, 61.36%; H, 4.58%; N, 15.90%. Found: C, 61.37%; H, 4.38%; N, 15.76%.

Solution Polycondensation

The following three examples are representative.

Poly-*N*-methylterephthalyhydrazide (in Oleum; PI-2). Methylhydrazine sulfate (2.95 g) and terephthalic acid (1.65 g) were heated in 30% fuming sulfuric acid (25 g) at 80°C for 2 hr and then at 100°C for 8 hr. After cooling, the viscous solution was poured into ice water with stirring. The precipitated polymer was separated, extracted with hot water for 24 hr, and dried under vacuum at 80°C. The yield was 0.95 g (54%). The inherent viscosity (at a concentration of 0.2 g/100 ml of *m*-cresol at 30°C) was 0.41; mp 275°C.

ANAL. Calcd for $(C_9H_5O_2N_2)_n$: C, 61.36%; H, 4.55%; N, 15.91%. Found: C, 55.86%; H, 4.47%; N, 15.74%.

Poly-*N*-methylterephthalyhydrazide (in PPA; PI-3). Methylhydrazine (2.9 g) and terephthalic acid (1.65 g) were heated in 116% polyphosphoric acid (25 g) at 140°C for 2 hr and then at 150°C for 28 hr. After cooling, the viscous solution was poured into ice water. The precipitated polymer was separated, extracted with hot water for 24 hr, and dried at 50°C under vacuum. The yield was 1.49 g (84%). The inherent viscosity was 0.11 (in *m*-cresol at a concentration of 0.2 g/100 ml at 30°C); mp 275°C.

Poly-*N*-methylterephthalyhydrazide from Terephthalic Acid, Hydrazine Sulfate, and Dimethyl Sulfate (in Oleum; PIII-2). Terephthalic acid (1.70 g), hydrazine sulfate (1.50 g), and dimethyl sulfate (3.8 g) were heated in 30% SO₃ fuming sulfuric acid (50 g) at 135°C for 1 hr. The viscous solution was poured into ice water with stirring. The polymer was washed with ammonium hydroxide, extracted with hot water for 24 hr, and dried. It weighed 1.70 g. The inherent viscosity was 0.92 (at a concentration of 0.2 g/100 ml of dichloroacetic acid at 30°C). It did not melt below 500°C but degraded above 320°C.

References

1. Y. Iwakura, K. Uno, and S. Hara, *J. Polym. Sci. A*, **3**, 45 (1965).
2. Y. Iwakura, K. Uno, S. Hara, and S. Kurosawa, *J. Polym. Sci. A-1*, **6**, 3357 (1968).
3. H. H. Hatt, *Org. Syn.*, **16**, 19 (1936); Coll. Vol. II, 209 (1943).
4. R. H. Benson and T. L. Cairns, *J. Amer. Chem. Soc.*, **70**, 2115 (1948).
5. G. v. Brüning, *Ann.*, **253**, 12 (1889).
6. L. Knorr and A. Köhler, *Ber.*, **39**, 3264 (1906).
7. I. Satoda, N. Yoshida, and K. Mori, *Yakugaku Zasshi*, **77**, 703 (1957); *Chem. Abstr.*, **51**, 17928d (1957).

Received April 15, 1968

Revised May 31, 1968

Polyhydrazides. III. N-Methylated Polyhydrazides by Ring-Opening of Poly-*p*-phenylene-1,3,4-oxadiazole

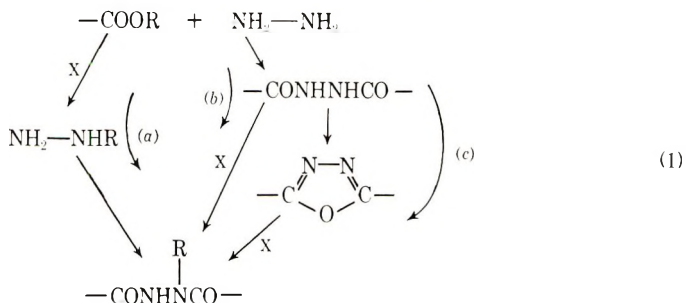
YOSHIO IWAKURA, KEIKICHI UNO, SHIGEYOSHI HARA,*
and SHIGERU KUROSAWA, *Department of Synthetic Chemistry, Faculty
of Engineering, University of Tokyo, Bunkyo-ku, Tokyo, Japan*

Synopsis

A new ring-opening reaction of 1,3,4-oxadiazole by methylating reagents was developed in fuming sulfuric acid or polyphosphoric acid and then, by applying this reaction to poly-*p*-phenylene-1,3,4-oxadiazole, a high molecular weight poly-*N*-methyl-terephthalyhydrazide was obtained. Various methylating reagents were investigated as ring-opening reagents. The degrees of ring-opening in polymers were estimated and related to the properties of the polymers.

INTRODUCTION

In the course of a study of preparation of poly-1,3,4-oxadiazoles,¹ we reported the reaction of dialkyl esters of dicarboxylic acids with hydrazine salts to give *N*-alkylated polyhydrazides in fuming sulfuric acid (oleum) or in polyphosphoric acid (PPA).² In the above reaction, there seemed to be three routes for forming the *N*-alkylhydrazide linkage; (a) the alkylation of hydrazine and the subsequent formation of the *N*-alkylhydrazide linkage, (b) the formation of acylhydrazine first and its subsequent alkylation, and (c) the ring-opening reaction of 1,3,4-oxadiazole formed by dehydration of diacylhydrazine [eq. (1), where X denotes alkylating reagent].

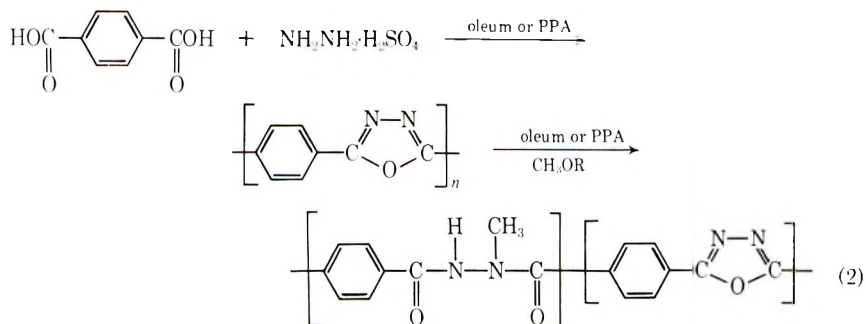


The first route (a) was denied by the fact that hydrazine was not methylated by dimethyl sulfate in oleum, but route (b) was studied in the preced-

* Present address: Teijin Limited, Tokyo, Japan.

ing paper and supported by some experimental facts.³ However, route (c) remained to be investigated.

In this study, the ring cleavage reaction of 2,5-diaryl-1,3,4-oxadiazole with methylating reagents was investigated both in oleum and in PPA in order to clear the mechanism of the condensation reaction of alkyl carboxylate and hydrazine. We found that the *N*-methylhydrazide linkage was formed through the ring cleavage of 1,3,4-oxadiazole, and then this result was applied to the reaction of poly-*p*-phenylene-1,3,4-oxadiazole to produce a high molecular weight poly-*N*-methylterephthalylhydrazide as shown in eq. (2),



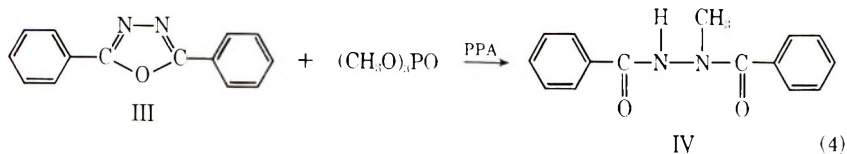
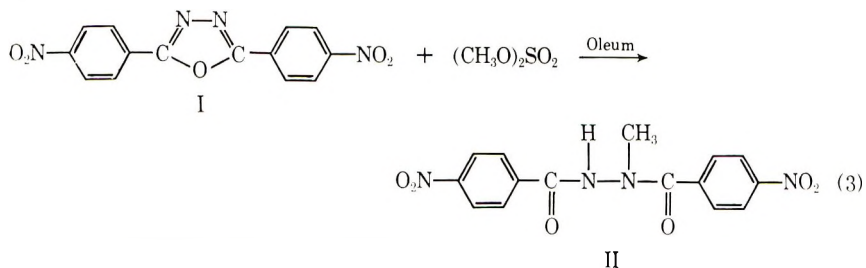
where R is $-\text{H}$, $-\text{SO}_3\text{CH}_3$, $-\text{PO}(\text{OCH}_3)_2$, $-\text{SO}_3\text{Na} \cdot \text{H}_2\text{O}$, $-\text{COC}_6\text{H}_5$, or $-\text{SO}_2\text{C}_6\text{H}_5$.

In this polymer reaction, a variety of ratios of hydrazide to 1,3,4-oxadiazole units in the resulting polymer chain could be obtained by regulating the ring-opening reaction.

RESULTS AND DISCUSSION

Model Reactions

The ring-opening reaction of 1,3,4-oxadiazole was investigated with two model compounds. In oleum, 2,5-bis-*p*-nitrophenyl-1,3,4-oxadiazole was used as a model compound to avoid the sulfonation of benzene rings.



By using an excess of dimethyl sulfate as a methylating reagent, the model compound I was converted to the corresponding *N*-methylhydrazide II at 130°C in oleum in good yield [eq. (3)]. This hydrazide II was identified by its infrared spectrum and elemental analyses. In PPA, the oxadiazole model compound III was heated at 150°C in the presence of an excess of trimethyl phosphate to give the expected *N*-methylated hydrazide IV in good yield [eq. (4)]. This hydrazide was identical to a known sample prepared from methylhydrazine and benzoyl chloride. When these reactions were carried out below 100°C, it was difficult to complete the reaction in several hours even if a large excess of methylating reagent was added. However, above 120°C, the reaction proceeded smoothly to give the corresponding *N*-methylated hydrazide.

In these reactions, the cleavage of the C—O bond took place with hydrazide formation. Generally, cleavage of the C—O bond takes place by attack of the nucleophilic reagent on C₂ or C₃,⁴ but here, strong methylating reagents such as dimethyl sulfate and trimethyl phosphate seemed to act as ring-opening reagents, first attacking the N or O of the oxadiazole ring. When the ring was attacked on the O, the methyl group would rearrange from the O to the N atom before or after the cleavage of the oxadiazole ring. Therefore, these reactions would be a new type of ring cleavage reaction for the 1,3,4-oxadiazoles. A detailed investigation of the reaction mechanism is now in progress.

These model reactions indicated that *N*-alkylhydrazide was also formed via route (c) of eq. (1) from alkyl carboxylate and hydrazine.

Polyhydrazides

The reactions of the model compounds described in the previous section suggested the formation of poly-*N*-methylterephthallylhydrazide on treatment of poly-*p*-phenylene-1,3,4-oxadiazole with appropriate methylating reagents in oleum or PPA above 120°C.

The reaction of poly-*p*-phenylene-1,3,4-oxadiazole with various methylating reagents such as dimethyl sulfate, trimethyl phosphate, methyl benzoate, methyl benzenesulfonate, methanol, and sodium methyl sulfate was carried out both in oleum and in PPA. Results are summarized in Tables I–III.

Table I shows the results of the reaction of poly-*p*-phenylene 1,3,4-oxadiazole with various amounts of dimethyl sulfate in oleum. The amount of dimethyl sulfate affected the structure and solubility of the resulting polymer. Treatment of the original polymer with a small amount of dimethyl sulfate gave polymers which were infusible and insoluble in organic solvents (PI-1, PI-2, and PI-3). However, the infrared spectra of these polymers gave strong amide absorptions in addition to the oxadiazole absorptions, as shown in Figure I. Treatment of the original polymer with a large amount of dimethyl sulfate gave polymers which were fusible and soluble in organic solvents (PI-5, PI-6, and PI-7). In the infrared spectra of these polymers, the amide absorptions became stronger with the increase of the amount of

TABLE I
Preparation of *N*-Methylated Polyhydrazides from Poly-*p*-phenylene-1,3,4-oxadiazole and Dimethyl Sulfate in Oleum^a

No.	Amt (CH ₃ O) ₂ SO ₂		Reaction conditions			Polymers		
	g	(mole)	Temp, °C	Time, hr	Yield, g	PMT, °C ^b	η_{inh}^c	η_{inh}^e
PI-1	0.32	(0.0025)	125	7	1.4	Inf. ^d	0.35 ^e	0.09 ^f
PI-2	0.63	(0.005)	130	6	1.4	Inf.	0.32 ^e	0.07 ^f
PI-3	1.30	(0.01)	125	5	0.9	Inf.	0.35 ^e	0.01 ^f
PI-4	1.30	(0.01)	130	7	1.5	Inf.	1.22	
PI-5	2.60	(0.02)	110	5	1.5	310	0.62	
			140	3		-321		
PI-6	3.80	(0.03)	115	4	1.5	315	0.74	
			125	4		-320		
PI-7	5.00	(0.04)	110	5	1.6	314	0.65	
			130	2		-320		

^a Amount of original poly-*p*-phenylene-1,3,4-oxadiazole used is 1.5 g; $\eta_{inh} = 2.06$ (0.2% in 95% sulfuric acid). The weight of oleum is 60 g.
^b Measured on the hot stage.

^c In *m*-cresol, at a concentration of 0.2 g/100 ml unless otherwise noted.

^d The polymer was infusible below 500°C, but degraded above 320°C.

^e In 10% SO₃-fuming sulfuric acid.

^f In 95% sulfuric acid.

TABLE II
Preparation of *N*-Methylated Polyhydrazide from Poly-*p*-phenylene-1,3,4-oxadiazole^a and Various Methylating Reagents in Oleum

No.	Methylating reagent		Wt oleum, g	Reaction conditions			Polymer	
	Type	Amt, g		Temp, °C	Time, hr	Yield, g	PMT, °C ^b	η_{inh}^c
PII-1	(CH ₃ O) ₂ PO	1.4	(0.01)	120	10	1.5	320	1.04
PII-2	C ₆ H ₅ CO ₂ CH ₃	5.44	(0.04)	120	10	1.3	Inf. ^d	1.56
PII-3	C ₆ H ₅ SO ₂ CH ₃	6.9	(0.04)	120	10	1.3	Inf.	0.89
PII-4	CH ₃ OH	2.6	(0.04)	120	10	1.5	310	1.01 ^e
PII-5	CH ₃ OSO ₂ Na·H ₂ O	6.1	(0.08)	120	10	1.4	315	0.66 ^e
PII-6	(CH ₃ O) ₂ SO ₂	1.3	(0.01)	130	7	1.5	Inf.	1.22 ^e

^a Amount of original poly-*p*-phenylene-1,3,4-oxadiazole used is 1.5 g (0.01 mole), $\eta_{inh} = 2.06$ (0.2% in 95% sulfuric acid).
^b Measured on the hot stage.

^c Measured in dichloroacetic acid at a concentration of 0.2 g/100 ml at 30°C unless otherwise noted.

^d The polymer was infusible below 500°C, b it degraded gradually above 320°C.

^e Measured in *m*-cresol.

TABLE III
Preparation of *N*-Methylated Polyhydrazides from Poly-*p*-phenylene-1,3,4-oxadiazole and Various Methylating Reagents in PPA^a

No.	Methylating reagents		PPA, g	Reaction conditions			Polymer	
	Type	Amt, g		(mole)	Temp, °C	Time, hr	Yield, g	η_{inh}^c
PIII-1	(CH ₃ O) ₂ PO	1.5	(0.01)	130	7	1.6	314	0.45
PIII-2	C ₆ H ₅ CO ₂ CH ₃	5.5	(0.04)	130	7	1.5	302	0.24
PIII-3	C ₆ H ₅ SO ₂ CH ₃	6.9	(0.04)	130	8	1.6	314	0.30
PIII-4	CH ₃ OH	1.3	(0.04)	135	7	1.6	306	0.31
PIII-5	CH ₃ O-SO ₂ -Na·H ₂ O	6.1	(0.04)	135	9	1.4	308	0.34

^a Poly-*p*-phenylene-1,3,4-oxadiazole was prepared preliminarily from terephthalic acid (1.66 g) and hydrazine sulfate (1.40 g) in PPA at 150°C. It is known that the resulting polymer has an inherent viscosity of nearly 2 after several hours' polycondensation.¹

^b Measured on the hot stage.

^c Measured in *m*-cresol at a concentration of 0.2 g/100 ml at 30°C.

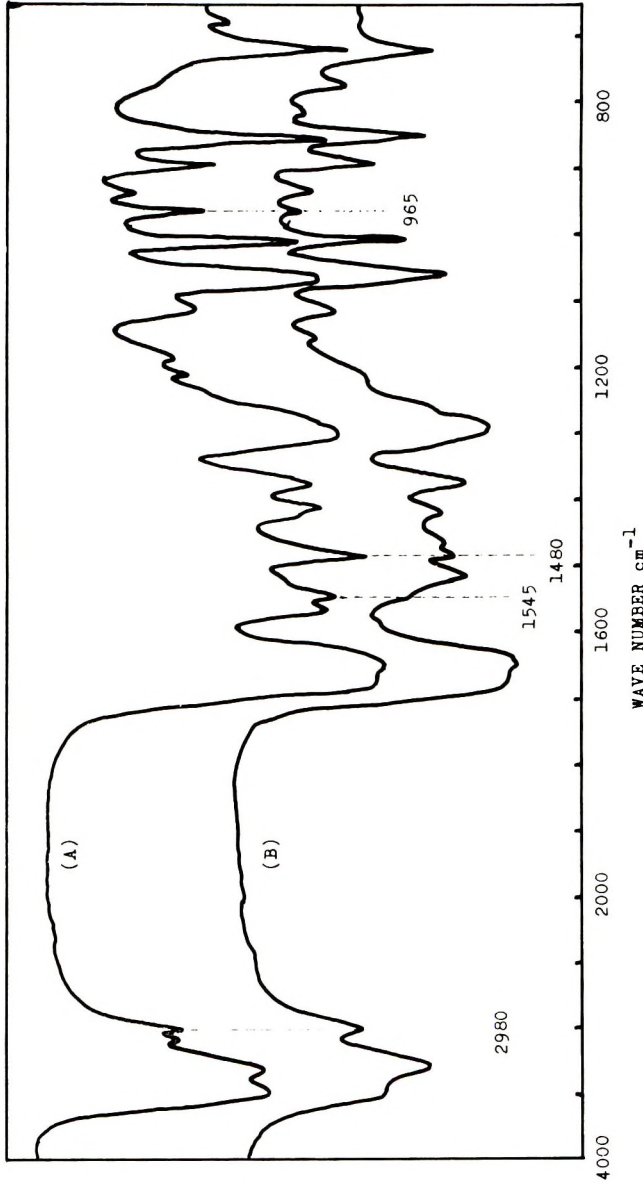


Fig. 1. Infrared spectra of polymers treated with methylating reagents: (A) PI-3 (contains a large amount of 1,3,4-oxadiazole); (B) PI-5 (contains a small amount of 1,3,4-oxadiazole).

dimethyl sulfate used. The inherent viscosities of these polymers measured in 10% SO_3 -fuming sulfuric acid or in *m*-cresol were high, while those measured in 95% sulfuric acid were very low. The infrared spectra of the polymers recovered from 95% sulfuric acid gave absorptions characteristic of the carboxyl group instead of amide in addition to the absorptions of the oxadiazole.

These data indicate that the resulting polymers are composed of two kinds of linkages as shown in eq. (2).

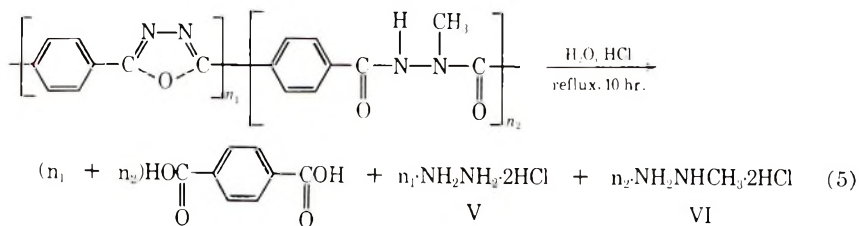
The relation between the ratio of these two kinds of linkages and the properties of the polymers will be discussed later.

Besides dimethyl sulfate, the methylesters of various acids and methanol were used as methylating reagents in the reaction described above. Tables II and III show the results of the reaction of poly-*p*-phenylene-1,3,4-oxadiazole carried out with the use of different methylating reagents in oleum and in PPA. In the reaction carried out in oleum, infusible polymers (PII-2 and PII-3) were obtained with methyl benzoate and methyl benzenesulfonate. On the contrary, fusible polymers were obtained in PPA (PIII-2 and PIII-3) at nearly the same conditions. The fusibility of these polymers is some measure of the extent to which the ring-opening reaction takes place, as discussed later. Therefore, PPA seems to be better for the ring-opening reaction. However, concerning the molecular weight, all the polymers obtained in oleum gave higher inherent viscosities in comparison with those obtained in PPA. PPA is known to give higher molecular weight PPA easily on elimination of water from low molecular weight PPA at a high temperature. This property of PPA might give the results described above.

As described above, the degree of ring opening of the polymers obtained depended upon two factors: (1) the amount of methylating agent, and (2) the reaction temperature. The reaction time was also a factor. When the reaction was stopped soon after addition of the methylating agent, polymers containing a large proportion of oxadiazole units were obtained even if a large excess of alkylating agent was added at a temperature sufficient for ring opening. Therefore, by the variation of these three factors, polymers with various degrees of ring opening were obtained.

Estimation of Degree of Ring Opening

The degree of ring opening of the resulting polymers were estimated as follows.



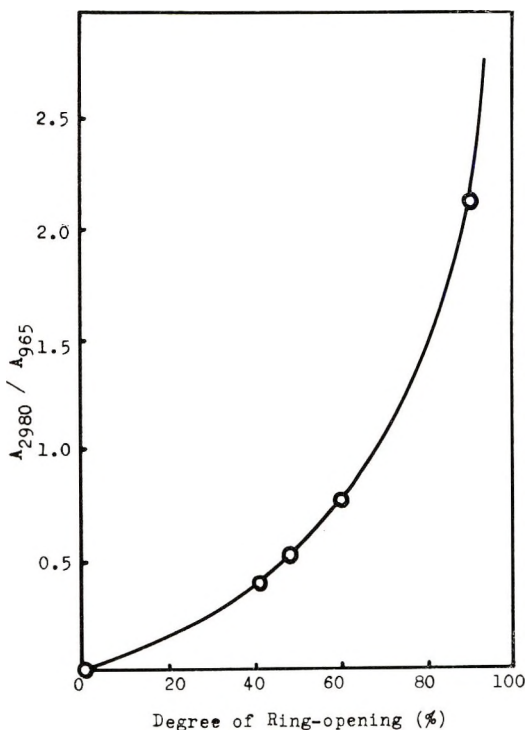


Fig. 2. Relation between the degree of ring opening and the ratio of the absorbance 2980 cm^{-1} to the absorbance at 965 cm^{-1} in the infrared spectra of the polymers.

Heating the polymer in 20% hydrochloric acid under reflux yielded terephthalic acid and two kinds of hydrazines [eq. (5)]. Terephthalic acid was separated completely from the reaction mixture by filtration of the precipitated terephthalic acid, and passage of the filtrate through a column containing a strong anion-exchange resin. To the aqueous solution of two hydrazines thus obtained was added hydrochloric acid. The mixture of hydrazines was obtained as salts by removing water. From elemental analysis of the mixture of V and VI, the molar ratio of the two components was estimated. Preliminary experiments with a mixture having a known ratio of two hydrazine salts confirmed the accuracy of this method. Carbon analysis gave a high accuracy and a good reproducibility, but nitrogen analysis did not. The molar percentage of methylhydrazine salt in this hydrazine mixture indicates the degree of ring-opening reaction of the polymer.

The infrared spectrum of the polyhydrazide-oxadiazole obtained here showed characteristic absorptions at 2980 cm^{-1} due to the C-H stretching of methyl group, and a sharp absorption at 965 cm^{-1} characteristic of 1,3,4-oxadiazole. Though these absorptions are not so strong, they do not overlap with the other peaks. Therefore the ratio of absorbances of these peaks could be well correlated with the degree of ring opening. Figure 2

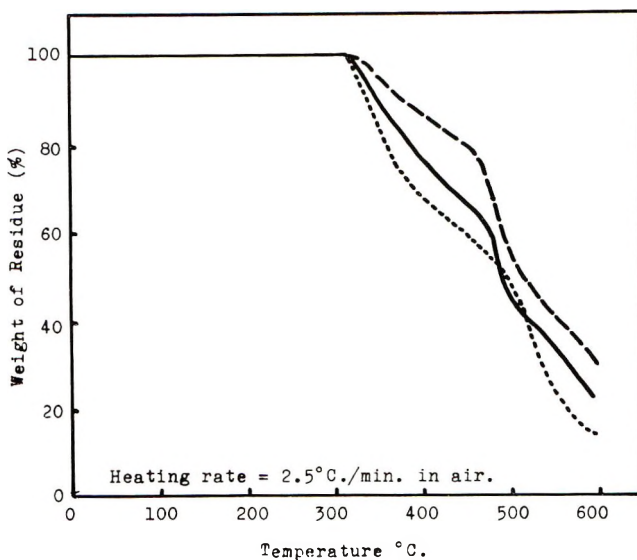
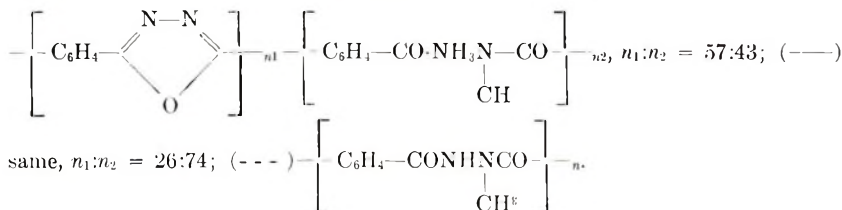


Fig. 3. Thermogravimetric analyses of polymers: (---)



shows the relations between the degree of ring opening reaction obtained from the analysis of hydrolyzate of the polymer, the mixture of hydrazine and methylhydrazine, and the ratio of the absorbance at 2980 cm^{-1} to the absorbance at 965 cm^{-1} . By the use of this calibration curve, the degree of ring-opening reaction could easily be estimated from the infrared spectrum of the polymer film.

Properties of Polymers

The polymers containing a large amount of 1,3,4-oxadiazole units were yellow, but the color gradually got whiter with increasing degree of ring-opening reaction. While polyoxadiazole was infusible and insoluble in all organic solvents, the *N*-methylated polyhydrazides showed melting temperatures and were soluble in such organic polar solvents as dichloroacetic acid, *m*-cresol, dimethylacetamide, dimethylformamide, dimethyl sulfoxide and formic acid, and from those solutions of polymers, clear tough films could be cast. Consequently, poly-*N*-methylterephthalylhydrazide containing some oxadiazole units showed considerable differences in PMT and the solubility, depending on the degree of ring opening. Table IV shows the relations between the degree of ring-opening reaction, PMT and the qualitative solubility of polymers.

TABLE IV
Relations between the Degree of Ring Opening and PMT and Solubility of Poly-*N*-methylterephthalylhydrazide

Degree of ring opening, %	PMT, °C	Solubility ^a		
		Dichloroacetic acid	<i>m</i> -Cresol	Dimethylacetamide
35	Inf.	+	-	-
41	Inf.	+	-	-
43	Inf.	++	±	-
45	Inf.	+++	±	-
47	Inf.	+++	+	-
60	Inf.	+++	+	-
70	Inf.	+++	++	±
74	310-321	+++	++	±
83	310-321	+++	+++	+
86	307-320	+++	+++	+
90	307-320	+++	+++	+

^a Solubility: (+++) soluble at room temperature; (++) soluble on warming; (+) partially soluble on warming; (±) swelling on warming; (-) insoluble.

Thermogravimetric properties of polymers of various degrees of ring opening are shown in Figure 3. The weight loss began at 320°C in all cases, independent of the degree of ring opening, but the slope of the curve between 320°C and 450°C becomes more gentle as the oxadiazole content increased. This may be due to the thermal stability of 1,3,4-oxadiazole ring. Thus, as the degree of ring opening decreases, the qualitative solubility of polymers becomes poorer, but the thermal stability increases.

EXPERIMENTAL

Model Compounds

2,5-Diphenyl-1,3,4-oxadiazole. The procedure was that of the literature.⁵ The compound was recrystallized from ethanol; mp 137-138°C (lit.⁵ mp 138°C).

2,5-Bis-*P*-nitrophenyl-1,3,4-oxadiazole. Hydrazine sulfate (1.30 g) and *p*-nitrobenzoic acid (1.67 g) were heated in polyphosphoric acid (50 g) for 3 hr at 130°C. The resulting solution was poured into 500 g of ice water with vigorous stirring. The yield was 1.5 g. Recrystallization from acetone yielded product with mp 299-301°C (lit.⁶ mp 302°C).

***N*-Methyl-*N,N'*-dibenzoylhydrazine.** Trimethyl phosphate (1.40 g) and 2,5-diphenyl-1,3,4-oxadiazole (2.22 g) were heated in polyphosphoric acid (50 g) for 5 hr at 150°C. The resulting yellow solution was poured into ice water with stirring. The precipitate was separated by filtration and dried. The yield was 2.1 g (83%). Recrystallization from a mixture of ethanol and water yields a product with mp 143.5-144.5°C (lit. mp 143°C,⁷ 145°C⁸).

***N*-Methyl-*N,N'*-di-4-nitrobenzoylhydrazine.** Dimethyl sulfate (0.39 g) and 2,5-bis-*p*-nitrophenyl-1,3,4-oxadiazole (0.62 g) were heated in fuming sulfuric acid (20 g) for 5 hr at 130°C. The yellow crystals were separated by filtration and dried. The yield was 0.60 g (87%) and recrystallization from a mixture of ethanol and water yielded a product with mp 182.0–182.5°C.

ANAL. Calcd for $C_{15}H_{12}N_4O_6$: C, 52.33%; H, 3.51%; N, 16.28%. Found: C, 52.31%; H, 4.09%; N, 15.64%.

Polymers

Typical preparations of poly-*N*-methyl-terephthalyhydrazide by the ring-opening reaction of poly-*p*-phenylene-1,3,4-oxadiazole are described below. Poly-*p*-phenylene-1,3,4-oxadiazole used here was prepared from terephthalic acid and hydrazine sulfate by the solution polycondensation method described in the previous paper.¹

Poly-*N*-methylterephthalyhydrazide (in oleum; PI-4). Crushed poly-*p*-phenylene-1,3,4-oxadiazole (1.44 g, $\eta_{inh.} = 2.06$ in sulfuric acid) was added to 30% SO_3 -fuming sulfuric acid (60 g). The mixture was stirred and heated for 4 hr at 110°C. During that time, polyoxadiazole dissolved to oleum to form a homogeneous solution. Dimethyl sulfate (1.30 g) was added dropwise to this solution, and the temperature was raised to 130°C. Soon the solution became less viscous. After being kept for 7 hr at this temperature, the solution was poured into 1 liter of ice water with vigorous stirring. The precipitated polymer was washed with water several times and dipped in dilute aqueous ammonia for a day. After being washed again with water and dried, the polymer weighed 1.5 g. The product was white. The inherent viscosity was 1.22 (0.2% in *m*-cresol at 30°C). It did not melt below 500°C, but decomposed gradually above 320°C.

ANAL. Calcd for $(C_8H_4N_2O)_n$: C, 66.66%; H, 2.80%; N, 19.44%. Calcd for $(C_9H_8N_2O)_n$: C, 61.36%; H, 4.58%; N, 15.90%. Found: C, 57.28%; H, 5.53%; N, 14.81%.

Poly-*N*-methylterephthalyhydrazide (in PPA; PIII-1). Terephthalic acid (1.66 g) and hydrazine sulfate (2.0 g) were heated with mechanical stirring for 8 hr at 180°C in 116% polyphosphoric acid (50 g). The reaction mixture gradually became viscous and finally forced us to discontinue stirring. The solution was cooled to 100°C. Trimethyl phosphate (1.5 g) was added dropwise to this solution with vigorous stirring, and the temperature was raised again to 130°C and kept for 7 hr at this temperature. The solution gradually became a little less viscous. After cooling, the solution was poured into 1 liter of ice water with vigorous stirring. The precipitated polymer was separated by filtration and washed several times until the filtrate became neutral. After drying 1.60 g of a white powder was obtained. The inherent viscosity in *m*-cresol (0.2%, 30°C) was 0.45; mp 310–314°C.

ANAL. Found: C, 60.14%; H, 5.10%; N, 18.21%.

References

1. Y. Iwakura, K. Uno, and S. Hara, *J. Polym. Sci. A*, **3**, 45 (1965).
2. Y. Iwakura, K. Uno, S. Hara, and S. Kurosawa, *J. Polym. Sci. A-1*, **6**, 3357 (1968).
3. Y. Iwakura, K. Uno, S. Hara, and S. Kurosawa, *J. Polym. Sci. A-1*, **6**, 3371 (1968).
4. A. Hetzheim and K. Möckel, *Advan. Heterocyclic Chem.*, **7**, 204 (1966).
5. W. Neugebauer, Japan. Pat. 256,946 (1959).
6. R. Stolle and A. Banbach, *J. Prakt. Chem.*, **74**, 22 (1906).
7. G. Brüning, *Ann.*, **253**, 12 (1889).
8. A. Michaelis and E. Handanck, *Ber.*, **41**, 3289 (1908).

Received April 15, 1968

Revised May 31, 1968

Electron-Transfer Polymers. XXXVII. Preparation and Redox Behavior of Polycarbonates with Incorporated Hydroquinone Units

GERHARD WEGNER,* NOBUO NAKABAYASHI,
STEPHEN DUNCAN, and HAROLD G. CASSIDY, *Sterling
Chemistry Laboratory, Yale University, New Haven, Connecticut 06520*

Synopsis

Preparation of polycarbonates from a quinonediol and phosgene, and from the quinonediol and various bischloroformates, is described. Some of the bischloroformates were prepared from poly(ethylene oxides) with two terminal hydroxyl groups by phosgenation. The quinone groups incorporated into the polymer chain were reduced to hydroquinone groups. Some of these polymers were titrated oxidatively in 90% acetic acid. Their redox behavior cannot be described by a simple Nernst equation. It is assumed that the differences between theoretically expected and experimentally obtained potentials express the amount of work needed to reshape the polymer coil according to a thermodynamically stable distribution of the redox groups.

INTRODUCTION

Through polycondensation of quinonediacetals with appropriate difunctional compounds such as diacylchlorides or diisocyanates it is possible to obtain polymers with incorporated quinone units.^{1,2} This method allows one to prepare redox polymers in a single step and there is no need to protect the redox groups during the formation of the polymer. A second advantage is the possibility of varying the distance between individual redox groups by using difunctional compounds of different chain length. This distance is of importance for the behavior of the polymer as well as for oligomers. It was shown that a distance smaller than 5 CH₂ units between adjacent hydroquinone units leads to interactions explainable through the inductive effect of one polar redox group upon the other.^{3,4} The following report describes the preparation of polycarbonates from 2,5-bis(3'-hydroxypropyl)-1,4-benzoquinone and phosgene and of mixed polycarbonates from phosgene, various poly(ethylene glycols) and the quinonediol. The quinone units in these polymers are reduced easily by the usual methods. Some of the polymers obtained in this work are soluble in 90% acetic acid and may be titrated to analyze their redox behavior.

* Present address: Institute for Physical Chemistry, Johannes Gutenberg University, Mainz, Germany.

EXPERIMENTAL

Spectra

Ultraviolet spectra were recorded on a Bausch and Lomb Spectronic 505 spectrometer. Tetrahydrofuran (THF) for spectroscopic use as well as for redox titrations was purified and distilled shortly before use, then diluted with 5% water to obtain a 95% solution (v/v). Spectrograde CH_2Cl_2 was used for spectra measured in this solvent. Infrared spectra were recorded on a Perkin-Elmer 421 spectrometer. Polymer samples were measured as films cast from THF solution on a sodium chloride plate.

Materials

All reaction solvents were of reagent grade and were used without further purification, except as otherwise stated. All other reagents were freshly distilled or recrystallized before use. Polyethyleneglycols were obtained from Matheson, Coleman & Bell. They were used without further treatment.

Preparation of the poly(ethylene glycol bischloroformates)

The commercially obtained poly(ethylene glycols) were analyzed quantitatively for endgroups by the usual method.⁵ The \bar{M}_n values were calculated. After phosgenation samples of the polymers with chloroformate endgroups were quantitatively hydrolyzed with alcoholic potassium hydroxide. Titration of the excess potassium hydroxide gave a second value for the amount of endgroups. In Table I the values for \bar{M}_n obtained by both methods are compared. \bar{M}_n calculated from hydrolysis of the chloroformate endgroups is slightly higher than \bar{M}_n calculated from acetylation of the hydroxyl endgroups. That is because it was not possible to completely remove the solvent (benzene) from the phosgenation without decomposing the chloroformate endgroups. However this is not necessary because for proper stoichiometry the number of moles endgroups/gram of the reactant only is of importance. In a typical run 5.6 ml (0.08 mol) phosgene was condensed in a suitable glass apparatus and a solution of 0.04 mol of the

TABLE I
Analytical Data of Poly(ethylene glycols) for Preparation of Redox Polycarbonates

\bar{M}_w according to supplier ^a	Data from acetylation of endgroups		\bar{M}_n by hydrolysis of chloroformate ^b	η_{sp}/c , cm^3/g^c	No. of poly- carbonate
	\bar{M}_n	\bar{P}_n			
380-420	398	8.5	463	2.6	SD-3
1300-1600	1310	30	1340	6.0	SD-4
15000-20000		340-450	6.8×10^{-6}	28.5	SD-6

^a Matheson, Coleman & Bell.

^b Given as mol bischloroformate/g, because the solvent could not be removed quantitatively.

^c In 95% THF; $c = 5 \text{ g/l}$.

polymer (calculated to the amount of endgroups) dissolved in 50 ml benzene was slowly dropped in with vigorous stirring. Phosgene refluxed on a Dry Ice cooler. The temperature of the reaction mixture was allowed to rise to room temperature slowly during 2 hr. The mixture was then heated to 50°C for an additional 3 hr. Excess phosgene was swept out by a stream of dry nitrogen and absorbed in alcoholic potassium hydroxide solution. Benzene was distilled off *in vacuo* at a bath temperature of 50°C. The remaining residue was analyzed for chloroformate endgroups.

Preparation of the Polymers

Preparation of SD-2. 2,5-Bis(3'-hydroxypropyl)-1,4-benzoquinone (1.79 g, 8.00 mmol) was dissolved in 35 ml THF and 5.0 ml pyridine. The mixture was cooled to -20°C and 1.0 ml phosgene was slowly dropped in with vigorous stirring. Pyridinium hydrochloride started to separate. The temperature was allowed to rise to 0°C and the mixture was stirred for 1 hr at this temperature. Excess phosgene was driven off by a stream of dry nitrogen. The mixture was filtered through a glass filter. The filtrate was poured into 300 ml *n*-pentane. The polymer separated as a dark yellow oil. It was redissolved in THF and precipitated again from *n*-pentane, forming brown-yellow flakes. Drying *in vacuo* formed a brittle yellow solid. The polymer was soluble in solvents like acetone, chloroform, THF, dimethylformamide; it was insoluble in water, aliphatic hydrocarbons, and acetic acid. Yield of the purified polymer was 80%.

Preparation of SD-7. This is a typical example for the other polymers. Exactly 1.794 g (8.00 mmol) 2,5-bis(3'-hydroxypropyl)-1,4-benzoquinone was dissolved in 30 ml THF and exactly 1.848 g (8.00 mmol) diethylene-glycol bischloroformate were added. Care was taken to exclude moisture during the preparation of the mixture. It was cooled in an ice bath, and 4.0 ml pyridine was added with a syringe under vigorous stirring with a magnetic stirrer. Pyridinium hydrochloride started to separate immediately, and the solution became viscous. The mixture was brought to room temperature and kept for 2 hr with stirring. It was then filtered and worked up as described above. Yield of the purified polymer was 70%.

Reduction of the Polymeric Quinones

In all cases reduction with sodium hydrosulfite in a THF-water mixture (saturated with ammonium chloride) gave excellent results.² Reduction with hydrogen in 90% acetic acid over Pd/C catalyst was also successful. The yield is quantitative for both methods; the polymeric hydroquinones form white to slightly yellow oils or waxes. Upon reoxidation, polymer with the original spectrum and viscosity is obtained.

Titration

The apparatus and the method used were exactly as described elsewhere.⁶ The titrations were carried out in a thermostat at 25°C. Potentials were

TABLE II
Structure and Properties of Redox Polycarbonates from 2,5-Bis(3'-hydroxypropyl)benzoquinone and Various Bischloroformates

No.	Structure ^a	State ^b	η_{sp}/c , cm ³ /g ^c	Ultraviolet data ^c		Infrared frequencies, cm ^{-d}		Remarks
				λ_{max} , m μ	ϵ_{max} $\times 10^{-3}$	Due to quinone	Due to carbonate	
SD-1	$\text{—R—O—}\overset{\text{O}}{\parallel}\text{C—O(CH}_2\text{)}_3\text{O—}\overset{\text{O}}{\parallel}\text{C—O}$	Ox Red	12.6 14.4	256 299	15.5 ^e 4.0	1658 1613 None	1750 1260 1748; 1730 1270	Brittle, yellow solid Colorless wax
SD-2	$\text{—R—O—}\overset{\text{O}}{\parallel}\text{C—O}$	Ox Red	9.3 16.5	256 298	16.5 ^e 3.9	1655 1611 None	1745 1265 1745; 1724 1275	Brownish-yellow solid Slightly yellow wax
SD-3 SD-8	$\text{—R—OC(=O)CH}_2\text{CH}_2\text{[CH}_2\text{]}_{3,4}\text{OC(=O)}$	Ox Red	14.0 17.0 17.5 21.5	257 300	16.6 ^e 4.4	1656 1612 None	1745 1263 1748 1270	Dark yellow oil Colorless oil

SD-4	$\text{—R—OC(=O)[OCH}_2\text{CH}_2]_{30}\text{OCO}$	Ox	13.5	257	16.5 ^c	1655 1611	1745 1270 1749 1270	Brown-yellow solid Colorless wax
SD-6	$\text{—R—OC(=O)[OCH}_2\text{CH}_2]_{100}\text{OCO}$	Red	13.2	206	4.2 ^c	None	1745 1280 1750	White powder White powder
SD-7	$\text{—R—OC(=O)[OCH}_2\text{CH}_2]_2\text{OCO}$	Ox Red	33.6	255	19.2	1659	1745 1260 1748 1270	Dark brown oil Slightly yellow oil
		Red	16.1	209	4.4	None		



^b Ox denotes oxidized; red denotes reduced.

^c In 95% THF unless otherwise stated.

^d Film on sodium chloride plate.

^e In methylene chloride.

measured against a saturated calomel electrode calibrated on the hydrogen scale. Thus all potentials were reported on the hydrogen scale and have been calculated to pH 0. The pH was measured with a glass electrode. During titration the pH change was less than 0.1 pH unit and was neglected for calculations. For titrations in 90% acetic acid (v/v) ceric ammonium nitrate, $\text{Ce}(\text{NH}_4)_2(\text{NO}_3)_6$, was used as oxidizing agent dissolved in 90% acetic acid. For titrations in 90% THF, *N*-bromosuccinimide was used as oxidizing agent dissolved in distilled water. 90% THF was obtained by mixing 900 ml purified THF with 100 ml 2*N* sulfuric acid. The pH of this mixture was 0.25 as measured with a glass electrode. It did not change more than 0.1 pH unit during titration. In a typical run about 0.1 mmol of the hydroquinone polymer (calculated on the repeating unit) was dissolved in 100 ml solvent. The endpoint of the titration was reached with about 3 ml of the titrant added. The pH values were determined by means of a Leeds and Northrup pH indicator, Model 7664.

Viscometry

Viscosity measurements were done in 95% THF as solvent. A Cannon-Fenske-Ostwald type of viscometer was used in a thermostatted bath at 25°C. Viscosity values η_{sp}/c were calculated according to eq. (1), t being the flow time of the polymer solution, t_0 the flow time of the pure solvent, and c the concentration of the polymer.

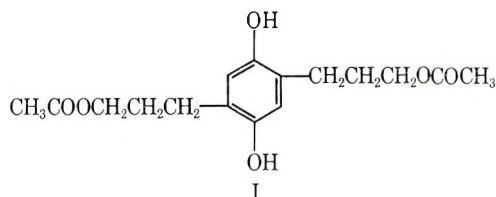
$$\eta_{sp}/c = (t - t_0)/t_0c \quad (1)$$

RESULTS AND DISCUSSION

Structure and properties of the various polycarbonates obtained in this work are compared in Table II. It is interesting that the viscosities of the reduced polymers are always higher than those of the polymers in the quinone form. Only polymer SD-4 is an exception. This polymer contains, however, very few redox units per molecule, separated by long chains of poly(ethylene oxide) structure. Both forms of this polymer are soluble in water. Most of the other polymers are insoluble in water but soluble in 90% acetic acid, a medium of choice for organic redox titrations. The quinone polymers are brown-yellow solids or waxes. Reduction of the quinone groups to hydroquinones with hydrosulfite or with hydrogen over a catalyst is quantitative. This can be demonstrated with the infrared and ultraviolet spectra. The quinone absorption around 256 $m\mu$ disappears fully and the hydroquinone absorption appears around 299 $m\mu$. The extinction coefficients are in the expected range. The typical absorptions of the quinone rings around 1655 and 1610 cm^{-1} in the infrared spectra disappear upon reduction, whereas the absorptions due to the carbonate groups remain. Only their frequencies change a little according to the possible increase in hydrogen bonding between the newly formed phenolic hydroxyl groups and the ester carbonyls. The polymers in the hydroquinone form are white to slightly yellow waxes. Solutions of the polymers in 90%

acetic acid are quite stable. The initially obtained η_{sp}/c values did not change for three days for a 10% solution of SD-8 at 25°C.

Of particular interest are the results of the redox titrations. Titrations of model compounds allow certain predictions for the redox behavior of the polymers. First of all, the redox groups should not "know" about each other because the distance between adjacent groups is larger than 5 CH₂ units.³ This means that there should not be an interaction between adjacent redox units through inductive effects. Second, the midpoint potential E_0 should be the same for all polymers because the side chains of the quinone units are very much the same. We expect the midpoint potential to be similar to that of the acetate I, which can be



looked at as a model substance for the polymers. This compound has a midpoint potential of 616 mV in 90% acetic acid. Polymers SD-4 and SD-3 show a theoretical 2-electron transfer curve with a midpoint potential of 616 mV. These compounds contain only a small amount of redox groups per molecule. Upon increase of molecular weight the behavior changes dramatically. SD-8, which has the same structure as SD-3 but probably twice its molecular weight, shows a quite different behavior. Titration curves for both polymers are compared in Figure 1. Whereas titration of the polymer with lower molecular weight showed rapid equili-

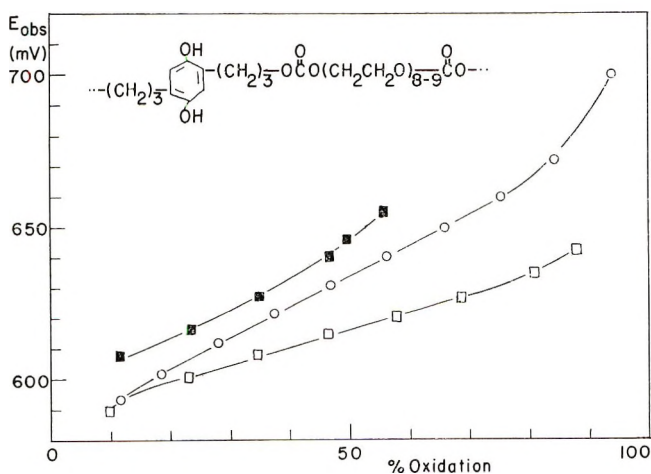


Fig. 1. Redox titration with ceric ammonium nitrate in 90% acetic acid at 25°C: (a) (□) SD-3 ($E_m = 616$ mV); (b) (■) SD-8; (c) (○) SD-8, 5% 2,5-dimethylhydroquinone added ($E_m = 634$ mV).

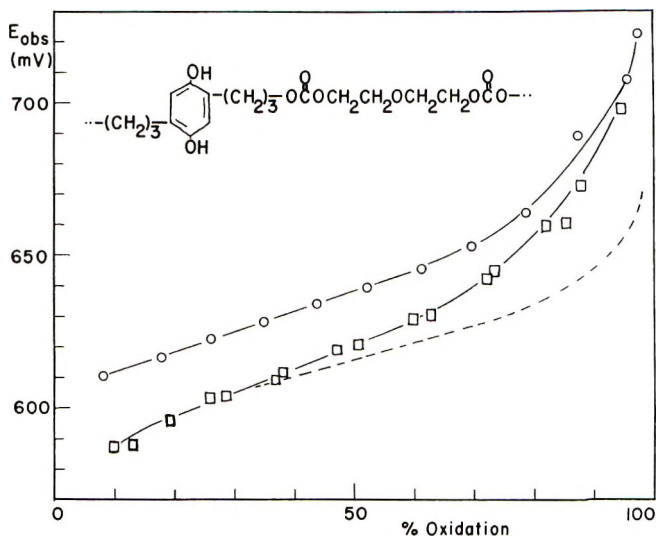


Fig. 2. Redox titration with ceric ammonium nitrate in 90% acetic acid at 25°C; (a) (○) SD-7 ($E_m = 638$ mV); (b) (□) SD-7, 5% 2,5-dimethylhydroquinone added ($E_m = 621$ mV); (c) (---) 2,5-bis(3'-acetoxypropyl)hydroquinone ($E_m = 616$ mV) as model compound and theoretical 2-electron-transfer curve.

bration and stable potentials (Fig. 1a), titration of the polymer with higher molecular weight was a tedious process. After addition of each portion of the oxidant the potentials dropped rapidly at first, then slowly in the direction of the desired equilibrium.⁶ It was not possible to obtain stable potentials even after a period of several hours. The reported values were taken if the drop in potential was less than 3 mV/hr (Fig. 1b). With increasing degree of oxidation the adjusting of the potentials became slower and slower. The reason for this behavior was laid to poor interactions between the redox groups in the coiled macromolecule and the electrode, and it was also laid to the slow process of distribution of reduced and oxidized groups throughout the polymer to the thermodynamically stable arrangement.⁶ Complications through intramolecular charge-transfer interactions could be excluded, since no unusual coloration could be detected during the oxidation process nor was there a charge-transfer band observed in the ultraviolet.

Addition of a "mediator" changed the whole picture. 2,5-Dimethylhydroquinone was chosen as mediator because its redox potential (602 mV) is close to the expected potential of the polymer. One does not need, therefore, to correct the titration curve. The function of the mediator is to work as a kind of catalyst and to establish a rapid equilibration between the individual redox groups fixed to the polymer matrix and the platinum electrode. Addition of 5% of dimethylhydroquinone (calculated to the amount of redox groups in the polymer chain) had the desired effect. Upon addition of oxidant a rapid equilibration took place, and after about 30 min a stable potential was reached. However, the shape of the titration

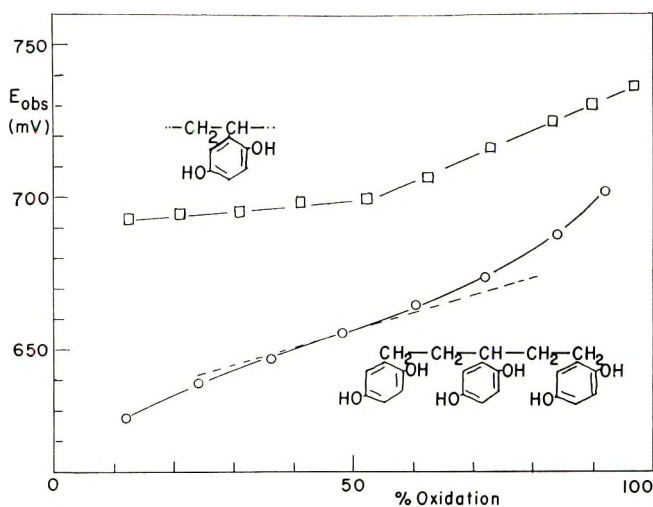
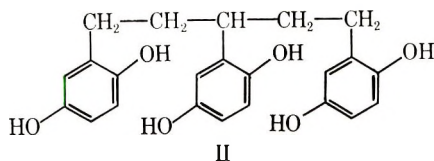


Fig. 3. Redox titration of polyvinylhydroquinone and of a hydroquinone trimer at 25°C: (a) (□) polyvinylhydroquinone titrated in 90% THF with *N*-bromosuccinimide ($E_m = 700$ mV); (b) (○) 1,3,5-tris-(2,5'-dihydroxyphenyl)pentane titrated with ceric ammonium nitrate in 90% acetic ($E_m = 651$ mV); (---) slope of a theoretical curve for 2-electron-transfer with the same midpoint.

curve (Fig. 1c) does not follow the theoretical expectations. It is too steep and shows a midpoint potential of 634 mV instead of 616 mV.

Similar results were obtained for the polymer SD-7 (for the structure see Table II). Titration without a mediator was tedious; stable potentials could not be obtained. The potentials used for the titration (Fig. 2a) were taken if the drop was less than 2 mV/hr. The curve is too steep and the midpoint potential too high. Addition of 5% 2,5-dimethylhydroquinone had the desired effect. Stable potentials were rapidly reached, indicating an equilibrium measurement. The midpoint potential dropped to 621 mV, but the curve (Fig. 2b) is still too steep and does not follow the simple Nernst equation. For comparison, the titration curve with theoretical shape for the model compound I is drawn as a dotted line in Figure 2.

These results were somewhat surprising, and we like to compare them with the redox behavior of polyvinylhydroquinone. Figure 3a shows the result of titration of polyvinylhydroquinone with 5% 2,5-dimethylhydroquinone added; 90% THF was the solvent, and *N*-bromosuccinimide was the oxidant. Stable potentials were reached in less than 1 hr after each addition of oxidant. The curve has a peculiar shape, too flat up to 50%



oxidation, too steep above that region. For comparison the titration curve for a hydroquinone trimer (II) is given.⁷ This trimer can be used as a model compound for the polymer. Its redox behavior also cannot be described by the simple Nernst equation, but it can be analyzed for the possible intermediates of the oxidation and their contributions to the shape of the curve.^{3,4} Interactions between adjacent redox groups are to be expected because they are separated by 3 CH₂ units in the trimer as well as in the polyvinylhydroquinone. It is therefore surprising that the curve for the polymer (Fig. 3a) is not as steep or even steeper than the curve for the trimer (Fig. 3b).

Three points have to be emphasized in attempting an explanation of the results of redox titrations. Titration in the presence of a mediator yielded stable potentials, the emf measured describes a thermodynamic equilibrium. Interactions between neighboring redox groups are not probable in the case of the polycarbonates. Formation of charge-transfer complexes cannot be of importance; there is no color development upon mixing oxidized and reduced form of the same polymer and no charge-transfer band in the ultraviolet. We have also to consider that there is always a change in viscosity going from the reduced form to the oxidized form; the values of η_{sp}/c become considerably smaller.

It is well known from the literature that the same hydroquinone has different standard potentials if measured in different solvents. That is because the contributions to the total free energy change ΔG by the solvation energy of quinone and hydroquinone are different in different solvents. If we now assume that the redox groups in the polymers are solvated by their own main chain as well as by the solvent it is immediately clear that the amount of solvation through main chain and through surrounding solvent may be different for hydrophilic hydroquinone groups and for hydrophobic quinone groups. A better solubility of the quinone groups in their own polymer matrix would similarly mean a tighter coiling of the polymer molecule and therefore a decrease in viscosity upon oxidation. It would also mean that the remaining hydroquinone groups would be drifted to the outside of the molecule if they are less soluble in the matrix and better in the outside solvent. This and the decrease in size of the molecule would mean a change in the entropy of the system, the solvation of the groups by their own polymer matrix or the solvent would change the enthalpy. It would be tedious to discuss all possibilities for better or poorer solvation of both forms of the molecule, since we do not have information about the ΔH and ΔS values of the individual cases. However, the final shape of the titration curve is a sum of all such contributions, and we point out only that the order of magnitude of deviation from the theoretical Nernst equation is in the order of magnitude for such processes, namely, ~ 2 kcal/mol. The whole thing can be expressed in a different way by postulating that the redox groups at the inside of the polymer coil have a different redox potential than groups at the outside.⁸ We can therefore assume that the potential at any given stage of oxidation is composed of a potential related to

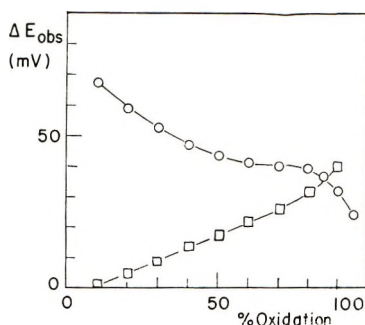


Fig. 4. Differences between theoretically expected and experimentally obtained redox potentials as function of the degree of oxidation. (○) polyvinylhydroquinone (values taken from Fig. 3); (□) polycarbonate SD-8 (values taken from Fig. 1).

the oxidation reaction and of a potential related to the work needed to rearrange the redox groups and the shape of the whole molecule. This second contribution which is only observed in polymers and not in low molecular weight compounds, has to be dependent on the degree of oxidation, as discussed above. If we plot the difference between the theoretically expected potentials (e.g., of model compounds) and the experimentally obtained potentials against per cent oxidation, the area under the curve is a measure of the free energy change related to the rearranging and recoiling of the polymer molecule. Such a plot is done in Figure 4 for a redox polycarbonate and for polyvinylhydroquinone. Unfortunately polyvinylhydroquinone is insoluble in 90% acetic acid. The curve from the titration in 90% THF (Fig. 3) is therefore compared with the curve of the model compound, which was titrated in 90% acetic acid. But the shape of the curve seems to be the same for many polyvinylhydroquinones and derivatives in different solvents.⁶ It is not surprising that one obtains very different curves for the two polymers if one considers the differences in the main chain of both polymers. The polyether and ester groups of the polycarbonate are hydrophilic, the backbone of polyvinylhydroquinone is extremely hydrophobic. At the present time it seems impossible to separate the contributions to the final shape of a titration curve according to the individual processes, especially since redox titration of polymers is experimentally a very difficult task.

We are glad to acknowledge the technical assistance of Mrs. Irmilind Stronkowski in this work. The work was supported by a Public Health Service Research Grant GM 10864, National Institutes of Arthritis and Metabolic Diseases.

References

1. G. Wegner, N. Nakabayashi, and H. G. Cassidy, *J. Org. Chem.*, **32**, 3155 (1967).
2. G. Wegner, N. Nakabayashi, and H. G. Cassidy, *J. Polym. Sci. B*, **6**, 97 (1968).
3. G. Wegner, T. F. Keys, III, N. Nakabayashi, and H. G. Cassidy, in preparation.
4. G. Manecke and D. Zerpner, *Makromol. Chem.*, **108**, 198 (1967).
5. Houben-Weyl, *Methoden der organischen Chemie*, Vol. 14/2, Georg Thieme, Stuttgart, 1963, p. 17.

6. H. G. Cassidy and K. A. Kun, *Oxidation-Reduction Polymers*, Interscience, New York, 1965.

7. R. E. Moser and H. G. Cassidy, *J. Org. Chem.*, **30**, 2602 (1965) [cf. W. Lautsch, W. Broser, W. Bandel, W. Biedermann, W. Gehrman, E. Schröder, H. Grichtel, I. Zermisch, G. Kurth, R. Kruger, and H.-J. Kraege, *Kolloid-Z.*, **138**, 129 (1954)].

8. W. Lautsch and W. Broser, reviewed in ref. 6, p. 82 ff.

Received May 1, 1968

NOTES

Influence of Dioxane on the Anionic Polymerization of Styrene in Benzene

It has been known for some time¹ that small amounts of polar solvents, such as ethers have a marked effect on the rate of anionic polymerization in a basically nonpolar medium. The only detailed kinetic study on this type of system was carried out by Bywater and Worsfold² using small amounts of tetrahydrofuran (THF) in benzene. In this study it was found necessary to postulate the successive formation of a mono-etherate and a di-etherate of polystyryllithium, both active in polymerization, as the THF concentration was increased up to about 0.1 molar in benzene. Tetrahydrofuran is an ether with a relatively high dielectric constant ($\epsilon = 7.4$ at 20°C. and dipole moment 1.7 D). Dioxane is often used in similar polymerization systems, and since this ether has a low dielectric constant (2.2) and essentially zero dipole moment, it is of obvious interest to study etherate formation with it as additive in order to provide information on the factors which give rise to specific ether solvation in anionic systems.

Experimental

The experimental procedures were those described previously.^{2,3} Benzene was chosen as the base solvent. Polymerization was initiated with *n*-butyllithium. Concentrations are in moles/liter; the operating temperature was 30°C.

Results

Anionic polymerization proceeds in two overlapping steps, chain initiation and chain propagation. In pure benzene, chain initiation is slow and under commonly used experimental conditions may be occurring over much of the polymerization process. It was found previously² that even with amounts of THF present comparable with the initiator concentration, chain initiation is complete in a few seconds. Similar amounts of dioxane increase the initiation rate over that in pure benzene, but initiation requires a minute or two. It is, of course, virtually instantaneous at higher dioxane levels. No detailed analysis of the effect on the initiation rate was, however, made.

The effect of small amounts of dioxane on the propagation rate is shown in Figure 1 at two different concentrations of polystyryllithium. The ordinate represents rate of polymerization [$R_p = (-1/M)(dM/dt)$] divided by the concentration of polystyryllithium. A common line will result at different concentrations of active centers where the reaction is first-order in them. This point is reached at dioxane concentrations above 0.05 *M*. Below this, the propagation rate is clearly of lower order as in pure benzene. Figure 2 shows the results up to 0.01 *M* dioxane plotted with ordinate propagation rate divided by the square root of the polystyryllithium concentration over a twenty-fold range of the latter. All the points fall on a single line which indicates that here the reaction is of half order in polystyryllithium as it is in pure benzene. Presumably between 0.01 and 0.05 *M* dioxane marks the transition range where the order changes.

Discussion

The behavior of the dioxane-benzene system exactly parallels that of tetrahydrofuran-benzene. The propagation rates go through a maximum at quite low concentrations of polar solvent. The most plausible explanation for the results is that advanced previously² and which involves the existence of four forms of polystyryllithium (*P*₁) in rapidly established equilibria,

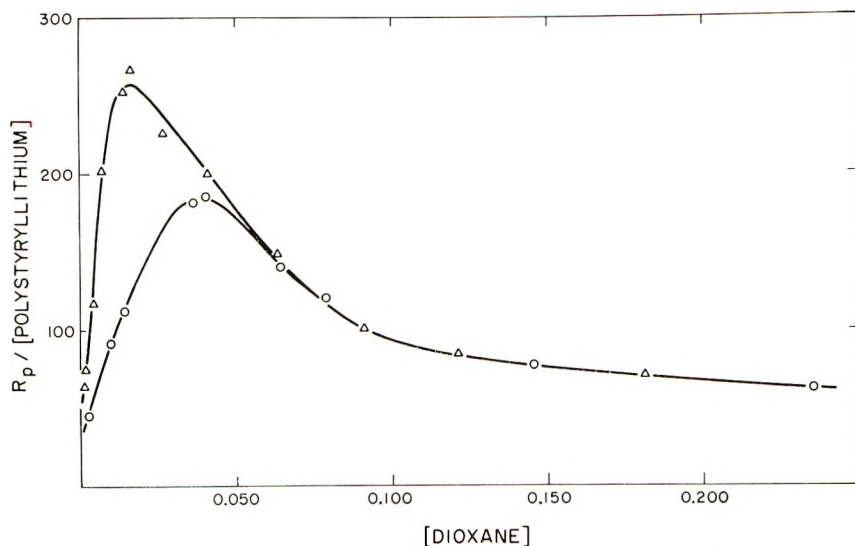
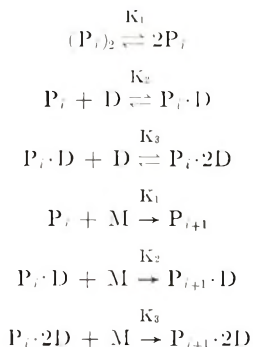


Fig. 1. Effect of molar concentration of dioxane on the propagation rate (in l./mole-min) at various concentrations of active centers: (Δ) $2 \times 10^{-4}M$; (\circ) 2×10^{-3} .



where $P_i \cdot D$ and $P_i \cdot 2D$ are specific dioxanates of polystyryllithium.

At low dioxane concentrations this scheme leads² to:

$$-d \ln[M]/dt = \{k_1 K_1^{1/2} + k_2 K_1^{1/2} K_2 [D]\} [(P_i)_2]^{1/2}$$

Since $(P_i)_2$ is virtually equal to one half the total polystyryllithium concentration under these conditions the results will be of the form shown in Figure 2. The intercept and slope give $k_1 K_1^{1/2} = 1.24$ and $k_2 K_1^{1/2} K_2 = 453$.

At high dioxane concentrations, the reaction is first-order in active centers and only equilibria 2 and 3 can be important.

$$-d \ln[M]/dt = k_2 [P_i \cdot 2D] / K_3 [D] + k_3 [P_i \cdot 2D]$$

The concentration of $P_i \cdot D$ must eventually reach low levels, and we may then approximate $[P_i \cdot 2D] = [\text{polystyryllithium}]_{\text{total}}$. A plot of $-d \ln[M]/dt$ divided by total polystyryllithium should be linear in the reciprocal of dioxane concentration, as shown in Figure 3 which enables an evaluation of k_3 and k_2/K_3 as 32 l./mole-min. and 7 l.²/mole²-min, respectively.

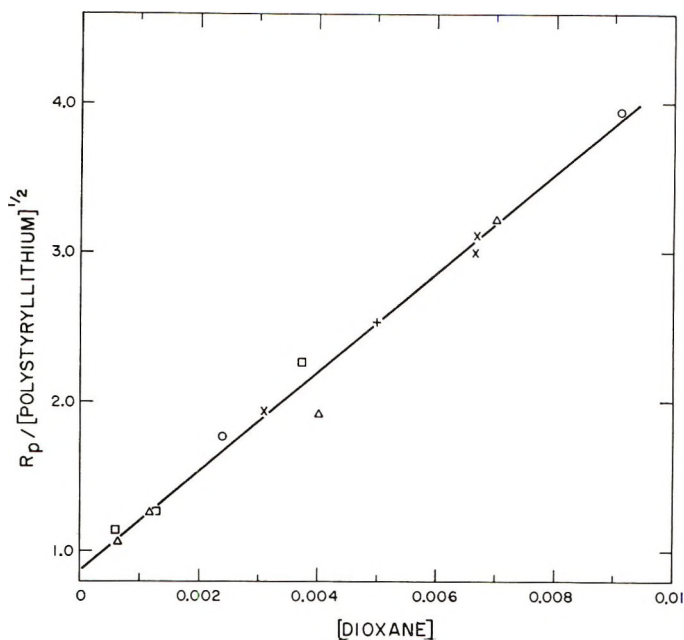


Fig. 2. Effect of molar concentration of dioxane on propagation rate (in $l^{1/2}/mole^{1/2}\text{-min}$) at low concentrations and various concentrations of active centers: (\square) $1 \times 10^{-4}M$; (\triangle) $2 \times 10^{-4}M$; (+) $6 \times 10^{-4}M$; (\times) $1 \times 10^{-3}M$; (\circ) $2 \times 10^{-3}M$.

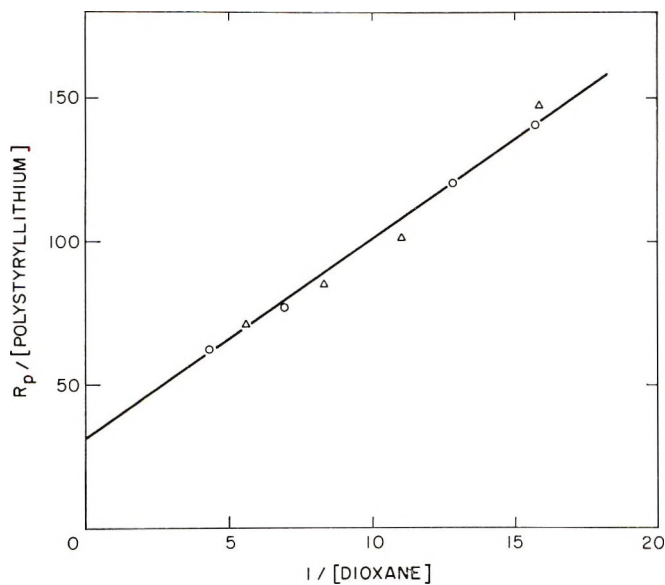


Fig. 3. Effect of reciprocal dioxane concentration on propagation rate at higher concentrations up to $0.2M$. Symbols as in Fig. 1.

The only rate constant which can be evaluated directly is that of the dietherate (k_2) which is 32 l./mole-min for dioxane and 70.5 l./mole-min for tetrahydrofuran at 30°C. The reactivity of this solvated species is clearly not very dependent on the nature of the ether. The activation energy for k_2 is, within experimental error, equal to that found with tetrahydrofuran. Experiments between 20 and 40°C and around 0.4*M* dioxane, where the dietherate is the predominant species, indicate an activation energy of 10.6 kcal/mole. Although individual association constants cannot be evaluated it is clear that dioxane is an efficient complexing agent, but slightly weaker than THF.

The absolute rate constant for the dietherate in the range 0.07–0.2 molar dioxane in benzene established from the kinetic scheme presented is virtually the same as that determined in pure dioxane (38 l./mole-min).⁴ A somewhat higher figure (56 l./mole-min) was determined earlier⁵ in dioxane. This behavior is in strong contrast to the behavior in tetrahydrofuran, where the propagation constant is very much higher than that of the dietherate in solutions containing little tetrahydrofuran. In dioxane-benzene mixtures the dielectric constant changes little over the whole concentration range so that the dielectric constant effect suggested⁶ as the cause of the rapid change in rate in the presence of high concentrations of tetrahydrofuran would be absent. Alternatively if the rapid rise in rate of reaction of the ion-pair in tetrahydrofuran-rich mixtures was caused by the formation of a small fraction of highly reactive solvent-separated ion pairs,⁷ none would be expected to form in dioxane. In either case, if the dietherate predominantly formed by about 0.2*M* dioxane persisted through to pure dioxane, the propagation rate would not change further.

References

1. K. F. O'Driscoll and A. V. Tobolsky, *J. Polym. Sci.*, **35**, 259 (1959).
2. S. Bywater and D. J. Worsfold, *Can. J. Chem.*, **40**, 1564 (1962).
3. D. J. Worsfold and S. Bywater, *Can. J. Chem.*, **38**, 1891 (1960).
4. D. J. Worsfold and B. E. Lee, unpublished.
5. D. N. Bhattacharyya, J. Smid, and M. Szwarc, *J. Phys. Chem.*, **69**, 624 (1965).
6. S. Bywater and D. J. Worsfold, *J. Phys. Chem.*, **70**, 162 (1966).
7. T. E. Hogen-Esch and J. Smid, *J. Amer. Chem. Soc.*, **88**, 307 (1966).

S. BYWATER
I. J. ALEXANDER

Division of Applied Chemistry
National Research Council of Canada
Ottawa, Canada

Received January 10, 1968

Dilatometer for Chemically Initiated Reactions

Description of the Apparatus

We describe below a sensitive dilatometer capable of being used with a redox or other chemical initiator system. The problems associated with degassing the separate chemical components before mixing, and mixing and warming within short periods of time have been overcome. It was designed specifically for the emulsion polymerization of a dilute solution of monomer in water, but is believed to have general utility. A relative volume change on the order of two parts per million was readily measurable under the conditions employed. Greater sensitivity could be obtained with more precise temperature control.

Construction and Calibration

The dilatometer consists of four parts, designated in Figure 1 as: the reaction vessel A, a two neck, flat-bottomed flask with a stopcock a; the capillary B with an inner diameter of ca. 1 mm, having a stopcock b at one end; a 25 ml buret C into which has been sealed a 30-ml capacity bulb; and a 300 ml bulb D in which a gas dispersion tube has been sealed in a manner such that the sintered glass tip extends to the very bottom of the bulb. Two stopcocks, c and d, and three standard-taper joints are also part of D. Stirring is provided by a Teflon-covered magnetic bar. The stopcocks used are all hollow-plug vacuum types.

The capillary was calibrated with a plug of mercury approximately 7 cm long, section by section: the average dimensions are $(1.10 \pm 0.01) \times 10^{-2}$ ml/cm for capillary B-1, $(1.29 \pm 0.01) \times 10^{-2}$ ml/cm for capillary B-2. Water was used to calibrate the capacity of the dilatometer flask. With capillary B-1 attached to unit A, the capacity is 280.9 ± 0.1 ml; with B-2, it is 286.1 ± 0.1 ml.

Operation

The dilatometer is operated in the following manner, the emulsion polymerization of methyl methacrylate being used as an example. Measured amounts of monomer, sodium dodecyl sulfate (solid), and a solution of Mohr's salt $[\text{Fe}(\text{NH}_4)_2(\text{SO}_4)_2 \cdot 6\text{H}_2\text{O}]$ are introduced into flask A. Parts B and D are then attached to A through the appropriate joints, and connected to the vacuum line through d. Deaeration is carried out by the customary freezing-thawing cycles (three cycles) at a pressure no greater than 10^{-4} torr. With the apparatus evacuated, stopcocks a and b are finally closed, the assembly is removed from the vacuum line, and carefully purified nitrogen is admitted to D through stopcock d. About 300 ml of demineralized water is poured into D and is deaerated by means of four cycles of alternate evacuating and nitrogen purging. One cycle comprises 2 min evacuation (during which the water boils) and 2 min of nitrogen purging. This has been shown to reduce dissolved O_2 concentration to below 0.3 ppm or $10^{-5}M$.¹ A three-way stopcock e, is provided for connecting the system to either a mechanical pump or to the nitrogen source (Fig. 2). By proper manipulation of stopcocks c, d, e, and f it is possible to purge through the fritted glass gas-diffusion tube (stopcocks c and f) and evacuate through the other opening (stopcocks d and f). The glass frit also serves the important function of nucleating boiling so that outgassing occurs efficiently throughout the entire body of liquid instead of just from the surface or irregularly through "bumping."

Stopcock a is opened, and with the magnetic stirrer on, about 200 ml of water is added to dissolve the contents of the flask. The space under stopcock a is filled by applying a

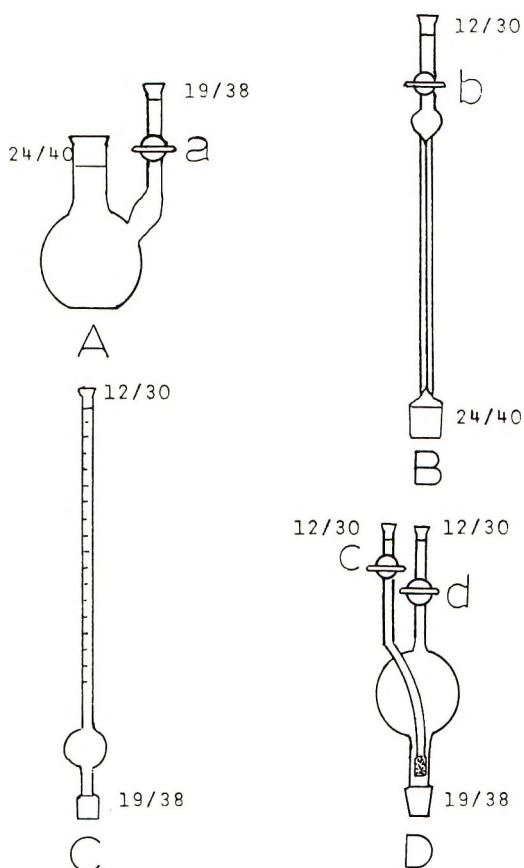


Fig. 1. Dilatometer used for kinetic studies.

slightly diminished pressure from D. More water is added from D to bring the level in the flask to a desired mark, the height of which will be determined by the volume of initiator solution subsequently added. Stopcock a is closed, and the capillary assembly (B) is connected to the nitrogen source; b is opened quickly, so that vapor bubbles are collapsed immediately. Stopcock b is closed, D is replaced with the buret C, the apparatus is immersed in a water bath which is set on a magnetic stirrer to agitate the contents of flask A, and temperature is controlled at $30 \pm 0.002^\circ\text{C}$ (YSI Model 72, Proportional Temperature Controller). Freshly prepared solutions of $\text{K}_2\text{S}_2\text{O}_8$ and NaHSO_3 are pipetted into column C. Deaeration of the mixed initiating solutions in the column is accomplished by a short period of repeated, alternating evacuation and nitrogen purging. Column C is connected to a nitrogen source at the end of deaeration. A period of 30 min is sufficient for the solution in the flask to attain thermal equilibrium with the surrounding bath; for the initiating solution in the buret, 15 min is required.

To initiate the polymerization, stopcock b is opened to the atmosphere, the initiating solution is quickly introduced through stopcock a, and timing is started. The liquid level is brought up to a desired height in the capillary B, whereupon a is closed. The addition of initiating solution is finished in about 15 sec, while the first reading of the cathetometer usually requires another 30–40 sec. The amount of initiator is determined from the difference in initial and final buret readings. The reaction mixture is stirred at constant rate throughout the entire period of polymerization. Two timers record the

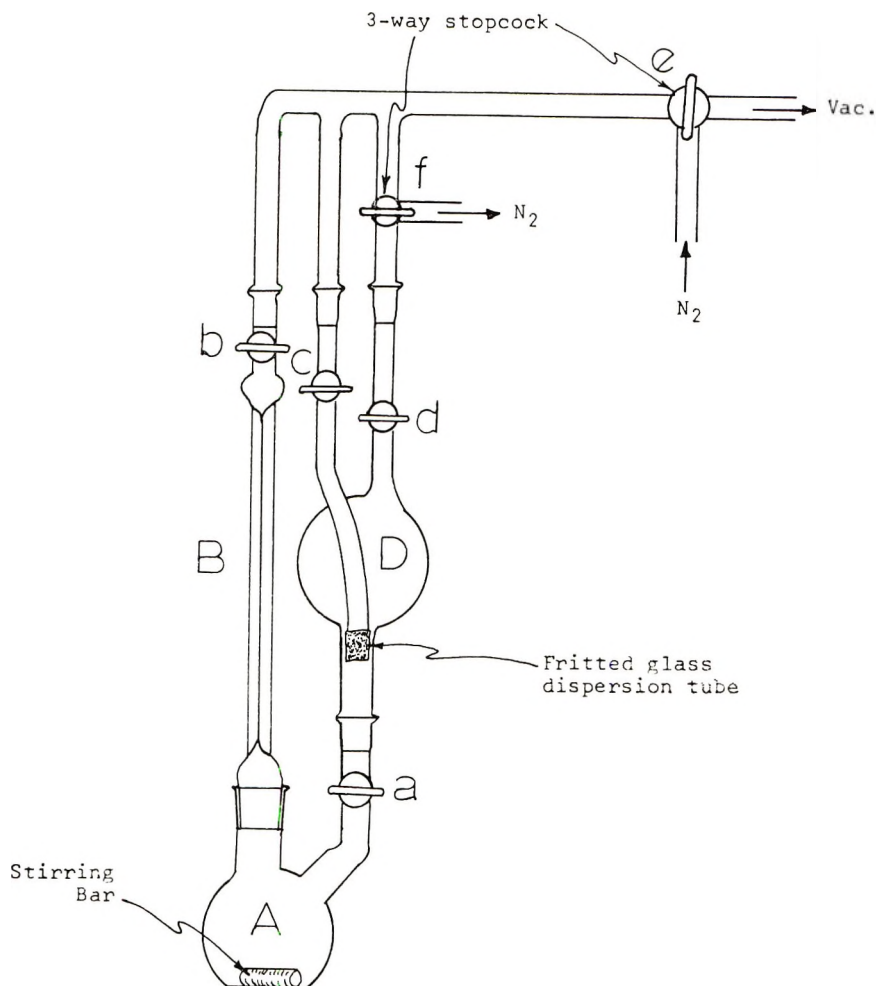


Fig. 2. Dilatometer assembly.

reaction rate continuously without interruption. At each reading both timers are "punched" simultaneously, starting one and stopping the other. The sum of the times read on both gives the total time elapsed.

Performance

No period of inhibition could be observed when degassing was performed as described. Thus the hazardous* freezing-thawing procedure of Dainton² has been obviated by our technique.

Reproducibility of experimental rates was good: the average standard deviation of 15 experiments was 4.85% of the mean rate. Considering the number of experimental variables involved, this is an acceptably narrow distribution of errors.

An estimate of the error introduced by the maximum observed fluctuation in temperature ($5 \times 10^{-2}^{\circ}\text{C}$) from the geometry of our apparatus ($V = 280 \text{ cc}$) and the coefficient

* Hazardous in that when a large volume of aqueous solution is frozen in glass, the chances of breakage are considerable.

of thermal expansion of water gives 2.9×10^{-4} cc. This would be read as a change in height of 2.8×10^{-2} cm in our capillary of radius 5.73×10^{-2} cm, and would result in an error of 0.2% conversion in the calculated value for conversion when the initial monomer concentration was $3.45 \times 10^{-2}M$.

Premixing of Redox Initiator Components

Theoretically, it would be desirable to keep the persulfate and bisulfite separate during the period of degassing and achievement of thermal equilibrium. Attempts to place solid NaHSO_3 in with the monomer for freeze-thaw degassing always resulted in polymerization immediately upon addition of water even though no persulfate was present. Presumably oxygen, adsorbed onto the surface of the bisulfite crystals, is not removed upon degassing, and reacts to form free radicals in an aqueous environment.

The rate of the redox reaction has been calculated from the kinetic equation of Fritsche and Ulbricht³ and found to be sufficiently slow so that it may be considered constant throughout the warm-up and reaction periods. Other redox initiator systems may not exhibit this behavior and would require separation of their components during degassing. This would add to the complexity of the dilatometer superstructure in that a double bulb-buret system or its equivalent would be required in place of unit C.

Automation

The dilatometer described above can readily be converted to an automatic recording device by various ways already described in the literature. The simplest method is probably that of Ley and Hummel, where a mercury-filled capillary in which is placed a platinum wire of known linear coefficient of electrical resistance⁴ is used. A mercury-column variable capacitance device has also been described.⁵

This work was supported in part by a Frederick Gardner Cottrell grant from the Research Corporation.

References

1. R. D. Dendinger, MS Thesis, North Dakota State University, Fargo N. D. September 1966.
2. F. S. Dainton and P. H. Seaman, *J. Polym. Sci.*, **39**, 279 (1959).
3. P. Fritsche and J. Ulbricht, *Faserforsch. Textiltech.*, **14**, 320, 517 (1963).
4. D. Hummel, G. Ley, and C. Schneider, in *Polymerization and Polycondensation Processes*, Advances in Chem. Series, No. 34, Am. Chem. Soc., Washington, D.C., 1962, pp. 60-86.
5. G. F. K. Acres and F. L. Dalton, *Nature*, **184**, 335 (1959).

ROBERT M. FITCH*
TSANG-JAN CHEN†

Department of Chemistry
North Dakota State University
Fargo, North Dakota 58102

Received May 16, 1968
Revised June 24, 1968

* Present address: Department of Chemistry, University of Connecticut, Storrs, Connecticut 06268.

† Present address: Research Laboratories, Eastman Kodak Co., Rochester, New York 14616.

*Near-Infrared Spectrophotometric Analysis of
Styrene-Acrylonitrile Copolymer*

Composition analysis of styrene-acrylonitrile copolymers is usually carried out by using the infrared method proposed by Schedde.¹ In the work, relative absorbance between a nitrile $\nu(\text{CN})$ mode at 4.4μ and a phenyl $\nu(\text{CC})$ mode at 6.2μ is used. In this note, results of a near-infrared study of styrene-acrylonitrile copolymers by use of combination- and overtone-bands are presented.

Four random copolymers, polyacrylonitrile (AN) and polystyrene (St) were used as samples. The composition of the copolymers was calibrated by Duma's method of nitrogen estimation. The films for the near-infrared analysis ranged from 0.5 to 0.6 mm in thickness and were molded in a hot press with the use of 150 mg of the samples at 180°C for 20 min in a nitrogen atmosphere. The film of AN alone was cast on a glass surface from its dimethyl sulfoxide solution to prevent thermal degradation. After the film was air-dried at room temperature, it was removed from the surface, then kept in boiling water for 2 hr, and finally dried in a vacuum oven at 90°C for 24 hr. Examination of the infrared spectra of the prepared films in the region $2\text{--}16 \mu$ showed that the films had not been oxidized or thermally degraded to any appreciable extent. The near-infrared spectra from 1.6 to 2.2μ were obtained with a Shimadzu spectrophotometer, Model RV-50. The instrument was calibrated with the use of 1,2,4-trichlorobenzene as a standard.²

Typical near-infrared spectra of the copolymers and the homopolymers are shown in Figure 1. The bands which occur in the region $1.6\text{--}2.2 \mu$ result from overtones and combination tones which occur, respectively, in the regions $1.6\text{--}1.8 \mu$ and $1.9\text{--}2.2 \mu$.

The band near 1.68μ is assigned as an overtone of phenyl $\nu(\text{CH})$ mode near 3000 cm^{-1} ($3000 \times 2 = 6000 \text{ cm}^{-1} = 1.67 \mu$), and its absorbance is directly proportional to the St content of the copolymer and the film thickness. The band near 1.75μ is assigned as an overtone of aliphatic $\nu(\text{CH})$ mode near 2900 cm^{-1} ($2900 \times 2 = 5800 \text{ cm}^{-1} = 1.724 \mu$) and both AN and St absorb at this wavelength. Bands at 1.910 and 1.952μ are combination tones of AN and are assigned as, respectively, $\nu(\text{CN}) + \nu_{\text{asym}}(\text{CH}_3)$ ($2237 + 2940 = 5177 \text{ cm}^{-1} = 1.932 \mu$) and $\nu(\text{CN}) + \nu_{\text{sym}}(\text{CH}_3)$ ($2237 + 2870 = 5107 \text{ cm}^{-1} = 1.958 \mu$).

For calculation of the absorbance of these four characteristic bands, two different baseline methods were used, as shown in Figure 1.

The reproducibility of the determination expressed as a percentage of the standard deviation of the average is presented in Table I. The observation was made with four replicate samples of the copolymer containing 24 wt-% of AN. The method using the extrapolated baseline from 2μ introduces less deviation than the other baseline method. Among the four absorbance ratios, $A_{1.675}/A_{1.910}$ proved to be the best one. The same trend mentioned above was observed with the other copolymers.

TABLE I
Reproducibility of the Determination

Absorbance ratio (A_i/A_j) ^a	Relative standard deviation, % ^b	
	Baseline (—)	Baseline (---)
1.675/1.910	1.0	0.7
1.75/1.910	2.9	1.6
1.675/1.952	5.6	2.6
1.75/1.952	6.0	3.4

^a i, j = microns.

^b See Fig. 1.

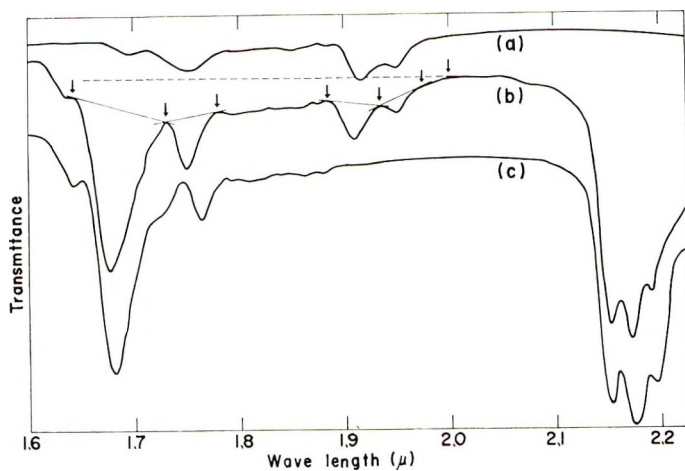


Fig. 1. Near-infrared spectra: (a) polyacrylonitrile; (b) styrene-acrylonitrile copolymer (AN content 25.7 wt-%); (c) polystyrene.

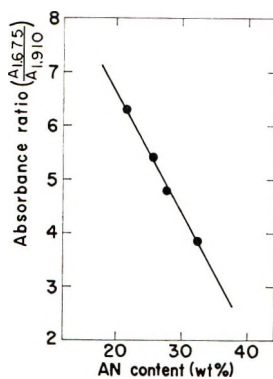


Fig. 2. Relationship between absorbance ratio and AN content of styrene-acrylonitrile copolymers.

TABLE II
Precision Data

Sample	Content of AN, wt-% (A) ^a	Absorbance ratio ($A_{1.675}/A_{1.910}$)	Calculated content of AN, wt-% (B) ^b	Deviation (B - A), wt-%
1	21.6	6.31	21.5	-0.1
2	25.7	5.41	25.4	-0.3
3	27.6	4.79	28.1	+0.7
4	32.3	3.85	32.0	-0.3

^a Determined by elementary analysis of nitrogen.

^b Calculated by eq. (1).

Figure 2 shows a calibration curve obtained by the method using the extrapolated baseline and the absorbance ratio $A_{1.675}/A_{1.910}$. The points represent the observed values and the solid line is obtained by the method of least squares. A linear relationship can be represented as follows;

$$0.0206x + 0.0882y = 1 \quad (1)$$

where x is weight per cent of AN and y is the absorbance ratio $A_{1.675}/A_{1.910}$.

Precision data are listed in Table II.

As the relative absorbance ratio method is employed, the calibration curve is not sensitive to small changes of the thickness of the film. Although thermal degradation was not observed in this work, it must be considered during the film preparation of the copolymers with such a high content or block segments of AN. The difficulty may be overcome by use of a solution or a cast film method.

References

1. R. T. Scheddel, *Anal. Chem.*, **30**, 1303 (1958).
2. E. K. Plyler, L. R. Blaine, and M. Nowak, *J. Res. Natl. Bur. Stand.*, **58**, 195 (1957).

TSUGIO TAKEUCHI
SHIN TSUGE
YOSHIHIRO SUGIMURA

Department of Synthetic Chemistry
Faculty of Engineering
Nagoya University
Nagoya, Japan

Received April 12, 1968

Revised May 21, 1968

Estimation of Diglycidyl Ether in Epoxide Resins

The estimation of diglycidyl ether (DGE) of bisphenol-A and also other components present in an epoxide resin enables the correct evaluation of it since its properties are influenced¹ by the amount of DGE initially present which is in turn dependent on the molar ratio of reactants.^{1,2}

The present investigation deals with a column chromatographic method (CCM) for the quantitative isolation of DGE and with a preparative thin layer chromatographic (TLC) method for the determination of overall composition of the resin.

The resin was prepared, as usual, by condensing 10 moles of epichlorohydrin, 2 moles of bisphenol-A with 2 moles of NaOH in *sec*-butyl alcohol at 80–85°C. It had an epoxide equivalent of 191, hydroxyl value of 0.16 per molecule, and, on T.L.C. analysis according to Weatherhead,³ indicated the presence of six components as represented in Figure 1.

The separation of DGE from other components of the resin was made by CCM, wherein activated silica gel (BDH) was used as adsorbent and chloroform (E. Merck) as eluting solvent in a column of 1 cm² cross section with an effective length of 32 cm loaded with 0.1869 g of the resin. Fractions (2 ml each) denoted by test tube numbers in Figure 2 were collected at an elution rate of 1 ml/min and weighed. The purity of the fractions was monitored with the help of TLC.³ The sequence of separation is represented in Figure 2. The recovery of DGE was quantitative, amounting to 77.5% of the resin having an OH value of 0, epoxide equivalent of 170.5, and C/H = 10.5. Total recovery of the material from the column was 93.9%.

Since the separation of all the components besides DGE was not effective by CCM (*cf.* Fig. 2) further investigation on quantitative determination of individual component in the resin was made by a preparative TLC method using Silica Gel G, 0.8 mm in thickness, and chloroform as eluting solvent. Each plate was loaded in band form with 50 mg of 4% resin solution. The components thus separated in band form were located

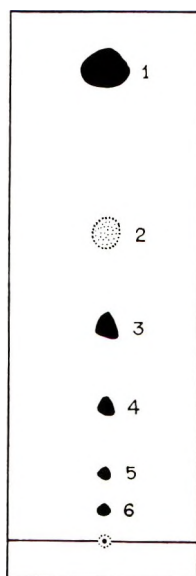


Fig. 1. Thin-layer chromatographic separation of the components of epoxide resin. The silica gel G plate was eluted once with chloroform and developed by spraying with 50% sulphuric acid, followed by heating at 150°C for 20 min. in an air oven, and reproduced by tracing the outlines of the spots.

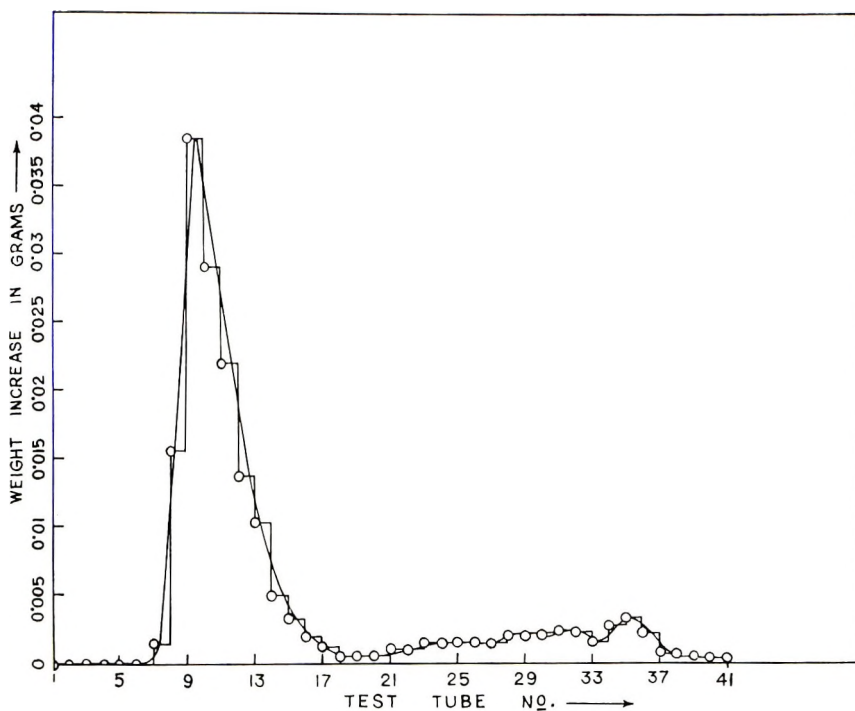


Fig. 2. Plot of test-tube number vs. amount of residue left in each test tube.

by using an indicator band of the sample along the edges of the plate. These components were detected by spraying with 0.005% aqueous Rhodamine B (visible under uv light) and finally estimated gravimetrically after extracting a separated fraction from each of three such plates with warm chloroform. The individual components present in the resin were thus found to be 75.5, 2.1, 12.4, 5.6, and 4.4% corresponding to spot number 1 (DGE), 2, 3, 4, and 5, 6 (combined) respectively (cf. Fig. 1).

References

1. P. K. Ghosh and A. N. Saha, *Indian J. Appl. Chem.*, in press.
2. H. Lee and K. Neville, *Epoxide Resins*, McGraw-Hill, New York, 1957, page 10.
3. R. G. Weatherhead, *Analyst*, **91**, 245 (1966).

P. K. GHOSH
C. BANDYOPADHYAY
A. N. SAHA

Department of Applied Chemistry
University College of Science & Technology
Calcutta, India

Received March 5, 1968

Revised April 1, 1968

AUTHOR INDEX, VOLUME 6

- Abe, K.: see Matsuda, M.
- Ahn, T.: see Wiley, R. H.
- Alexander, A. E.: see Friend, J. P.
- Alexander, I. J.: see Bywater, S.
- Alwani, D. W.: see Smith, W. E.
- Anand, L. C., Dixit, S. S., and Kapur, S. L.: Polymerization of styrene with VCl_4 -aluminum alkyls, 909
- Anderson, D. K.: see Kern, E. E.
- Anderson, J. D.: Electrochemical synthesis of living anions, 3185
- Andrews, M. W.: see Ingram, P.
- Ansporn, H. D.: see Smith, W. E.
- Aoki, S., Harita, Y., Tanaka, Y., Mandai, H., and Otsu, T.: Relative reactivities of cyclic ethers in cationic copolymerizations: Effects of ring strain and basicity, 2585
- Artymyshyn, B.: see Jordan, E. F., Jr.
- Asahara, T., Ikeda, K., and Yoda, Y.: Salt effect in the base-catalyzed polymerization of unsaturated amide compounds. III. Nature of the polymerization system, 2489
- and Yoda, N.: Salt effect in the base-catalyzed polymerization of unsaturated amide compounds. II. Polymerization of *p*-vinylbenzamide and acrylamide, 2477
- : see Sanui, K.
- Asai, M.: see Tazuke, S.
- Ashby, G. E.: see Werber, F. X.
- Aso, C., Kunitake, T., and Ishimoto, Y.: Studies of polymers from cyclic dienes. IV. Determination of the structure of polycyclopentadiene, 1163. V. Cationic polymerization of cyclopentadiene, influence of polymerization conditions on the polymer structure, 1175
- , —, Matsuguma, Y., and Imaizumi, Y.: Studies on the polymerization of bifunctional monomers. XVI. Cyclopolymerization of *o*-divinylbenzene with triphenylmethyl fluoroborate and presumption of the presence of the free growing cation in this system, 3049
- Ayscough, P. B., Roy, A. K., Croce, R. G., and Munari, S.: Electron spin resonance study of the radiation-induced polymerization of *N*-vinylcarbazole, 1307
- Bahary, W. S., and Bsharah, L.: Molecular structure of synthetic rubber. I. Light-scattering properties of styrene-butadiene copolymers, 2819
- Baijal, M. D.: see Thyrion, F. C.
- Bailey, S.: see Brewer, R. J.
- Baines, F. C., and Bevington, J. C.: A tracer study of the hydrolysis of methyl methacrylate and methyl acrylate units in homopolymers and copolymers, 2433
- Baldwin, M. G., and Reed, S. F., Jr.: Polymerization studies on allylic compounds. III. α -(Substituted methyl)styrenes, 2627
- Bandyopadhyay, C.: see Ghosh, P. K.
- Barefoot, R. D.: see Tompa, A. S.
- Barrett, E. J.: see Hoyer, H. W.
- Bartoň, J.: Peroxide crosslinking of poly(*n*-alkyl methacrylates), 1315
- Beaulieu, R. D.: see Zavitsas, A. A.
- Becker, A. J.: see Freeman, E. S.
- Bedford, M. A.: see Stille, J. K.
- Benning, C. J., Wszolek, W. R., and Werber, F. X.: Crystalline titanium dichloride—An active catalyst in ethylene polymerization. II. Polymer structure, polymerization variables, and scope, 755
- : see Werber, F. X.
- Berger, J., and Lazár, M.: Polymerization of methyl methacrylate in a tetrahydrofuran-maleic anhydride system. Part II, 3109
- Berr, C. E.: see Gay, F. P.
- Bevington, J. C.: see Baines, F. C.
- Bilbo, A. J., Douglas, C. M., Fetter, N. R., and Herring, D. L.: Synthesis and thermogravimetric analysis of diol-linked tetrameric hexaphenyldichlorophosphonitrile polymers, 1671
- Blais, P., and St. John Manley, R.: Morphology of nascent polyolefins

- prepared by Ziegler-Natta catalysis, 291
- Block, B. P.: see Maguire, K. D.
- Bly, D. D.: Determination of theoretical plates in gel permeation chromatography by using polydisperse materials (polymers), 2085
- Board, R. D.: see Lal, J.
- Bochvar, D. A.: see Rodè, V. V.
- Bond, J., and Lee, P. I.: Cupric sulfate-hydrazine system as an initiator of vinyl polymerization. II. Polymerization of methyl methacrylate in aqueous solution in the absence of oxygen, 2621
- Bondarenko, E. M.: see Rodè, V. V.
- Bower, G. M., Freeman, J. H., Traynor, E. J., Frost, L. W., Burgman, H. A., and Ruffing, C. R.: Thermosetting polyimides, 877
- Braden, M.: Water-absorption properties of an acetal copolymer, 1227
- Bradford, E. B., and Vanzo, E.: Ordered structures of styrene-butadiene block copolymers in the solid state, 1661
- Bressler, S. E., Erussalimsky, B. L., and Kulevskaya, I. V.: Molecular weight distributions in polymerizing systems with different coexisting active centers, 2795
- Brewer, R. J., Tanghe, L. J., Bailey, S., and Burr, J. T.: Molecular weight distribution of cellulose esters by gel permeation chromatography and fractional precipitation, 1697
- Brown, D. W., and Wall, L. A.: The radiation-induced copolymerization of tetrafluoroethylene and 3,3,3-trifluoropropene under pressure, 1367
- Brownstein, S.: see Fujii, K.
- Brydges, T. G., Dawson, D. G., and Lorimer, J. W.: Preparation of ion-selective membranes from crosslinked copolymers of styrene and *p*-vinylbenzenesulfonic acid, 1009
- Bsharah, L.: see Bahary, W. S.
- Burgman, H. A.: see Bower, G. M.; Frost, L. W.
- Burr, J. T.: see Brewer, R. J.
- Butler, P. E.: see Wei, P. E.
- Bywater, S., and Alexander, I. J.: Influence of dioxane on the γ -anionic polymerization of styrene in benzene, 3407
- Campbell, D.: see Liepins, R.
- Caporiccio, G.: see Sianesi, D.
- Carmichael, J. B.: see Levin, G.
- Cassidy, H. G.: see Nakabayashi, N.; Uno, K.; Wegner, G.
- Chatterjee, P. K., and Conrad, C. M.: Thermogravimetric analysis of cellulose, 3217
- Chaudhuri, A. K., and Palit, S. R.: Mode of termination in the copolymerization of vinyl acetate-isobutyl methacrylate and methyl methacrylate-methyl acrylate at 60°C, 2187
- Chen, J. C. W.: Polymer reactions. II. Thermal decomposition of polyethylene hydroperoxide, 375
- and Jabloner, H.: Polymer reactions. IV. Thermal decomposition of polypropylene hydroperoxides, 393
- , Vandenberg, E. J., and Jabloner, H.: Polymer reactions. III. Structure of polypropylene hydroperoxide, 381
- Chiklis, C. K., and Haas, H. C.: Polymerization of 2,2,2-trifluoroethyl vinyl ether, 2573
- Cho, I.: see Overberger, C. G.
- Choudhury, P. K.: see Permanik, A. G.
- Chow, R. C. L., and Marvel, C. S.: Preparation and copolymerization of vinyl 10,11-epoxyundecanoate, 1273. Copolymerization of allyl esters of some fatty acids, 1515
- Christie, P. A.: see Dyer, E.
- Christman, E. M.: see Meyers, R. A.
- Chūjō, R.: see Ohsumi, Y.
- Colombo, P., Fontana, J., and Steinberg, M.: Radiation-induced copolymerization of ethylene and sulfur dioxide in the liquid and gas phases, 3201
- Conrad, C. M.: see Chatterjee, P. K.
- Cooper, S. L., McKinnon, A. J., and Prevorsek, D. C.: Morphological changes of twisted nylon 66 and poly(ethylene terephthalate) monofilaments, 353
- Coopes, I. H.: The optical rotation of gelatin films, 1991
- Croce, R. G.: see Ayscough, P. B.
- Culbertson, B. M., Sedor, E. A., Dietz, S., and Freis, R. E.: Aminimides. V. Preparation and polymerization studies of trimethylamine-4-vinylbenzimidazole, 2197
- and Slagel, R. C.: Aminimides. IV.

- Homo- and copolymerization studies on trimethylamine methacrylimide, 363
- Cunningham, R. E., and Dove, R. A.:
The composition of catalysts prepared from tri-*n*-propylaluminum, anisole, and titanium tetrachloride, 1751
- Dall'Asta, G.: Polymerization of cyclobutene rings. VI. Influence of the organometallic compound of the Ziegler-Natta catalysts on the mechanism of polymerization of cyclobutene and 3-methylcyclobutene, 2397
- and Motroni, G.: Polymerization of cyclobutene rings. VII. Polymerization of bicyclo[4,2,0]octa-7-ene and bicyclo[3,2,0]hepta-2,6-diene with Ziegler-Natta catalysts and with group VIII metal halides, 2405
- Dannels, B. F., and Shepard, A. F.:
Inorganic esters of novolacs, 2051
- Dawson, D. G.: see Brydges, T. G.
- Deanin, R. D., Margosiak, S. A., Farrar, G. L., and Storms, P. W.: Polymers of hydrogenated and chlorinated naphthalene-2,5-dicarboxylic acids, 235
- Delman, A. D., Kovacs, H. N., and Simms, B. B.: Thermal stability of silicon-containing amide, benzimidazole, hydrazide, and oxadiazole polymers, 2117
- : see Kovacs, H. N.
- Deshpande, A. B.: see Malhotra, S. L.
- Devenuto, A.: see Wiley, R. H.
- Dietrich, H. J.: Polymerization of 2-(chlorinated methyl)-4-methylene-1,3-dioxolanes, 2255
- : see Raes, M. C.
- Dietz, S.: see Culbertson, B. M.
- Dillon, J. G.: see Mulvaney, J. E.
- Dine-Hart, R. A.: Hydrazine based polyimides and model compounds, 2755
- Dixit, S. S.: see Anand, L. C.
- Donnet, J. B., Wetzel, J. P., and Riess, G.: Polymérisation "basse pression" de l'éthylène en présence de noir de carbone, 2359
- Douglas, C. M.: see Bilbo, A. J.
- Dove, R. A.: see Cunningham, R. E.
- Duncan, S.: see Wegner, G.
- Dyer, E., and Christie, P. A.:
Polytetrazoles and polyaminotetrazoles, 729
- Eargle, D. H., Jr., and Mouiz, W. B.:
Anion radicals of polyphenylsiloxanes, 1153
- Eastham, A. M.: see Fujii, K.
- Enomoto, Y.: see Minoura, Y., Ergova, Yu. V.: see Korshak, V. V.
- Erussalimsky, B. L.: see Bressler, S. E.
- Faber, J. W. H.: see Klanderma, B. H.
- Farrar, G. L.: see Deanin, R. D.
- Fehn, G. M.: Steady-state drawing of polymer melts, 247. *Erratum*, 3197
- Fetter, N. R.: see Bilbo, A. J.; Slota, P. J., Jr.
- Fijolka, P., and Shabab, Y.:
Contribution to the study of the mechanism of curing of unsaturated resins, 1217
- Flagg, E. E.: see Schmidt, D. L.
- Fleš, D.: see Janovič, Z.
- Fletcher, J. P., and Persinger, H. E.:
Molecular weight distribution of liquid poly(ethylene glycols): Determination by gas chromatography, 1025
- Fock, J.: On the synthesis and pyrolysis of a tetrafluoroethylene-acrylonitrile graft copolymer, 963. Pyrolysis of a tetrafluoroethylene-acrylonitrile copolymer, 969
- Fontana, C. M.: Polycondensation equilibrium and the kinetics of the catalyzed transesterification in the formation of polyethylene terephthalate, 2343
- Fontana, J.: see Colombo, P.
- Franco, S.: see Leoni, A.
- Freeburger, M. E.: see Stille, J. K.
- Freeman, E. S., and Becker, A. J.:
Thermal degradation of nadic methyl anhydrido-crosslinked Novolac epoxy resin, 2827
- Freeman, J. H.: see Bower, G. M.; Frost, L. W.
- Freeman, L. P.: see Slota, P. J., Jr.
- Freis, R. E.: see Culbertson, B. M.
- Friend, J. P., and Alexander, A. E.:
Effect of surfactants on the polymerization of acrylamide in aqueous solutions, 1833
- Frost, L. W., Bower, G. M., Freeman, J. H., Burgman, H. A., Traynor, E. J., and Ruffing, C. R.: Benzimidazole- and oxadiazole-modified aromatic polyimides, 215
- : see Bower, G. M.
- Fry, F. H.: see Watt, W. R.
- Fueno, T.: see Okuyama, T.

- Fujii, K., Brownstein, S., and Eastham, A. M.: Reactions of trifluoroacetic acid with poly(vinyl alcohol) and its model compounds. Effect of neighboring hydroxyl groups on the reaction, 2377. Fluorine magnetic resonance spectra and tacticities of poly(vinyl trifluoroacetate), 2387
- Fujimoto, T., Kawabata, N., and Furukawa, J.: Infrared studies of stereoregular polymerization of methyl methacrylate and methacrylonitrile by organometallic compounds, 1209
- Fujioka, S., Ichimura, T., Shinohara, Y., and Hayashi, K.: Radiation-induced polymerization of isoprene in aqueous solution of silver nitrate, 1109
- Fujita, Y.: see Morimoto, T.
- Fukuda, W., and Marvel, C. S.: Polymers from the vinyl esters of different samples of hydrogenated rosins, 1050. Polymers from the vinyl ester of dehydroabietic acid, 1281
- , Saga, M., and Marvel, C. S.: Homopolymers and copolymers of vinyl ethers of rosin-derived alcohols, 1523
- Fukui, K.: see Kagiya, T.; Yokota, H.
- Fukumi, A.: see Nishizaki, S.
- Fukutani, H.: Price, C. C.
- Furukawa, J.: see Fujimoto, T.; Okuyama, T.
- Furuno, H.: see Kujirai, C.
- Gardon, J. L.: Emulsion polymerization. I. Recalculation and extension of the Smith-Ewart theory, 623. II. Review of experimental data in the context of the revised Smith-Ewart theory, 643. III. Theoretical prediction of the effects of slow termination rate within latex particles, 665. IV. Experimental verification of the theory based on slow termination rate within latex particles, 687. V. Lowest theoretical limits of the ratio k_t/k_p , 2851. VI. Concentration of monomers in latex particles, 2857
- Gay, F. P., and Berr, C. E.: Polypyromellitimides: Details of pyrolysis, 1935
- : see Heacock, J. F.
- Gaylord, N. G., Hoffenberg, D. S., Matyska, B., and Mach, K.: Lewis acid-catalyzed reactions on polystyrene, 269
- , Kössler, I., Matyska, B., and Mach, K.: Cyclo- and cyclized diene polymers. XVI. Nature of the active species and a proposed mechanism of cyclopolymerization of isoprene with catalysts containing ethylaluminum halides, 125
- Gebura, S. E.: see Smith, W. E.
- Gervasi, J. A., Gosnell, A. B., Woods, D. K., and Stannett, V.: Reactions of living polystyrene with difunctional nitriles to produce specifically placed grafting sites, 859
- Ghosh, P. K., Bandyopadhyay, C., and Saha, A. N.: Estimation of diglycidyl ether in epoxide resins, 3418
- Goins, O. K.: see Deusen, R. L. van
- Golemba, F. J., Guillet, J. E., and Nyburg, S. C.: Synthesis and crystal structure of isotactic poly-4-phenyl-1-butene, 1341
- Golub, M. A., and Stephens, C. L.: Photoinduced microstructural changes in 1,4-polyisoprene, 763
- Gosnell, A. B.: see Gervasi, J. A.
- Grassie, N., and Torrance, B. J. D.: Thermal degradation of copolymers of methyl methacrylate and methyl acrylate. I. Products and general characteristics of the reaction, 3303. II. Chain scission and the mechanism of the reaction, 3315
- Grotewold, J., Lissi, E. A., and Villa, A. E.: Vinyl monomer polymerization mechanism in the presence of trialkylboranes, 3157
- Guillet, J. E.: see Golemba, F. J.; Kells, D. I. C.
- Gulbekian, E. V.: The emulsion polymerization of vinyl acetate. Factors controlling particle surface area and rate of polymerization, 2265
- Haack, R.: see Rembaum, A.
- Haas, H. C.: see Chiklis, C. K.
- Hagiwara, M., Mitsui, H., Machi, S., and Kagiya, T.: Liquid carbon dioxide as a solvent for the radiation polymerization of ethylene, 603. Kinetics of the γ -radiation-induced polymerization of ethylene in liquid carbon dioxide, 609. Two-stage irradiation study on propagation and termination in the γ -radiation-induced

- polymerization of ethylene in liquid carbon dioxide, 721
- : see Mitsui, H.; Suganuma, F.
- Haldon, R. A., and Hay, J. N.:
Dehydrochlorination reactions in polymers. III. Vinylidene chloride-styrene copolymers, 951
- Han, G. E.: see Smith, W. E.
- Hammond, R. J., and Work, J. L.:
Dynamic mechanical properties of plasticized poly(vinyl chloride). Linear free energy relationship in the poly-(vinyl chloride)-ester system, 73
- Hansch, C., and Helmer, F.:
Extrathermodynamic approach to the study of the adsorption of organic compounds by macromolecules, 3295
- Hara, S.: see Iwakura, Y.
- Harada, H.: see Minoura, Y.
- Harita, Y.: see Aoki, S.
- Harris, F. W.: see Stille, J. K.
- Hartman, R. D., and Pohl, H. A.:
Hyperelectronic polarization in macromolecular solids, 1135
- Hasegawa, M.: see Iguchi, M.; Takahashi, H.
- Hashiya, S.: see Kujirai, C.
- Hatada, K.: see Yuki, H.
- Hattori, K.: see Iwakura, Y.
- Hay, J. N.: Thermal reactions of polyacrylonitrile, 2127
- : see Haldon, R. A.
- Hayano, F.: see Iwakura, Y.
- Hayashi, K.: see Fujioka, S.; Nakayama, Y.
- Hancock, J. F., Mallory, F. B., and Gay, F. P.: Photodegradation of polyethylene film, 2919
- Helmer, F.: see Hansch, C.
- Hergenrother, P. M.: Aliphatic polyphenylquinoxalines, 3170
- and Levine, H. II.:
Polybenzothiazoles. III. A-B Polymers, 2937
- Herring, D. L.: see Bilbo, A. J.
- Hermann, A. M.: see Rembaum, A.
- Herweh, J. E.: see Work, J. L.
- Higashimura, T., Kusudo, S., Ohsumi, Y., Mizote, A., and Okamura, S.:
Cationic polymerization of α,β -disubstituted olefins. IV. Stereospecific polymerization of propenyl alkyl ethers catalyzed by $\text{BF}_3 \cdot \text{O}(\text{C}_2\text{H}_5)_2$ and $\text{Al}_2(\text{SO}_4)_3 \cdot \text{H}_2\text{SO}_4$ complex, 2511
- , —, —, and Okamura, S.:
Cationic polymerization of α,β -disubstituted olefins. V. Reactivity of propenyl alkyl ethers in cationic polymerization, 2523
- : see Miki, T.; Mizote, A.; Ohsumi, Y.
- Higashiura, K., and Oiwa, M.:
Retardation of radical polymerization by phenylacetylene and its *p*-substituted derivatives, 1857
- Higgins, J. P. J., and Weale, K. E.:
Soluble high polymers from allyl methacrylate, 3007
- Hirashara, T., Nakano, T., and Minoura, Y.:
Effects of mercaptides on the butyllithium-initiated polymerization of methyl methacrylate, 485
- Hironaka, H.: see Minoura, Y.
- Hirooka, M., Yabuuchi, H., Iseki, J., and Nakai, Y.:
Alternating copolymerization through the complexes of conjugated vinyl monomers-alkylaluminum halides, 1381
- Hladký, E.: see Kučera, M.
- Hodgdon, R. B., Jr.:
Polyelectrolytes prepared from perfluoroalkylaryl macromolecules, 171
- and Macdonald, D. I.:
Preparation and polymerizability of substituted α,β,β -trifluorostyrenes, 711
- Hoffenberg, D. S.: see Gaylord, N. G.
- Hoglen, J. J.: see Trifan, D. S.
- Holmer, D. A.:
Polyamide and polyester derivatives of homoterephthalic acid, 3177
- Hori, Y.: see Takahashi, T.
- Horio, K., Mita, I., and Kambe, H.:
Calorimetric investigation of polymerization reactions. I. Diffusion-controlled polymerization of methyl methacrylate and styrene, 2663
- Hosemann, R., and Schramek, W.:
Statistische Methoden zur Ermittlung der Verteilung der Molekülgrößen in hochpolymeren Systemen aus Experimentalergebnissen der fractionierten Fällung. IV. Berücksichtigung der Polydispersität der Fraktionen, 109
- Hosoi, F.: see Mitsui, H.
- Howard, P., and Parikh, R. S.:
Solution properties of cellulose triacetate. II. Solubility and viscosity studies, 537
- Hoyer, H. W., Santoro, A. V., and Barrett, E. J.:
Activation energies for

- styrene polymerization by differential thermal analysis, 1033
- Hrabak, F.: Isomerization of *cis*-1,4-polybutadiene by $\text{RhCl}_3 \cdot 3\text{H}_2\text{O}$, 3259
- Ichimura, T.: see Fujioka, S.
- Iguchi, M., Nakanishi, H., and Hasegawa, M.: Crystals of polymers derived from divinyl compounds by photoradiation in the solid state, 1055
- Ikeda, K.: see Asahara, T.
- Ikeda, M.: see Okajima, S.
- Imai, H.: see Saegusa, T.,
- Imai, Y.: see Iwakura, Y.,
- Imaizumi, Y.: see Aso, C.
- Imanishi, Y.: see Kohjiya, S.
- Ingram, P., Williams, J. L., Stannett, V., and Andrews, M. W.: Radiation grafting of vinyl monomers to wool. III. Location of the grafted polymer, 1985
- Inoue, T.: see Yuki, H.
- Ise, N.: see Sakurada, I.
- Iseki, J.: see Hirooka, M.
- Ishii, Y.: see Yokota, K.
- Ishikawa, K.: see Takizawa, A.
- Ishimoto, Y.: see Aso, C.
- Iwahori, K.: see Shibukawa, T.
- Iwakura, Y., Imai, Y., and Yagi, K.: Preparation of highly branched graft copolymers by the ceric ion method, 801. Preparation of polymers containing sugar residues, 1625
- , Izawa, S., and Hayano, F.: Aromatic polydiketopiperazines, 1097
- , Nabeya, A., and Nishiguchi, T.: 1,5-Polymerization of 1-thioacylaziridines, 2591
- , Toda, F., and Hattori, K.: Copolymerization of vinylsilanes with styrene, 1633. Reaction between ethanol and silicon-hydrogen of poly(*p*-vinylphenyldimethylsilane), 1643
- , —, Torii, Y., and Murata, K.: Synthesis of polyamideamines from 5-oxazolones, 785
- , —, —, and Sekii, R.: Polyaddition reaction of pseudoxazolones with dimercaptans, 1877. Copolymerization of 2-isopropenyl-4,4-dialkyl-5-oxazolones with styrene, 2681
- , Uno, K., Hara, S., and Kurosawa, S.: Polyhydrazides. I. *N*-Alkylated polyhydrazides from diesters and hydrazine, 3357. II. Methylated polyhydrazides by direct solution polycondensations of methylated hydrazines and dicarboxylic acid components, 3371. III. *N*-Methylated polyhydrazides by ring-opening of poly-*p*-phenylene-1,3,4-oxadiazole, 3381
- , —, and Kobayashi, N.: Polymerization of isocyanates. III. Chemical behavior and structure of polyisocyanates, 1087. IV. Polymerization by aqueous initiator systems, 793. V. Thermal degradation of polyisocyanates, 2611
- , —, and Oya, M.: Polymerization of α -amino acid *N*-carboxy anhydrides. III. Mechanism of polymerization of L- and DL-alanine NCA in acetonitrile, 2165
- , —, and Takiguchi, T.: Syntheses of aromatic polyketones and aromatic polyamide, 3345
- : see Uno, K.
- Iwatsuki, S., Kokubo, T., and Yamashita, Y.: Studies on the charge transfer complex and polymerization. XIV. Spontaneous copolymerization of 1-methylcyclopropene and sulfur dioxide, 2441
- , Okada, T., and Yamashita, Y.: Studies on the charge transfer complex and polymerization. XVI. Spontaneous copolymerization of cyclopentene and sulfur dioxide, 2451
- Izawa, S.: see Iwakura, Y.
- Izu, M.: see Kagiya, T.
- Jabloner, H.: see Chien, J. C. W.
- Janović, Z., and Fleš, D.: Preparation of *p*-[(S) (-)-2-phthalimidopropionyl] polystyrene, 1871
- Jedlinski, Z., and Maslinska-Solich, J.: Polymerization of cyclic acetals. I. Polymerization of 2-vinyl-1,3-dioxane and 2-isopropenyl-1,3-dioxane, 3182
- Jerassi, R. A., and McCormick, M. R.: Aryl end-capping of 2,6-dimethyl-1,4-polyphenylene oxide, 3167
- Jin, J. I.: see Wiley, R. H.
- Jokl, J., Kopeček, J., and Lím, D.: Mechanism of three-dimensional polymerization of the system methyl methacrylate-glycol dimethacrylate. I. Determination of the structure of the three-dimensional product, 3041

- Jordan, E. F., Jr.: Heterogeneity parameters by light scattering for statistical copolymers incorporating long side-chain comonomers, 2209
- , Artymyshyn, B., and Wrigley, A. N.: Chain transfer for vinyl monomers polymerized in *N*-allylstearamide, 575
- Kagiya, T., Izu, M., Kawai, S., and Fukui, K.: Solid-state polymerization of maleimide by 2,2'-azobisisobutyronitrile, 1719
- , —, Matsuda, T., Matsuda, M., and Fukui, K.: Synthesis of ordered copolyamides by the interfacial polycondensation of the hydrolyzate of bisimidazoline with diacid chloride, 2059
- : see Hariwara, M.; Mitsui, H.; Suganuma, F.; Yokota, H.
- Kai, A.: see Okajima, S.
- Kalló, A.: see Kollár, L.
- Kamachi, M., and Miyama, H.: Determination of elementary rate constants of styrene polymerization catalyzed by rhenium pentachloride, 1537
- Kamath, Y.: see Wiley, R. H.
- Kambe, H.: see Horio, K.
- Kamiya, Y.: Autoxidation of polypropylene catalyzed by cobalt salt in the liquid phase, 2561
- Kamogawa, H., Kato, M., and Sugiyama, H.: Syntheses and properties of photochromic polymers of the azobenzene and thiazine series, 2967
- : see Kato, M.
- Kanbe, M., and Okawara, M.: Synthesis of poly-*p*-xylylene from *p*-xylylenebis(dimethylsulfonium) tetrafluoroborate, 1058
- Kani, M.: see Yokota, K.
- Kapur, S. L.: see Anaud, L. C.; Malhotra, S. L.
- Karabinos, J. V.: see Raes, M. C.
- Kasabo, T.: see Minoura, Y.
- Kasica, H., Kryszewski, M., Szymaniski, A., and Włodarczyk, M.: Electrical conductivity of *N*-substituted polyamides, 1615
- Kato, M., and Kamogawa, H.: Polymerization of allyl(vinyl phenyl) ethers and reactions of the resulting polymers, 2933
- : see Kamogawa, H.
- Katz, D., and Relis, J.: Free-radical polymerization of 9-vinylanthracene, 2079
- Kawabata, N.: see Fujimoto, T.
- Kawai, S.: see Kagiya, T.
- Kawai, W.: Cationic polymerization of 4-methyl-1,3-dioxene-4 and copolymerization with tetrahydrofuran, 137. Copolymerization of 4-methyl-1,3-dioxene-4 with maleic anhydride and terpolymerization with styrene as the third component, 1945
- Kells, D. I. C., Koike, M., and Guillet, J. E.: Direct determination of crosslinking and chain scission in polymers, 595
- Kennedy, J. P.: Olefin polymerizations and copolymerizations with aluminum alkyl-cocatalyst systems. I. Cocatalysts with Brønsted acid systems, 3139
- Kern, E. E., and Anderson, D. K.: The structure and transport properties of poly(methacrylic acid) in aqueous solution, 2765
- Kitahama, Y.: Polymerization of 2,5-dimethyl-3,4-dihydro-2*H*-pyran-2-carboxaldehyde (methacrolein dimer). II, 2309
- Klenderman, B. H., and Faber, J. W. H.: Novel bridged anthracene derivatives and polyesters and copolyesters therefrom, 2955
- Kobayashi, N.: see Iwakura, Y.
- Kobayashi, S.: see Tsuda, K.
- Kössler, I.: see Gaylord, N. G.
- Kohjiya, S., Imanishi, Y., and Okamura, S.: Cationic polymerization of cyclic dienes. V. Polymerization of the methylcyclopentadiene, 809
- Koike, M.: see Kells, D. I. C.
- Kokubo, T.: see Iwatsuki, S.
- Kollár, L., Simon, A., and Kalló, A.: Study of Ziegler-Natta catalysts. Part III. Effect of the structure of titanium trichloride on the polymerization of propylene, 937
- , —, and Osváth, J.: Study of Ziegler-Natta catalysts. I. Valence state and polymerization activity, 919. II. The liquid phase and polymerization activity of the catalyst, 927
- Kondo, M.: see Yokota, H.
- Konomi, T.: see Tani, H.
- Kopeček, J.: see Jokl, J.
- Korshak, V. V., Mozgova, K. K., and

- Ergova, Yu. V.: Synthesis and investigation of properties of repeatedly grafted copolymers (pemosors), 2715
 —: see Rodě, V. V.
- Koshijima, T., and Muraki, E.: Radical grafting on lignin. I. Radiation-induced grafting of styrene onto hydrochloric acid lignin, 1431
- Kottle, S.: see McGaugh, M. C.
- Kovacs, H. N., Delman, A. D., and Simms, B. B.: Silicon-containing amide, benzimidazole, hydrazide, and oxadiazole polymers, 2103
 —: see Delman, A. D.
- Krongauz, E. S.: see Rodě, V. V.
- Kryszewski, M.: see Kascia, H.
- Kubota, H.: see Ogiwara, Yoshitaka
- Kučera, M., Hladký, E., and Majerová, K.: Kinetics of the polymerization of tetrahydrofuran in the presence of water, 901
 —and Majerová, K.: Effect of the initiator solvation on the change in polymerization rates of dioxolane and tetrahydrofuran, 527
- Kujirai, C., Hashiya, S., Furuno, H., and Terada, N.: Photochemical cross-linking of polypropylene, 589
- Kulevskaya, I. V.: see Bressler, S. E.
- Kun, K. A., and Kunin, R.: Macroreticular resins. III. Formation of macroreticular styrene-divinylbenzene copolymers, 2689
- Kunin, R.: see Kun, K. A.
- Kunioka, E.: see Tajima, Y.
- Kunitake, T.: see Aso, C.
- Kuroda, T.: see Ohsumi, Y.
- Kurosawa, S.: see Iwakura, Y.
- Kusudo, S.: see Higashimura, T.
- Labana, S. S.: Kinetics of high-intensity electron-beam polymerization of a divinyl urethane, 3083
- Lal, J., McGrath, J. E., and Board, R. D.: Effect of polymer structure on ease of hydrogen abstraction by cumyloxy radicals, 821
- Laurin, D., and Parravano, G.: Polymerization of 4-vinylpyridine by sodium in liquid ammonia, 1047
- Laverty, J. L.: see Mulvaney, J. E.
- Lazár, M.: see Berger, J.
- Leblanc, J. R.: see Zavitsas, A. A.
- Lee, P. I.: see Bond, J.
- Leoni, A., Franco, S., and Polla, G.: Polymerization with hydrogen migration of acrylamide, 3187
- Levin, G., and Carmichael, J. B.: Molecular weight distribution and thermal characterization of polydimethylsilimethylene, 1
- Levine, H. H.: see Hergenrother, P. M.
- Levy, A., and Litt, M.: Polymerization of cyclic iminoethers. III. Effect of ring substituents, 57. IV. Oxazoline polymerization in solvents containing different functional groups, 63. V. 4,3-Oxazolines with hydroxy-, acetoxy-, and carboxymethyl-alkyl groups in the 2 position and their polymers, 1883
- Liepins, R., Campbell, D., and Walker, C.: 1,2-Dinitrile polymers. I. Homopolymers and copolymers of fumaronitrile, malconitrile, and succinonitrile, 3059
- Lím, D.: see Jokl, J.
- Lissi, E. A.: see Grotewold, J.
- Litt, M.: see Levy, A.
- Lorimer, J. W.: see Brydges, T. G.
- Lovering, E. G., and Wright, W. B.: Evidence for several species of active sites in Ziegler-Natta catalysts, 2221
- Ludwig, B. A.: see Pittman, A. G.
- Macchi, E. M., Morosoff, N., and Morawetz, H.: Polymerization in the crystalline state. X. Solid-state conversion of 6-aminocaproic acid to oriented nylon 6, 2033
- MacCallum, J. R., and Tanner, J.: Preparation of poly(diphenyl phosphazene), 3163
- McCormick, M. R.: see Jerassi, R. A.
- Macdonald, D. I.: see Hodgdon, R. B., Jr.
- McGaugh, M. C., and Kottle, S.: The thermal degradation of acrylic acid-ethylene polymers, 1243
- McGrath, J. E.: see Lal, J.
- McGuchan, R., and McNeill, I. C.: Studies of chlorinated polyisobutenes. Part I. Investigations of structure by proton magnetic resonance and of thermal stability by thermal volatilization analysis, 205
- Mach, K.: see Gaylord, N. G.
- Machi, S.: see Hagiwara, M.; Suganuma, F.
- McIntosh, C. R.: see Stephens, W. D.
- McKinnon, A. J.: see Cooper, S. L.

- McNeill, I. C.: see McGuchan, R.,
McSweeney, G. P.: Ozonolysis of
natural rubber, 2678
- Maguire, K. D., and Block, B. P.:
Inorganic coordination polymers. X.
Observations on the formation and
nature of poly(di- μ -diphenylphosphina-
tohydroxyaquochromium) (III),
 $\{\text{Cr}(\text{H}_2\text{O})(\text{OH})[\text{OP}(\text{C}_6\text{H}_5)_2\text{O}]_2\}_z$, 1397
- Majerová, K.: see Kučera, M.
- Makita, M.: see Uno, K.
- Malhotra, S. L., Deshpande, A. B., and
Kapur, S. L.: Polymerization of
styrene with ZrCl_4 and ZrCl_3 in
combination with $\text{Al}(\text{C}_2\text{H}_5)_3$, 193
- Mallon, B. J.: X-ray degradation of
Penton and its potential use as a
dosimeter for the 4–15 keV range,
2637. Observation of gel formation
in Penton with low-energy x-rays, 2677
- Mallory, F. B.: see Heacock, J. F.
- Mandai, H.: see Aoki, S.
- Margosiak, S. A.: see Deanin, R. D.
- Marshall, J.: The interaction of ions with
nylon. 1. Absorption of simple acids,
1583. 2. Diffusion of simple
acids, 1913
- Marshall, M. C.: see Shaw, J. N.
- Marvel, C. S.: see Chow, R. C. L.;
Fukuda, W.; Okada, Masahiko; Wolf,
R.
- Maslińska-Solich, J.: see Jedlinski, Z.
- Mate, R. D.: see Purdon, J. R., Jr.
- Matsuda, M., and Abe, K.:
Polymerization initiated by the
charge-transfer complex of styrene and
maleic anhydride in the presence of
cumene and of cumene and liquid
sulfur dioxide, 1441
- Matsuda, T.: see Kagiya, T.
- Matsuguma, Y.: see Aso, C.
- Matsumoto, S. I.: see Saegusa, T.
- Matsuzaki, K., Uryu, T., Okada, M.,
and Shiroki, H.: The stereoregularity
of polyacrylonitrile and its dependence
on polymerization temperature, 1475
- Matyska, B.: see Gaylord, N. G.
- Meller, A.: Method for computing the
specific rate of hydrolysis of glucosidic
bonds in some trisaccharides, 2415
- Meyers, R. A., and Christman, E. M.:
Solid-state initiation of polymerization
of *N*-vinylcarbazole by gases, 945
- Meyersen, K., and Wang, J. Y. C.:
Cyclocopolymerization of dicyclic
dienes and maleic anhydride to fused
ring systems (*erratum*), 2031
- Miki, T., Higashimura, T., and Okamura,
S.: Solution polymerization of trioxane
catalyzed by stannic chloride, 3031
- Millich, F., and Sinclair, R. G., II:
Polyisocyanides. II. Heterophasic
catalytic synthesis of poly(α -
phenylethylisocyanide) and of poly(*n*-
hexylisocyanide), 1417
- Minoura, Y., and Enomoto, Y.: Effect
of chlorosilanes on the radical
polymerization of styrene and methyl
methacrylate, 13
- , Hironaka, H., Kasabo, T., and Ueno,
Y.: Reaction of chlorine-containing
polymers with living polymers, 2773
- , Shiina, K., and Harada, H.: Lithiation
of diene polymers, 559
- , Shundo, M., and Enomoto, Y.: The
preparation of polysiloxane-vinyl
monomer graft and block copolymers,
979
- and Yamaguchi, H.: Preparation of
optically active polymethyl vinyl
carbinol, 2013
- : see Hirahara, T.
- Mita, I.: see Horio, K.
- Mitsui, H., Hosoi, F., Hagiwara, M., and
Kagiya, T.: Effect of acetylene on the
 γ -radiation-induced polymerization of
ethylene, 2879
- : see Hagiwara, M.; Sugauma, F.
- Miyama, H.: see Kamachi, M.
- Miyazaki, T.: see Nagai, T.
- Mizote, A., Higashimura, T., and
Okamura, S.: Cationic polymerization
of the geometrical isomers of β -
methylstyrene and anethole, 1825
- : see Higashimura, T.
- Moedritzer, K., and Van Wazer, J. R.:
Linear molecules based on
dimethylgermanium and dimethylsilicon
groups bridged with oxygen atoms and
terminated with chlorine atoms, 547
- Moniz, W. B.: see Largle, D. H., Jr.
- Morawetz, H.: see Macchi, E. M.
- Morelli, F., Tartarelli, R., and Moriconi,
A.: Effect of agitation on the
heterogeneous polymerization of
trioxane in solution, 2421
- Mori, K.: see Nakamura, Y.
- Moriconi, A.: see Morelli, F.
- Morimoto, S.: On the heat of solution of
polymer with solvent:

- Polydimethylsiloxane-solvent systems, 1547
- Morimoto, T., Fujita, Y., and Takeda, A.: Cyclic oligomer of diethyleneglycol terephthalate, 1044
- Morosoff, N.: see Macchi, E. M.
- Motroni, G.: see Dall'Asta, G.
- Mozgova, K. K.: see Korshak, V. V.
- Munari, S.: see Ayscough, P. B.
- Mulvaney, J. E., and Dillon, J. G.: Anionic polymerization and copolymerization of acrylophenone, 1849
- , —, and Laverty, J. L.: Polymerization and copolymerization of α -methacrylophenone, 1841
- Murahashi, S.: see Yuki, H.
- Muraki, E.: see Koshijima, T.
- Murano, M., and Yamadera, R.: Studies on the tacticity of polyacrylonitrile. III. NMR spectra of stereoisomers of 2,4,6-tricyanoheptane as model compounds of polyacrylonitrile, 843
- Fitch, R. M., and Chen, K. J.: Dilatometer for chemically initiated reactions, 3411
- and Terada, A.: Aminobutadienes. X. Polymerization and copolymerization of 2-phthalimidomethyl-1,3-butadiene, 2945
- : see Iwakura, Y.
- Nabeya, A.: see Iwakura, Y.
- Nagai, M., and Nishioka, A.: Solvent effect on NMR spectra of poly-(methyl methacrylate), 1655
- Nagai, T., Miyazaki, T., Sonoyama, Y., and Tokura, N.: On the blue-colored species, possibly assignable to a radical cation, formed by the aromatic hydrocarbon-sulfur dioxide-oxygen system: The polymerization of olefins initiated by aromatic hydrocarbons-oxygen in liquid sulfur dioxide, 3087
- Nakabayashi, N., Wegner, G., and Cassidy, H. G.: Electron-transfer polymers. XXX. Preparation of poly(1-vinyl-3,4,6-trimethyl-2,5-benzoquinone), 869
- : see Wegner, G.
- Nakagawa, T., and Okawara, M.: Retardation of discoloration of poly(vinyl chloride) and decolorization of discolored poly(vinyl chloride) with diimide, 1795
- Nakai, Y.: see Hirooka, M.
- Nakamura, Y., and Mori, K.: Modification of poly(vinyl chloride). X. Crosslinking of poly(vinyl chloride) with a soft segment of an elastomer containing thiol groups, 3269
- Nakanishi, H.: see Iguchi, M.
- Nakano, T.: see Hirahara, T.
- Nakayama, Y., Hayashi, K., and Okamura, S.: Copolymerization of phenanthrene and maleic anhydride, 2418
- Natarajan, L. V., and Santappa, M.: Polymerization of acrylamide and methacrylamide photoinitiated by azidopentamminecobalt(III), 3245
- Negishi, T.: see Takizawa, A.
- Nettleton, H. R.: see Stevenson, R. W.
- Neuse, E. W., and Rosenberg, H.: Polycarboxyhydrazides with ferrocenylene groups in the main chain, 1567
- Nicora, C.: see Borsini, G.
- Nishi, T., and Wada, Y.: Relaxations of selenium in crystalline and amorphous states, 1597
- Nishiguchi, T.: see Iwakura, Y.
- Nishioka, A.: see Nagai, M.
- Nishizaki, S., and Fukami, A.: Thermal stability of aromatic polyamides from 4,4'-oxydibenzoic acid, 1769
- Nyburg, S. C.: see Golemba, F. J.
- O'Donnell, J. H., and Sothman, R. D.: Radiation-induced, solid-state polymerization of derivatives of methacrylic acid. I. Postirradiation polymerization of zinc methacrylate, 1073
- Ogata, N.: see Sanui, K.
- Ogiwara, Yoshitaka, Kubota, H., and Ogiwara, Yukie: Studies of the graft copolymerization of methyl methacrylate by means of the photochemical reduction of ceric ion adsorbed on cellulosic materials, 3119
- , Ogiwara, Yukie, and Kubota, H.: The mechanism of consumption of ceric salt with cellulosic materials, 1489
- Ogiwara, Yukie: see Ogiwara, Yoshitaka
- Ohara, M.: see Uno, K.
- Ohsumi, Y., Higashimura, T., Okamura, S., Chūjō, R., and Kuroda, T.: Cationic polymerization of α,β -disubstituted olefins. VI. Steric structure of poly(methyl propenyl ether) obtained by cationic catalysts, 3015
- : see Higashimura, T.

- Ohta, K.: see Yuki, H.
- Oiwa, M.: see Higashiura, K.
- Okada, Masahiko, and Marvel, C. S.:
Polymers with quinoxaline units. III.
Polymers with quinoxaline and thiazine
recurring units, 1259.
Polytriphenodithiazine, 1774
—: see Wolf, R.
- Okada, Munehisa: see Matsuzaki, K.
- Okada, T.: see Iwatsuki, S.
- Okajima, S., Ikeda, M., and Takeuchi,
A.: A new transition point of
polyacrylonitrile, 1925
—and Kai, A.: Investigation of the
change in the fine structure of valonia
cellulose upon wet heating and
mercerization, 2801
- Okamura, S.: see Higashimura, T.;
Kohjiya, S.; Miki, T.; Mizote, A.;
Nakayama, Y.; Ohsumi, Y.; Tazuke, S.
- Okawara, M.: see Kanbe, M.; Nakagawa,
T.
- Okuyama, T., Fueno, T., and Furukawa,
J.: Structure and reactivity of α,β -
unsaturated ethers. II. Cationic
copolymerizations of propenyl
isobutyl ether, 993
—, —, —, and Uyeo, K.: Structure and
reactivity of α,β -unsaturated ethers.
III. Cationic copolymerizations of
alkenyl alkyl ethers, 1001
- Ooi, S.: see Uno, K.
- Osgan, M.: Catalytically active form of
ferric acetate hydroxide for the insertion
polymerization of propylene oxide,
1249
- Osváth, J.: see Kollár, L.
- Otsu, T., and Yamaguchi, M.: Metal-
containing initiator systems. IV.
Polymerization of methyl methacrylate
by systems of some activated metals
and organic halides, 3075
—: see Aoki, S.; Tsuda, K.;
Yamamoto, T.
- Overberger, C. G., and Cho, I.: Optically
active imidazole-containing polymers,
2741
—and Parker, G. M.: The synthesis of
some optically active *C*-methylated
2-oxohexamethyleneimines, 513
- Oya, M.: see Iwakura, Y.
- Palit, S. R.: see Chaudhuri, A. K.;
Pramanick, D.
- Parikh, R. S.: see Howard, P.
- Parker, G. M.: see Overberger, C. G.
- Parmanik, A. G., and Choudhury, P. K.:
Physicochemical and macromolecular
properties of sodium amylose xanthate
in dilute solution, 1121
- Parravano, G.: see Laurin, D.
- Persinger, H. E.: see Fletcher, J. P.
- Pittman, A. G., Sharp, D. L., and
Ludwig, B. A.: Polymers derived from
fluoroketones. II. Wetting properties
of fluoroalkyl acrylates and
methacrylates, 1729
—, Ludwig, B. A., and Sharp, D. L.:
Polymers derived from fluoroketones.
III. Monomer synthesis,
polymerization, and wetting properties
of poly(allyl ether) and poly(vinyl
ether), 1741
- Pittman, C. U., Jr.: Ferrocene-containing
polyesters and polyamides, 1687
- Pobiner, H.: see Watt, W. R.
- Pohl, H. A.: see Hartman, R. D.
- Polla, G.: see Leoni, A.
- Prabhakara Rao, S., and Santappa, M.:
Graft polymers from poly(vinyl
chloride) and chlorinated rubber,
95
- Pramanick, D., and Palit, S. R.: Studies
in some new initiator systems for
vinyl polymerization. II. Ammonia-
halogen system as the redox initiator,
2179
- Prevorsek, D. C.: Cooper, S. L.
Price, C. C., and Fukutani, H.:
Syndiotactic and isotactic poly-
(*tert*-butylethylene oxide), 2653
- Price, E.: see Tompa, A. S.
- Purdon, J. R., Jr., and Mate, R. D.:
Calibration of the gel permeation
chromatograph, 243
- Pyler, R. E.: see Whistler, R. L.
- Raes, M. C., Karabinos, J. V., and
Dietrich, H. J.: Copolymers of chloral
and heterocumulenes, 1067
- Raff, R. A. V., and Sharan, A. M.:
Thermal degradation of polymers
through an inductively heated insert,
1035
- Ravve, A.: Study on modification of
polymers with the aid of the Schmidt
reaction, 2887
- Reed, S. F., Jr.: see Baldwin, M. G.
- Reich, E.: see Wiley, R. H.
- Relis, J.: see Katz, D.
- Rembaum, A., Hermann, A. M., and
Haack, R.: Charge transfer complexes

- of *N*-ethylcarbazole and poly-*N*-vinylcarbazole, 1955
- Riess, G.: see Donnet, J. B.
- Rode, V. V., Bondarenko, E. M., Korshak, V. V., Rusanov, A. L., Krongauz, E. S., Bochar, D. A., and Stankevich, I. V.: Thermostability of some isomeric polyoxadiazoles, 1351
- Rogers, C. E., Sternberg, S., and Salovey, R.: Preparation and analysis of asymmetric membranes, 1409
- Rosenberg, H.: see Neuse, E. W.
- Roy, A. K.: see Ayscough, P. B.
- Ruffing, C. R.: see Bower, G. M.; Frost, J. W.
- Ruffini, G.: see Whistler, R. L.
- Rusanov, A. L.: see Rodb, V. V.
- Saegusa, T., Imai, H., and Matsumoto, S. I.: Polymerization of tetrahydrofuran by $AlEt_3-H_2O$ promoter system: Rate of propagation reaction, 459
- and Matsumoto, S. I.: Determination of concentration of propagating species in cationic polymerization of tetrahydrofuran, 1559
- Saga, M.: see Fukuda, W.
- Saha, A. N.: see Ghosh, P. K.
- St. John Manley, R.: see Blais, P.
- Sakurada, I., Tanaka, Y., and Ise, N.: Cationic polymerization of α -methylstyrene catalyzed by boron trifluoride etherate in 1,2-dichloroethane under an electric field, 1463
- Salovey, R.: see Rogers, C. E.
- Santappa, M.: see Natarajan, L. V.; Prabhakara Rao, S.; Subramanian, S. V.
- Santoro, A. V.: see Hoyer, H. W.
- Sanii, K., Asahara, T., and Ogata, N.: Room-temperature polycondensation of β -amino acid derivatives. I. Polyamide from amino alcohols and acrylates, 1195
- Sasaki, M.: see Yokota, K.
- Sato, I.: see Takahashi, T.
- Schmidt, D. L., and Flagg, E. E.: Preparation and properties of poly(phosphonatoalanes) chloride, 3235
- Schramek, W.: see Hosemann, R.
- Sedor, E. A.: see Culbertson, B. M.
- Sekii, R.: see Iwakura, Y.
- Sewell, P. R., and Skidmore, D. W.: Identification of diene comonomer by time-averaged NMR spectroscopy, 2425
- Shabab, Y.: see Fijolka, P.
- Sharan, A. M.: see Raff, R. A. V.
- Sharp, D. L.: see Pittman, A. G.
- Shaw, J. N., and Marshall, M. C.: Infrared spectroscopic studies of polystyrene emulsion polymers: Effect of oxidation during polymerization, 449
- Shelden, R. A.: see Trifan, D. S.
- Shepard, A. F.: see Dannels, B. F.
- Shibukawa, T., Sone, M., Uchida, A., and Iwahori, K.: Light-scattering study of polyacrylonitrile solution, 147
- Shima, K.: see Minoura, Y.
- Shinohara Y.: see Fujioka, S.
- Shiroki, H.: see Matsuzaki, K.
- Shuudo, M.: see Minoura, Y.
- Sianesi, D., and Caporiccio, G.: Polymerization and copolymerization studies on vinyl fluoride, 335
- Sicrec, A. J.: see Deussen, R. L. van
- Simms, B. B.: see Delman, A. D.; Kovacs, H. N.
- Simon, A.: see Kollár, L.
- Sinclair, R. G., II: see Millich, F.
- Sircar, A. K., and Stanonis, D. J.: Identification of cellulose phenylpropionylphenylpropionate as a side product in the reaction of cotton cellulose with phenylpropionyl chloride, 1061
- Skidmore, D. W.: see Sewell, P. R.
- Slagel, R. C.: see Culbertson, B. M.
- Slota, P. J., Jr., Freeman, L. P., and Fetter, N. R.: Metal coordination polymers. I. Synthesis and thermogravimetric analysis of beryllium phosphinate polymers, 1975
- Smith, H. A.: Effect of urethane groups on the reaction of alcohols with isocyanates, 1299
- Smith, W. E., Ham, G. E., Ansporn, H. D., Gebura, S. E., and Alwani, D. W.: Polylactones derived from polymethacrolein and styrene-methacrolein copolymerizations, 2001
- Sone, M.: see Shibukawa, T.
- Somoyama, Y.: see Nagai, T.
- Sothman, R. D.: see O'Donnell, J. H.
- Stankevich, I. V.: see Rode, V. V.
- Stannett, V.: see Gervasi, J. A.; Ingram, P.
- Stanonis, D. J.: see Sircar, A. K.
- Steinberg, M.: see Colombo, P.
- Stephens, C. L.: see Golub, M. A.
- Stephens, W. D., McIntosh, C. R., and Taylor, C. O.: Synthesis of low

- molecular weight hydroxy-terminated *cis*-1,3-polybutadiene, 1037
- Sternberg, S.: see Rogers, C. E.
- Stevenson, R. W., and Nettleton, H. R.: Polycondensation rate of poly(ethylene terephthalate). I. Polycondensation catalyzed by antimony trioxide in presence of reverse reaction, 889
- Stille, J. K., and Bedford, M. A.: Polymers from 1,3-dipole addition reactions: The syndone dipole, 2331
- and Froeburger, M. E.: Ladder polyphenoxazines, 161
- and Harris, F. W.: Polymers from 1,3-dipole addition reactions: The nitrilimine dipole from acid hydrozine chlorides, 2317
- Storms, P. W.: see Deanin, R. D.
- Strecker, R. A., and Tompa, A. S.: Investigation of reactions in carboxyl-terminated polybutadiene and tris-[1-(2-methyl)aziridinyl] phosphine oxide, 1233
- Subramanian, S. V., and Santappa, M.: Vinyl polymerization initiated by ceric ion reducing agent systems in sulfuric acid medium, 493
- Suganuma, F., Machi, S., Mitsui, H., Hagiwara, M., and Kagiya, T.: Effects of alcohols on the gamma-radiation-induced polymerization of ethylene, 2069
- , Mitsui, H., Machi, S., Hagiwara, M., and Kagiya, T.: Kinetics of the gamma-radiation-induced polymerization of ethylene in *tert*-butyl alcohol, 3127
- Sugimura, Y.: see Takeuchi, T.
- Sugiyama, H.: see Kamogawa, H.
- Sumi, K.: see Tsuchiya, Y.
- Szymaniski, A.: see Kasica, H.
- Tajima, Y., and Kunioka, E.: Ethylene polymerization by titanium compounds containing titanium-nitrogen bonds, 241
- Takahashi, H., and Hasegawa, M.: Linear polyhydrazides, 1449
- Takahashi, T.: Polymerization of vinylcyclopropanes. II, 403. III. Cationic polymerization of stereoisomers of 1-halo-2-vinylcyclopropanes, 3327
- , Hori, Y., and Sato, I.: Coordinated radical polymerization and redox polymerization of acrylamide by ceric ammonium nitrate, 2091
- Takeda, A.: see Morimoto, T.
- Takeuchi, A.: see Okajima, A.
- Takeuchi, T., Tsuge, S., and Sugimura, Y.: Near-infrared spectrophotometric analysis of styrene-acrylonitrile copolymer, 3415
- Takiguchi, T.: see Iwakura, Y.
- Takizawa, A., Negishi, T., and Ishikawa, K.: Sorption of water vapor by poly(vinyl alcohol): Influence of polymer crystallinity, 475
- Tanaka, T., Yokoyama, T., and Yamaguchi, Y.: Quantitative study on hydrogen bonding between urethane compound and ethers by infrared spectroscopy, 2137. Effects of methyl sidegroup on the extent of hydrogen bonding and modulus of polyurethane elastomers, 2153
- Tanaka, Y.: see Aoki, S.; Sakurada, I.
- Tanghe, L. J.: see Brewer, R. J.
- Tani, H., and Konomi, T.: Some properties of poly- α -piperidone, 2281. Polymerization of α -piperidone with MAlEt_3 , MAIEt_3 , or KAlEt_3 (piperidone) as catalysts and *N*-acetyl- α -piperidone as initiator, 2295
- Tanner, J.: see MacCallum, J. R.
- Tartarelli, R.: see Morelli, F.
- Taylor, C. O.: see Stephens, W. D.
- Tazuke, S., Asai, M., and Okamura, S.: Effects of metal salts on polymerization. Part V: Polymerization of *N*-vinylcarbazole initiated by sodium chloroaurate, 1809
- and Okamura, S.: Photo and thermal polymerization sensitized by donor-acceptor interaction. I. *N*-Vinylcarbazole-acrylonitrile and related systems, 2905
- Terada, A.: see Murata, K.
- Terada, N.: see Kujirai, C.
- Thryion, F. C., and Baijal, M. D.: Electron spin resonance study of polyglycols, 505
- Toda, F.: see Iwakura, Y.
- Tokarzewska, M.: Polyaryläther-Kondensationsprodukte des 4,4'-Bis(chloromethylphenyl)äthers mit manchen Diphenolen, 777
- Tokura, N.: see Nagai, T.
- Tompa, A. S., Barefoot, R. D., and Price, E.: Wide line and pulsed NMR studies of carboxyl-terminated polybutadiene polymers and binders, 2785

- : see Strecker, R. A.
- Torii, Y.: see Iwakura, Y.
- Torrance, B. J. D.: see Grassie, N.
- Traynor, E. J.: see Bower, G. M.; Frost, L. W.
- Trifan, D. S., Shelden, R. A., and Hoglen, J. J.: The polymerization of 1,4-pentadiene to [3.3.1]bicyclo-linked chains, 1605
- Tsuchiya, Y., and Sumi, K.: Thermal decomposition products of polyethylene, 415
- Tsuda, K., Kobayashi, S., and Otsu, T.: Vinyl polymerization. 178.
Copolymerizations of *p*-substituted phenyl vinyl sulfides, 41
- Tsuge, S.: see Takeuchi, T.
- Tsuruoka, K.: see Uno, K.
- Uchida, A.: see Shibukawa, T.
- Ueno, Y.: see Minoura, Y.
- Uno, K., Makita, M., Ooi, S., and Iwakura, Y.: Polymerization and copolymerization of methacrylic esters derived from glycidyl methacrylate, 257
- , Ohara, M., and Cassidy, H. G.: Electron-transfer polymers. XXIX. Copolymerizability of vinylhydroquinone derivatives, 2729
- , Tsuruoka, K., and Iwakura, Y.: Cyclopolymerization of diallylcyanamide, 85
- : see Iwakura, Y.; Yuki, H.
- Uryu, T.: see Matsuzaki, K.
- Uyeo, K.: see Okuyama, T.
- Vandenberg, E. J.: see Chien, J. C. W.
- Van Deusen, R. L., Goins, O. K., and Sicree, A. J.: Thermally stable polymers from 1,4,5,8-naphthalenetetracarboxylic acid and aromatic tetraamines, 1777
- Van Wazer, J. R.: see Moedritzer, K.
- Vanzo, E.: see Bradford, E. B.
- Villa, A. E.: see Grotewold, J.
- Wada, Y.: see Nishi, T.
- Walker, C.: see Liepins, R.
- Wall, L. A.: see Brown, D. W.
- Wang, J. Y. C.: see Meyersen, K.
- Watt, W. R., Fry, F. H., and Pobiner, H.: Polymerization of ethylene catalyzed by diethylaluminum chloride and titanium(III) acetylacetonate, 2703
- Weale, K. E.: see Higgins, J. P. J.
- Wegner, G., Nakabayashi, N., and Cassidy, H. G.: Electron-transfer polymers. XXXIV. Redox polyurethanes from *p*-benzoquinone-2,5-diols and diisocyanates, 3151
- , —, Duncan, S., and Cassidy, H. G.: Electron-transfer polymers. XXXVII. Preparation and redox behavior of polycarbonates with incorporated hydroquinone units, 3395
- : see Nakabayashi, N.
- Wei, P. E., and Butler, P. E.: Synthesis and polymerization studies of several chloro and cyano epoxides, 2461
- Weigmann, H.-D.: Reduction of disulfide bonds in keratin with 1,4-dithiothreitol. I. Kinetic investigation, 2237
- Werber, F. X., Benning, C. J., Wszolek, W. R., and Ashby, G. E.: Crystalline titanium dioxide—An active catalyst in ethylene polymerization. I. Catalyst activation, 743
- : see Benning, C. J.
- Wetzel, J. P.: see Donnet, J. B.
- Whistler, R. L., Ruffini, G., and Pyle, R. E.: Grafting of monosaccharide derivatives to cellulose acetate, 2501
- Wiley, R. H., and Ahn, T.: Monomer reactivity ratios for the copolymerization of styrene with 1,2,4-trivinyl and *p*-divinylbenzenes, 1293
- , —, and Kamath, Y.: Rates of sulfonation of divinylbenzene-crosslinked polystyrene in dimethyl sulfoxide, 1414
- and Devenuto, A.: Rate of sulfonation of bead polymers of styrene crosslinked with 1,2,4- and 1,3,5-trivinylbenzene, 1501
- , Jin, J. I., and Kamath, Y.: Isolation of pure *p*-divinylbenzene from commercial divinylbenzene, 1065
- and Reich, E.: The peroxide-induced degradation of sulfonated polystyrenes crosslinked with *m*- and *p*-divinylbenzenes, 3174
- Williams, J. L.: see Ingram, P.
- Wirick, M. G.: Study of the substitution pattern of hydroxyethylcellulose and its relationship to enzymic degradation, 1705. A study of the enzymic degradation of CMC and other cellulose ethers, 1965
- Włodarczyk, M.: see Kasica, H.
- Wolf, R., Okada, M., and Marvel, C. S.: Polymers with quinoxaline units. IV.

- Polymers with quinoxaline and oxazine units, 1503
- Woods, D. K.: see Gervasi, J. A.
- Work, J. L., and Herweh, J. E.: Thermal and mechanical properties of some polysulfonates, 2022
—: see Hammond, R. J.
- Wright, W. B.: see Lovering, E. G.
- Wrigley, A. N.: see Jordan, E. F., Jr.
- Wszolek, W. R.: see Benning, C. J.; Werber, F. X.
- Yabuuchi, H.: see Hirooka, M.
- Yagi, K.: see Iwakura, Y.
- Yamadera, R.: see Murano, M.
- Yamaguchi, H.: see Minoura, Y.
- Yamaguchi, M.: see Otsu, T.
- Yamaguchi, Y.: see Tanaka, T.
- Yamamoto, T., and Otsu, T.: Vinyl polymerization. 179. Effects of substituents on chain transfer reaction of substituted cumenes toward poly(methyl methacrylate) radical, 49
- Yamashita, Y.: see Iwatsuki, S.
- Yoda, N.: see Asahara, T.
- Yokota, H., Kondo, M., Kagiya, T., and Fukui, K.: Cationic polymerization of formaldehyde in liquid carbon dioxide. I, 425. II. A kinetic study of the polymerization, 435
- Yokota, K., Kani, M., and Ishii, Y.: Determination of propagation and termination rate constants for some methacrylates in their radical polymerization, 1325
—, Sasaki, M., and Ishii, Y.: Preparation and polymerization of 2-pyridyl methacrylate, 2933
- Yokoyama, T.: see Tanaka, T.
- Yuki, H., Hatada, K., and Inoue, T.: Anionic copolymerization of 1,1-diphenylethylene and 2,3-dimethylbutadiene, 3333
—, Ohta, K., Uno, K., and Murahashi, S.: Polymerization of *n*- α -methylbenzyl methacrylate by *n*-butyllithium and the tacticity and optical rotation of the polymer, 829
- Zavitsas, A. A.: Formaldehyde equilibria: Their effect on the kinetics of the reaction with phenol, 2533
—, Beaulieu, R. D., and Leblanc, J. R.: Base-catalyzed hydroxymethylation of phenol by aqueous formaldehyde. Kinetics and mechanism, 2541
- Zelinger, J.: see Zitek, P.
- Zitek, P., and Zelinger, J.: PVC-rubber blends. VI. The structure, 467

SUBJECT INDEX, VOLUME 6

- Acetal copolymer, 1227
Acetals, cyclic, 3182
Acetonitrile, 2165
Acetylene, 2881
N-Acetyl- α -piperidone, 2295
Acid hydrazide chlorides, 2317
Acids, simple, 1583, 1913
Acrylamide, 1833, 2091, 2477, 3187, 3245
Acrylates, 1195
Acrylic acid-ethylene polymers, 1243
Acrylophenone, 1849
Activated metals, 3075
Activation energies, 1033
Active centers, coexisting, 2795
Activity, polymerization, 919, 927
Adsorption, 3295
Agitation, 2421
L- and *DL*-Alanine NCA, 2165
Alcohols, 1299, 2069
 rosin-derived, 1523
N-Alkalated polyhydrazides, 3357
Alkenyl alkyl ethers, 1001
Alkylaluminum halides, 1381
Allyl esters, 1515
Allylic compounds, 2627
Allyl methacrylate, 3007
N-Allylstearamide, 575
Allyl(vinyl phenyl) ethers, 2993
Alternating copolymerization, 1381
Aluminum alkyl-cocatalyst systems, 3139
Amide polymers, 2117
Amides, unsaturated, 2477, 2489
Aminimides, 363, 2197
 α -Amino acid *N*-carboxy anhydrides, 2165
 β -Amino acid derivatives, 1195
Amino alcohols, 1195
Aminobutadienes, 2945
6-Aminocaproic acid, 2033
Ammonia, liquid, 1047
Ammonia-halogen system, 2179
Amorphous state, 1597
Anethole, 1825
Anionic copolymerization, 3333
Anionic polymerization, 1849, 3407
Anion radicals, 1153
Anisole, 1751
Anthracene derivatives, bridged, 2955
Antimony trioxide, 889
Aqueous solution, 1109, 2621
Aromatic hydrocarbon-sulfur dioxide-oxygen system, 3087
Aromatic polyamides, 1769
Aryl end-capping, 3167
Autoxidation, 2561
Azidopentamminecobalt(III) chloride, 3245
Azobenzene and thiazine series, 2967
2,2'-Azobisisobutyronitrile, 1719
Base-catalyzed polymerization, 2477, 2489
Bead polymers, 1501
Benzene, 3407
Benzimidazole polymers, 2117
p-Benzoquinone-2,5-diols, 3151
Beryllium phosphinate, 1975
Bicyclo(3,2,0)hepta-2,6-diene, 2405
[3.3.1]Bicyclo-linked chains, 1605
Bicyclo(4,2,0)octa-7-ene, 2405
Bifunctional monomers, 3049
4,4'-Bis(chloromethylphenyl)ether, 777
Bisimidazoline, hydrolyzate of, 2059
Block copolymers, 979
Boron trifluoride etherate, 1463
Brønsted acid systems, 3139
tert-Butyl alcohol, 3217
n-Butyllithium, 829
Butyllithium-initiated polymerization, 485
Calorimetry, 2663
Carbon black, 2359
Carbon dioxide, liquid, 603, 609, 721
Carboxymethylcellulose, 1965
Catalyst activation, 743
Catalysts, 1751
Cationic catalysts, 3015
Cationic copolymerizations, 993, 1001, 2585
Cationic polymerization, 809, 1175, 1463, 1559, 1825, 2511, 2523, 3015, 3327
 formaldehyde, 425, 435
 4-methyl-1,3-dioxene-4, 137
Cellulose, 3217
Cellulose acetate, 2501
Cellulose esters, 1697
Cellulose ethers, 1965
Cellulose phenylpropionylphenylpropionate, 1061
Cellulose triacetate, 537
Cellulosic materials, 1489, 3119

- Ceric ammonium nitrate, 2091
Ceric ion, 3119
Ceric ion method, 801
Ceric ion reducing agent systems, 493
Ceric salt, 1489
Chain scission, 595, 3315
Chain transfer, 575
Charge-transfer complexes, 1441, 1955, 2441, 2451
Chloral and heterocumulenes, 1068
2-(Chlorinated methyl)-4-methylene-1,3-dioxolanes, 2255
Chlorine-containing polymers, 2773
Chlorosilanes, effect on radical polymerization, 13
Cobalt salt, 2561
Cocatalysis, 3139
Comonomers, long side-chain, 2209
Complexes, 1381
Consumption, mechanism of, 1489
Coordination polymers, inorganic, 1397
Copolyamides, ordered, 2059
Cotton cellulose, 1061
Crosslinked copolymers, 1009
Crosslinking, 595
Crystalline state, 1597, 2033
Crystallinity, 475
Crystals, 1055
Crystal structure, 1341
Cumene, 1441
 and vinyl polymerization, 49
Cumyloxy radicals, 821
Cupric sulfate-hydrazine, 2621
Curing, mechanism of, 1217
Cyclic ethers, 2585
Cyclic iminoethers, 1883
Cyclobutene rings, 2397, 2405
Cyclopentadiene, 1175
Cyclopentene, 2451
Cyclopolymerization, 3049
 diallylcyanamide, 85
 isoprene, 125
Dehydroabiatic acid, 1281
Dehydrochlorination, 951
Diacid chloride, 2059
Diallylcyanamide, cyclopolymerization of, 85
Dicarboxylic acids, 3371
1,2-Dichloroethane, 1463
Diene comonomer, 2425
Dienes, 559
 cyclic, 809, 1163, 1175
 cyclo and cyclized, 125
Diesters, 3357
Diethylaluminum chloride, 2703
Diethyleneglycol terephthalate, 1044
Differential thermal analysis, 1033
Diffusion-controlled polymerization, 2663
Diglycidyl ether, 3418
Diimide, 1795
Diisocyanates, 3151
Dilatometer, 3411
Dimercaptans, 1877
2,3-Dimethylbutadiene, 3333
2,5-Dimethyl-3,4-dihydro-2*H*-pyran-2-carboxaldehyde, 2309
Dimethylgermanium, 547
2,6-Dimethyl-1,4-polypheylene oxide, 3167
Dimethylsilicon groups, 547
Dimethyl sulfoxide, 1414
1,2-Dinitrile polymers, 3059
Diol-linked tetrameric hexaphenyldichlorophosphonitrile polymers, 1671
Dioxane, 3407
Dioxolane, 527
1,1-Diphenylethylene, 3333
1,3-Dipole addition reactions, 2317, 2331
Discoloration, retardation of, 1795
 α,β -Disubstituted olefins, 2511, 2523, 3015
Disulfide bonds, 2237
1,4-Dithiothreitol, 2237
m- and *p*-Divinylbenzenes, 3174
o-Divinylbenzene, 3049
p-Divinylbenzene, 1065, 1293
Divinylbenzene-crosslinked polystyrene, 1414
Divinyl compounds, 1055
Divinyl urethane, 3283
Donor-acceptor interaction, 2907
Dosimeter, 2637
Dynamic mechanical properties, poly-(vinyl chloride), 73
Elastomers, 3269
Electrical conductivity, 1615
Electric field, 1463
Electrochemical synthesis, 3185
Electron beam, high-intensity, 3283
Electron spin resonance, 505, 1307
Electron-transfer polymers, 869, 2729, 3151, 3395
Emulsion polymerization, 623, 643, 665, 687, 2265, 2853, 2859
Emulsion polymers, polystyrene, 449
Enzymic degradation, 1705, 1965
Epoxide resins, 3418
Epoxides, chloro and cyano, 2461
Epoxy resin, novolac, 2829
Esters, inorganic, 2051
Ethanol, 1643

- Ethers, 2137
N-Ethylcarbazole, 1955
Ethylene, 603, 609, 721, 2069, 2359, 2703, 3201, 3217
Ethylene polymerization, by titanium compounds, 241, 743, 755
Extrathermodynamic approach to adsorption, 3295
Fatty acids, 1515
Ferric acetate hydroxide, 1249
Ferrocene-containing polyesters and polyamides, 1687
Ferrocenylene, 1567
Film, polyethylene, 2921
Fine structure, 2801
Fluorine magnetic resonance spectra, 2387
Fluoroalkyl acrylates, 1729
Fluoroalkyl methacrylates, 1729
Fluoroketones, 1729, 1741
Formaldehyde, aqueous, 2541
 cationic polymerization, 425, 435
 equilibria in, 2533
Fractional precipitation, 1697
Free growing cation, 3049
Free-radical polymerization, 2079
Fumaronitrile, 3059
Gas chromatography, 1025
Gases, 945
Gelatin films, 1991
Gel formation, 2677
Gel permeation chromatography, 1697, 2085
 calibration, 243
Glucosidic bonds, 2415
Graft copolymerization, 3119
Graft copolymers, 963, 979
 highly branched, 801
Grafting, radiation-induced, 1431
Grafting sites, specifically placed, 859
Graft polymers, from chlorinated rubber, 95
 from poly(vinyl chloride), 95
Halides, organic, 3075
1-Halo-2-vinylcyclopropanes, 3327
Heat of solution, 1547
Heterogeneity parameters, 2209
Heterogeneous polymerization, 2421
Heterophase catalytic synthesis, 1417
Hexaphenyldichlorophosphonitrile polymers, diol-linked tetrameric, 1671
Homopolymers and copolymers, 1523, 3059
Homoterephthalic acid, 3177
Hydrazide, 2117
Hydrazine, 3357
Hydrazine-based polyimides, 2755
Hydrochloric acid lignin, 1431
Hydrogen abstraction, 821
Hydrogen bonding, 2137, 2153
Hydrogen migration, 3187
Hydrolysis, 2433
 specific rate of, 2415
Hydroquinone units, 3395
Hydroxy-, acetoxy-, and carboxymethyl alkyl groups, 1883
Hydroxyethylcellulose, 1705
Hydroxyl groups, 2377
Hydroxymethylation, base-catalyzed, 2541
Hyperelectronic polarization, 1135
Imidazole-containing polymers, optically active, 2741
Iminoethers, cyclic, polymerization of, 57, 63
Infrared spectroscopy, 449, 2137
Initiator solvation, 527
Initiator systems, 2179
 aqueous, 793
 metal-containing, 3075
Insertion polymerization, 1249
Ion-selective membranes, 1009
Irradiation, two-stage, 721
Isocyanates, 793, 1087, 1299, 2611
Isomerization, 3259
Isomers, geometrical, 1825
Isoprene, 1109
 cyclopolymerization of, 125
2-Isopropenyl-4,4-dialkyl-5-oxazolones, 2681
2-Isopropenyl-1,3-dioxane, 3182
Keratin, 2237
Kinetics, 609, 2343, 2533, 2541, 3127, 3283
 cationic polymerization of formaldehyde, 435
 of polymerization, 901
Latex particles, 665, 687, 2859
Light scattering, 2209, 2819
 polyacrylonitrile, 147
Lignin, 1431
Linear molecules, 547
Lithiation of dienes, 559
Living anions, 3185
Living polymers, 2773
Maleic anhydride, 1441, 1945, 2418
Maleimide, 1719
Maleonitrile, 3059
Melts, steady-state drawing of, 247
Membranes, asymmetric, 1409

- Mercaptides, 485
Mercerization, 2801
Metal coordination polymers, 1975
Metal salts, 1809
Methacrolein dimer, 2309
Methacrylamide, 3245
Methacrylates, 1325
Methacrylic acid, derivatives of, 1073
Methacrylic esters, polymerization, 257
Methacrylonitrile, 1209
 α -Methacrylophenone, 1841
Methyl acrylate, 2433, 3303, 3315
C-Methylated 2-oxohexamethyleneimines, 513
N-Methylated polyhydrazides, 3371, 3381
n- α -Methylbenzyl methacrylate, 829
3-Methylcyclobutene, 2397
Methylcyclopentadiene, 809
1-Methylcyclopropene, 2441
4-Methyl-1,3-dioxene-4, 1945
 cationic polymerization, 137
 copolymerization with tetrahydrofuran, 137
Methyl methacrylate, 485, 1209, 2433, 2621, 2663, 3075, 3109, 3119, 3303, 3315
 radical polymerization, 13
Methyl methacrylate-glycol dimethacrylate, 3041
Methyl methacrylate-methyl acrylate, 2187
Methyl sidegroup, 2153
 α -Methylstyrene, 1463
 β -Methylstyrene, 1825
Microstructural changes, photoinduced, 763
Model compounds, 2755
Molecular weight distribution, 1025, 1697, 2795
 polydimethylsilmethylene, 1
Monosaccharide derivatives, grafting of, 2501
Morphology, nylon 66, 353
 poly(ethylene terephthalate), 353
 polyolefins, 291
Nadic methyl anhydride-crosslinked novolac epoxy resin, 2829
Naphthalene-2,6-dicarboxylic acids, polymers of, 235
1,4,5,8-Naphthalenetetracarboxylic acid, 1777
Natural rubber, 2678
Near-infrared spectrophotometry, 3415
Nitriles, difunctional, 859
Nitrilimine dipole, 2317
Novolac epoxy resin, 2829
Novolacs, 2051
Nuclear magnetic resonance spectra, 843, 1655
 time-averaged, 2425
 wide line and pulsed, 2785
Nylon, 1913
 interaction of ions with, 1583
Nylon 6, oriented, 2033
Nylon 66, morphology, 353
Olefin polymerizations and copolymerizations, 3139
Olefins, 3087
Oligomer, cyclic, 1044
Optically active *C*-methylated 2-oxohexamethyleneimines, 513
Optical rotation, 829, 1991
Organometallic compounds, 1209
Oxadiazole polymers, 2117
Oxazine units, 1503
Oxazoline polymerization, of cyclic iminoethers, 63
1,3-Oxazolines, 1883
5-Oxazolones, 785
Oxidation during polymerization, effect of, 449
2-Oxohexamethyleneimines, *C*-methylated, 513
4,4'-Oxydibenzoic acid, 1769
Oxygen, 2621
Ozonolysis, 2678
Particle surface area, factors controlling, 2265
Pemosors, 2715
1,4-Pentadiene, 1605
Penton, 2637, 2677
Perfluoroalkylaryl macromolecules, polyelectrolytes from, 171
Peroxide crosslinking, 1315
Peroxide-induced degradation, 3174
Phenanthrene, 2418
Phenol, 2533, 2541
Phenylacetylene, 1857
Phenylpropionyl chloride, 1061
Phenyl vinyl sulfides, *p*-substituted, copolymerization of, 41
Photo and thermal polymerization, 2907
Photochemical crosslinking, 589
Photochemical reduction, 3119
Photochromic polymers, 2967
Photodegradation, 2921
Photoinitiation, 3245
Photoradiation in the solid state, 1055
2-Phthalimidomethyl-1,3-butadiene, 2945

- p*-[(*S*)(-)-2-Phthalimidopropionyl]
 polystyrene, 1871
- α -Piperidone, 2295
- Polyacrylonitrile, 843, 1475, 1925
 light scattering, 147
 thermal reactions of, 2127
- Polyaddition reaction, 1877
- Poly(*n*-alkyl methacrylates), 1315
- Poly(allyl ether), 1741
- Polyamide, aromatic, 3345
- Polyamideamines, 785
- Polyamide derivatives, 3177
- Polyamides, 1195, 1687
 N-substituted, 1615
- Polyaminotetrazoles, 729
- Poly(aryl ethers), 777
- Polybenzothiazoles, 2939
- Polybutadiene, carboxyl-terminated,
 1233
- cis*-1,3-Polybutadiene, low molecular
 weight hydroxy-terminated, 1037
- cis*-1,4-Polybutadiene, 3259
- Poly(*tert*-butylethylene oxide), syndio-
 tactic and isotactic, 2653
- Polycarbonates, 3395
- Polycarboxyhydrazides, 1567
- Polycondensation, equilibrium, 2343
 interfacial, 2059
 room-temperature, 1195
- Polycondensation rate, 889
- Polycyclopentadiene, 1163
- Poly(di- μ -diphenylphosphinatohydroxy-
 aquochromium)(III), 1397
- Polydiketopiperazines, 1097
- Polydimethylsilmethylene, molecular
 weight distribution, 1
- Polydimethylsiloxane-solvent systems,
 1547
- Poly(diphenyl phosphazene), 3163
- Polydisperse materials, 2085
- Polyelectrolytes, from perfluoroalkylaryl
 macromolecules, 171
- Polyester derivatives, 3177
- Polyester resins, unsaturated, 1217
- Polyesters, 1687
 and copolyesters, 2955
- Polyethylene, thermal decomposition, 415
- Polyethylene film, 2921
- Poly(ethylene glycols), liquid, 1025
- Poly(ethylene hydroperoxide), thermal
 decomposition, 375
- Poly(ethylene terephthalate), 2343
 morphology, 353
- Polyglycols, 505
- Poly(*n*-hexylisocyanide), 1417
- Polyhydrazides, 3357, 3371, 3381
 linear, 1449
- Polyimides, benzimidazole- and oxa-
 diazole-modified, 215
 hydrazine-based, 2755
 thermosetting, 877
- Polyisobutenes, structure, 205
- Polyisocyanates, 1087, 2611
- Polyisonitriles, 1417
- 1,4-Polyisoprene, 763
- Polyketones, aromatic, 3345
- Polylactones, 2001
- 1,5-Polymerization, 2591
- Polymethacrolein, 2001
- Poly(methacrylic acid), 2765
- Poly(methyl methacrylate), 1655
- Poly(methyl propenyl ether), 3015
- Polymethyl vinyl carbinol, optically
 active, 2013
- Polyolefins, morphology, 291
- Polyoxadiazoles, isomeric, 1351
- Polyphenoxazines, 161
- Poly-4-phenyl-1-butene, 1341
- Poly-*p*-phenylene-1,3,4-oxadiazole, 3381
- Poly(α -phenylethylisocyanide), 1417
- Polyphenylquinoxalines, aliphatic, 3170
- Polyphenylsiloxanes, 1153
- Poly(phosphonatoalanes), 3235
- Poly- α -piperidone, 2281
- Polypropylene, 589
- Polypropylene hydroperoxide, structure,
 381
 thermal decomposition, 393
- Polypyromellitimides, 1935
- Polysiloxane-vinyl monomer graft and
 block copolymers, 979
- Polystyrene, 449, 1414
 Lewis-acid catalyzed reactions, 269
 living, 859
 sulfonated, 3174
- Polysulfonates, 2022
- Polytetrazoles, 729
- Polytriphenodithiazine, 1774
- Polyurethane elastomers, 2153
- Polyurethanes, redox, 3151
- Poly(vinyl alcohol), 475, 2377
- Poly-*N*-vinylcarbazole, 1955
- Poly(vinyl chloride), 1795, 3269
 dynamic mechanical properties, 73
 graft polymers from, 95
- Poly(vinyl chloride)-rubber blends, 467
- Poly(vinyl ether), 1741
- Poly(*p*-vinylphenyldimethylsilane),
 1643
- Poly(vinyl trifluoroacetate), 2387

- Poly(1-vinyl-3,4,6-trimethyl-2,5-benzoquinone), 869
- Poly-*p*-xylylene, 1058
- Postirradiation polymerization, 1073
- Propagating species, concentration of, 1559
- Propagation rate constants, 1325
- Propagation reaction, rate of, 459
- Propagation and termination, 721
- Propenyl alkyl ethers, 2511, 2523
- Propenyl isobutyl ether, 993
- Propylene, 937, 2561
- Propylene oxide, 1249
- Proton magnetic resonance, polyisobutenes, 205
- Pseudoxazolones, 1877
- 2-Pyridyl methacrylate, 2935
- Pyrolysis, 963, 969, 1935
- Quinoxaline units, 1259, 1503
- Radiation grafting, 1895
- Radiation-induced copolymerization, 1367, 3201
- Radiation-induced grafting, 1431
- γ -Radiation-induced polymerization, 721, 1109, 1307, 2069, 2881, 3127
of ethylene, 609
- Radiation-induced solid-state polymerization, 1073
- Radical cation, 3087
- Radical grafting, 1431
- Radical polymerizations, 1325
coordinated, 2091
methyl methacrylate, 13
retardation of, 1857
styrene, 13
- Rate constants, elementary, 1537
- Rate of polymerization, factors controlling, 2265
- Reactivity ratios, monomer, 1293
- Redox initiator, 2179
- Redox polymerization, 2091
- Reducing agent systems, ceric ion, 493
- Relative reactivities, 2585
- Resins, epoxide, 3418
macroreticular, 2689
unsaturated polyester, 1217
- Rhenium pentachloride, 1537
- Ring-opening, 3381
- Ring structure and basicity, 2585
- Rosins, hydrogenated, 1050
- Rubber, chlorinated, graft polymers from, 95
synthetic, 2819
- Rubber-poly(vinyl chloride) blends, 467
- Salt effect, 2477, 2489
- Schmidt reaction, 2889
- Selenium, relaxations of, 1597
- Silicon-containing polymers, 2117
- Silicon-hydrogen, 1643
- Silver nitrate, 1109
- Smith-Ewart theory, 623, 643
- Sodium amylose xanthate, 1121
- Sodium chloroaurate, 1809
- Solid state, 1661
- Solid-state conversion, 2033
- Solid-state initiation, 945
- Solid-state polymerization, 1073, 1719
- Solubility, 537
- Solution, dilute, 1121
- Solution polycondensations, direct, 3371
- Solution polymerization, 3031
- Solution properties, 537
- Solutions, aqueous, 1833
- Solvent effect, 1655
- Sorption of water vapor, 475
- Spontaneous copolymerization, 2441, 2451
- Stannic chloride, 3031
- Stereoisomers, 843, 3327
- Stereoregularity, 1475
- Stereoregular polymerization, 1209
- Stereospecific polymerization, 2511
- Styrene, 909, 1009, 1033, 1293, 1431, 1441, 1501, 1537, 1633, 1945, 2663, 2681, 3407
polymerization with $ZrCl_3$ and $ZrCl_4$, 193
radical polymerization, 13
- Styrene-acrylonitrile copolymer, 3415
- Styrene-butadiene block copolymers, 1661
- Styrene-butadiene copolymers, 2819
- Styrene-divinylbenzene copolymers, macroreticular, 2689
- Styrene-methacrolein, 2001
- p*-Substituted derivatives, 1857
- α (Substituted methyl)styrenes, 2627
- Succinonitrile, 3059
- Sugar residues, 1625
- Sulfonation, rates of, 1414, 1501
- Sulfur dioxide, 2441, 2451, 3201
liquid, 1441, 3087
- Sulfuric acid medium, 493
- Surfactants, 1833
- Sydnone dipole, 2331
- Tacticity, 829, 843, 2387
- Termination, mode of, 2187
- Termination rate, slow, within latex particles, 665, 687
- Termination rate constants, 1325
- Terpolymerization, 1945
- Tetraamines, aromatic, 1777

- Tetrafluoroethylene, 1367
Tetrafluoroethylene-acrylonitrile graft copolymer, 963, 969
Tetrahydrofuran, 459, 527, 901, 1559
 copolymerization with 4-methyl-1,3-dioxene-4, 137
Thermal decomposition, polyethylene, 415
 polyethylene hydroperoxide, 375
 polypropylene hydroperoxides, 393
Thermal degradation, 1035, 1243, 2611, 2829, 3303, 3315
Thermally stable polymers, 1777
Thermal stability, 1769
 polyisobutenes, 205
Thermogravimetric analysis, 1671, 1975, 3217
Thermostability, 1351
Thiazine recurring units, 1259
1-Thioacylaziridines, 2591
Thiol groups, 3269
Three-dimensional polymerization, mechanism of, 3041
Titanium(III) acetylacetonate, 2703
Titanium dichloride, crystalline, 743, 755
Titanium tetrachloride, 1751
Titanium trichloride, 937
Transesterification, catalyzed, 2343
Transport properties, 2765
Trialkylboranes, 3157
2,4,6-Tricyanoheptane, 843
Trifluoroacetic acid, 2377
2,2,2-Trifluoroethyl vinyl ether, 2573
3,3,3-Trifluoropropene, 1367
 α,β,β -Trifluorostyrenes, substituted, 711
Trimethylamine methacrylimide, polymerization studies, 363
Trimethylamine-4-vinylbenzamide, 2197
Trioxane, 2421, 3031
Triphenylmethyl fluoroborate, 3049
Tri-*n*-propylaluminum, 1751
Trisaccharides, 2415
Tris-[1-(2-methyl)aziridinyl] phosphine oxide, 1333
1,2,4-Trivinylbenzene, 1293, 1501
1,3,5-Trivinylbenzene, 1501
 α,β -Unsaturated ethers, 993, 1001
Urethane, 2137
Urethane groups, 1299
Valance state, 919
Valonia cellulose, 2801
Vinyl acetate, 2265
Vinyl acetate-isobutyl methacrylate, 2187
9-Vinylanthracene, 2079
p-Vinylbenzamide, 2477
p-Vinylbenzenesulfonic acid, 1009
N-Vinylcarbazole, 945, 1307, 1809
N-Vinylcarbazole-acrylonitrile, 2907
Vinyl chloride, low-temperature polymerization, 21
Vinylcyclopropanes, 403, 3327
2-Vinyl-1,3-dioxane, 3182
Vinyl 10,11-epoxyundecanoate, 1273
Vinyl esters, 1050, 1281
Vinyl ethers, 1523
Vinyl fluoride, polymerization, 335
Vinylhydroquinone derivatives, 2729
Vinylidene chloride-styrene copolymers, 951
Vinyl monomers, 575, 1895, 3157
 conjugated, 1381
Vinyl polymerization, 41, 49, 493, 2179, 2621
4-Vinylpyridine, 1047
Vinylsilanes, 1633
Viscosity, 537
Water, 901
Water-absorption properties, 1227
Water vapor, sorption of, 475
Wetting properties, 1729, 1741
X-ray degradation, 2637
X-rays, low-energy, 2677
p-Xylylenebis(dimethylsulfonium) tetrafluoroborate, 1058
Ziegler-Natta catalysts, 919, 927, 937, 2221, 2397, 2405
Zinc methacrylate, 1073